THE DEVELOPMENT OF ACIDIC PROTEIN APTAMERS USING CAPILLARY ELECTROPHORESIS METHODS AND THEIR USE IN SURFACE PLASMON RESONANCE

JON ASHLEY

(MChem, PGCE, NUS)

A THESIS SUBMITTED FOR THE DEGREE OF DOCTORATE OF CHEMISTRY

DEPARTMENT OF CHEMISTRY

NATIONAL UNIVERSITY OF SINGAPORE

2013

Declaration Page

I hereby declare that this thesis is my original work and it has been written by me in its entirety, under the supervision of Professor Sam, Fong, Yau, Li, (Lab:S5-02-05), Chemistry department, National University of Singapore, between 16/01/2009 and 07/04/2013.

I have duly acknowledged all the sources of information which have been used in the thesis.

This thesis has also not been submitted for any degree in any university previously.

The content of the thesis has been partly published in:

1) Ashley J, Ji K, Li SFY: Selection of bovine catalase aptamers using non-SELEX. *Electrophoresis* 2012; 33:2783-2789.

1. J. Ashley, and S.F.Y. Li, Three-dimensional selection of leptin aptamers using capillary electrophoresis and implications for clone validation. Analytical Biochemistry 434 (2013) 146-152.

Jon Ashley	S Ashley	18/03/2013
Name	Signature	Date

Acknowledgements

We acknowledge financial support from the National University of Singapore, National Research Foundation and Economic Development Board (SPORE, COY-15-EWI-RCFSA/N197-1) and Ministry of Education (R-143-000-441-112).

I would like to thank the Singaporean government for allowing me to come to undertake my doctorate degree at the National University of Singapore. I would also like to acknowledge my supervisor Professor Sam Fong Yau Li for his support and guidance during my time here. I also wish to thank my fellow research group members for all their help and advice. In particular I would like to thank Dr. Grace Birungi and Dr. Junie Tok for training me on the use of capillary electrophoresis, Dr. Zuo Xing Bing for teaching me PCR, associate professor Christoph Winkler for training and advice on agarose gels, Kaili Ji for help with the cloning and general discussions on aptamers, and the proteomic centre for the use of the BIAcore T3000 SPR. I would like to acknowledge the work done by the students I mentored, Dong Jia on the hybridized-SELEX using magnetic beads, Lim Wee Siang on the non-SELEX of hemoglobin aptamers and Lin weili for her work on the development of aptamers for β-lactoglobulin A using CE-SELEX

I'd also like to thank my friends and family for their patience and support and my girlfriend Hyojae Park for her love and support.

Table of Contents

Outline

Aptamers are ssDNA or ssRNA which show affinity towards a wide range of biomolecules and small molecules. We can screen for aptamers by incubating the target with a library of random oligonucleotides, separating binding oligonucleotides, amplifying them by Polymerase chain reaction (PCR) and regenerating the oligonucleotides by strand separation. This is known as systematic evolution of ligands by exponential enrichment (SELEX). Traditionally scientists have used affinity chromatography or nitrocellulose membrane filters to select these aptamers. Selection of aptamers can take a long time to finish due to the number of rounds needed to achieve an enriched library, typically >10 rounds. A number of post SELEX modifications have appeared in the literature that decrease the time required for selection. CE-SELEX and non-SELEX are capillary based methods that take advantage of the higher efficiency of separation and can reduce the number of rounds to <5 rounds of selection. These CE based methods allow for the selection of aptamers without immobilization of the target, and the selection of aptamers with both fast and slow binding kinetics. It also can be used to accurately determine the binding affinities, kinetics and specificity of aptamer sequences.

In my PhD, the use of CE-SELEX to select DNA aptamers for human leptin protein was demonstrated. Four rounds of selection were performed and aptamers were screened for binding affinity. An aptamer with high nanomolar binding affinity and specificity towards leptin was found.

In the second project the use of non-SELEX to select aptamers which bind to human hemoglobin and bovine catalase protein was achieved. Improvements in the selection were demonstrated by inducing a stacking effect to increase the signal sensitivity of the complex peak and, increase the internal diameter of the capillaries used to maximize the number of sequences screened without

losing resolution. For the catalase aptamers were selected after 2 rounds of selection. The enriched library was cloned and sequenced. Aptamers with high nanomolar binding affinity and high specificity were found for both targets.

In the next part of the thesis, an alternative CE based method called hybridized-SELEX was proposed. A single round of selection using a nitrocellulose filter combined with 2 rounds of CE based partitioning without intermediate amplification, allowed for a greater number of aptamers to be screened. This method also allows for the aptamers to be screened in two different environments, namely either with the target immobilized or with the target in free solution. An advantage is that it is compatible with a large range of partitioning techniques. This method also removes the necessity to carry out a negative round of selection in the case of acidic protein targets. An aptamer with high nanomolar binding affinity and specificity was selected.

In the last part of the thesis, we developed an aptamer based SPR biosensor for the detection of bovine catalase in milk. The aptamer was immobilized onto the surface by streptavidin affinity capture. The sensor showed good specificity and reproducibility towards bovine catalase in milk and the limit of detection (LOD) was then determined to be 68 nM.

.

List of Tables

List of Figures

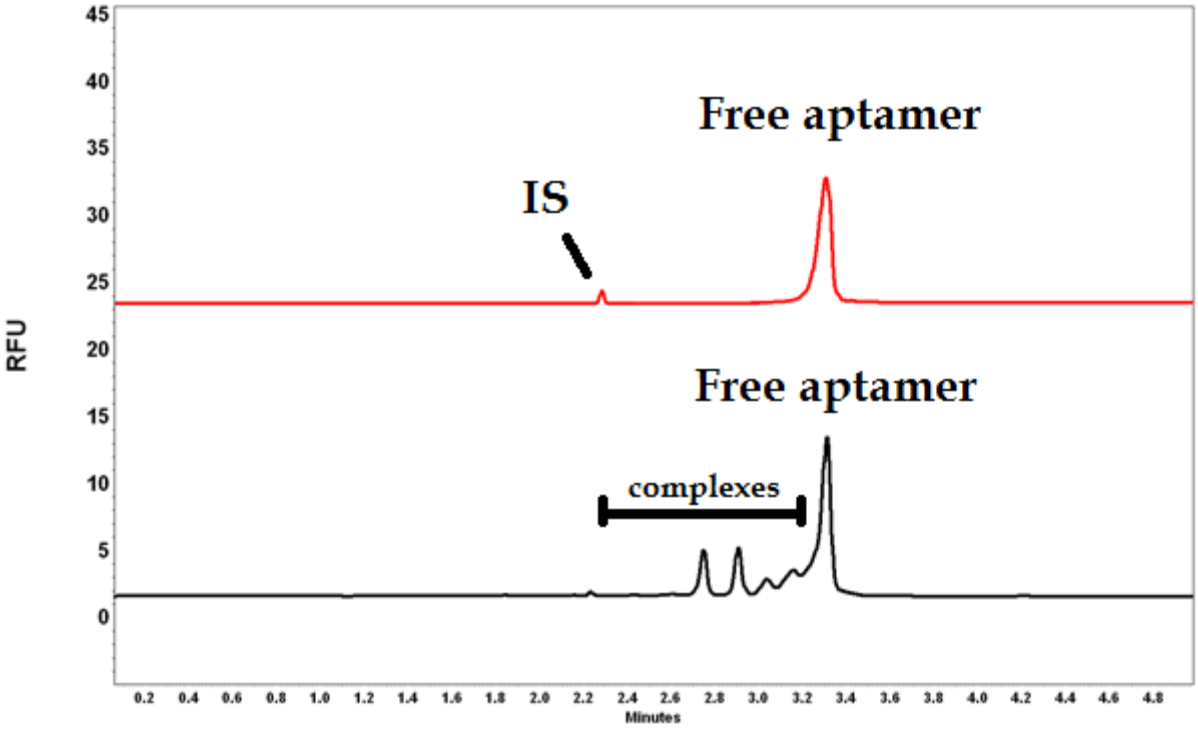

Figure c.9 NEECEM analysis of CES 3 aptamer; 100nM aptamer and 500nM leptin were incubated for 30 minutes and injected onto the capillary by hydrodynamic injection (9.90 nl), 666Vcm^{-1} separation with LIF detection. The areas of the free DNA, dissociated DNA and complex peak were used to determine K_D and experiments were performed in triplicate. 190

List of Abbreviations

ACE	Affinity capillary electrophoresis
BP	Base pair
BSA	Bovine serum albumin
CAT	Catalase
CE	Capillary electrophoresis
CEC	Capillary electrokinetic chromatography
CES	Cholesterol esterase
CLADE	Closed loop aptameric directed evolution
DNA	Deoxyribonucleic acid
dsDNA	Double stranded deoxyribonucleic acid
ECEEM	Equilibrium capillary electrophoresis of equilibrium mixtures
EDC	1-Ethyl-3-(3-dimethyl aminopropyl)-carbodiimide
EDTA	Ethylenediaminetetraacetate
ELISA	Enzyme-linked immunosorbent assay
EMSA	Electophoretic mobility shift assay
FAM	Fluorescein amidite
FRET	Fluorescence resonance energy transfer
GO	Graphene oxide
GST	Glutathione-S-transferase
HAU	Hemagglutination units

HB	Hemoglobin
HEPES	(4-(2-hydroxyethyl)-1-piperazineethanesulfonic acid)
HIV	Human immunodeficiency virus
HKE	HEPES-potassium chloride-EDTA
HPLC	High performance liquid chromatography
ID	Internal diameter
IgE	Immunoglobulin E
LB	Lysogeny broth
Lep	Human leptin
LIF	Laser induced fluorescence
LOD	Limit of detection
11-MUA	11-Mercaptodecanoic acid
NHS	N-hydrosuccinimide
NECEEM	Non equilibrium capillary electrophoresis of equilibrium mixtures
PCR	Polymerase chain reaction
PDA	Photo diode array
PDGF	Platelet-derived growth factor
QCM	Quartz crystal microbalance
RBP 4	Retinol binding protein
RNA	Ribonucleic acid
RT-PCR	Reverse transcriptase polymerase chain reaction

SAM	Self-assembly monolayer
SELEX	Systematic evolution of ligands by exponential enrichment
SOC	Super optimal broth
SPR	Surface plasmon resonance
ssDNA	Single stranded DNA
TBST	Tris-buffered saline, Tween
TGK	Tris-glycine-phosphate buffer
Tris	Tris (hydroxymethyl) aminomethane
UV-vis	Ultraviolet-visible
VHSV	Marine derived pathogenic virus

1 Literature review

1.1 Aptamers

Aptamers are ssDNA, ssRNA or peptide oligonucleotides that bind to a large number of different biomolecules or small molecules and display a high degree of binding affinity and specificity towards their targets. Aptamers are an attractive alternative to antibodies with a distinct number of advantages[1; 2].

When compared to antibodies, aptamers can be produced cheaply and in large quantities. This is because DNA, RNA and peptides can be synthesized chemically by well-defined methods in the lab. Antibodies however require the use of animals to produce an immune response to a particular protein or molecule. This can be both expensive and give large batch to batch variations in terms of yield. The extent, to which antibodies can be produced, depends on the immune response that the animal exhibits to an antigen. Often if the immune response is weak, biologists can add the antigen to a complex mixture of agents called adjuvants. Antibodies also suffer from faster degradation when compared to aptamers. DNA aptamers can last for several months or even years if stored properly. Aptamers are smaller than antibodies having average molecular weight of ~25 kDa which is considerably smaller than antibodies which have an average molecular weight of ~150 kDa. This can give aptamers an advantage over antibodies where the mass of the ligand is important. For example, the size of aptamers makes them more desirable in biosensors. This can improve the sensitivity of the biosensor. Researchers can

tailor aptamers with predefined properties to fit their intended application. For example, they can design aptamers with a specific kinetic property such as a slow k_{off} rate or modifying the base groups on the aptamer to make them more resistant to enzyme degradation. In contrast antibodies generally are limited to physiological conditions.

1.2 A comparison of different types of aptamer

Although both ssDNA and ssRNA aptamers can form diverse secondary structures, ssRNA can form more complex 3D structures than ssDNA due to the extra 3' hydroxyl group which can result in aptamers with higher binding affinity. However ssRNA is less stable than ssDNA and is particularly susceptible to nuclease degradation. ssRNA aptamers typically have half-lives of minutes when used *in vivo*. ssDNA, although also susceptible to nuclease enzymes, is generally more stable when used *in vivo*[3]. Both ssRNA and ssDNA aptamers can bind the targets using the whole sequence, although smaller aptamer sequences are more desirable due to the lower cost.

Recently researchers have used peptides as a new class of aptamer[4]. The peptide contains a sequence, displayed on an inert protein scaffold. They show similar properties to antibodies and they are even smaller than DNA and RNA aptamers. They are also very stable, and have a higher solubility. However they are challenging to develop compared to DNA and RNA.

1.3 Uses of aptamers

Research groups and biotech companies have developed aptamers for a large number of applications for the last 20 years. Aptamers have found use in areas such as analytical chemistry,

the pharmaceutical industry, and even environmental applications. Despite being used for the last 20 years, interest in the application of aptamers is still growing.

1.3.1 Bioanalytical uses of aptamers

A large number of research papers for the application of aptamers in bio analytical chemistry, have appeared in the literature in recent years[5]. Aptamers have found use as affinity ligands in separation techniques such as chromatography, microfluidics and capillary electrophoresis[6]. These aptamers can help facilitate the improved purification and separation of proteins and small molecules. For example in affinity chromatography, highly specific aptamer-ligand interactions can allow for good separation of biomolecules in biological samples. The analyst injects the analyte onto a column which is packed with immobilized aptamers. The target analyte interacts with the aptamers and will be retained on the column while the rest of the sample elutes through. The analyte can then be eluted using a high salt buffer which disrupts the aptamer-ligand interaction. Scientists have explored using packed bed columns, open tubular columns and monolithic columns as stationary supports for aptamer immobilization[7; 8]. One example recently reported was for a chromatographic affinity assay for the detection and purification of thrombin protein using two different aptamers as affinity agents. This allowed for a detection limit of 0.1 nM to be obtained[9]. In microfluidics, researchers used aptamer based stationary phases to develop a method for the enrichment, sorting and detection of multiple cancer cells[10]. Microfluidics offer many advantage over conventional methods by being able to integrate sample pre-treatment, separation and detection on a single chip. The technique only requires a small amount of sample allowing for continuous analysis and faster separations.

In affinity capillary electrophoresis (ACE), aptamers were used as affinity probes for the detection of inorganic metal ions[11]. Tagging aptamers with fluorescence fluorophores also allows for extremely sensitive assays to be developed. Several recent papers described the use aptamers as affinity probes in ACE include IgE, HIV type 1 reverse transcriptase, thrombin and antithrombin III[12-14].

The use of aptamers in biosensors is becoming a huge area of interest in bioanalytical chemistry. A biosensor consists of a recognition element which is usually a biomolecule such as an antibody and a transducer which can be based on an electrochemical, optical or mass change. Biosensors are a viable alternative to traditional techniques which often require more sample preparation. Aptamers are useful as the recognition element in biosensors and these sensors are often referred to as aptasensors. Aptamer based electrochemical sensors, allow for the detection of biomolecules with high sensitivity, rapid response, and potential for miniaturization[15]. Researchers have also developed chemiluminescence-based aptasensors due to low cost, high sensitivity and simplicity[16; 17].

Fluorescence-based aptasensors have also been developed and offer one of the most sensitive techniques for detection of biomolecules and a large number of different method platforms have been reported [17]. In 2004 Nutiu *et al* reported the on the use of aptamers as signaling agents to monitor the conversion of adenosine 5'monophosphate into adenosine by alkaline phosphatase[18]. Li *et al* reported the use of fluorophore tagged aptamers *in vivo* as probes for real time imaging of proteins in cells[19]. Fluorescence resonance energy transfer (FRET) based assays have been employed in a thrombin based graphene assembled aptasensor[20]. The dye labeled aptamer causes a quenching effect due to the non-covalent assembly between the aptamer and the graphene. The

presence of thrombin allows the fluorescence to return to the probe making it possible to quantify the analyte.

Molecular beacons are typically based on aptamers and contain both a fluorophore and a quencher tag. Upon binding with the target, a change in conformation can cause the quencher and fluorophore to move away from one another or vice versa, which induces a change in the fluorescence signal. Aptamer based molecular beacons have been developed to bind to DNA, as hybridization probes and for the detection of proteins[21]. Examples of aptamers used in molecular beacons, which detect proteins include thrombin and platelet-derived growth factor **(**PDGF**)**[22-25].

The use of quantum dots in aptamer research and biosensors can increase the sensitivity of detection. In comparison to fluorescent organic dyes, they are more photostable and varying the size and composition can cause the wavelength of emitted light to change[26]. Quantum dots also display broad excitation wavelengths and very narrow emission wavelengths. One example where aptamers were used with quantum dots was in a sandwich based assay for the detection of *Camplyobacter* in food samples[27].

Research into biosensors based on mass changes is of great interest in bioanalytical chemistry. These techniques rely on the analyte mass to induce a sensitive response. Hence the detection of small molecules is more challenging. One technique called Quartz crystal microbalance (QCM) is a mass sensitive technique which works on the principle of the pizoelectric effect [28]. An applied voltage across the quartz crystal causes oscillations of a particular frequency known as the resonance frequency. The resonance frequency changes as the thickness of the surface of the crystal changes. As the mass of the surface changes, the resonance frequency also changes allowing the quartz crystal in effect to act like a small balance. The surface of the quartz crystal

is usually coated with a layer of gold, allowing for a large number of chemistries to be used. Researchers have started using aptamers in QCM as the recognition element and they have the advantage of being smaller than antibodies, allowing for a more sensitive assay. Recently Yao *et al* developed an aptamer and antibody based QCM biosensor for the detection of IgE protein[27; 29]. They both gave a similar linear range of detection, but the aptamer showed a lower limit of detection (LOD). Other protein targets studied include HIV-1, tat protein and marine derived pathogenic virus (VHSV)[30; 31]. The use of nanoparticles in QCM sensors has also been reported recently to amplify the QCM signal for detection of thrombin[32]. Nanoparticles can act as a heavy functional molecule which also contains the ligand. The nanoparticle binds to the analyte which causes an increase in mass upon binding to the ligand on the surface of the sensor and causing a boost in signal. Another mass sensitive biosensor which is of increasing interest in the life sciences is surface plasmon resonance (SPR). Researchers have used this technique to study bio interactions of biomolecules. For example, in protein-protein and DNA-protein interactions, SPR can determine kinetic information such as dissociation constants. The method works on the principle that as an incident ray of polarized light shines onto a gold-glass interface and it can be totally internally reflected at a certain incident angle.

The light photons can interact with the electrons in the gold surface forming plasmon waves. This causes a change in the reflected light intensity, giving rise to a response. When a biomolecule interacts with the surface of the SPR there is a change in the response. This is due to the change in refractive index. Unfortunately the SPR signal can also change due to temperature fluctuations, composition of the metal surface, as well as the refractive index of the medium. As with QCM, the SPR chip contains a gold surface and again is an ideal choice for a

large range of chemistries. This change in signal that allows for the use of SPR as a real time analysis technique for kinetic studies and concentration based assays.

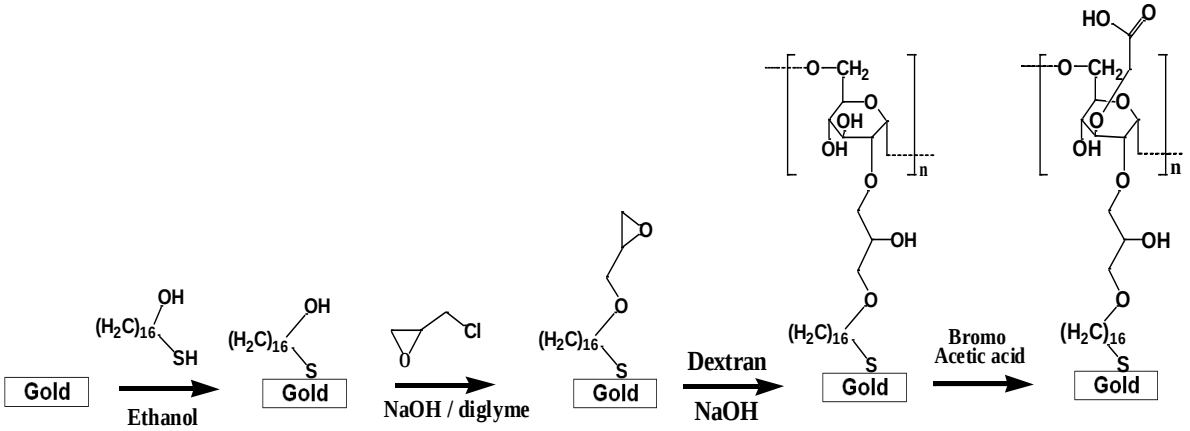

Figure 1.1 The immobilization of carboxylated dextran sensor (The BIAcore CM5 chip).

The aptamer ligands must be attached to the sensor surface in order for an analyte-ligand interaction to be detected. There are a number of methods that can be used to achieve this. The bioreceptor can be directly immobilized onto the sensor surface by functionalizing the bioreceptor with a thiol group although this does not guarantee a stable surface and is susceptible to non-specific binding[33; 34].

The most popular method for immobilizing the bioreceptor involves forming self-assembled monolayers (SAMs) such as thiol alkanes to prevent the analyte from interacting with the gold surface itself[35; 36]. These SAM's can have functionalized groups such as a carboxylic acid, hydroxyl, or amine groups in order to couple the bioreceptor to the surface. Most commercially available chips incorporate dextran based surfaces onto their chips which contain various functional groups such as carboxylic acids. Dextran minimizes non-specific binding of the analyte to the gold. **Figure 1.1** shows the immobilization of carboxylated dextran onto a gold

sensor surface using thiol alkane. The thiol alkane reacts with a halo epoxide. The epoxide then reacts with dextran, which is functionalized with carboxylated groups. This forms the basis of the BIAcore CM5 chip[37; 38]. These functionalized groups can then undergo covalent coupling with aptamer ligands onto the SAM. A wide range of methods are available to attach the Ligands to the surface of the SAM, although the tagging of aptamers with functional groups is currently limited to a few methods such as tagging with biotin, thiol groups or amines[39]. Amine coupling where a carboxylic acid functional group on the SAM is activated using N-hydroxysuccinimide (NHS) and 1-ethyl-3-(3-dimethyl aminopropyl)-carbodiimide (EDC) followed by reaction of a amine terminated aptamer is by far the most popular method for immobilizing aptamers[40]. **Figure 1.2** shows the immobilization of 11-mercaptoundecanoic acid (11-MUA) onto a gold surface followed by amine coupling with the aptamer.

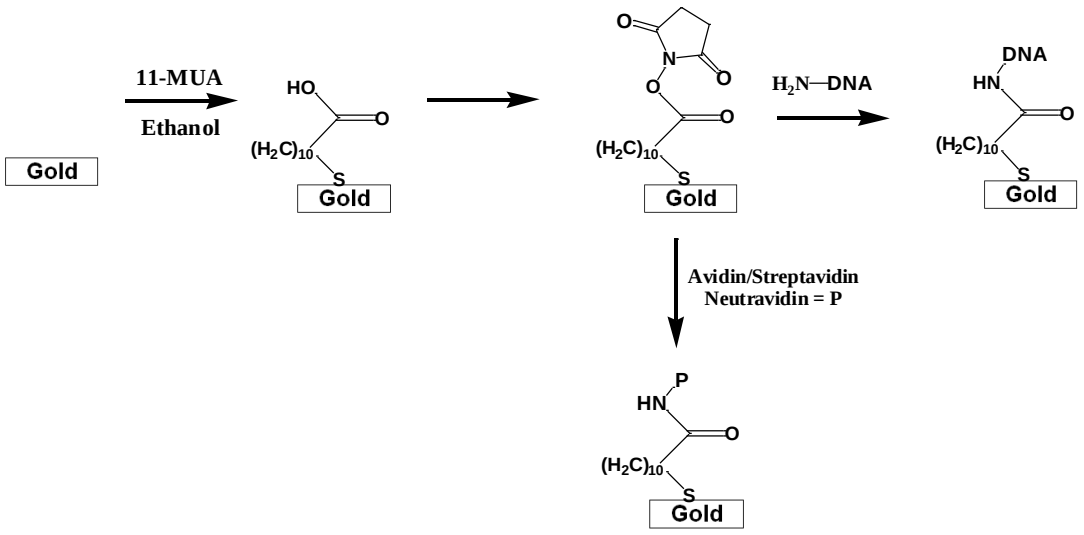

Figure 1.2 Immobilization of 11-MUA onto a gold surface, followed by amine coupling to the a protein or DNA based receptor.

Thiol functionalized aptamers have also been immobilized using 11-amino-1-undecanethiol hydrochloride based SAMs[41]. This coupling reaction involves activating the SAM with

sulfosuccinimidyl 4-(N-maleimidomethyl)cyclohexane-1-carboxylate followed by coupling with the thiol aptamer.

Affinity capture of aptamers offers an alternative method to direct covalent coupling although the biomolecules still need to undergo covalent coupling to attach the affinity agent. One example of affinity capture in aptamer based aptasensors is the biotin-streptavidin interaction, partly due to the ease of which the aptamer can be biotinylated[42]. The biotin-streptavidin interaction is one of the strongest interactions in nature with a dissociation constant K_D of 10^{-15} M and can only be removed by 8M Guanidine HCl solution. Other affinity capture techniques include, poly histidine tags and glutathione-S-transferase (GST), although these types of affinity capture have not been demonstrated on aptamer based biosensors as of yet.

To date there has been a number of aptasensors developed to detect and quantify proteins. In 2005 Tombellini developed an RNA aptamer-based biosensor for QCM and SPR to detect tat protein using the streptavidin-biotin affinity capture to immobilize the aptamer[31]. Lee *et al* developed an aptamer based SPR sensor for retinol binding protein (RBP4) using an aptamer based system again using a streptavidin interaction[43]. They reported a limit of detection (LOD) of 75 nM which was comparable to the conventional immunoassay based methods. A sandwich style SPR aptasensor assay was developed in 2009 for the detection of IgE protein allowing for a detection limit of 2.07 ng/ml[44]. More recently, a SPR aptasensor was developed for the rapid detection of H5N1 avian influenza and reported a detection range of between 0.128 and 1.28 Hemagglutination units (HAU)[42]. In 2012 Chang *et al* developed a SPR based biosensor for the detection of Interferon-gamma achieving a linear dynamic range of between 0.3-333nM and a detection limit down to picomolar range[45].

1.4 Selection of Aptamers

A combinatorial approach to find aptamers that bind to a particular target allows for a large number of oligonucleotides to be screened. A random library of oligonucleotides can be synthesized by automated solid phase synthesis. The 5' end of a Deoxygribonucleoside 3'-phosphoramitide is protected using dimethoxytrityl (DMT) and the 3' phosphate is protected with β-cyanomethyl protecting groups. This is followed by coupling to a base group attached to a resin bead using hydrolysis in anhydrous conditions. Iodine is then selected to reduce the phosphite triester to a phosphotriester group. The DMT protecting group can then be removed using dichloroacetic acid (DCA). The resultant deprotected chain can then be elongated with randomized base groups until the desired size of oligonucleotide is obtained. The final step involves removing the β-cyanomethyl protecting groups using ammonium hydroxide. The oligonucleotides can then be removed from the bead and purified using PAGE. DNA libraries consist of oligonucleotides with a constant region of about 20 bp at both the 5' and 3' ends and a 20-50 bp randomized region in the middle. Shorter random regions have been reported to lead to GC bias while longer regions can be expensive to produce. In the case of RNA, the DNA library is transcribed into RNA using the T7 transcriptase and a T7 promoter region incorporated onto the 5' constant end of the oligonucleotide. A 40bp random region library would give rise to 10^{24} sequences requiring 40kg of DNA. It is therefore acceptable only to use a small fraction of the total number of sequences and typically libraries containing 10^{17} sequences can be used.

1.4.1 Partitioning methods

Aptamers are selected from a library of random sequences of DNA using a method called Systematic Evolution of Ligands by Exponential Enrichment (SELEX). The constant primer region is complementary to the primers allowing for amplification by PCR.

First developed independently by Elington and Tuerk in 1990, the process involves incubating a library of random DNA or RNA with the target molecule and partitioning the bound sequences from the unbound sequences[46; 47]. Subsequent amplification of the bound sequences by PCR for DNA and reverse transcriptase RT-PCR for RNA results in a library of sequences which show high affinity towards the target molecule. Regeneration of ssDNA and ssRNA allows for another round of selection. After a certain number of rounds of selection, an enriched library is obtained and a negative selection is carried out. This allows for the separation of non-specific binding sequences from those that bind the target molecule. **Figure 1.3** shows the general scheme of SELEX.

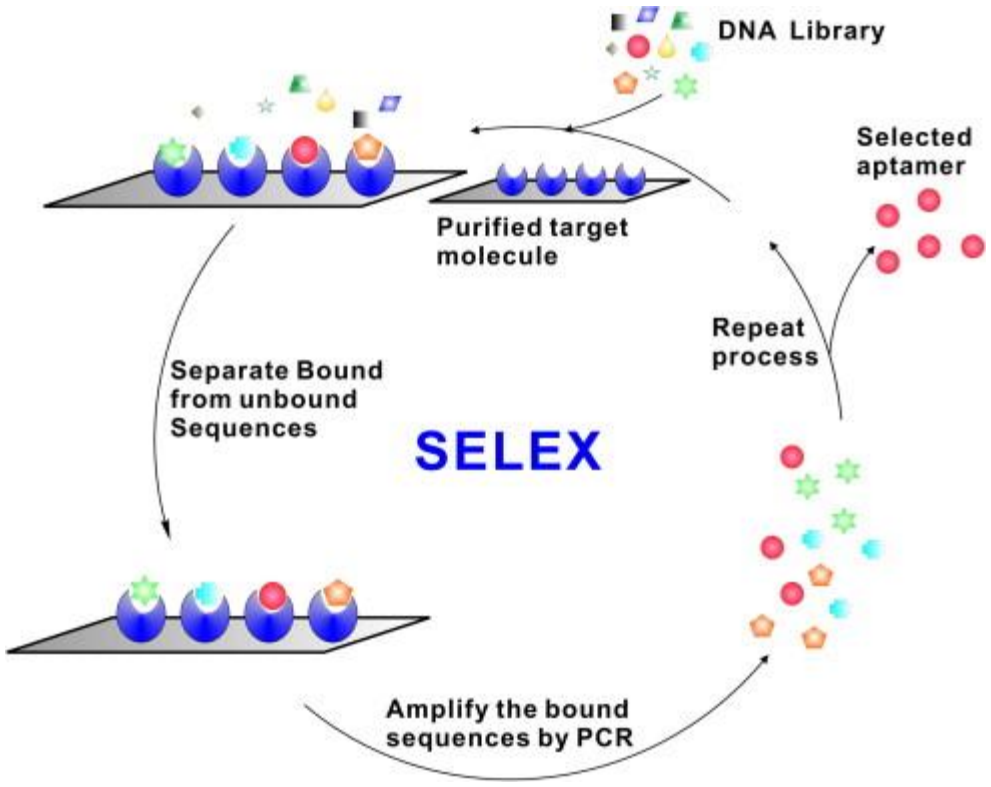

Figure 1.3 A general scheme for SELEX. A number of positive selections separating bound DNA from the unbound DNA followed by PCR amplification and regeneration of the ssDNA. Often a negative round of selection is used to remove non-specific binding aptamer sequence[48].

Aptamer libraries are then cloned and sequenced to determine the sequence of the aptamer. These aptamer sequences must be synthesized and validated against the target for secondary structure folding, binding affinity and specificity. A successful aptamer sequence will display a good folding structure with negative Gibbs free energy, high binding affinity and a high specificity.

Affinity columns are a widely used method for the partitioning step. The target is immobilized onto a packed column. The nucleic acid library passes through the column and binding sequences will bind with the target and stay on the column. The non-binding DNA passes through the column and elutes straight through. Types of affinity column that have been used for

partitioning include biotin-streptavidin, glutathione S-transferase (GST), polyhistidine tagging and Immobilized metals[49; 50].

Biotin-streptavidin was originally used for affinity column based SELEX procedures[51]. The target is tagged with biotin and incubated with streptavidin agarose beads which are packed into the column. They are a readily available, cheap and easy to setup. Poly-histidine tags have also been used in a number of selection studies due to their ease of use. Poly-histidine has an affinity towards nickel or cobalt and so the target containing the histidine tag can bind onto an immobilized metal affinity column[52]. Scientists have used Immobilized metals on their own as targets for selection such as in the selection of arsenic specific aptamers[53].

The use of GST is also of interest in SELEX. The tagging of the target with the GST fusion protein onto its N terminus allows for the immobilization onto a solid support by binding to its substrate Glutathione[54-56].

As well as affinity columns, other affinity surfaces can be used for the partitioning step. Magnetic beads and agarose beads are a convenient platform for immobilizing a target protein and can act as a heterogeneous type selection[57; 58]. Immobilization of the target onto the beads makes use of similar chemistries used in affinity columns. The beads facilitate selection by incubating with the target in solution. Researchers can then remove the binding sequences by magnet or spin columns. Another affinity surface technique reported in the literature used a microtitre plate to select aptamers against human oncostatin M and influenza virus[59-61]. There are a wide range of micro well plates that incorporate the same affinity chemistries mentioned for the affinity columns. The target is again immobilized onto the plate using the desired tag and the unbound sites are blocked using a blocking agent such as bovine serum Albumin (BSA).

Incubation of the target on the plate and the washing of unbound DNA allows for the selection to proceed.

Nitro cellulose membrane filters are a quick and easy separation method for SELEX[62]. It also makes it possible to select aptamers against smaller targets such as small molecules and peptides. However, efficiency of membrane filters is quite low and >10 rounds of selection are often required. This technique was originally used for the first selection described by Gold and Tuerck for the selection of organic dye molecules and this technique is the most common method for partitioning. Research groups have used this technique to select aptamers for proteins such as mouse prion protein and human IgE and protein kinase C[63-65].

Over the years researchers have developed a number of modifications and alternative partitioning methods. In 1996 Geiger *et al* demonstrated the use of negative selection to remove non-specific binding nucleic acid sequences[66]. Separation using non-immobilized target allows for non-specific binders to stay on the membrane or stationary support while allowing non-binding sequences to elute through. In 1994 the Gold group, developed counter-SELEX, as a way of developing aptamers that can differentiate between closely related proteins[67]. By changing the target in between rounds they were able to select the aptamers that didn't bind to the target. Methods that result in aptamers that can distinguish targets in complex mixtures are of enormous interest to the scientific community. For example, Deconvolution-SELEX is a method which can select aptamers against complex targets[68]. This allows for the selection to be done against the target in its native form and medium, avoiding problems associated with validation and use of the aptamers at a later stage.

In recent years the desire to develop immobilization-free methods of selection is of great importance. Shangguan *et al* in 2006 used whole cells as the target for selection of aptamers termed cell-SELEX[69]. The cells were incubated with the DNA and the cells along with the bound DNA can be separated using ultracentrifugation or flow cytometry. The cells act as a pseudo stationary phase. As there are hundreds of membrane proteins on the cell surface, the target for SELEX is unknown until the aptamers have been validated and the selection is in essence performed using 1000's of membrane protein targets. This can result in aptamers with high affinity but very low specificity.

More recently, a group from Korea developed an immobilization free partitioning technique using graphene oxide called GO-SELEX[70]. The graphene oxide can be used as a scavenging agent to selectively remove all the unbound oligonucleotides and could potentially select aptamers for small molecules.

Due to the large number of rounds required for selection, of aptamers for a particular target as well as the time taken to validate individual aptamer candidates, a number of methods have demonstrated a much greater efficiency of selection. CE-SELEX takes advantage of the higher separation efficiency of capillary electrophoresis and does not require the target to be immobilized[71]. CE-SELEX involves the use of capillary electrophoresis to separate bound DNA due to the differences in electrophoretic mobilities of the complex and the free DNA. This technique involves the incubation of a target protein with a native DNA library followed by injecting onto a capillary. This technique has been used to select a variety of targets including HIV reverse transcriptase, Y neuropeptide, protein kinase C-Delta, and ricin toxin[72-76]. CE is considered to be a more efficient separation tool for SELEX and has the advantages of allowing for the selection of aptamers which bind the whole target in free solution. It takes less than 5

rounds to complete the selection and only requires small injection volumes allowing the researcher to save precious sample. A further modification to the CE-SELEX was reported by Ruff *et al* where they use implemented an alternative method for CE-Selection without using LIF detection[77]. Real time-PCR was used to indirectly measure aptamer-target complexes. This method was used to select aptamers against BSA protein.

In 2005 Berezovski *et al* reported further modifications to the CE-SELEX method called non-SELEX[78] and is shown in **figure 1.4**. The technique further reduces the number of rounds to ≤3 rounds and again does not require target immobilization.

Non-SELEX involves repeated rounds of partitioning using capillary electrophoresis without the need for amplification and strand separation after each subsequent round of selection reducing the error rate associated with PCR. Each collected pool is amplified individually for subsequent strand separation and K_D determination[79]. Non-SELEX can be described in terms of two modes of operation. The first mode is Non equilibrium capillary electrophoresis of equilibrium mixtures (NECEEM)[13; 80]. This mode relies on forming an equilibrium mixture by incubating the target and library. Injection of a small plug of equilibrium mixture is followed by

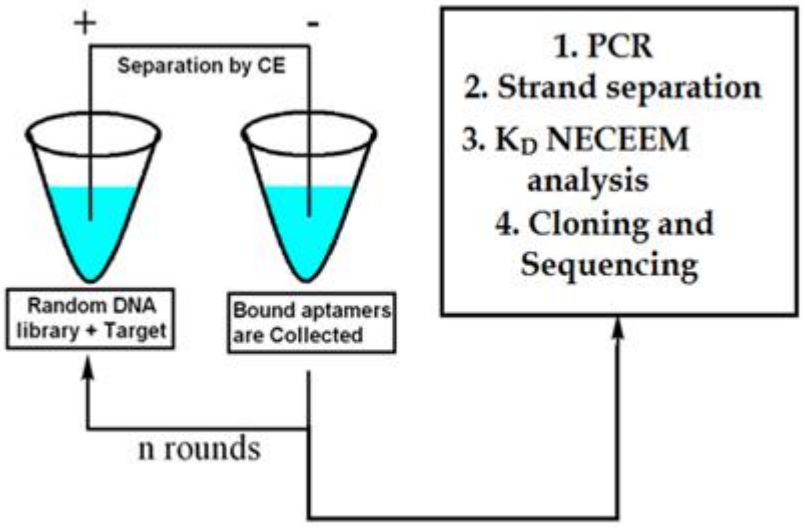

Figure 1.4 General scheme of non-SELEX; selection is carried out using capillary electrophoresis. DNA is collected into a vial containing the target and then re injected. 1-3 rounds are achieved without intermittent amplification. Each round of selection is amplified using PCR and the bulk affinity of each round is monitored for the bulk affinity K_D.

separation and can result in easy collection of the bound DNA. As with CE-SELEX, the unbound DNA sequences, the complex of DNA and the target and excess unbound target molecule all migrate at different rates due to the difference in their electrophoretic mobilities, allowing for separation and collection of bound DNA. Aptamers with the highest k_{off} rates will dissociate from the complex during migration through the capillary, forming an exponential decay region in the electrophoretogram. Therefore this method allows for the collection of aptamers with all possible k_{off} rates. A typical profile of NECEEM is shown in **figure 1.5.**

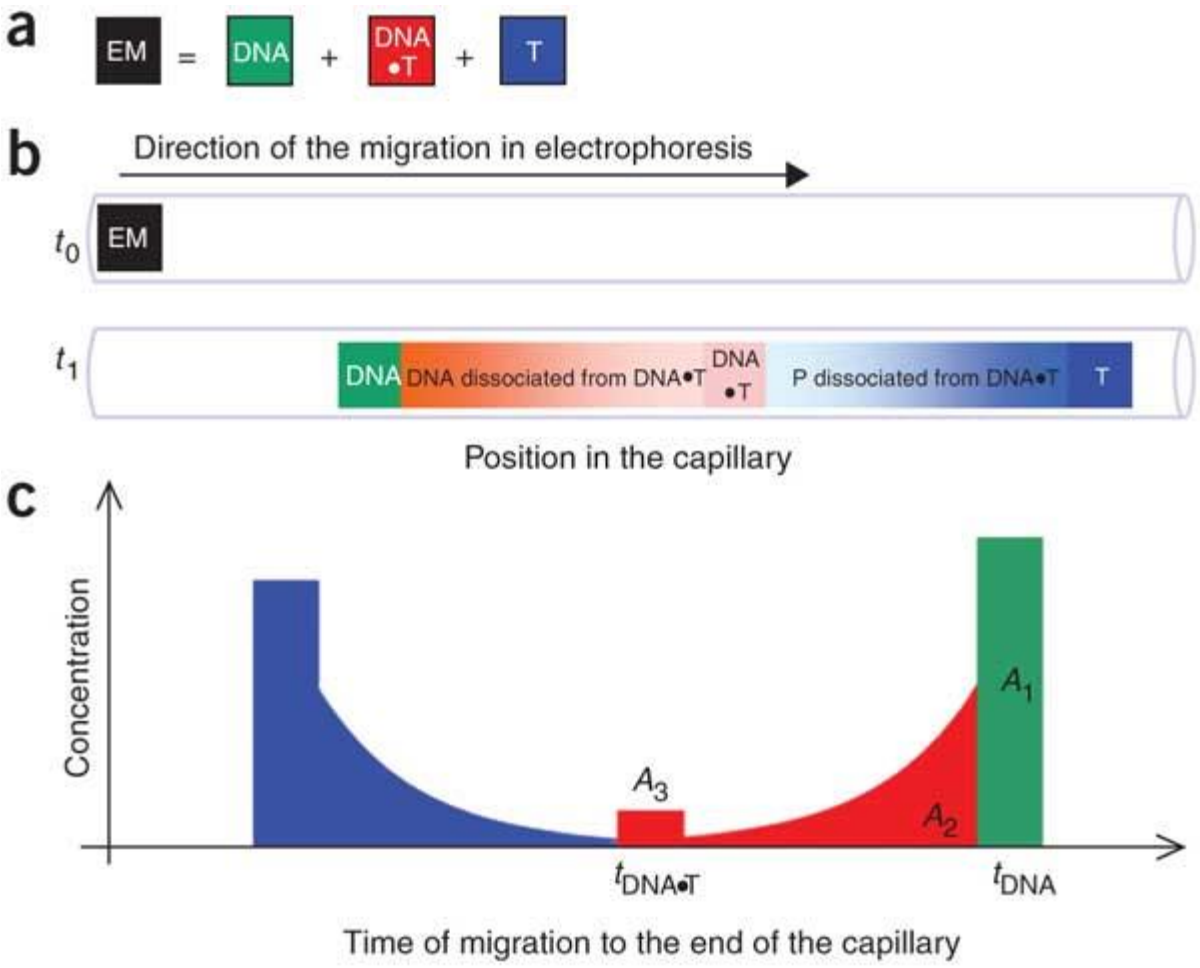

Figure 1.5 (a) The equilibrium mixture (EM) consists of the unbound DNA (DNA), complex (DNA•T) and unbound target (T); (b) relative positions of the constituents of the equilibrium in the capillary at t0 and t1; (c) electrophoretogram plot profile of the equilibrium mixture with the area of the unbound DNA library (A1), the area of the dissociated DNA (A2) and the area of the complex peak (A3)[79].

Equilibrium capillary electrophoresis of equilibrium mixtures (ECEEM), the other mode of non-SELEX relies on similar conditions as described for NECEEM with the exception that the target is added to the run buffer to allow for a quasi-equilibrium to form in the capillary[81]. Whereas NECEEM allowed for the selection of aptamers with predefined k_{off}, ECEEM selection allows for the selection of aptamers with predefined K_D's. As the run progresses, aptamers with higher K_D values are collected (**figure 1.6**).

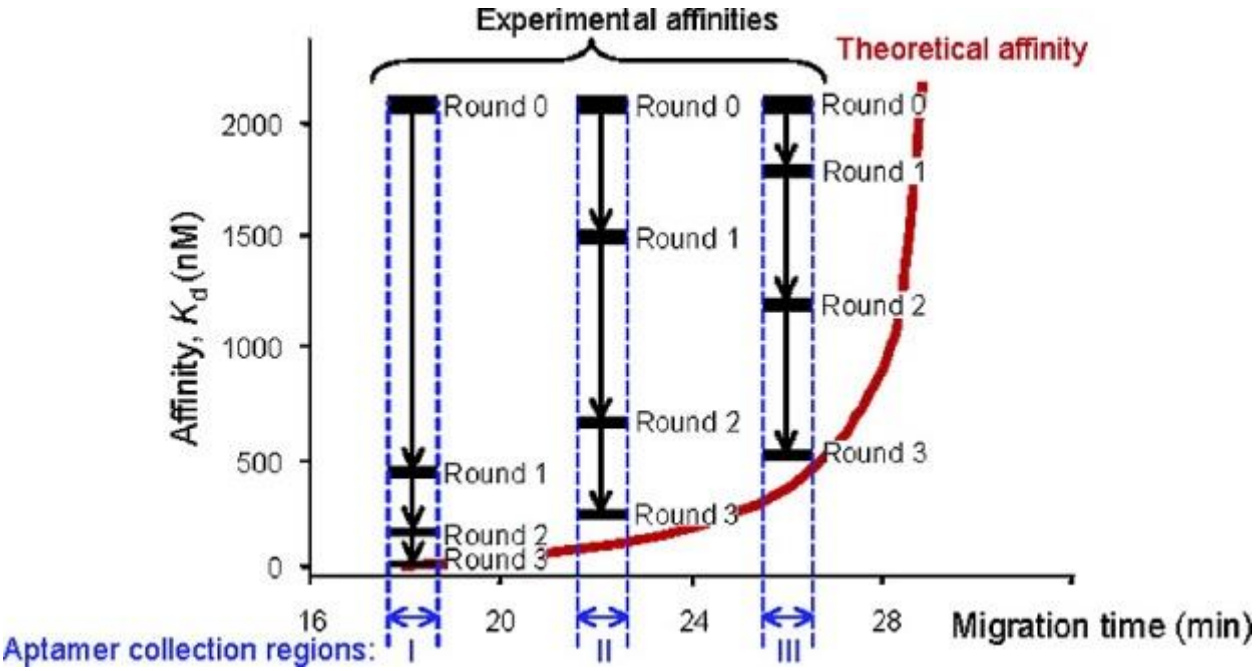

Figure 1.6 A general scheme showing the progression of fractions collected using ECEEM for three rounds of selection at fraction collection points I, II and III. Shorter collection times result in aptamers being collected with typically lower K_D values and subsequent drops in K_D are greater at shorter collection times[81].

Similarly to CE-SELEX, non-SELEX also takes advantage of small injection volumes as well as homogenous separation. The NECEEM method was used to select aptamers that recognize h-RAS protein and farnesyltransferase protein with comparable low micro to nanomolar K_D values reported[78; 80]. ECEEM based non-SELEX was used to select MutS protein[81]. Recently *Tok et al* obtained aptamers that bind to transduction proteins using NECEEM based non-SELEX achieving micro to nano molar K_D values[82].

Due to the fact that both the non-SELEX and CE-SELEX use on capillary detection, the point of elution has to be determined using the **equation 1.1** where *f* is the elution factor, L_{tot} is the total length of the capillary and L_{det} is the length of the capillary from the detection window to the inlet end.

$$f = \frac{L_{tot}}{L_{det}}$$

Equation 1.1 Determination of the elution factor f where L_{tot} is the total length of the capillary and L_{det} is the length of the capillary from the detection window to the inlet end. The elution factor is multiplied by the migration time to get the point of elution.

The elution factor can then be used to correct the elution time by multiplying the elution factor by the migration time of the complex peak. If no complex is observed then the end time of the collection window is used as the migration point.

Despite these promising developments, there are obvious disadvantages associated with both the CE-SELEX and non-SELEX. For both the non-SELEX and CE-SELEX methods, despite the decrease in the number of rounds needed for selection, lengthy buffer optimization prevents the selection from progressing quickly and inducing a stable complex peak is difficult. Due to the small amounts of sample needed for capillary electrophoresis, fewer sequences are screened when compared to conventional methods resulting in lower binding affinities[83]. So far the literature has only reported the use non-SELEX and CE-SELEX on protein targets due to limitations in size and charge, and so these methods have not been demonstrated on small molecules. However, Drabovich *et al* recently developed a proof of concept selection of small molecule ligands from combinatorial libraries against protein targets using kinetic capillary electrophoresis[84]. Protein adsorption onto the capillary surface is a challenging problem, meaning that for proteins with a p*I* >7, coated capillaries and reverse polarity are often required. The non-SELEX method also has physical limitations in the sensitivity of the detector, and after each round of selection there is a reduction in the sensitivity due to the dilution of the analyte.

1.4.2 Determination of binding affinities K_D and specificity

During the selection of aptamers, binding affinities assays can demonstrate the progress of selection. The lower the $K_{D,}$ the more tightly bound the aptamer is to the target. Estimates in the bulk affinity binding can help monitor the selection progress. After cloning, the binding affinity must also be measured for each cloned aptamer sequence to determine how well aptamers bind to the target. A large number of methods have been described in the literature and some of these methods are commonly linked to the partitioning method used for selection of aptamers[85]. Methods can be divided into two main categories. The first contains mixture-based methods which can allow for direct measurement of binding affinities and are a popular choice of methods. Fluorescence is a highly sensitive method which can measure K_D's down to 10^{-10} M and aptamers can easily be tagged with a fluorophore[86]. The use of UV-Vis absorption can measure K_D's to 10^{-6} M, but is not as sensitive as fluorescence based methods[87]. A widely used method for the determination of binding affinity and specificity of aptamers, which can utilize either colorimetric measurement or fluorescence detection, is Enzyme-linked immunosorbent assay (ELISA). This method was used to validate aptamers against anthrax protective antigen, and a sandwich style assay was used to determine the specificity of Hepatitis C virus aptamers[88; 89]. SPR is fast becoming the method of choice for the determination of binding affinity[90]. This is due to the fact that it allows for real time determination of kinetic parameters such as K_D, k_{off} and k_{on} of protein-aptamer interactions. It is also a sensitive method allowing for the measurement of K_D down to 10^{-12} M[91]. Isothermal titration calorimetry is a mixture based method that requires a large number of targets in order to calculate binding affinity and 10^{-9} M K_D's were demonstrated in the literature using the technique[92].

Separation based techniques, as the name suggests, relies on a separation and measurement of the complex peak or free DNA. HPLC was used to measure the K_D of Adenosine aptamers using the aptamer as the stationary phase and K_D's of 10^{-6} M were reported [93]. Dialysis was used to measure K_D's down to 10^{-8} M for the determination of binding affinity of orchatoxin aptamers[94]. Gel electrophoresis which has demonstrated the highest binding affinity range reported of K_D 10^{-13} M was used in the validation of high-mobility group protein B1 aptamers using radio isotope labeling[95]. Nitrocellulose membrane filters again have been used to measure K_D's down to 10^{-12} M using radio isotope labeling[96].

Electrophoretic mobility shift assay (EMSA) is a method which originally was used as qualitative measure of aptamer binding and specificity[97]. Similar to the gel electrophoresis, EMSA can utilize radio isotope labeling to give highly sensitive kinetic measurements[98].

Flow cytometry is often used as a method for the determination of binding affinity of aptamers against whole cells. This method was used to determine the K_D of CD30 expressing lymphoma cells aptamers down to 10^{-10} M K_D[99].

Affinity capillary electrophoresis (ACE) has been used in the study of protein-protein and protein-DNA interactions. A fluorescently labeled aptamer is titrated against increasing concentrations of protein forming the complex. This allows K_D's down to 10^{-9} M to be determined. Differences in electrophoretic mobilities between the complex and the unbound DNA and target cause the intensity of the free aptamer peak to decrease. Assuming no quenching effect, the complex peak can be seen. Using the nonlinear analysis, the K_D can be determined from **equation 1.2** where i_0 is the initial peak height of the aptamer, i is the peak height after addition of the target and [T] is the target concentration**.**

$$\frac{i_0 - i}{i_0} = \frac{constant}{K_D + [T]}$$

Equation 1.2 Determination of K_D using affinity capillary electrophoresis, where i_0 is the initial peak height of the aptamer, i is the peak height after addition of the target and [T] is the target concentration.

This technique was used to determine the binding affinity between IgE and its aptamer as well as in CE-SELEX [71]. A slight variation of this technique was developed by Berezovski and Krylov for the measurement of K_D, k_{off} and k_{on} and is called non equilibrium capillary electrophoresis of equilibrium mixtures (NECEEM)[79; 100]. This method was originally developed as a sensitive affinity protein assay employing aptamer technology. A mixture of aptamer and target protein is allowed to reach equilibrium. A sample of DNA and the target is allowed to reach equilibrium and is injected. The complex, the ligand and target can be separated. The aptamer peak migrates the slowest, the target migrates the fastest, and the complex peak migrates in between. Once the zones of the target, aptamer and complex are separated the complex is no longer in equilibrium and the aptamer and target can dissociate from the complex peak producing tail peaks with monomolecular rate allowing for the k_{off} rate to be calculated. Due to the high separation efficiency of CE, reassociation of the aptamer and target is negligible. The K_D can be determined by comparing the areas of the complex peak and free DNA and calculating using **equation 1.3** where A_1 is the area of the free DNA library, A_2 is the area of the DNA that has dissociated from the complex DNA after t_0 and A_3 is the area of the complex peak. $[T]_{tot}$ is the total concentration of the target and $[DNA]_{tot}$ is the total concentration of the DNA.

$$K_D = \frac{[T]_{tot}\{1+A_1/(A_2+A_3)\}-[DNA]_{tot}}{1+(A_2+A_3)/A_1}$$

Equation 1.3 Determination of K_D using NECEEM where A_1 is the area of the free DNA library, A_2 is the area of the DNA that has dissociated from the complex DNA after t_0, A_3 is the area of the complex peak, $[T]_{tot}$ is the total concentration of the target and $[DNA]_{tot}$ is the total concentration of the DNA.

As mentioned previously, NECEEM allows for the selection of aptamers with a wide range of k_{off} and k_{on} values. NECEEM analysis allows for these parameters to be determined experimentally from **equation 1.4** where tDNA■T is the migration time of the complex peak.

$$k_{off} = \frac{1}{tDNA\blacksquare T} ln\left(\frac{A_2+A_3}{A_3}\right)$$

Equation 1.4 Determination of k_{off} using NECEEM where tDNA■T is the migration time of the complex peak.

For ECEEM based aptamer selection, the measurement of K_D is not possible. Therefore, NECEEM was used as a complimentary technique for aptamer validation.

As well as measuring the binding affinity of aptamers towards the target, the specificity must also be determined. In general, aptamer binding affinity K_D can be measured against targets with similar structures or against the medium in which the target is found. Often K_D can be used as a measure of specificity using the same method as used for measuring the binding affinity of the original target. For example, during the CE-SELEX of IgE protein, the specificity of the aptamer was demonstrated on closely related globulin proteins by comparing the peak height of the DNA peaks[71].

1.5 Objectives and Scope of the dissertation

The focus of this thesis will be on the development of aptamers using capillary electrophoresis. We will initially investigate two different recently proposed methods, namely CE-SELEX and non-SELEX, to develop aptamers. We will look at how these two methods can be improved, what are the limitations that cannot be overcome, and what advantages do these methods have over classical SELEX techniques.

The specific goals of this thesis are:

1. To successfully select aptamers which bind to bovine catalase, hemoglobin, human leptin and cholesterol esterase with high affinity using capillary based methods.
2. To overcome the limitations associated with capillary based selection methods through the development of universal buffer conditions, use of sample stacking and maximizing the number of sequences screened.
3. To demonstrate the compatibility of FAM labelled aptamers with real time-PCR in the amplification of the enriched oligonucleotide libraries without the need for preparative PCR.
4. To demonstrate a fundamental limitation of aptamers selected using immobilization free selection methods in terms of use in applications where immobilization is required.
5. To develop an SPR based aptamer biosensor for the detection of catalase, a bio indicator of mastitis in milk samples.
6. To develop an alternative capillary based method for the selection of aptamers which increases the number of sequences screened.

The general plan of the projects performed in this dissertation is shown in **figure 1.7**

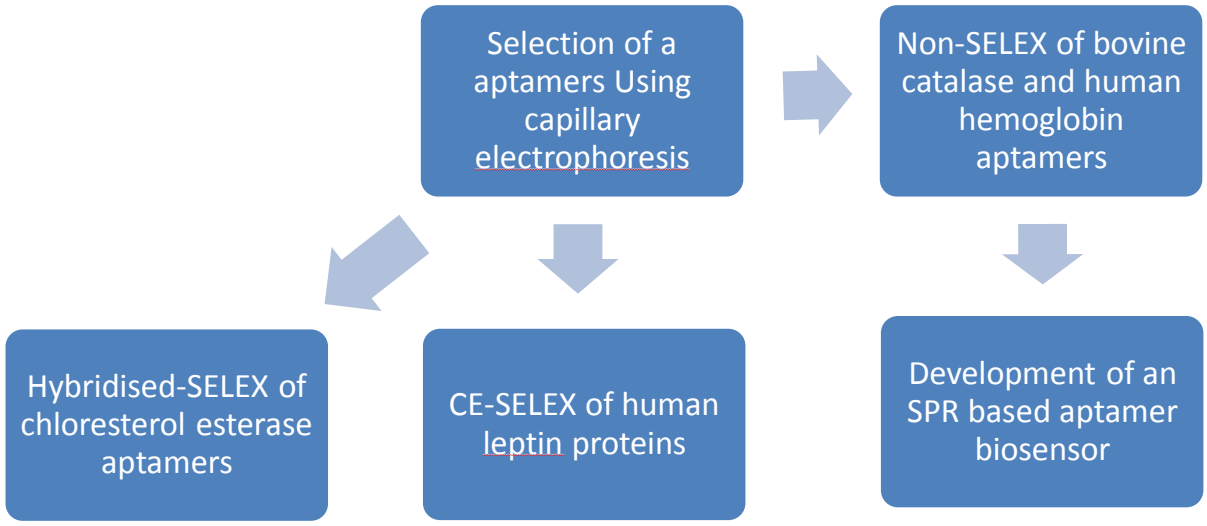

Figure 1.7 A general Scheme of work for the dissertation.

2 Methodology

2.1 Methods and materials

2.1.1 Selection of aptamers using CE-SELEX, Non-SELEX and Hybridised-SELEX

Human leptin protein),(MW: 16 kDa, *pI*: 5.84), catalase (250 kDa, *pI* 5.4), hemoglobin (67KDa, *pI* 6.7) and cholesterol esterase from p*seudomonas* (300 kDa, *pI* 5.95) were purchased from Sigma Aldrich (Singapore) and were dissolved in 25 mM Tris, 192 mM glycine, 5mM potassium phosphate buffer pH 8.3 (1xTGK) [101]. Random libraries of oligonucleotides were bought from 1st Base (Singapore) and contained the sequence 5'-FAM-CTT CTG CCC GCC TCC TTC C-(40N)-GGAGAC GAG ATAGGC GGA CAC T-3', with a fluorescein (FAM) fluorophore. N represents the 40 random DNA base groups. The Reverse-Primer (R-Primer) and Forward-Primer (F-Primer) were purchased from 1st Base and contained the sequence 5'-CTT CTG CCC GCC TCC TTC C-3' and 5'-AGT GTC CGC CTA TCT CGT CTC C-3' respectively for cloning and sequencing. A biotin tagged R-primer and a FAM tagged F primer were also purchased from 1st Base of the same sequences as the unlabeled primers. Capillaries with 50, 75 and 100 μm internal diameter (IDs) and with a total length of 60 cm and effective length of 50 cm were used for the partitioning step and NECEEM analysis for each aptamer selection. Nitro cellulose membrane filters and Lok syringe filter holders were purchased from Millipore-Merck (Billerica**,** MA) and used in the selection of cholesterol esterase aptamers. For the selection of leptin aptamers, an SsoAdvanced™ SYBR green mix was used to amplify the collected fractions (BioRad, Hercules CA, USA). For the selection of catalase, hemoglobin and cholesterol esterase aptamers, a preparative PCR was performed to amplify the collected fractions. PCR reagents

were bought from Fermantas (Singapore) and contained, taq polymerase, dNTP, PCR reaction buffer, $MgCl_2$, and nuclease-free water. All strand separation steps were carried out using Piece streptavidin high capacity agarose beads (Rockford, IL, USA) in a polyprep column (Biorad, Singapore), binding buffer, 0.15 M NaOH, and 0.15 M acetic acid. A 3 M sodium acetate, ice cold ethanol, and a 70:30 ethanol:water mixture were used for DNA precipitation. All buffers were filtered using a 45-μm filter and degassed using a sonicator.

2.1.2 Development of an aptamer based SPR biosensor

For the development of the aptamer based SPR biosensor, casein, β lactoglobulin A and bovine albumin proteins were purchased from Sigma Aldrich (Singapore) and dissolved in 10mM HEPES, 100mM KCl, 1mM EDTA and 0.5% BSA buffer, pH 7.4 (HKE-BSA). Standardised milk samples were purchased from a local supplier (Meiji, Singapore). For the formation of the self-assembly monolayer (SAM), 11-Mercaptoundecanoic acid (11-MUA) and 2-mercaptoethanol (2-ME) were purchased from (Sigma Aldrich, Singapore) and dissolved in absolute ethanol. N-hydroxysuccinimide and ethyl 1-Ethyl-3-(dimethylaminopropyl) carbodiimide were also purchased from Sigma Aldrich (Singapore) and dissolved in water. Streptavidin was purchased from Merck Chemicals (Singapore) and dissolved in 20 mM sodium acetate buffer pH 5.0. Biotinylated aptamer ligand of sequence CTTCTG CCC GCC TCC TTC CGACCTAG CAGTGGACA TGTGGCAGGGTG AAGTGGCA TCGTCGGAGAC GAG ATAGGC GGA CAC T/ 3'biotin was purchased from (1st Base, Singapore) and reconstituted in 10 mM HEPES, 100 mM KCl, 1mM EDTA, pH 7.4 (HKE) buffer. Aptamers were renatured using a DNA engine thermocycler (Bio-Rad, Singapore) by heating to 94 °C for 10 minutes and then cooling down at rate of 0.5 °C / second to room temperature. SIA AU kits containing bare gold chips were purchased from Biacore (Sweden). Bare gold sensor chips were also purchased

for the SensiQ (SensiQ Technologies, Inc, Okaholma, US). For all experiments, the machine was purged with run buffer. In the immobilization of streptavidin, the flow buffer was 20 mM sodium acetate buffer pH 5.0 and the flow rate was set to 5 µl/min. Prior to the aptamer ligand immobilization, the flow buffer was changed to HKE buffer pH 7.4 at a flow rate of 5 µl/min. For the optimization, catalase assay and real milk analysis a flow buffer of HKE:BSA buffer was used and the flow rate was set to 10 µl/min. All buffers were degassed by Sonication prior to analysis.

All capillary electrophoresis experiments were performed on a PA 800 plus Beckman CE instrument (Mississauga, ON, Canada). Using PDA UV-vis absorbance detection set at 214, 260, 280 nm and LIF detection at an excitation wavelength of 488 nm and an emission wavelength of 520 nm.

The determination of the sample collection window and optimization of buffer conditions were carried out using capillary electrophoresi for all aptamer selections. Capillaries were conditioned by pressure flushing at 20 psi (137.9 kPa) for 5 minutes with 0.1 M HCl, 1M NaOH, deionized water, and finally; 8.3 pH 75mM Tris, 576 mM glycine and 15 mM potassium phosphate (3x TGK) run buffer. This was followed by application of 333 Vcm^{-1} for 30 minutes.

DNA plasmid cloning was performed for all aptamer selections. A PCR reaction containing taq polymerase (0.05 U/ml), unlabeled forward primer (0.5 µM), unlabeled reverse primer (0.5 µM), nuclease free water and the enriched library DNA (10 µl) were mixed and a 3 step cycle was used to amplify the reaction. A TA overhang was introduced by preparing a mixture of taq polymerase 1 U/µl, adenosine triphosphate (0.5 µM) and the DNA sample. The mixture was heated to 70^{o}C for 20 minutes and quickly inserted into the Qiagen plasmid insert. The sample was transformed into competent E.coli cells and grown over night onto LB Agar plates. Colonies

were chosen using white blue screening and transferred to SOC medium and incubated for less than 16 hours. The colonies were sequenced to determine the structure.

2.2 The CE-SELEX procedure for leptin aptamers

The leptin protein solution was diluted to 1 μM. The naïve DNA library was folded with a Bio-Rad DNA engine thermocycler by heating the DNA to 94 °C and cooling down to 20 °C at a rate of 0.5 °C per second and diluted to a final concentration of 0.1 μM. A solution containing DNA only (0.1 μM) was injected using hydrodynamic injection (411 nl) and separated at 333 V cm^{-1} with LIF detection. A solution containing protein only (1 μM) was subsequently injected by hydrodynamic injection (411 nl) and separated at 333 V cm^{-1} with PDA detection at 214 and 280 nm wavelengths. The migration times of the unbound DNA and complex peaks were noted. The equilibrium mixture containing the DNA library (0.1 μM) and leptin protein (1 μM) was incubated for 30 min before being injected by hydrodynamic injection (411 nl) and separated at 333 V cm^{-1} using LIF detection (of 488 nm emission wavelength of 520 nm excitation wavelength). The migration times of the unbound DNA and complex peaks were noted, and the time between the protein peak and the free DNA peak was determined to be the time collection window.

The procedure for the fraction collection is based on that reported by Mosing and coworkers [73]. The initial round of selection was done by incubating the DNA (10 μM) with leptin protein (1 μM) for 30 min to allow the mixture to reach equilibrium. The equilibrium mixture was then injected by hydrodynamic injection (411 nl) and separated using 333 Vcm^{-1} with PDA detection at 254nm and 280nm. Fractions were collected into an outlet vial containing 5 μl of 3x TGK and

the corrected elution time was used to determine the fraction collection end point and was calculated from **equation 1.1**. A total of 3 injections for each round of selection were performed and DNA was collected into the same outlet vial for each round. The fractions collected from the first round were then amplified using real time-PCR. All amplification steps were performed on a CFX96™ Real-time PCR detection system (BioRad, Hercules CA, USA). One stock solution containing Ssoadvanced master mix (1x), FAM labeled forward primer (0.5 μM), biotin reverse primer (0.5 μM) and nuclease free water was prepared and split into 8 separate vials containing the template DNA and 1 vial containing the negative control. A three step cycle was used with annealing at 94 ^{o}C for 20 seconds, and an annealing temperature of 65 ℃ (-1 ℃ per cycle to 54 ℃) for 20 seconds, and an extension temperature of 72 ℃ for 20 seconds. The number of cycles was optimized by amplification graph. The specificity and the extent of amplification were checked by melting curve analysis. In order to account for interference from fluorescein the negative control was subtracted from the baseline signal.

The single stranded oligonucleotides were regenerated by using agarose streptavidin beads and weak base denaturing. The oligonucleotides were then purified by DNA ethanol precipitation. The oligonucleotides were then reconstituted in 1 x TGK (30 μl), assayed for purity and concentration on a Nanodrop spectrometer (Thermo Scientific, Wilmington, DE, USA). The DNA was then incubated with the protein and the selection was repeated. A total of 4 rounds of selection were performed and the progress of selection was monitored using NECEEM. For each round of selection, the stringency of selection was increased by decreasing the target protein concentration from 1 μM down to 100 nM and details of the selection are shown in **table 2.1**. The enriched library from round 4 was chosen for cloning and sequencing.

2.2.1 Validation of leptin clone sequences

Aptamer clone sequences were verified against leptin protein by NECEEM and fluorescence intensity methods. The NECEEM method employed the same conditions as described for the bulk affinity analysis. Each aptamer clone sequence (0.1 μM), was incubated with leptin protein (0.5 μM) and fluorescein internal standard (0.1 μM), before being injected by hydrodynamic injection (411 nl) and separated at 333 V cm^{-1} using LIF detection. The K_D binding affinity was calculated from the normalized areas of the free DNA, complex peak, and dissociated DNA. Three replicate samples were measured. For the fluorescence intensity method, the protein was immobilized onto a 96-well microplate (0.5 μg/well) in 25 mM 1 x TGK buffer (90 μl). The plate was incubated with shaking for 1 h at room temperature. The plate was then washed three times with Tris-buffered saline and Tween buffer (pH 8.4) containing 0.5 M Tris, 50 mM sodium chloride, and 0.5% Tween 20 (TBST, 90 μl), and the wells were blocked by incubating with 5% bovine serum albumin (BSA, 90 μl) for 1 h. The plate was then washed with 90 μl of TBST three times to remove non-bound BSA, and each well was incubated with a different concentration of aptamer (0–5000 nM) for 1 h with shaking at room temperature. The plate was then washed with 1 x TGK buffer three times to remove excess DNA, and the aptamer/leptin complex was placed in 90 μl of 1 x TGK buffer. A well containing 5% BSA and aptamer at 5000 nM without leptin was used as the negative control. All fluorescence intensity experiments were measured using BioTek Synergy 4 microplate reader (Singapore) with an excitation wavelength of 488 nm and an emission wavelength of 520 nm. All measurements were performed on the surface of the plate using and the baseline negative control was subtracted from the signal. A saturation graph of relative fluorescence intensity against the aptamer concentration was plotted, and nonlinear regression was used to calculate the binding affinity K_D.

The specificity of the aptamers was tested using a NECEEM based method. Here, Lep 3 aptamer (0.1 μM) was incubated with β-lactoglobulin (1 μM) and bovine catalase (1 μM) separately for 30 min before being injected by hydrodynamic injection (411 nl) and separated at 333 V cm^{-1} using LIF detection.

2.3 The Non-SELEX of catalase and hemoglobin aptamers

2.3.1 Optimization of the Non-SELEX procedure

All capillary electrophoresis experiments were performed on a Beckman PA800 plus capillary electrophoresis system (Mississauga, ON, Canada) with photodiode array (PDA) detection at 215 nm and 280 nm for the detection of the target and laser-induced fluorescence (LIF) detection at an excitation/emission wavelength of 488 nm and 520 nm for the detection of FAM-labeled DNA.

The the time collection window was determined for both proteins using the same conditions. 1 μM of the random DNA library was prepared in the selection buffer and denatured on an Eppendorf master thermocycler (Hamburg, Germany) at 94℃ for 10 min and cooled at 0.5 ℃/s to 20℃. 10 μM of catalase protein and hemoglobin where dissolved in the selection buffer separately. An equilibrium mixture was prepared by incubating 100 nM of the folded DNA with 2 μM of each protein for 30 min. The folded 100 nM DNA, 2 μM catalase, 2 μM hemoglobin and the two equilibrium mixtures were injected separately at 1 psi for 13 s and run on the capillary electrophoresis at 333 Vcm^{-1} to determine the migration times of the DNA library, the

protein peaks, and the complex peaks. The buffer conditions and protein concentrations were optimized to give the most stable complex peak.

2.3.2 The Non-SELEX procedure for bovine catalase aptamers

For the partitioning step in the selection of aptamers for catalase, manual fraction collection was used. In the first round of selection, the incubated mixture containing 50 μM of folded DNA and 10 μM of each protein was injected onto the capillary using the same conditions employed for the time window determination with the exception that the outlet vial contained 30 μL of 1 μM catalase and the complex peak was collected. This vial was allowed to reach equilibrium for 30min and then reinjected onto the capillary for the second round of selection and collected into another vial containing 30 μL of 0.1 μM of catalase repeated two more times. The collection end point was determined for each round from the elution factor which was calculated from **equation 1.1**. The free DNA was flushed to the waste using high pressure[78; 80]. All PCR experiments and ssDNA folding steps were performed on an Eppendorf master thermocycler (Hamburg, Germany). A touchdown program was used for the thermocycler using an initial denaturing step of 94℃ for 3 min. The 10–30 subsequent cycles consisted of a denaturing step of 94℃ for 20 s, an annealing step of 65℃ for 20 s with a −1℃ increment for each cycle to 55℃ for 20 s, and an extension step of 72℃ for 20 s. This was followed by a final extension step of 1 min. The PCR products were analyzed on a 2% agarose low Melting gel and the number of PCR cycles was optimized to give the best possible PCR yield. 1 μl of loading buffer was mixed with 6 μl of each sample and loaded on to the gel. The gel was run in 1x TAE buffer at 100 V. The gel was visualized using ethinum bromide dye and a Biorad gel reader.

The dsDNA PCR product was converted into ssDNA by agarose streptavidin column and base denaturing. The resultant ssDNA was recovered using sodium acetate ethanol precipitation and the pellet was lyophilized using a Christ freeze dryer (Martin Christ Gefriertrocknungsanlagen GmbH, Asterods, Germany).

2.3.3 Bulk affinity determination by NECEEM and validation of catalase aptamer clone sequences

The enriched libraries from each round of selection were resuspended in 30 μL of TGK and the concentration of the DNA was measured using a Thermo Scientific Nanodrop 1000 spectrometer (Massachusetts, USA). The bulk affinity of each enriched library was determined by incubating 100 nM of the folded DNA with 1 μM of catalase. The sample was injected into the capillary at 1 psi for 13 s and run at 333 Vcm^{-1}. The NECEEM equation from **equation 1.2** was used to estimate the bulk affinity K_D of the enriched library and a decrease in K_D showed that the selection was proceeding.

The enriched library from the 2nd round of selection was amplified using non labeled primers and analyzed on a 2% agarose gel with a negative control and a 100bp ladder. An adenosine overhang was added to the sequence and ligated into a pDrive cloning vector and introduced into Qiagen EZ competent cells by heat shock. The cells were then plated onto a petri dish and incubated overnight. The colonies that turned white were selected for sequencing and the plasmid DNA was purified and sequenced using single pass sequencing (1st Base, Singapore). The validation of the full structure of individual clone sequences was performed using both NECEEM and fluorescence intensity assays. The affinity of the aptamer was also determined using NECEEM. A total of 100 nM aptamer was incubated with 4 μM catalase and FAM internal

standard for 1 h and injected at 1 psi for 13 s on to a capillary. A voltage of 333 Vcm^{-1} was applied and the K_D was determined using NECEEM analysis.

For the fluorescence intensity method, the catalase protein was immobilized onto a 96-well microplate (0.5 µg / well) in 25 mM 1 x TGK buffer (90 µl). The plate was incubated with shaking for 1 h at room temperature. The plate was then washed three times with Tris-buffered saline and Tween buffer (pH 8.4) containing 0.5 M Tris, 50 mM sodium chloride, and 0.5% Tween 20 (TBST, 90 µl), and the wells were blocked by incubating with 5 % bovine serum albumin (BSA, 90 µl) for 1 h. The plate was then washed with 90 µl of TBST three times to remove non-bound BSA, and each well was incubated with a different concentration of aptamer (0–5000 nM) for 1 h with shaking at room temperature. The plate was then washed with 1 x TGK buffer three times to remove excess aptamer and the aptamer/catalase complex was placed in 90 µl of 1 x TGK buffer. A well containing 5 % BSA and aptamer at 5000 nM without immobilized catalase was used as the negative control. All fluorescence intensity experiments were measured using a BioTek Synergy 4 microplate reader (Singapore) with an excitation wavelength of 488 nm and an emission wavelength of 520 nm. All measurements were performed on the surface of the plate and the negative control signal was subtracted from each signal. A saturation graph of relative fluorescence intensity against the aptamer concentration was plotted, and nonlinear regression was used to calculate the binding affinity K_D[88].

The specificity of the aptamer was tested using a similar technique as described above. Four proteins, i.e. lysozyme, trypsinogen, chymotrypsinogen A, and myoglobin, were immobilized onto a 96-well plate (0.5 µg/well) in 25 mM 1 x TGK buffer (90 µl) and incubated for 1 hour. The plates were then washed with 100 µL TBST five times and 100 µL of 5% BSA solution was added to block the remaining sites in the well. Each well was then incubated with a different

concentration of aptamer for 1 h with shaking. The excess ssDNA was removed by washing with 1x TGK. The fluorescence was measured after each wash until the signal stayed relatively constant. The fluorescence was plotted against the ssDNA concentration using a saturation graph and the K_D and its standard deviation were estimated.

2.3.4 The Non-SELEX procedure for hemoglobin aptamers

For hemoglobin aptamers, manual fraction collections were performed using the same procedure as described for catalase. An equilibrium mixture, containing 25 µM DNA library and 14.9 µM hemoglobin was injected onto the capillary by a 13 s, 1 psi hydrodynamic injection, followed by separation at 333Vcm^{-1}. Bound DNA was collected into a vial containing 30 µl of 1 µM of hemoglobin in TGK buffer. The collection end point was determined to be the point just before the unbound DNA was detected. The elution time was calculated using the same method described for the catalase. The contents of the outlet vial were re-injected using the same conditions mentioned and the fraction collection was repeated using a vial containing 0.1 µM of hemoglobin. A total of 1 round was performed and a total of 3 collections were performed for each round. The capillaries were rinsed after each injection to prevent contamination of the fractions.

2.3.5 Bulk affinity analysis using ACE and validation of hemoglobin clone sequences

The enriched libraries from each round of selection were resuspended in 30 µL of TGK and the concentration of the DNA was measured using a Thermo Scientific Nanodrop 1000 spectrometer (Massachusetts, USA). The bulk affinity of each enriched library was determined by incubating 10 nM of the folded DNA library with hemoglobin (0-1000 nM) for 1 hour. The samples were injected into the capillary at 0.5 psi for 5 s and run at 333 Vcm^{-1}. The peak heights were

measured for the free DNA peak and the bulk affinity was determined by plotting a linear graph of fraction of bound DNA against the protein concentration. The enriched library from the 1st round of selection was amplified using non labeled primers and analyzed on a 2 % agarose gel. An adenosine overhang was added to the sequence and ligated into a pDrive cloning vector and introduced into Qiagen EZ competent cells by heat shock. The cells were then plated onto a petri dish and incubated overnight. The colonies that turned white were selected for sequencing and the plasmid DNA was purified and sequenced using single pass sequencing (1st Base, Singapore).

The K_D of the full individual aptamer clone structures were determined by affinity capillary electrophoresis. Samples of aptamer (10 nM) were titrated with different concentrations of hemoglobin (0-1000 nM) and fluorescein internal standard (10 nM) and incubated for 1h followed by injection at 0.5 psi for 5 s on to a capillary. A voltage of 333 Vcm^{-1} was applied. The peak height of the free DNA was measured and the K_D was determined by plotting a non-linear regression saturation plot of the ratio of bound DNA against the protein concentration. The specificity of hemoglobin aptamers was tested by CE using the same conditions as described for the affinity CE method. The aptamer clone sequences were incubated for 1 h with different proteins and injected at 1 psi for 13 s on to a capillary. A voltage of 333 Vcm^{-1} was applied and the K_D was estimated from the peak heights of the unbound aptamer.

2.4 Hybridised-SELEX Procedure

All capillary electrophoresis experiments were performed on a Beckman PA800 plus capillary electrophoresis system (Mississauga, ON, Canada) with photodiode array (PDA) detection at 215 nm and 280 nm for the detection of the target and laser-induced fluorescence (LIF) detection at an excitation wavelength of 488 nm and emission wavelength of 520 nm for the detection of FAM-labeled DNA

The time window for selection of aptamers using CE was determined by injection of solutions of the DNA library and protein separately. For the DNA library 0.1 µM was injected by hydrodynamic injection (51.46 nl) and separated (500 Vcm^{-1}) with LIF detection at 488nm excitation and 520 nm emission wavelength. For the target, 20 µM was injected using hydrodynamic injection (51.46 nl) and separated (500 Vcm^{-1}) with PDA detection at 280 nm. An equilibrium mixture containing 0.1 µM DNA library and the 20 µM target was also injected by hydrodynamic injection (51.46 nl) and separated (500 Vcm^{-1}) with LIF detection at 488 nm excitation and 520 nm emission wavelength.

For the NC round of selection, a NC membrane filter was washed with TGK buffer and an incubated mixture of DNA library (50 µM) and protein target (20 µM) was added onto the filter and incubated again for 30 minutes. The filter was then washed several times using 10 x 1 ml tris-buffered saline, Tween 20 buffer (TBST) containing 0.5 M Tris, 50 mM NaCl, and 0.5% tween solution at pH 8.4 to remove unbound DNA sequences. The bound DNA sequences were eluted by incubating the membrane in 1 ml of 7 M urea solution with shaking. The DNA was then purified using an isopropanol precipitation and resuspended in water. For subsequent rounds of selection, the DNA library was incubated with additional target protein (1 µM) and

injected hydro dynamically, followed by separation (500 Vcm^{-1}) using LIF detection. Fractions were collected into a micro vial containing 5 µl of run buffer and protein (0.5 µM) and the end point of detection was determined by the elution time of the complex peak and corrected to take into account time it takes for the complex peak to travel from the detector to the end of the capillary. The collection end point was calculated for each round using the elution factor as described previously in order to determine when the complex peak was eluted at the end of the capillary. The outlet vial containing the DNA and target was then re-injected using the same conditions. The partitioning step for each round of selection was repeated 3 times. The fractions from round NC, 1 and 2 were then amplified using PCR. All PCR experiments and ssDNA folding steps were performed on an Eppendorf Master thermocycler (Hamburg, Germany). A touchdown program was used for the thermocycler using an initial denaturing step of 94 ℃ for 3 min. The 10–30 subsequent cycles consisted of a denaturing step of 94 ℃ for 20 s, an annealing step of 65 ℃ for 20 s with a −1℃ increment for each cycle to 55 ℃ for 20 s, and an extension step of 72 ℃ for 20 s. This was followed by a final extension step of 1 min. The PCR products were analyzed on a 2% agarose low Melting gel and the number of PCR cycles was optimized to give the best possible PCR yield. 1 µl of loading buffer was mixed with 6 µl of each sample and loaded on to the gel. The gel was run in 1x TAE buffer at 100 V. The gel was visualized using ethinum bromide dye and a Biorad gel reader. The number of PCR cycles was optimized to give the best possible PCR yield.

2.4.1 Bulk affinity determination by NECEEM and validation of cholesterol esterase aptamer clone sequences

The bulk affinity of the initial DNA library, the NC round and round 1 and 2 of non-SELEX was determined by incubating the target (0.5 μM) with the DNA library (0.1 μM) for at least 30 minutes followed by hydrodynamic injection and separation at 500 Vcm^{-1} using LIF detection. The bulk affinity was determined using NECEEM analysis. The strands of the dsDNA PCR product were separated by an agarose streptavidin column and base denaturing. The resultant ssDNA was purified by ethanol precipitation and the pellet was lyophilized using a Christ freeze dryer (Martin Christ Gefriertrocknungsanlagen GmbH, Asterods, Germany).

The enriched libraries from each round of selection were resuspended in 10 μL of water and the concentration of the DNA was measured using a Thermo Scientific Nanodrop 1000 spectrometer (Massachusetts, USA). The bulk affinity of each enriched library was determined by incubating 100 nM of the folded DNA with cholesterol esterase (1 - 0.1 μM). The sample was injected into the capillary at 0.5 psi for 5 seconds (9.90 nl) and separated at 500 Vcm^{-1}. The NECEEM equation was used to estimate the bulk affinity K_D of the enriched library and a decrease in K_D showed that the selection was proceeding [79].

The enriched library from the 2nd round of selection was amplified using non labeled primers and analyzed on a 2% agarose gel. An adenosine overhang was added to the sequence and ligated into a pDrive cloning vector and introduced into Qiagen EZ competent cells by heat shock. The cells were then plated onto a petri dish and incubated overnight. The colonies that turned white were selected for sequencing and the plasmid DNA was purified and the sequence was determined using single pass sequencing (1st Base, Singapore).

The binding affinity K_D of the full aptamer clone sequences (CES 1-6) was determined using NECEEM. 0.2 µM of aptamer was incubated with 0.2 µM cholesterol esterase and 0.1µM FAM internal standard for 1 h and (0.5 psi for 5 seconds, 9.90 nl) was injected on to a capillary and separated (500 Vcm^{-1}). The binding affinity of the truncated aptamer clones (CES 3T and CES 4T) were also determined using NECEEM employing the same conditions used for the full structures. A fluorescence polarization experiment was performed to reconfirm the binding affinity of CES 4T using a BioTek Synergy 4 microplate reader (Singapore) with an excitation wavelength of 488 nm and an emission wavelength of 520 nm. All measurements were performed in solution. 50 µl of aptamer (10 nM) was incubated with 50 µl target (0.1-20000 nM) for 1 hour. A sample containing aptamer (10nM) only was used as the reference. The anisotropy was measured using a 485/588nm filter and the auto focus was set so that both the perpendicular and parallel intensities were over 10000. The anisotropy was calculated from the two intensity measurements and corrected using the aptamer only reference. A dose dependent graph of anisotropy against the log cholesterol esterase concentration was plotted and the binding affinity was calculated from the graph.

The specificity of CES 4T was tested by NECEEM. Using similar conditions as described for determining the affinity, 100 nM of aptamer was incubated with 1 µM of α glycol acid protein, amylose glycosylase, trypsin inhibitor and bovine catalase. The equilibrium mixtures were injected (9.90 nl each) and separated at 500 Vcm^{-1}. The K_D was determined by NECEEM.

2.5 Development of aptamer based SPR biosensor

For the development of the assay, a SensiQ discovery SPR machine (SensiQ Technologies, Inc, Okaholma, US) was used for the development and optimization of the method. The DNA

sequences were denatured and folded on a Bio Rad thermocycler. All real sample analysis was carried out on the BIAcore T3000 SPR machine (Sweden).

2.5.1 Preparation of the chip surface and optimization of the sensor

Preparation of chips sensors – SensiQ

A SensiQ discovery chip was docked in the machine and the signal was normalized. Absolute ethanol was degassed and pumped through the SPR machine at a flow rate of 5 µl/min through channels1 and 2. A solution containing 1mM 11-MUA and 6 mM 2-ME was dissolved in ethanol and 50 µl was injected onto the SPR sensor. The flow rate was stopped half way through the injection and all tubes were sealed to prevent air entering the system. The mixed thiol alkane SAM was left to react for 24 hours. The chip was then purged with ethanol followed by water and finally 20 mM sodium acetate buffer pH 5.0. The flow rate was then set to 5 µl/min and left until a stable baseline was achieved.

A solution of 0.1 M NHS and 0.4 M EDC was mixed (1:1) and 50 µl was injected onto both channels to activate the carboxylic acid groups on the 11-MUA. 50 µl of avidin and streptavidin (50 µg / ml) was then injected on separate chips on channels 1 and 2. The remaining unreacted ester groups were blocked by injecting 50 µl of 1M ethanol amine. The flow buffer was then changed to HKE buffer and the flow rate was set to 10 µl / min. 50 µl of 10 µM biotin tagged DNA was injected and captured onto the surface of channel 2 only.

Preparation of chips sensors - BIAcore

A gold slide was submerged in a solution containing 11-MUA 1mM and 6-ME 4mM in absolute ethanol for 24 hours. The slide was then rinsed with water and ethanol and dried by nitrogen. The gold slide is then inserted into the chip and docked into the machine. Sodium acetate buffer was flowed through the machine with a flow rate of 5 µl/min. A solution of 0.1 M NHS and 0.4 M EDC was mixed (1:1) and 50 µl was injected onto both channel 1 and 2 to activate the carboxylic acid groups on the 11-MUA. 50 µl of streptavidin 50 µg/ml was injected onto the sensor for all channels. The remaining unreacted ester groups were blocked using 50 µl of 1 M ethanol amine. The flow buffer was then changed to HKE buffer and the flow rate was set to 10 µl / min. 50 µl of 10 µM biotin tagged DNA was injected and captured onto the surface of channel 2 only.

2.5.2 Optimization of the catalase biosensor

Optimization of catalase biosensor- SensiQ

For avidin based chips, the system was purged with, HKE, 0.5% BSA buffer. For each cycle, the flow rate was set to 10 µl/min and injection of 50 µl of catalase (0.01- 4 µM) in HKE after 180s. After the endpoint of each injection of catalase, a dissociation time of 360s was applied and this was followed by injection of 50 µl of 0.1 M NaOH, 45 mM glycine in 5 % ethanol regeneration buffer. A further wait time of 180 seconds was applied after each injection to allow the baseline to stabilize. A calibration curve was plotted and the limit of detection LOD and linear range were determined. For the Streptavidin chip, samples of catalase (0.01- 4 µM) were injected onto the sensor. The surface of the sensor was then regenerated by injecting a solution of 0.1 M

NaOH, 45 mM glycine in 1.2 % ethanol (regeneration buffer). A calibration plot was made using linear regression and the limit of detection (LOD) was determined by measuring the standard deviation of three blank samples.

Optimization of catalase biosensor - BIAcore

For the BIAcore system the streptavidin based system was used. The BIAcore system was purged with HKE-BSA buffer. For each cycle the flow rate was set to 10 µl/min and injection of 50 µl of catalase (10- 1000 nM) in HKE-BSA after 180 seconds. After the endpoint of each injection of catalase, a dissociation time of 360 seconds was applied, followed by injection of 50 µl of 0.1M NaOH, 45mM glycine in 5% ethanol regeneration buffer. A further wait time of 180 seconds was applied after each injection to allow the baseline to stabilize. A calibration plot was made using linear regression and the limit of detection (LOD) was determined by measuring the standard deviation of three blank samples. Assays were performed in triplicate. The specificity was measured by injecting 1 µM of each protein (50 µl) and measuring the response using the same conditions employed for the catalase assay.

The specificity of the immobilized aptamer was determined by measuring the response of the sensor towards different milk proteins. 50 µl of 1 µM catalase, 54 µM β-lactoglobulin, 52 µM bovine casein and 15 µM bovine albumin was injected and the relative response was measured followed by a dissociation time of 360 seconds. The 50 µl of regeneration buffer was used to regenerate the surface followed by a wait time of 180 seconds to allow the baseline to stabilize.

2.5.3 Real sample analysis

The BIAcore T3000 system was purged with HKE:BSA buffer. Milk samples were prepared by spiking with different concentrations of catalase (67.7- 1000 nM). Spiked samples were centrifuged and the supernatant was transferred to a new vial and filtered through a 0.45 µm filter. For each cycle the flow rate was again set to 10 µl/min and injection of 50 µl of each sample after 180 seconds. After each injection of catalase, a dissociation time of 360 seconds was applied followed by injection of 50 µl of regeneration buffer. A further wait time of 180 seconds was applied after each injection to allow the baseline to stabilize. The response plots were normalized using a milk only negative control. A calibration plot was constructed by measuring the difference in response after injection at 480 seconds. A plot of relative response units against time was plotted and the sample percentage recoveries of the each sample were determined.

3 CE-SELEX of leptin aptamers and Implications for clone validation

3.1 Aim

For the first part of this thesis, an investigation into post SELEX modifications was conducted.

Proteins make up the largest group of targets for SELEX and to date well over 100 targets have been screened. From a scan of possible targets using various resources such as the aptamer database, we found that an DNA aptamer for human leptin had not been developed and as such we decided to use this as our target for the study[102; 103].

In this chapter, we describe the use of CE-SELEX to select aptamer sequences of high binding affinity against human leptin protein using buffer conditions that promote the stacking effect allowing for an improvement in the sensitivity of the complex peak (see chapter 4) and demonstrate the use of real time PCR on the amplification of FAM labelled DNA without the need for a preparative PCR step. We also report the apparent differences in K_D measurements using two different techniques, namely non equilibrium capillary electrophoresis of equilibrium mixtures (NECEEM) and fluorescence intensity[88; 104].

Leptin is a relatively small acidic protein (16 kDa MW) which plays an important role in the regulation of appetite and metabolism and the structure is shown in **figure 3.1**[105; 106].

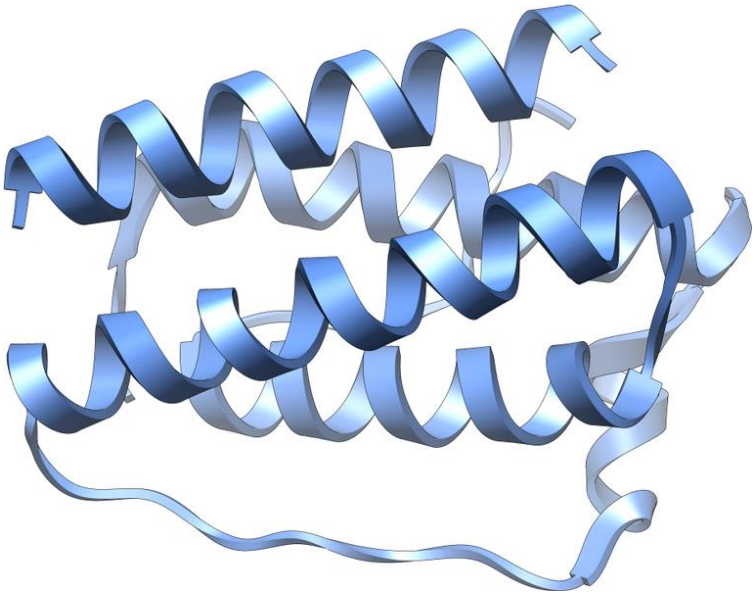

Figure 3.1 The structure of human leptin generated from the PDB[107].

Leptin acts as a signal molecule which limits the intake of food and increases energy used.

The protein interacts with receptors in the hypothalamus part of the brain and controls appetite by promoting the synthesis of the appetite suppressant α-melanocyte-stimulating hormone, inhibiting tetrahydrocannabinol and regulating neuropeptide Y^{106}. An aptamer developed against human leptin could be used to investigate leptin's role as an inflammatory marker and its mechanism. Leptin protein is made by the adipocytes in white adipose tissue (fat cells) and in the placenta of Brown adipose tissue. The degree of expression of leptin depends on the amount of body fat.

3.2 Results and Discussion

3.2.1 The CE-SELEX procedure for leptin aptamers

In order to separate aptamers that bind to the target, the buffer conditions had to be optimized to allow for the largest number of sequences to be screened, while maintaining a suitable resolution and sensitivity of the peaks. For this study, a selection buffer of 1x TGK was used to dissolve both the target and DNA library, and 3x TGK was used as a run buffer. From our preliminary studies, we observed a stacking effect due to the difference in ionic strength of the run and selection buffer which increased the sensitivity of the complex peak. The conditions were generally kept the same as for the non-SELEX (see chapter 3). The internal diameter was kept at 100 µm and the total length and effective length of the capillary were kept at 60 and 50 cm respectively.

The first part of the selection involved determining the time collection window of the protein and DNA. This would give us an idea of when the complex peak would elute and allow us to determine the elution time of the complex peak. It also allows us to check the protein for impurities. The time window is shown in **figure 3.2.** We can see that the protein migrates first at about 5.3 minutes and has an absorbance max at 280 nm. The DNA peak is also observed at around 15 minutes with an absorbance max at 254 nm. The DNA is more negatively charged than the protein which is seen by the fact that the DNA migrates last.

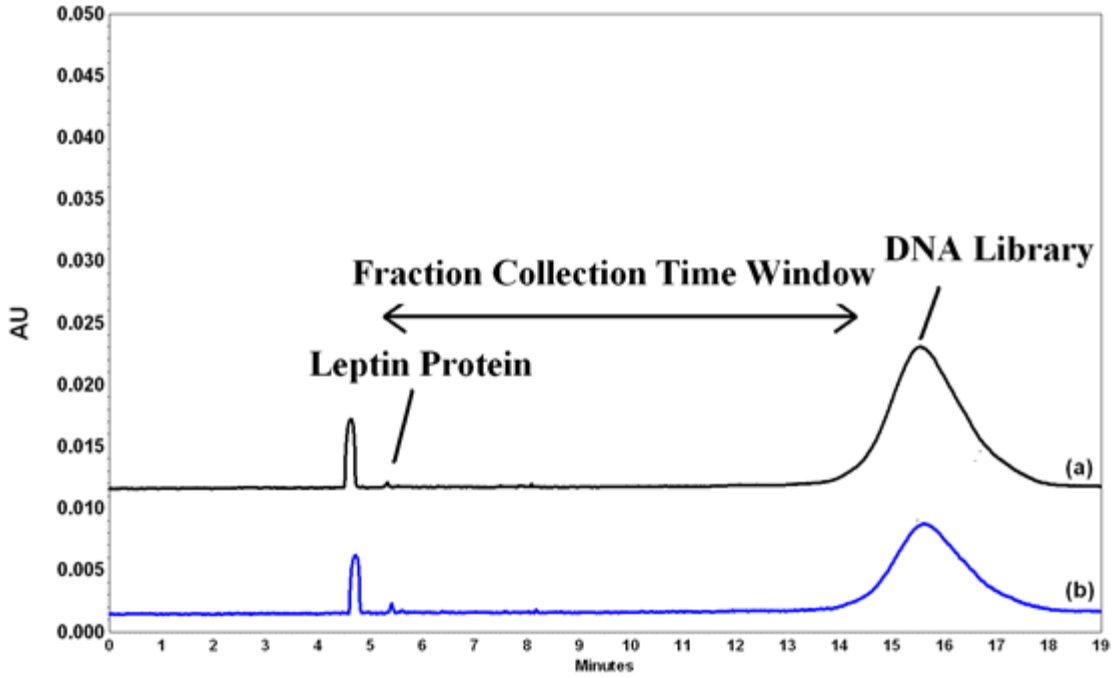

Figure 3.2 Electrophoretogram of the 10 μM random DNA library and 1 μM leptin were incubated for 30 minutes and injected onto a capillary by hydrodynamic injection (411nl), 333Vcm-1; (a) 254nM PDA detection; (b) 280nM PDA detection.

A peak at about 4.7 minutes is also observed which could be caused by electro osmotic Flow (EOF). The time collection window was determined to be from 5.5 minutes to 15 minutes. The bulk affinity K_D was determined by NECEEM analysis. An incubated mixture of naïve library 100 nM and 500 nM of human leptin was injected and separated using 333Vcm^{-1}. From the electrophoretogram shown in **figure 3.3** we can see that there is a small complex peak observed. The area of the unbound DNA library is quite broad which is expected for a highly heterogeneous sample of DNA. The bulk affinity was estimated to be 320 μM.

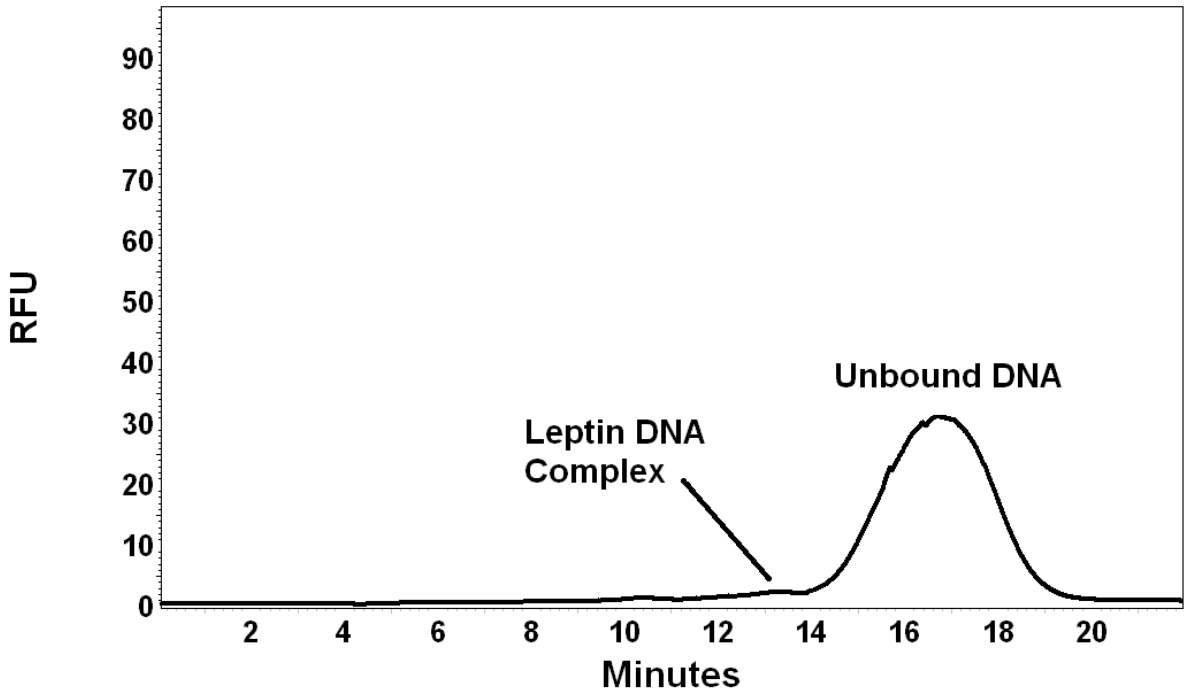

Figure 3.3 NEECEM bulk affinity analysis of round 0; 100nM DNA library and 500nM protein were incubated for 30 minutes and injected onto a capillary by hydrodynamic injection (411nl), 333Vcm-1, LIF detection. The areas of the free DNA, dissociated DNA and complex peak were used to estimate K_D.

Fractions were collected by replacing the outlet with 5 µl of 3X TGK buffer. The complex peak is collected by calculating the corrected elution time. The corrected elution time is multiplied against the elution factor which is calculated using **equation 1.1**. The partitioning step was carried out a total of 3 times for each round of selection. The fraction was amplified using RT-PCR using SsoAdvanced polymerase mix and the F and R primers. We choose to use RT-PCR to check the progress of the amplification in real time by monitoring the SYBR green fluorescence signal for each round of amplification. A negative control was added and used as the base line signal to remove the interference from the FAM labeled primers. A typical amplification graph is shown in **figure 3.4.** The PCR was stopped at the optimum number of cycles when there was no increase in signal (~16 cycles).

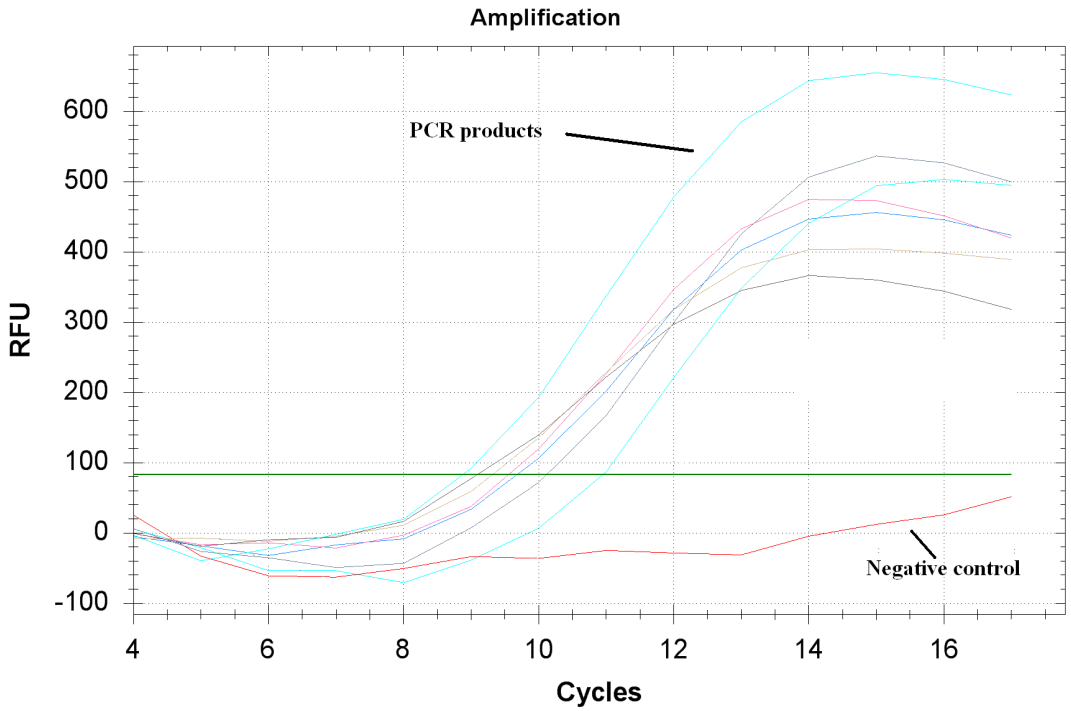

Figure 3.4 RT-PCR amplification plot of CE fractions from round 4 of selection and the negative control. The optimum amplification was observed at the 16th cycle.

The RT-PCR protocol was followed by melting point analysis. The melting point analysis allows for the PCR products to be analyzed without any loss of sample. Starting at the lowest temperature the fluorescence signal is measured at 1 degree increments and up until 95 ^{o}C. A graph of –d(RFU)/dT against temperature was plotted and a typical melting point graph is shown in **figure 2.5.** From the graph, we can see a single peak at about ~78 ^{o}C which suggests that only the PCR fragments were amplified. The negative control shows no peak which suggests that the polymerase used in the SsoAdvanced SYBR mix facilities high efficiency in amplifying small DNA fragments and that the sample was free from contamination.

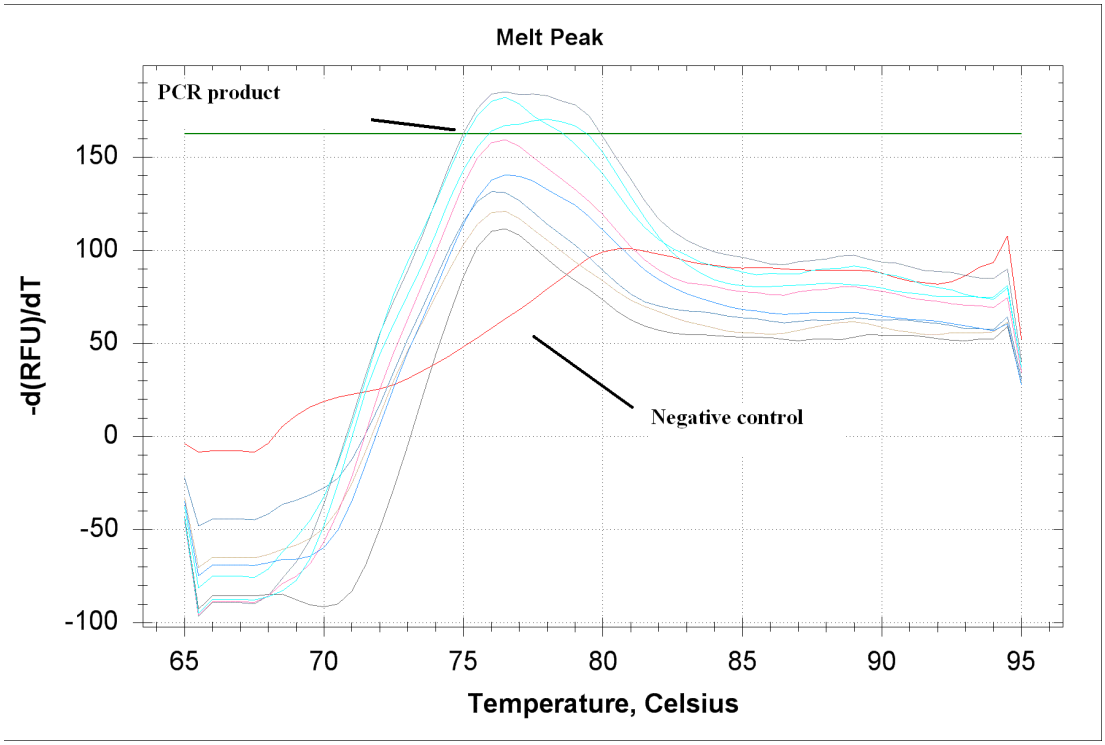

Figure 3.5 Melting curve analysis of round 4 enriched library. The one main peak corresponds to the 80bp DNA enrich library. No peak was observed in the negative control Each curve represents a different PCR reaction.

The dsDNA product was converted back to ssDNA using a streptavidin agarose beads and weak sodium hydroxide followed by isopropanol precipitation. Care was taken not to over dry the sample on the freeze dryer as an over dried sample would becomes difficult to reconstitute in buffer. The recovery of ssDNA was measured on the nanodrop spectrometer. The recovery of ssDNA varied between rounds from (15 ng / µl up to 50 ng/µl).

The bulk affinity was measured after each round of selection by NECEEM. The bulk affinity analysis allowed for the progress of selection to be monitored while only using a small volume. A decreasing K_D for each round showed that the selection was progressing. The bulk affinity K_D values after each round of selection is shown in **table 2.1.** The bulk affinity decreased from 320 µM for the initial library to 0.4 µM for round 4. A smaller K_D value corresponds to a higher binding affinity of the library. The NECEEM electrophoretogram for round 4 is shown in **figure**

2.6. When comparing this electrophoretogram to the one shown in **figure 2.2**, it can be seen that a complex peak has increased in area while the area representing the dissociated DNA has also increased in area suggesting that aptamers with wide range of k_{off} rates were present in the enriched library.

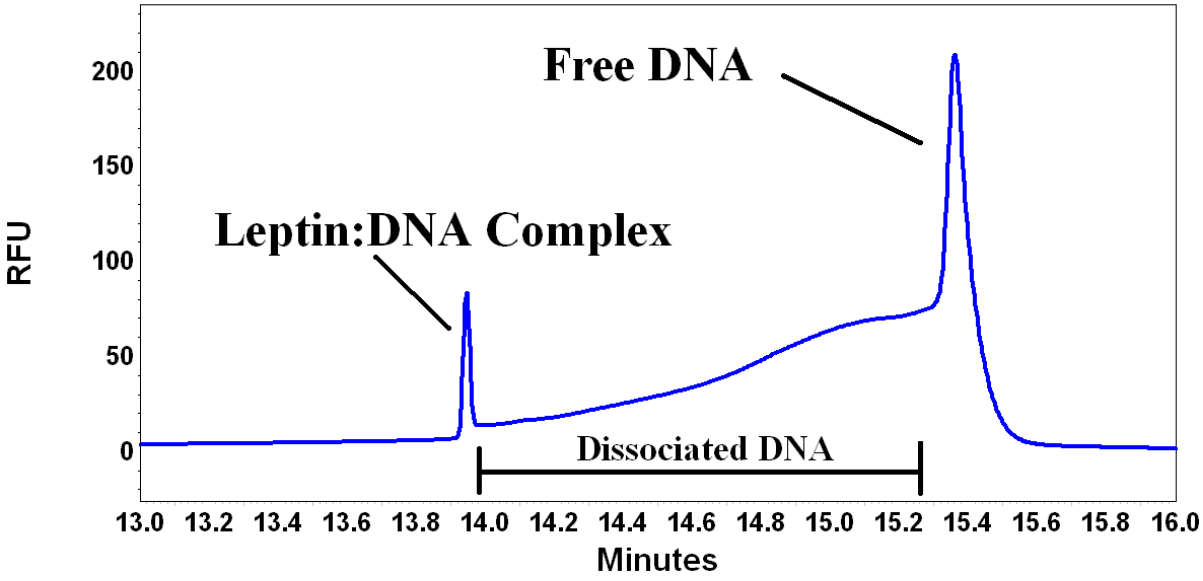

Figure 3.6 NEECEM bulk affinity analysis of round 4; 100nM enriched library and 500nM protein were incubated for 30 minutes and injected onto a capillary by hydrodynamic injection (411 nl), 333 Vcm-1, LIF detection. The areas of the free DNA, dissociated DNA and complex peak were used to estimate K_D.

Four rounds of selection were performed in total where there was no improvement in the bulk affinity value even with smaller concentrations of protein after round 4.

The conditions for the selection were varied from round to round. The target concentration of the equilibrium mixture was decreased after each round of selection to encourage competition between the DNA sequences while the DNA concentration did not vary much from round to round.

Table 3.1 A summary of the relative concentrations of protein and DNA for NECEEM and selection; bulk affinity K_D values. A decrease after each round suggested that the selection was proceeding.

		Rounds of Selection				
		0	1	2	3	4
NECEEM conditions	**Protein Concentration (μM)**	10	1	1	0.5	0.1
	DNA Concentration (μM)	0.1	0.1	0.1	0.1	0.1
Selection conditions	**Protein Concentration (μM)**	10	1	1	0.5	0.1
	DNA Concentration (μM)	1	1	1	1	1
	Bulk K_D (μM)	**320**	**47.3**	**13.07**	**0.57**	**0.4**

The DNA from round 4 was selected for cloning and sequencing. The DNA was amplified using RT-PCR with non-labelled primers added and purified using Qiaprep spin columns and isopropanol precipitation. The dsDNA was cloned, sequenced and a total of 10 clones were found, four of which were synthetized for validation.

3.2.2 Validation of leptin clone sequences

Of the ten sequences that were sequenced, 4 had a negative ΔG value which was determined using Oligoanalyzer software (IDT). The secondary structures were analyzed on OligoAnalyzer 3.1 for the hair pin structure. The secondary structure for Lep 3 gave a negative Gibbs free energy of -7.4 $kJmol^{-1}$ assuming standard ionic conditions (See Appendix 1, **figure a.1**). The truncated structure of Lep T3 showed an almost positive Gibbs free energy and differences in the secondary structures suggested that the constant region is involved in the binding. The full

secondary hairpin structures of aptamers Lep 1,2 and 4 also gave a negative Gibbs free energy and their truncated sequences Lep 1T, 2T and 4T also gave a near positive Gibbs free energy and all the structures are shown in Appendix 1, **figure a.2- a.4**. Two techniques were used to compare the binding affinity K_D of the individual aptamer clone sequences against the target protein in order to rigorously test the binding ability of each aptamer clone. First, NECEEM was used to determine the K_D of the aptamer-protein interaction in free solution (3D environment), without immobilization, 0.1µM of each aptamer was incubated with increasing concentrations of leptin until a complex was observed. The K_D was then calculated using **equation 1.3** by comparing the areas of the free aptamer, dissociated aptamer and complex peak. The electrophoretogram for Lep 3 aptamer is presented in **figure 3.7** and again, dissociated aptamer is observed as exponential decay from the unbound aptamer. The electrophoretograms of Lep 1, Lep 2 and Lep 3 are shown in appendix 1**, figure a.5-a.7** and they also show similar peak shapes.

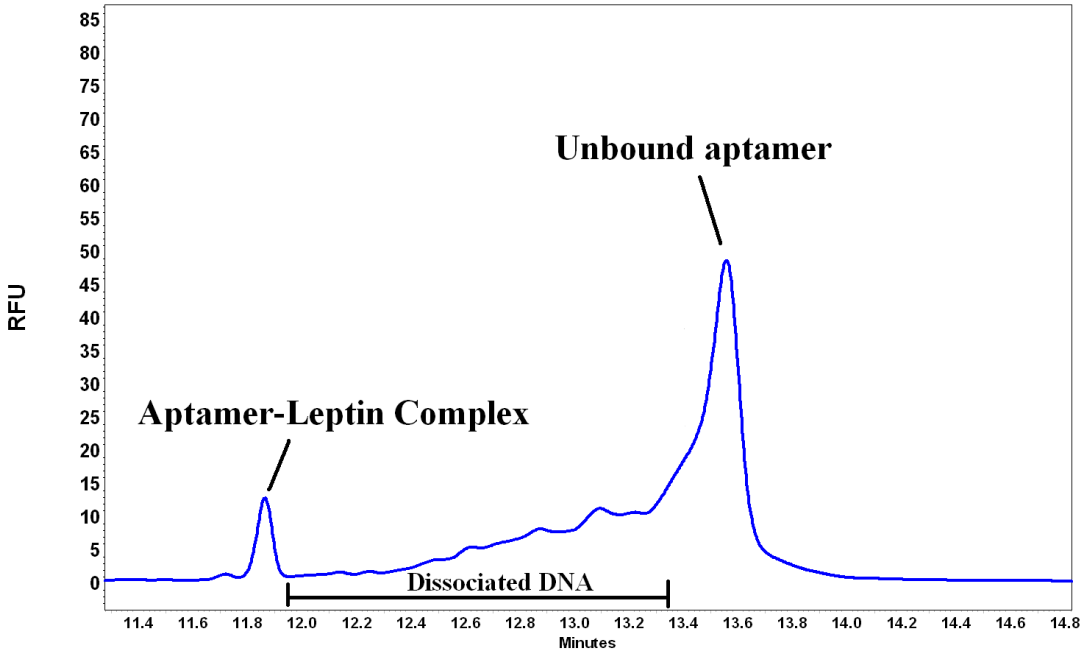

Figure 3.7 NEECEM analysis of Lep 3; 100nM aptamer and 500nM leptin were incubated for 30 minutes and injected onto the capillary by hydrodynamic injection (411nl), 333Vcm^{-1} separation with LIF detection. The areas of the free DNA, dissociated DNA and complex peak were used to determine K_D and 3 experiments were performed for each sequence.

The second technique used was a fluorescence intensity method which involved measuring the binding affinity, K_D of the aptamer against a protein target immobilized on a well plate (2D environment) and the saturation curve is shown in **figure 3.8**. A lower K_D value corresponds to a higher binding affinity. The target was immobilized onto a well plate at a constant concentration and incubated with a different concentration of each aptamer (5000-10nM) in each well. The plate was blocked with BSA to account for non-specific binding and a negative control of BSA was used to subtract the signal from the baseline. Experiments were performed in triplicate. Non-linear regression was used to determine B_{max} and K_D using GraphPad Prism.

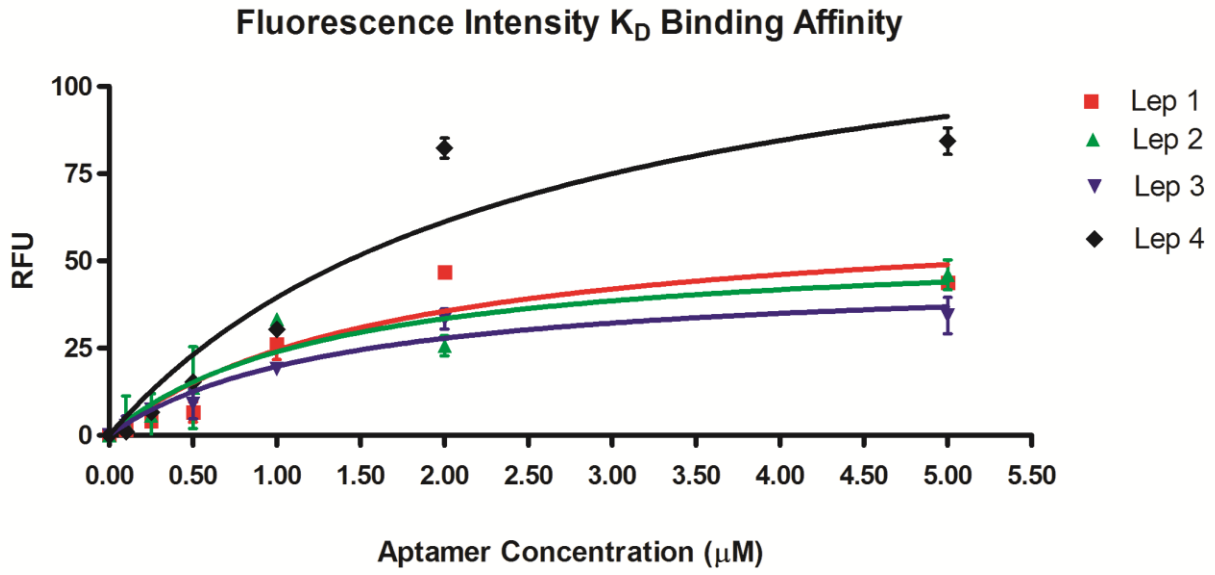

Figure 3.8 The saturation graphs of each aptamer sequence using fluorescence intensity. Experiments were performed in triplicate. Non-linear regression was performed using graph pad Prism.

Comparing the results obtained for the binding affinities, determined by NEECEM and fluorescence intensities, there are obvious discrepancies found in the values. The binding affinity

values for both techniques are shown in **table 3.2** NEECEM showed a higher binding affinity with the lowest K_D reported for Lep 3 aptamer (K_D = 0.32 μM). When Lep 3 was analyzed using the fluorescence intensity method, a lower binding affinity (K_D = 1.50 μM) was observed.

Table 3.2 A summary of the random sequences of aptamer sequences and the K_D values of NECEEM analysis and fluorescence intensity.

Name	Random sequence	NECEEM analysis K_D (μM)	Fluorescence intensity K_D (μM)
Lep 1	**TGTCACAATTTCCCCCCTCGCACATTTTGCAAGTAACTGA**	**0.87 ± 0.07**	**1.90 ± 0.53**
Lep 2	**TGGGTGGCCTCCCGTTTATTCGAGATTTGGTTGAATTTGT**	**0.41 ± 0.13**	**1.18 ± 0.39**
Lep 3	**GTTAATGGGGGATCTCGCGGCCGTTCTTGTTGCTTATACA**	**0.32 ± 0.50**	**1.50 ± 0.25**
Lep 4	**TCTATAAACTCTGTCCGGTTTTATAATAATAACATTTTAC**	**1.47 ± 0.14**	**3.00 ± 0.80**

These observed differences in K_D could be explained by a few reasons. Systematic errors could arise from a number of possible sources such as differences in the fluorescence signals produced by the two different machines because the NECEEM method relies on an LIF detector, whereas the fluorescence method relies on a microplate reader. Non-specific binding of the aptamer onto plastic can be considered as a source of systematic error but this effect was minimized by blocking the plastic with BSA and using a BSA-only control to normalize the signal. Another systematic error may arise from the k_{off} rates of the aptamer target, and this can affect the measurements of binding affinity[108]. In traditional SELEX procedures, there is a significant bias toward slow binding aptamers, meaning that fast binding sequences may dissociate quickly and be discarded. For the CE-SELEX procedure, both slow binding and fast binding sequences are selected. For all of the aptamers, there was a significant amount of dissociated DNA, suggesting that the k_{off} rate was higher for this particular target. It also suggests that for K_D measurements involving CE methods, the amount of DNA that dissociates from the target is taken into account and would give higher binding affinities. The fluorescence intensity method involves incubating

the aptamer with the protein target and washing the plate numerous times before measuring the fluorescence on the microplate reader. This could result in some dissociated DNA being washed away before the measurements are completed and leads to a significant slow binding kinetics bias and difference in K_D. Another possible reason for the difference in values is due to the environment in which the selection was carried out. During the CE–SELEX procedure, the aptamer library is free to bind with the whole protein target in solution, and if the molecular weight of the target is less than that of the DNA, then there is a possibility that the DNA can bind around the whole target. If the K_D of an aptamer selected by CE–SELEX is measured against an immobilized target, then the aptamer may be prevented from binding with the whole target due to changes in conformation of the protein on adsorption onto the plate, and this may give rise to significant differences in K_D. In conventional SELEX methods, which often involve the immobilization of the target onto the solid support, DNA molecules may be prevented from binding with the whole target due to steric hindrance of the linker molecule during selection. This effect may be more significant in low-molecular-weight targets where the relative size of the linker molecule increases in comparison with the target and is detrimental to aptamer binding to the target. Therefore, aptamers that are selected against an immobilized target are usually validated against an immobilized target, giving a binding affinity that mimics the environment in which they were selected and allowing the K_D to be measured with reasonable accuracy. Because characterization of aptamer–protein interactions has rarely been performed on aptamers selected against small targets in free solution, more investigations need to be carried out to confirm whether the binding kinetics of small target aptamer sequences selected in 3D environments is affected when introduced into a 2D environment such as being immobilized onto a surface. NECEEM has given comparable binding affinities in previous studies for thrombin binding

aptamers when compared with a nitrocellulose filter assay, with NECEEM and nitrocellulose filters giving 240 and 200 nM, respectively[13; 109]. Nitrocellulose filters can be considered as a 2D technique because the protein is immobilized onto the filter prior to incubation with the aptamer. The results demonstrate the successful selection of an aptamer for leptin protein by NECEEM. However, to compare binding constants determined by heterogeneous and homogeneous methods, systematic errors need to be kept to a minimum. Our results serve to provide more information on experimental parameters that need to be considered in future experiments to determine binding affinities. The specificity was tested by comparing the binding affinities of Lep 3 aptamer against different proteins. β-lactoglobulin was chosen because it has a similar molecular weight and isoelectronic point to that of human leptin. Bovine catalase was also chosen because in our separate studies, aptamers against this target had been selected using the same buffer conditions and so would account for any false negative results (See chapter 3). From the NECEEM based specificity electrophoretogram which is shown in **figure 3.9**, the binding affinities for β-lactoglobulin (2.3 ± 0.43 μM) and bovine catalase (3.1 ± 0.26 μM) towards Lep 3 aptamer were considerably lower than the binding affinity for human leptin.

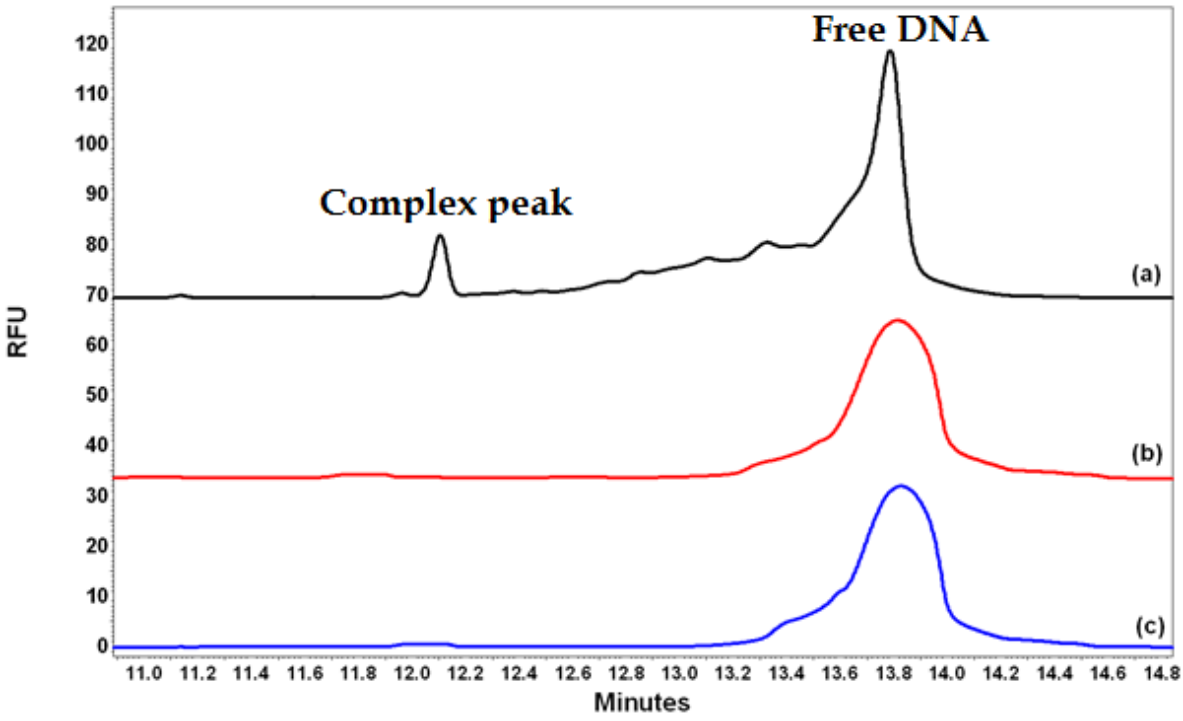

Figure 3.9 NEECEM specificity analysis Lep 3 aptamer against: (a) human leptin, (b) β-lactoglobulin and (c) bovine catalase; 100 nM aptamer and 500 nM of each protein were incubated for 30 minutes and injected onto a capillary by hydrodynamic injection (411 nl), 333 Vcm^{-1}, LIF detection. The areas of the free DNA, dissociated DNA and complex peak were used to determine K_D.

The electrophoretograms clearly shows a lack of complex peak but some dissociated DNA can be observed for both proteins. This demonstrates that Lep 3 aptamer shows high specificity towards human leptin protein in a free solution environment. However, specificity should always be retested when an aptamer is to be used in other experimental conditions.

3.3 Summary

The CE-SELEX method has been used to select aptamers against human leptin protein with K_D values in the low micromolar region. We also demonstrated the use of Real Time PCR amplification on FAM labelled oligonucleotides without the need for a preparative amplification step. As no aptamers with low nanomolar range were obtained, it suggests that there are still limitations in the CE-SELEX method in terms of number of aptamers screened and that K_D values obtained are could be target dependent. This problem could be overcome by developing a continuous injection method or by hybridizing conventional SELEX methods with the CE-SELEX method [83]. Also the apparent difference in K_D values obtained from the two methods (CE-SELEX and fluorescence intensity) suggests that K_D values should be determined using a method which simulates the environment in which the aptamer is intended to be used. In summary we have demonstrated the use of CE-SELEX to select a small protein with fast binding and our results could have implications for choice of binding affinity method for future capillary electrophoresis based SELEX and other non-immobilization based selection methods in terms of clone validation and possible applications of aptamers[70; 78; 83]. It will also be worth using X-ray crystallography to elucidate the mechanism of binding between the target and aptamer.

4 The Non-SELEX of bovine catalase and human hemoglobin aptamers

4.1 Aim

After the selection of aptamers against human leptin protein using CE-SELEX, a study of non-SELEX was performed to compare the two techniques. Non-SELEX is considered to be a faster method as the number of rounds is reduced to <3 rounds of selection. This reduction in the number of rounds of required is due to the higher separation efficiency of CE and the sensitive LIF detection which allows for the sample to be collected into a vial containing the target and reinjected with adequate sensitivity. This allows for enrichment of the library to be achieved rapidly in fewer steps. Also non-SELEX removes the requirement of PCR amplification between each round, reducing the error rate of PCR and preventing mispriming. However to date, only a small number of targets have been developed using the non-SELEX method. The non-SELEX procedure relies on successful detection of a complex peak in order to calculate the K_D using NECEEM. Another disadvantage of the non-SELEX is the difficulty of amplification using PCR. After each successive round of non-SELEX, the number of sequences collected is reduced further. This means that optimization of amplification is often required to get adequate recovery of ssDNA for the K_D determination and sequencing.

In this chapter, non-SELEX was used to select aptamers against two proteins, namely catalase protein from bovine liver and human hemoglobin protein. Also, some of the limitations associated with the non-SELEX procedure, namely the buffer optimization and the number of sequences screened were improved upon. To the best of our knowledge, the development of

aptamers for catalase from bovine liver and for human hemoglobin has not been previously reported. Catalase is a common acidic protein that is found in a large number of species and is responsible for the conversion of hydrogen peroxide into water and oxygen [110]. The protein plays an important role in the metabolism of the liver where it removes harmful hydrogen peroxide. It is also involved in the oxidation of metabolites as a catalyst although the exact mechanism is largely unknown. Catalase exists as a tetramer of four polypeptide chains which contain iron porphyrin heme groups. The full structure of catalase is shown in **figure 4.1[111].** These heme groups are responsible for the enzyme's activity[112].

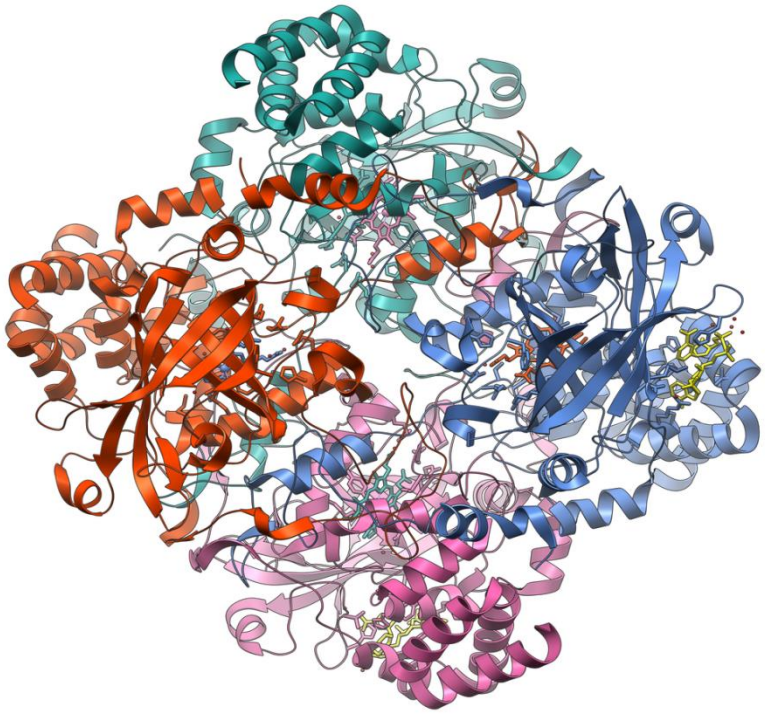

Figure 4.1 Full structure of bovine catalase enzyme generated from the PDB[112].

Inhibitors for catalase include heavy metal ions and cyanide[113]. Catalase has been linked to a number of physiological conditions in the body, although elucidating the exact role of catalase in

disease is difficult. A lack of catalase was found to increase the likelihood of developing type 2 diabetes [114]. Catalase has also been identified as a biomarker of oxidative stress in a large number of organisms, and it's presence at increased levels can demonstrate the presence of pollutants in environmental systems [115].

Hemoglobin is an iron containing oxygen transport protein, which is an important biomarker in a number of diseases and is one of the most assayed proteins in diagnostics [116]. The structure which is shown in **figure 4.2** exists as a quaternary structure with four subunits consisting of a packed protein structure and contains a non-protein heme group[117-119].

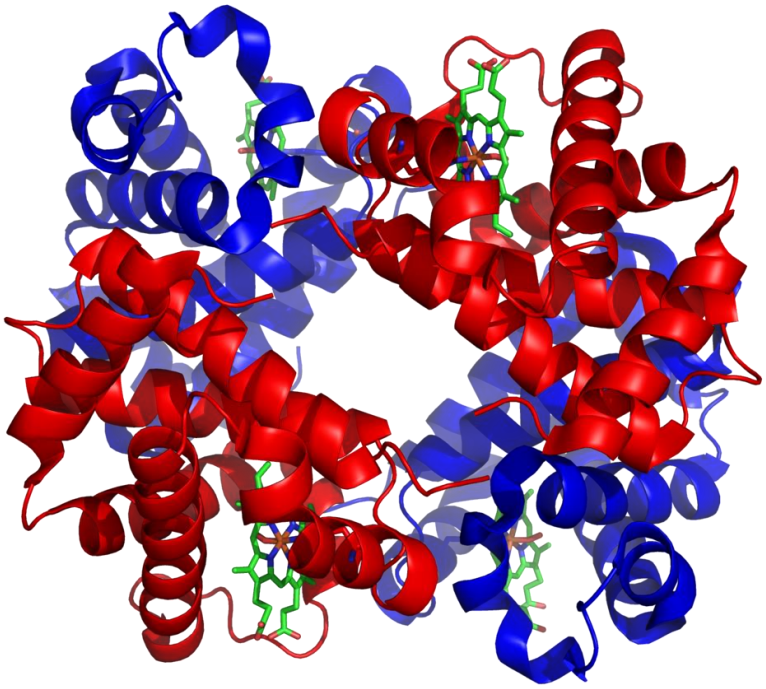

Figure 4.2 The full structure of haemoglobin[120].

An aptamers would be beneficial in a number of applications such as in the development of biosensors, Western Blot, Biomarker identification, and as a non-mutagenic inhibitor[121-125].

4.2 Results and Discussion

4.2.1 Optimization of the Non-SELEX procedure using catalase

For the initial experiments, the optimum conditions were determined so that the partitioning step, fraction collection and bulk affinity analysis could be performed. These conditions were used in all the capillary based selections in this thesis.

The non-SELEX method was optimized to improve the selection of aptamers from the library. To achieve this, the number of sequences screened was maximized. An experiment was performed to determine the effect of increasing the internal diameter of the capillary from 50 µm to 100 µm. A bare fused silica capillary with an effective length of 50 cm and total length of 60 cm was chosen for the analysis. For acidic proteins (*pI* <7) the buffer should be at least 2 pH units above the *pI* value so that the protein contains a net negative charge and the amount of protein adsorption to the capillary wall is minimal. For basic proteins (*pI* >7), which would have large net positive charges in lower pH buffers, protein adsorption is significant enough to give poor reproducibility and a coated capillary with reverse polarity is normally required. The DNA library was injected by hydrodynamic injection (1psi, 13seconds).

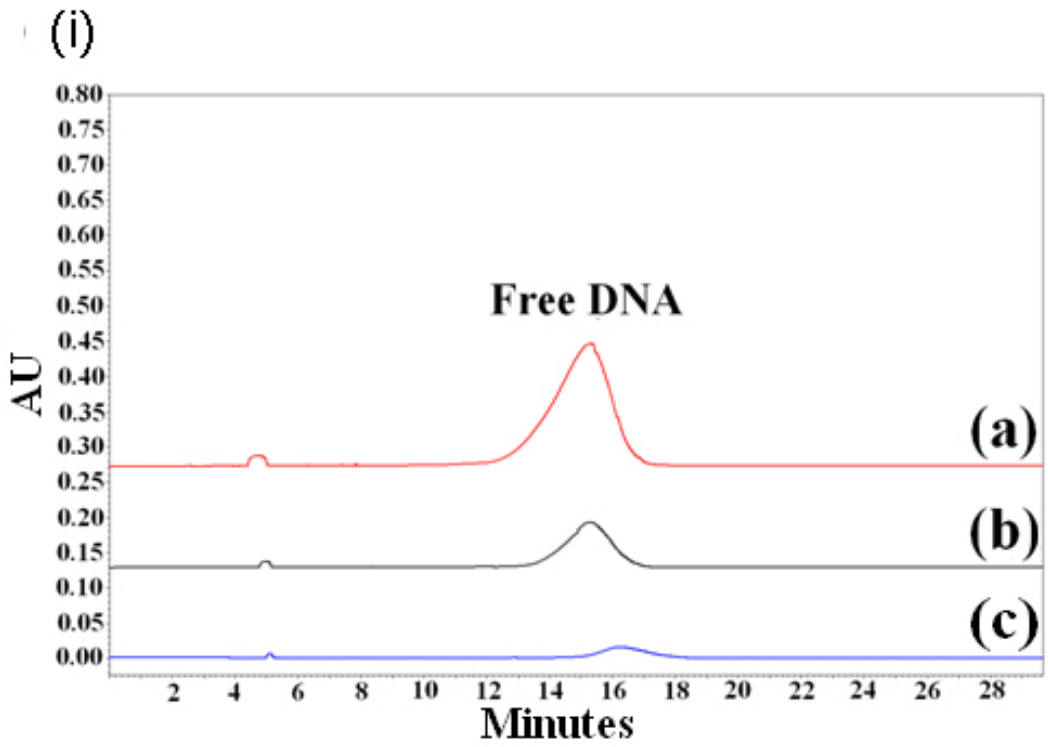

Figure 4.3 Optimization of the number of sequences injected and screened using capillary electrophoresis with PDA detection at 260nm, Run buffer: 3xTGK and selection buffer 1xTGK, 333Vcm^{-1}, 50μM Random library, 13 second injection 1psi; (a) 100μm ID; (b) 75μm ID and (c) 50μm ID.

The injection volume was maximized so that the number of sequences screened was increased while still maintaining good peak shape. A separation of 333 Vcm^{-1} at positive polarity was applied across the capillary as to keep the running current as low as possible to prevent Joule heating and PDA detection at 260nm was used to detect the DNA library. 3x TGK buffer was used as the run buffer due to the fact that this buffer was shown to facilitate the aptamer protein complex[101]. ***Figure 4.3*** shows the electrophoretogram for the DNA library peak for 50, 75 and 100 µm.

As the internal diameter of the capillary is increased, the injection volume increased and hence the number of sequences also increases. The estimated number of sequences for each diameter of capillary is shown in **table 4.1**. The number of sequences screened was calculated from the injection volume and average molecular weight of the DNA library. The increase in diameter also allowed for a bigger fraction to be collected. The 100µm internal diameter was chosen for the selection procedure as the highest number of sequences could be screened while still maintaining adequate resolution during the bulk affinity determination.

Table 4.1 A summary of the estimated injection volume and number of sequences injected for different capillary internal diameters.

Internal Diameter (µm)	Injection volume (nl)	Number of sequences injected
50	**25.73**	**7.7×10^{12}**
75	**130.27**	**3.9×10^{13}**
100	**411.70**	**1.2×10^{14}**

We also maximized the number of sequences screened and collected them by increasing the protein concentration. Equilibrium mixtures containing 2 µM, 1 µM and 200 nM of catalase protein were incubated with 100 nM DNA for 30 minutes. These samples were injected onto the capillary and separated using 333 Vcm^{-1} with LIF detection at excitation wavelength 488 nm and 528 nm emission wavelength.

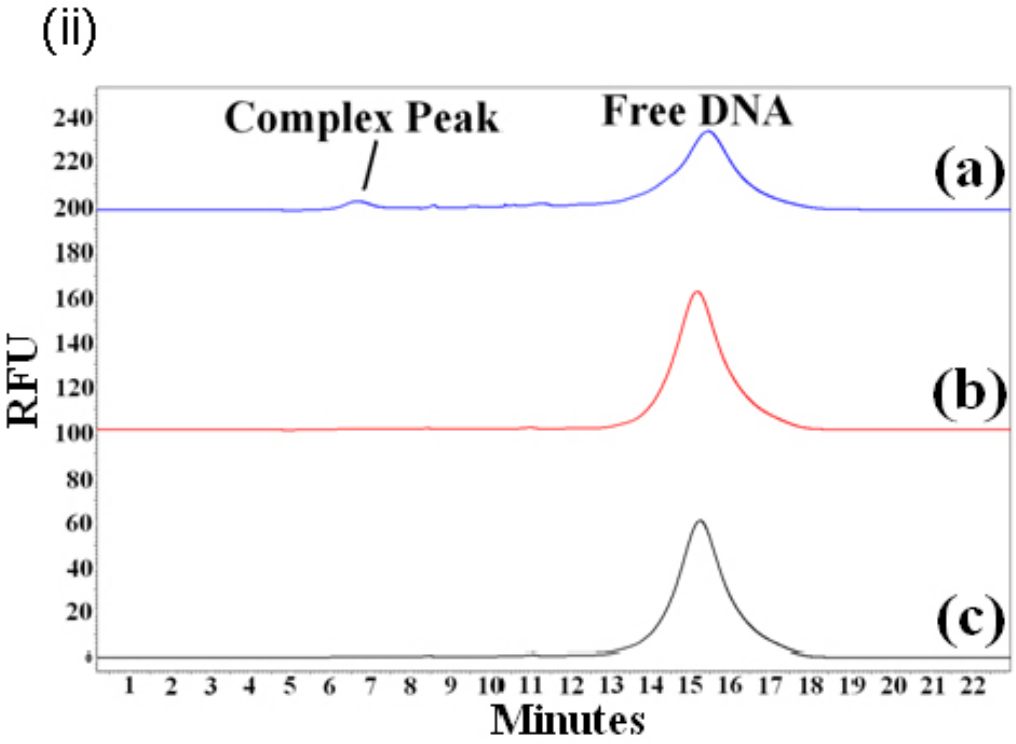

Figure 4.4 Effect of protein concentration on the area of the complex using, 13 second 1 psi injection, 333 Vcm^{-1}, using LIF detection; (a) 2 μM protein incubated with 100 nM DNA library; (b) 1 μM protein incubated with 100 nM DNA library and (c) 200 nM Catalase protein incubated with 100 nM DNA library.

For the initial round of selection and bulk affinity analysis, the protein concentration is an important consideration in ensuring a high enough efficiency of selection and to ensure that there is adequate sensitivity for the detection of the complex peak. After subsequent rounds of selection, the protein concentration should be lowered to increase the stringency of selection and to ensure that the aptamers with the highest binding affinity will be selected. As the library becomes enriched with high binding aptamers the complex peaks are more observable at lower concentrations. From **figure 4.4** the optimum protein concentration for the initial round of selection was shown to be 2 μM which gave a significant complex peak area. No dissociation

was observed as the degree of dissociation of the aptamer from the complex may not be high enough to give a detectable signal and can be assumed to be negligible. At lower concentrations, no complex was observed. At concentrations > 2 μM no significant change in the area of the complex peak was observed.

The second improvement we made was in the run buffer and selection buffer conditions. Often the detection of complex peaks has proven difficult due to the stability, sensitivity and resolution of the complex peak from the unbound DNA. A more ionic run buffer can decrease the EOF resulting in a higher resolution of the peaks but higher capillary Joule heating. The pH is also an important factor in controlling the EOF. The run buffer pH and the selection buffer pH were kept at around 8.2 as a high pH would result in a higher EOF and an acidic pH would cause degradation of the DNA. Therefore the pH could not be altered too much. A run buffer of 3x TGK and the selection buffer 1x TGK were chosen based on the improved stability of the complex peak and a lower Joule heating effect[101]. Two samples, both containing 2μM of protein and 100nM of the library but with one of the samples dissolved in 1X TGK and the other sample dissolved in 3X TGK were prepared. The difference in ionic strength between the run buffer and selection buffer is believed to induce a stacking effect which in turn increased the signal of the complex peak. This effect is shown in **figure 4.5.**

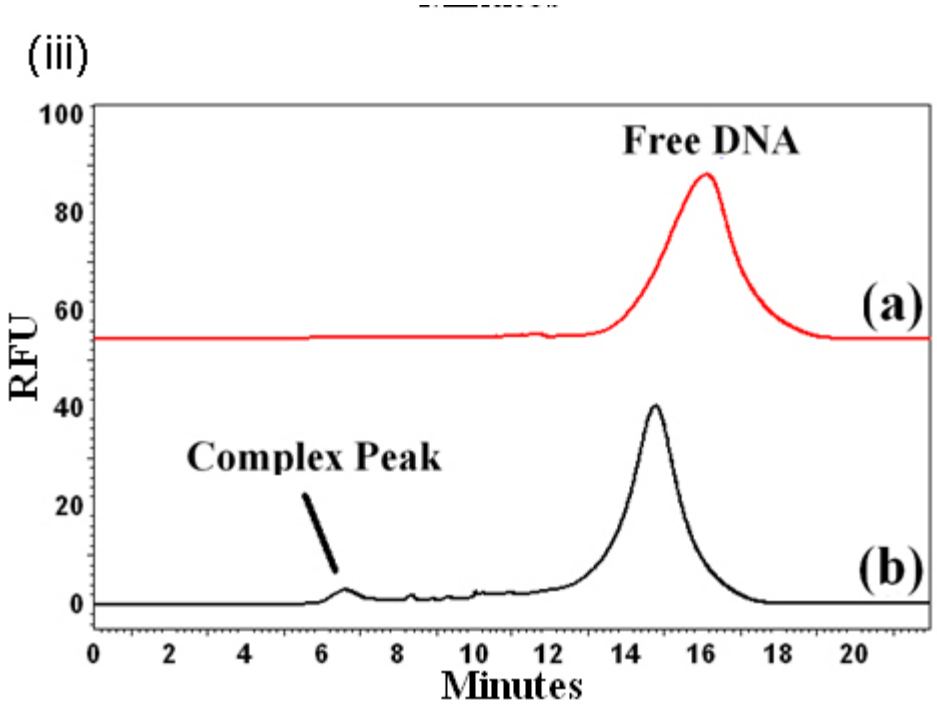

Figure 4.5 The effect of sample stacking on affinity analysis of initial library, 13 second, 1psi injection, 333 Vcm^{-1}, using LIF detection; (a) 100 nM of random DNA library incubated with 2 μM catalase protein sample dissolved in 3x TGK buffer and (b) 100 nM of random DNA library incubated with 2 μM catalase protein sample dissolved in 1X TGK buffer.

4.2.2 The Non-SELEX of catalase aptamers

The migration time was determined from the time collection window and was determined to be between 9 and 14 minutes and is shown in **figure 4.6.** A wide collection window allows for more sequences to be collected and prevents the collection of non-binding sequences.

For the fraction collection and multi-round partitioning, the concentration of the DNA Library was increased up to 50 μM while the final protein concentration was increased to 10 μM. The

protein concentration is thus in excess of the naïve library concentration and the concentration of protein after each round was decreased in order to increase the stringency of the selection.

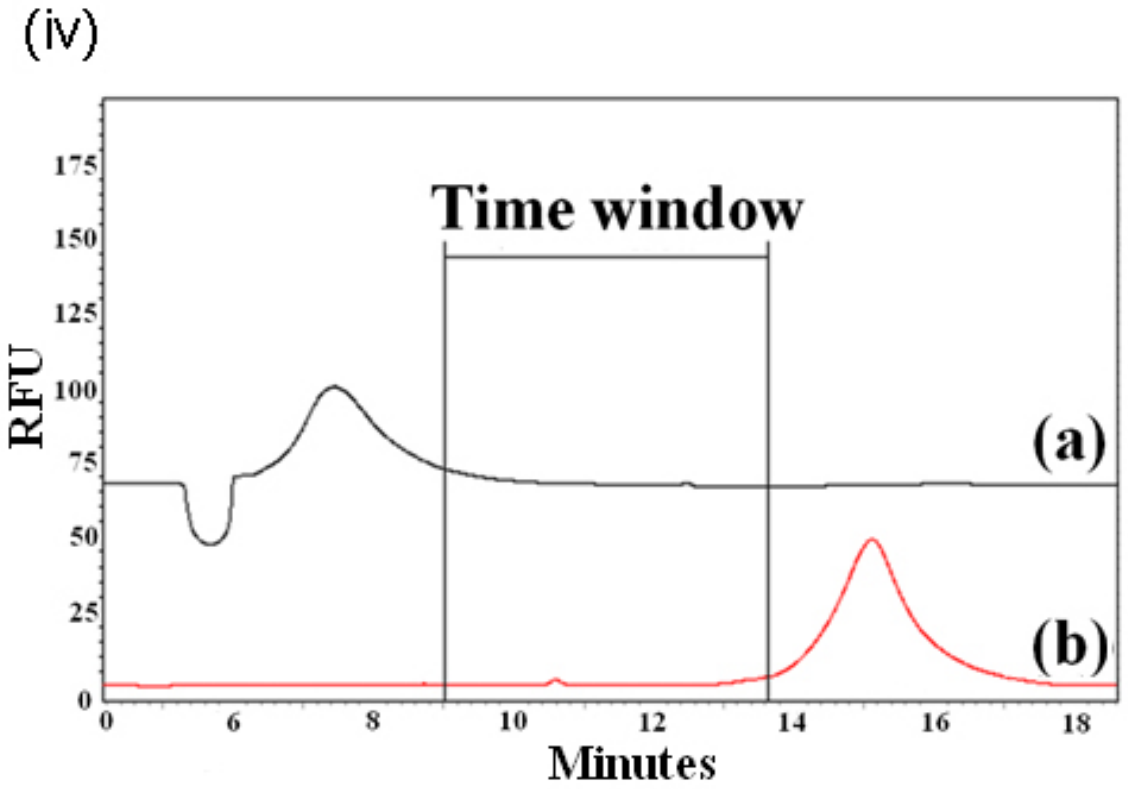

Figure 4.6 Time window determination using capillary electrophoresis; Run buffer: 3xTGK and selection buffer 1x TGK, 333 $Vcm^{-1}V$, 13 second injection 1 psi, 100μm ID; (a) 2μM catalase protein using PDA detection; (b) 100 nM random library using LIF detection.

A photo diode array (PDA) detector was used for the first round of selection due to its suitable detection range. Subsequent rounds of selection were performed using LIF detection as the sensitivity of the complex peak and free DNA decreased substantially. A manual fraction collection was carried out by replacing the outlet buffer with a micro vial containing 30 μl of run buffer and 1 μM of protein for round 1 and 0.1 μM of protein for round 2. The protein and complex peak can be collected by firstly determining the time at which the peak would elute at

the end of the capillary which can be determined by **equation 1.1**. The sample was injected and collected a total of 3 times for each round of selection in order to maximize the number of template DNA sequences for PCR amplification and a total of 2 rounds of selection were completed.

The use of RT-PCR was not available in this project so preparative PCR with agarose gels was used instead to amplify the libraries. The fractions from each round of selection were amplified using PCR for subsequent bulk affinity analysis. This is to increase the concentration of DNA to get adequate signal in the LIF. The fractions were split into 8-10 different reactions with 5 µl of DNA template added to each reaction tube. The PCR reaction was optimized to determine the optimum number of cycles. The number of cycles required for adequate amplification varies between each fraction due to the differences in DNA sequences collected.

A touchdown method was used to limit the amount of non-specific amplification and formation of primer dimers. The touch down protocol can also eliminate the need for annealing temperature optimization. The forward primer was labelled with a FAM fluorophore and the reverse primer was labelled with biotin to facilitate strand separation. The primer concentration was varied to give the optimum degree of amplification while again avoiding the formation of non-specific products. The products were analysed on 2 % agarose gel and is shown in **figure 4.7**.

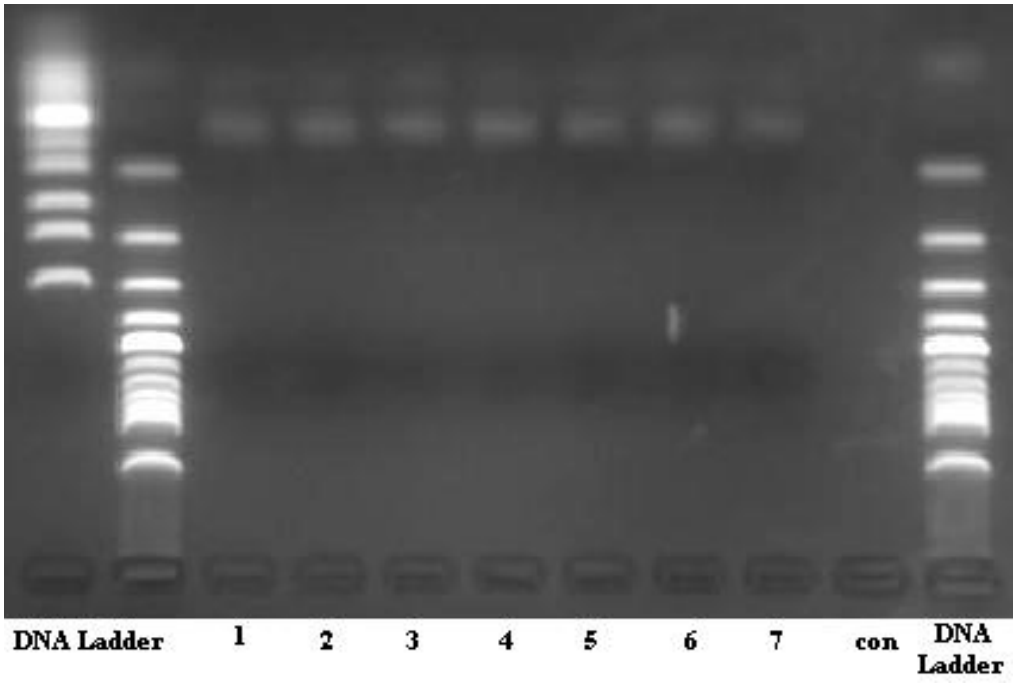

Figure 4.7 Typical gel analysis; 2% agarose gel with ethinium bromide stain; from left ultra low molecular weight ladder, 100bp ladder, 1-7 PCR products of fraction collection; negative control and 100bp DNA ladder.

The gel analysis showed a band at less than 100 bp which corresponds to the aptamer. A negative control was added to the PCR reaction which consisted of nuclease free water instead of the DNA template. This is the standard practice for determining whether there is contamination present in the PCR mixture. Two DNA markers were used in the gels because the aptamer has 80 bp. The standard DNA marker has size markers up to 100 bp and the ultra-low DNA marker has DNA markers that go down to 25 bp.

The subsequent dsDNA product of each round were converted to the ssDNA using streptavidin agarose beads as described for the CE-SELEX of leptin aptamers. The aptamers were incubated with streptavidin agarose beads for 30 minutes. The streptavidin binds to the biotin on the reverse strand of the DNA. The forward strand can then be separated by heating or adding weak

base. We chose to use weak base as previous research had shown that heating may cause bleaching of streptavidin. The denaturing step was repeated twice for 20 each and neutralized with weak acetic acid followed by isopropanol precipitation. Sometimes a pellet is not visible due to the fact that the DNA is transparent. The DNA was reconstituted in selection buffer and the purity and concentration of recovered library was then checked on a nanodrop spectrometer. The purity is measured by comparing the ratio of absorbance at 260 nm and 280 nm. A ratio greater than 1.8 suggests that the DNA was pure. The concentration was recorded for the bulk affinity analysis and concentrations up to 1 μM were recovered.

Bulk affinity analysis was performed on each enriched library fraction to estimate the degree of binding affinity. An adequate determination of bulk binding affinity on a highly heterogeneous sample is not possible due to the small differences in molecular weight of each individual DNA strand and hence can only be estimated. Nevertheless the bulk affinity analysis can indicate the progress of selection with a decrease in K_D suggesting that the selection is proceeding. The bulk affinities of the initial library, the enriched library from round 1 and the enriched library from round 2 are shown in **table 4.2**.

Table 4.2 Conditions for Non-SELEX selection of catalase aptamers and bulk affinity analysis of enriched aptamer libraries after each round of selection using capillary electrophoresis.

		Rounds of Selection		
		0	1	2
Selection conditions	Protein concentration (μM)	10	1	0.1
	DNA Library concentration (μM)	50	not determined	Not determined
Bulk Affinity capillary electrophoresis	Protein concentration (μM)	1	1	1
	DNA Library concentration (μM)	0.1	0.1	0.1
	Bulk affinity K_D (μM)	>100	6	0.75

The initial library showed a bulk binding affinity of > 100 μM. After each round of selection, a decrease in K_D was observed. The 1st round of selection showed a bulk affinity of 1 μM and the 2nd round of selection showed a bulk affinity of 0.75 μM. This decrease in K_D confirmed that the selection of aptamers was progressing. The electrophoretogram of the enriched library from round 1 is shown in appendix 2, **figure b.1.** The second round of selection showed no improvement in the bulk affinity. The electrophoretogram for the 2nd round aptamer library is shown in **figure 4.8**.

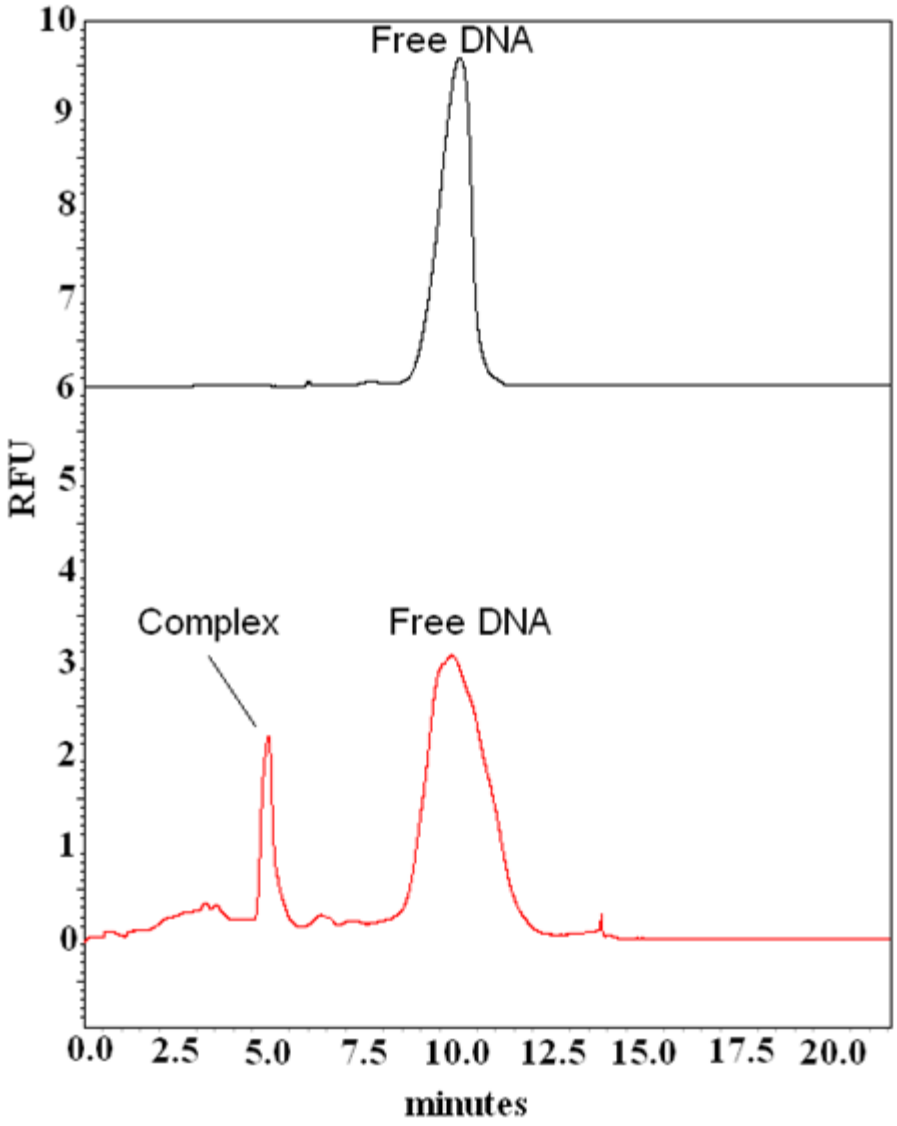

Figure 4.8 Bulk affinity analysis of the 2nd enriched library using capillary electrophoresis; Run buffer: 3xTGK and selection buffer 1xTGK, 333 Vcm^{-1}, 13 second injection, 1psi, 100 μm ID capillary; (a); 100 nM random library with LIF detection (b) 1 μM catalase protein and 100 nM enriched DNA library with LIF detection.

Comparing the electrophoretogram of the enriched DNA library of round 2 in **figure 4.8** with the electrophoretogram shown in **figure 4.5(b)** of the initial library, it can be seen that there is an increase in area of the complex peak and that the width of the DNA peak decreases. This suggests that the library has become more homogenous as the selection has progressed. When compared to the **figure 4.6** there is also a shift in the migration times of the library which is

possibly due to the library becoming more homogenous in nature and also due to the longer capillary size used.

4.2.3 Validation of catalase aptamer clone sequences

The enriched library from round 2 was selected for cloning and sequencing. The DNA was amplified using Taq polymerase and unlabelled primers, as labelled primers would interfere with the insertion into the vector. If a non-proof reading enzyme such as Taq polymerase is used, an adenosine overhang has to be added to the end of the DNA allowing for the easy inclusion into the clone vector which contains a T overhang. If a proof reading polymerase enzyme is used then an adenosine overhang can be introduced by simply heating the PCR product with ATP and taq polymerase at 74 °C. The DNA product was purified using an ethanol precipitation. For cloning pDrive vector was used. A ligation mixture was prepared on ice using the PCR product, the pDrive vector and distilled water. The mixture was mixed together and incubated at 4 °C. The ligation mixture was left overnight to give a more efficient ligation yield. The E. coli competent cells were thawed and immediately used for the transformation. The ligation mixture was mixed with the competent cells and incubated for 5 minutes on ice. The mixture was then subjected to heat shock at 42 degrees for 30 seconds and then returned to ice for a further 2 minutes. 250 µl of SOC medium was added to each transformation mixture and 100 µl plated onto a LB agar plate containing ampicillin using a spreader and incubated overnight at 37 °C. Blue white screening helps to determine the number of colonies that contain the PCR product. A white colony confirmed the presence of the PCR product in the bacteria colony. Each of the white colonies were cut out of the agar plate and transferred to a tube containing SOC medium. Each tube was incubated with shaking overnight.

The plasmid DNA was extracted using a plasmid extraction kit and purified. Then each sample was sequenced using single pass sequencing.

Out of the 20 colonies that were selected 4 gave successful sequences (CAT 1-4). The lack of successful sequences may suggest that the diversity of aptamers is very low. Each sequence was analysed on the OligoAnalyzer 3.1 software to determine whether sequences from specific conformations.

The secondary structures of the full sequences (CAT 1 – 4) and those of the truncated sequences (CAT 1T - 4T) are shown in appendix 2, **figure b.2 – b.5.** The full sequences showed significant folding in their secondary structures and they all displayed a negative Gibbs free energy. When compared to the truncated aptamer secondary structures, the truncated aptamers displayed a smaller negative Gibbs free energy and the secondary structures of the truncated sequences are also significantly different to those of the full structures suggesting that the constant region is involved in the formation of the structure.

The full aptamer sequences of CAT 1-4 were validated using two different binding affinity methods and the highest binding aptamer was accessed for specificity. The binding affinity K_D for both the affinity capillary electrophoresis and fluorescence intensity methods and the sequences of (CAT 1-4) are shown in **table 4.3**. As with the leptin selection, NECEEM allowed for the aptamers to be validated in free solution (3D), while the fluorescence method allowed for the aptamers to be validated against an immobilized target (2D). Validating the aptamer using two different methods gave a more robust analysis of the aptamers binding ability.

Table 4.3 A summary of the random region sequences and binding affinities of aptamers CAT 1-4 using both the NECEEM and fluorescence intensity methods.

	Random region Sequence	K_D NECEEM	K_D fluorescence intensity
CAT 1	**GACCTAGCAGTGGACATGTGGCAGGGTGAAGTGGCATCGTC**	**0.237µM ±0.13**	**0.430 µM ±0.4**
CAT 2	**ACTGGGCAGATTAACGGTCCTATATTTTCGGTTCTGGAAA**	**1.29µM ±0.2**	**3.53 µM ±0.7**
CAT 3	**CTTCCATGTTGAGGCGTTTATACCAGTTATCATCGGACTA**	**43.4µM ±2.2**	**14.6 µM ± 0.8**
CAT 4	**AGTGGCGAGGGGGGTAGGTAAAGTATCCTTAGTGTGTTTG**	**2.49µM ±3**	**8.36 µM ± 1.4**

Both methods showed that the best aptamer sequence (CAT 1) has affinity in the low micro molar region and validates the aptamer against both the free target and the immobilized target. The capillary electrophoresis electrophoretogram analysis of CAT 1 is shown in **figure 4.9**. The aptamer formed a stable complex which is confirmed by lack of DNA dissociation in the electrophoretogram. The electrophoretograms of CAT 2-4 are also shown in appendix 2, **figure b.6-b.8**. The non-linear regression graph for CAT 1 using the fluorescence intensity is shown in appendix 2, **figure b.9**. The binding affinity was determined from non-linear regression and plotted on GraphPad Prism.

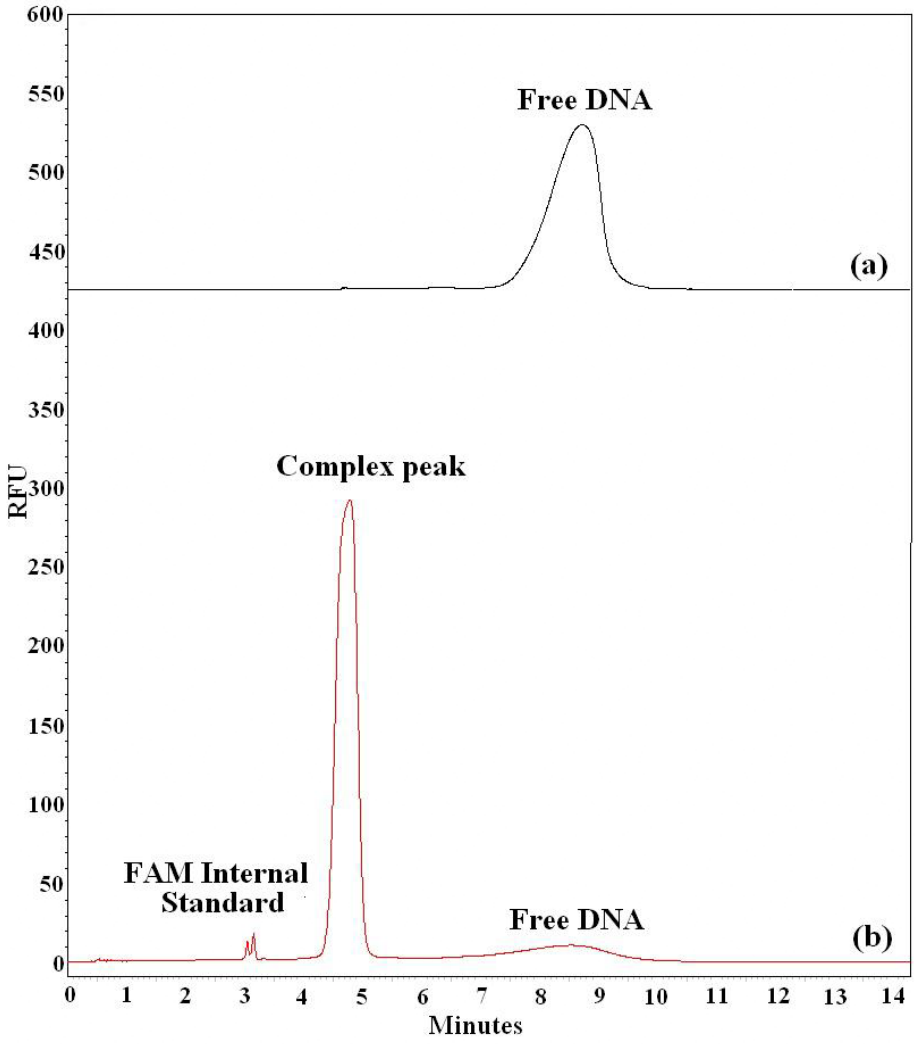

Figure 4.9 NECEEM analysis of CAT 1 aptamer; Run buffer: 3xTGK and selection buffer 1xTGK, 20 kV 13 second injection 1 psi, 100μm ID capillary; (a) 100 nM DNA library with LIF detection; (b) incubated mixture of 4 μM catalase, 100 nM catalase aptamer 1 and 10nM FAM internal standard with LIF detection.

.

The differences in binding affinities between the two methods suggest that there are some systematic errors associated with each method. The NECEEM method allowed for K_D determination of the target and aptamer in free solution, whereas the fluorescence intensity method relies on immobilizing the protein onto a well plate. As there is little control on the

orientation of the protein upon immobilization, systematic errors can arise from the aptamer being prevented from binding to the protein due to conformational and steric effects[126]. The NECEEM method relies on high reproducibility of injections which can vary from injection to injection, a source for some error in K_D although the use of an internal standard can account for this. Also the buffer conditions and ionic conditions of the two systems are different which could lead to a change in confirmation of the aptamer causing differences in the binding. DNA at lower concentrations has also been observed to adsorb to the sample vial wall which could be a source of error[127]. Overall the choice of method for K_D determination should depend on the application of the aptamer, choosing the NECEEM method for aptamers which will be used in a free solution application such as in the development of molecular beacons or using the fluorescence intensity when the aptamer is to be immobilized as in the case of biosensors. The apparent differences in the two techniques were also observed in the selection of leptin aptamers but in this study the difference in binding affinities between two methods was much less suggesting that systematic errors aren't the only factor in measuring the binding affinities.

For the specificity, the fluorescence intensity assay was performed on 4 different proteins to analyze the specificity of CAT 1 aptamer. A similar method to the fluorescence intensity method was used. The proteins were immobilized onto a microplate and a non-linear regression graph was plotted of the fluorescence signal against the aptamer concentration which is shown in appendix 2, **figure b.10**. A negative control of BSA only incubated with aptamer was used as the baseline signal. The binding affinity was measured against lysozyme, trypsinogen, chymotrypsinogen A and myoglobin protein and their binding affinities are shown in **table 4.4.** The aptamer displayed at least a 100 fold decrease in affinity towards these four proteins and this confirms that the aptamer exhibits a distinct specificity towards bovine catalase. Lysozyme had

the highest binding affinity of 15 ± 0.3 μM. Although specificity has been demonstrated, the specificity should be retested in the medium that the aptamer is intended to be used.

Table 4.4 Binding affinities of lysozyme, trypsinogen, chymotrypsinogen A and myoglobin using fluorescence intensity against CAT 1 aptamer sequence.

Protein	Lysozyme	Trypsinogen	Chymotrypsinogen A	Myoglobin
K_D	15 μM±0.3	593μM±7	<1mM	20 μM±0.24

4.2.4 The Non-SELEX of hemoglobin aptamers

The migration time for the collection of hemoglobin aptamers was determined to be between 3.5 and 8 minutes as shown in **figure 3.10.**

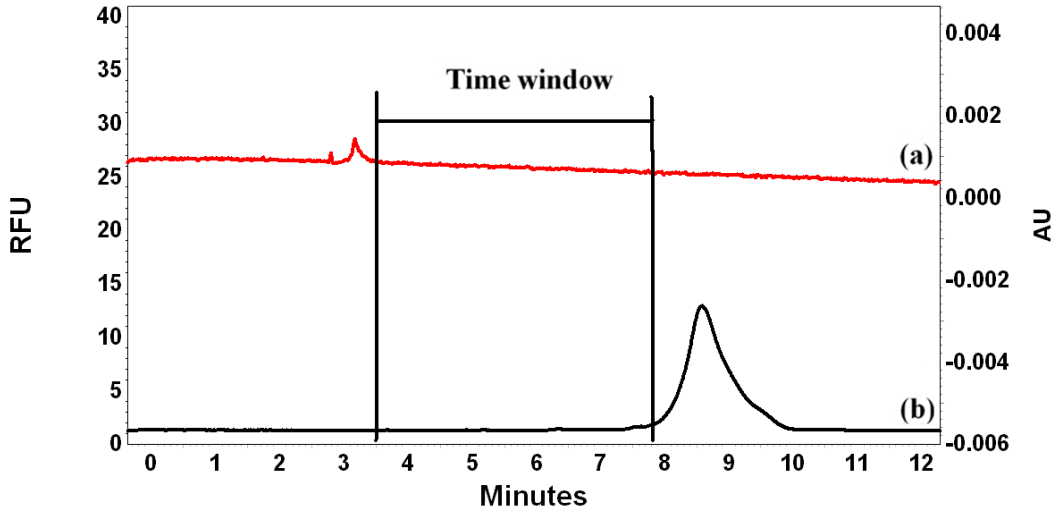

Figure 4.10 Time window for hemoglobin binding aptamer collection using capillary electrophoresis, Run buffer: 3xTGK and selection buffer 1xTGK, 333Vcm^{-1}V, 13 second, 1psi injection 100μm ID; (a) 2μM catalase protein using PDA detection 280nm; (b) 100nM random library using LIF detection.

As with the other selections, the hemoglobin, and DNA library will migrate after the EOF, with hemoglobin migrating before the DNA. The fraction collection was completed using the same conditions that were previously reported for the catalase selection with the exception that no complex peak was seen and as a result the fraction collection was carried out blind. 2 rounds of selection were carried out as there was no improvement in the bulk affinity binding even upon increasing the hemoglobin concentration. The fractions collected were amplified using PCR as described before and analysed using a 2 % agarose gel. The resultant dsDNA was then separated using streptavidin as described for the catalase selection. The bulk affinity of the aptamer library was measured using affinity capillary electrophoresis. For this selection we choose affinity analysis instead of NECEEM due to the lack of complex peak observed in the electrophoretogram as shown in **figure 4.11**.

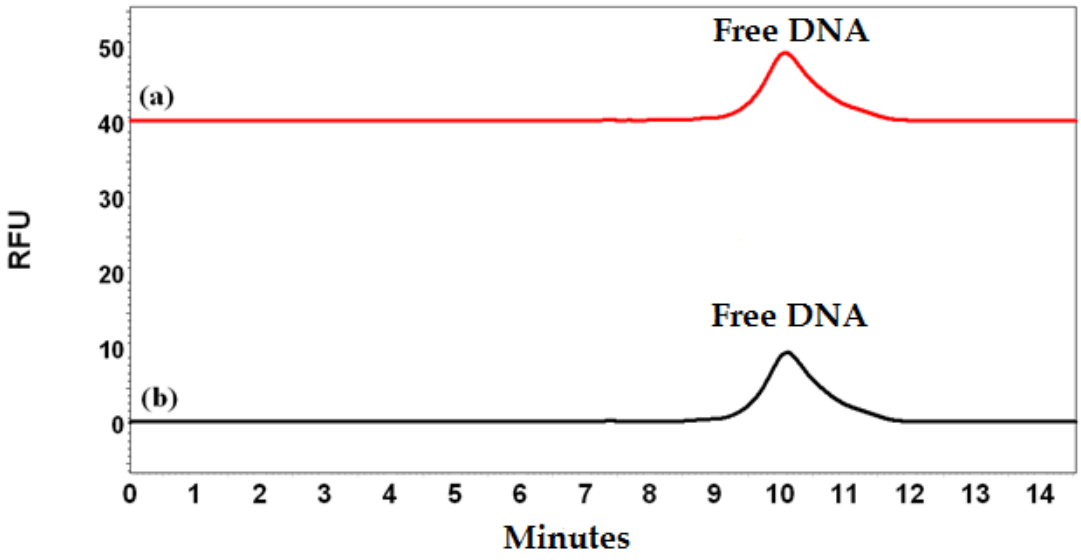

Figure 4.11 Electophoretogram of the 1st enriched library using capillary electrophoresis; Run buffer: 3xTGK and selection buffer 1xTGK, 333Vcm^{-1}, 13 second, 1psi injection, 100μm ID capillary; (a) 100nM random library with LIF detection; (b) 13.9 μM haemoglobin protein and 100nM enriched DNA library with LIF detection.

Affinity capillary electrophoresis relies on the measuring the peak height of the unbound DNA and comparing the peak heights of the unbound DNA without the target to the peak heights of the unbound DNA in the presence of different concentrations of target. This allows us to determine the ratio of bound DNA and hence the complex concentration assuming 1 to 1 binding. The difference between this method and NECEEM is that affinity capillary electrophoresis does not need a complex peak to be observed when determining the K_D. This is useful when there is a quenching effect between the target and the DNA fluorophore. As with the catalase selection bulk affinity K_D cannot be accurately determined for highly heterogeneous library of DNA. However it is an indicator of the progress of selection and a decrease in K_D tells us that the selection is progressing. The conditions of selection and the bulk affinity analysis by affinity capillary electrophoresis are shown in **table 4.5.**

Table 4.5 A summary of the conditions for non-SELEX selection of Hemoglobin aptamers and bulk affinity analysis of enriched aptamer libraries after each round of selection using capillary electrophoresis.

		Rounds of Selection		
		0	1	2
Selection conditions	Protein concentration (µM)	20.5	1	0.1
	DNA Library concentration (µM)	50	Not determined	Not determined
Affinity capillary electrophoresis (ACE)	Protein concentration (µM)	0 - 20	0 - 14.64	0 - 14.64
	DNA Library concentration (nM)	10	10	10
	Bulk affinity K_D (µM)	>100	2.2	3.1

From the table we can see that there was no improvement in the bulk affinity K_D from round 1 to 2 even upon a decrease of target concentration suggesting that the library had reached enrichment. The electrophoretogram and linear regression plots of round 1 are shown in appendix 2, **figure b.11** and **b.12** respectively.

4.2.5 Validation of hemoglobin aptamers clone sequences

We chose the enriched library from round 1 for cloning and sequencing and 26 white colonies were successfully cloned and 3 sequences were found.

The full sequences (HB 1-3) and the truncated sequences (HB 1T-3T) were analysed on OligoAnalyzer 3.1 to determine the Gibbs free energy and the secondary structures are shown in Appendix 2, **figure b13 – b15**. From all the full aptamer sequences found, all three displayed a negative Gibbs free energy which suggests that the aptamer sequences easily fold into distinct aptamer conformations. Comparing the secondary structures of the full and truncated structures, we can see that there are differences in the conformation between the full and the truncated structures suggesting that the whole structure of the aptamer is involved in the binding with hemoglobin. The truncated structure of (HB 1T-3T) showed lower Gibbs free energies suggesting that they are less likely to fold into distinct conformations.

The full aptamer sequences were validated for binding affinity and specificity. As stated previously, there was no complex peak observed during selection and so we chose to validate the aptamer using affinity capillary electrophoresis. A summary of the K_D binding affinities of the 3 aptamers is shown in **table 4.6.**

Table 4.6 A summary of the random region sequence and binding affinities for each full hemoglobin aptamer using affinity capillary electrophoresis.

	Random region Sequence	K_D ACE
HB 1	**CAATGTCTAGTTTCGTTACGCCGTGAAAAGCTGACGACCG**	**0.187 µM ± 0.01**
HB 2	**GCGCATTTGAGACGTAAGGGCCTACAACTCGGCTGCCTA**	**1.60 µM ±0.12**
HB 3	**CACCCTGACTACTATTTTGCATTCGGCTACTTTCCTTCAC**	**1.32 µM ± 0.15**

Affinity capillary electrophoresis was chosen as the method for validating the aptamers binding affinity towards the target due to the lack of a complex peak in the electrophoretogram. The absence of a complex peak maybe due to a quenching effect between the aptamer and the target upon binding, or it may be that the complex peak is too small to be detected using LIF. For the affinity capillary electrophoresis assay, 10 µM – 10 nM of hemoglobin was titrated against 10 nM of each aptamer. The heights of the peaks were corrected against the internal standard and total bound aptamer was determined using **equation 1.2**. The electrophoretogram is shown in **figure 4.12.** When a higher concentration of protein is titrated against the aptamer, the peak height decreases suggesting that a complex is indeed formed. This is due to a change in electrophoretic mobility of the complex in comparison to the free aptamer and the target. Again no complex peak was observed, possibly due to a quenching effect. Aptamer HB1 showed the highest binding affinity with a K_D of 0.187 ± 0.01 µM. The difference in K_D between this and the bulk affinity is considerable and suggests that the bulk affinity is in no way an indicator of the K_D of individual aptamer sequences or even accurate.

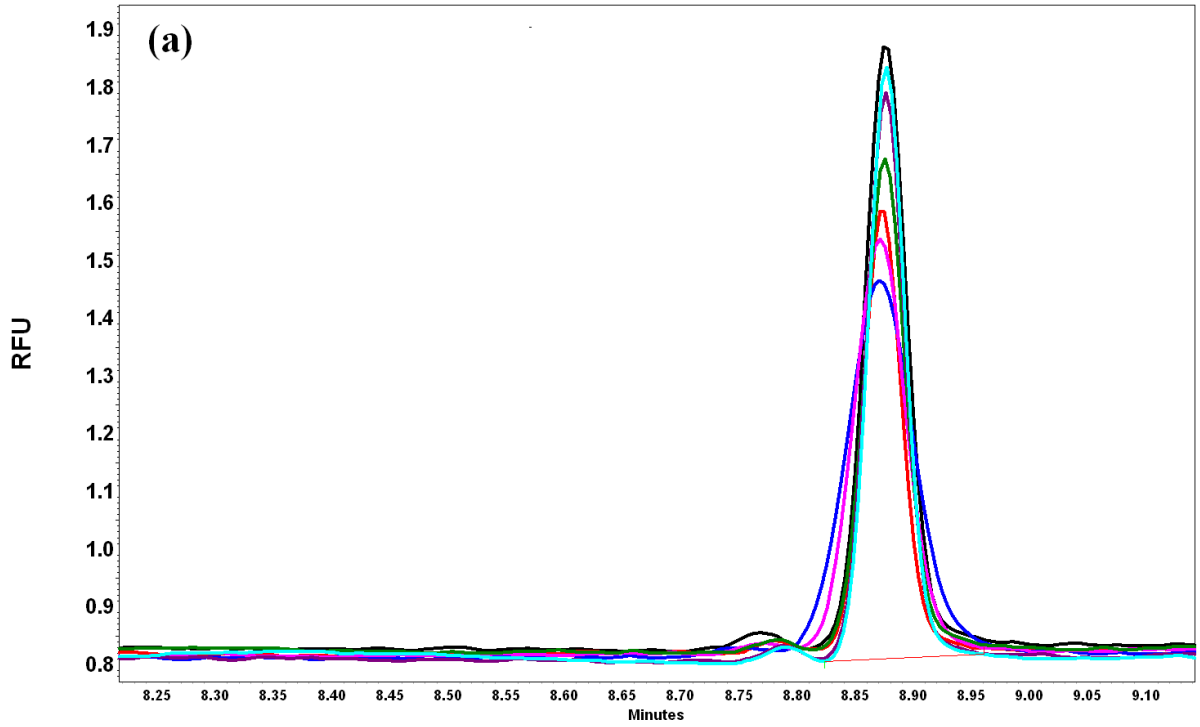

Figure 4.12 ACE electrophoretogram of hemoglobin HB1; (10µM - 10nM) of protein is titrated against 10nM of aptamer and the peak heights were corrected using 10nM of fluorescein internal standard. The analysis was performed in triplicate.

A non-linear regression curve was plotted of ratio of bound DNA in terms of concentration against the protein concentration and is presented in **figure 4.13**. 1:1 binding is assumed a R^2 value of 0.998 was fitted. The non-linear regression graphs of HB 2 and HB3 are shown in appendix 2, **figure b.16** and **b.17** and gave lower binding affinities than for HB1.

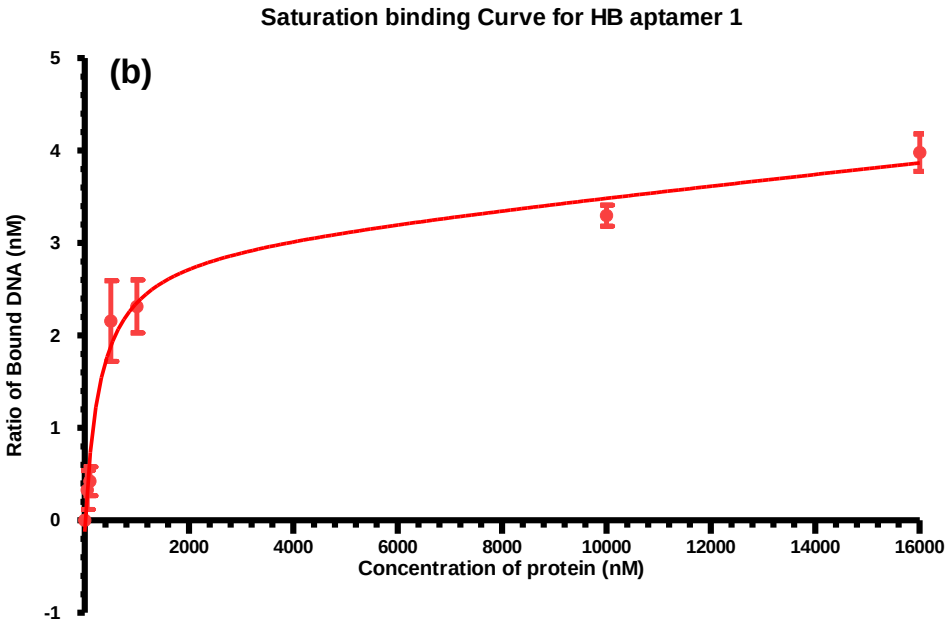

Figure 4.13 Non-linear regression analysis of HB1 aptamer; The ratio of bound DNA to unbound DNA in terms of concentration is plotted against protein concentration. The binding affinity K_D was determined using equation. 1.2.

The specificity of the HB1 was analyzed by using a method described by Mendosa *et al* [71]. The peak heights of 4 different acidic proteins were measured. The binding affinity of each protein can be estimated by comparing the peak heights of the aptamers at different concentrations. If the peak height does not decrease upon addition of each protein compared to the peak height of the initial aptamer where no protein has been added, then the aptamer will display specificity towards hemoglobin. The point at which the peak height starts to decrease is the point at which the K_D can be estimated. **Figure 4.14** shows the specificity plots of HB1 against catalase, α acid glycol protein, cholesterol esterase and trypsin inhibitor. The estimated binding affinites of each protein towards HB1 aptamer are shown in **table 4.7.**

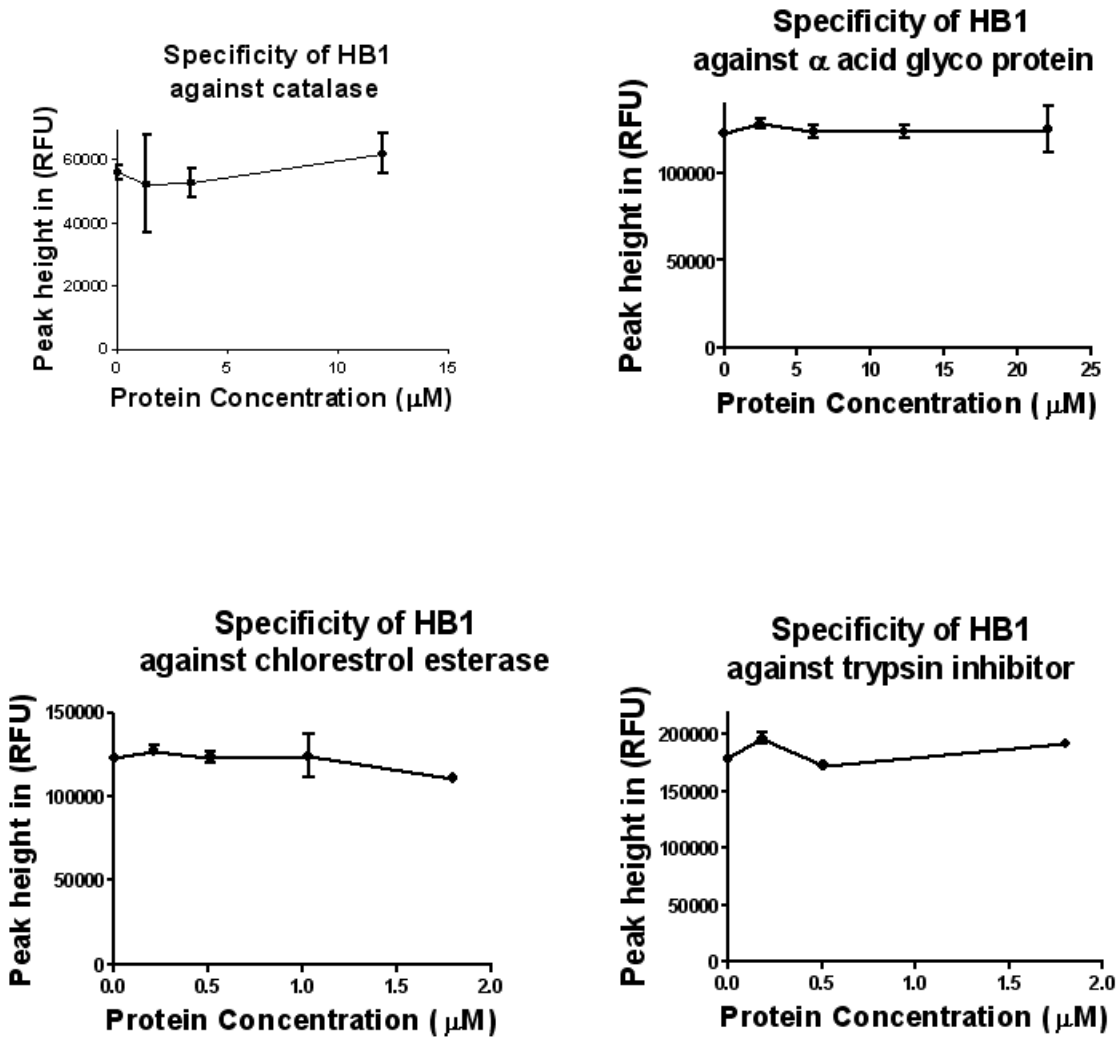

Figure 4.14 Plots showing the specificity of HB1 against different proteins. The peak height was measured at various concentrations (0-20 μM).

Table 4.7 A summary of the estimated binding affinities of different proteins towards HB1 aptamer.

	Bovine catalase	**α acid glycol protein**	**cholesterol esterase**	**trypsin inhibitor**
K_D	>12 μM	>22.5 μM	>1.8 μM	>2 μM

From the estimated binding affinities, we can see that both bovine catalase and α acid glycol protein showed considerably lower binding affinities towards HB1 compared with hemoglobin.

The cholesterol esterase and trypsin inhibitor showed higher binding affinities towards HB1 but they are still low when compared to hemoglobin. These results suggest that the aptamer demonstrates good specificity towards hemoglobin. However it is important to note that the specificity should always be tested again in the application of the aptamer.

4.3 Summary

The non-SELEX method was successfully used to find aptamers (CAT 1 and HB1) with high nanomolar range for bovine catalase and human hemoglobin. Although this is not the lowest K_D reported in the literature for protein targets, the K_D is acceptable for application in SPR which is demonstrated in the next chapter of this thesis. When looking at the full range of targets reported K_D can vary from the picomolar range to micromolar range. Clearly there are more factors at play regarding the selection of aptamers with high binding affinities. Some proteins have been shown to interact with ssDNA in nature and this would make them more predisposed to interact with aptamers.

Both CAT 1 and HB 1 showed good specificity towards bovine catalase and human hemoglobin respectively. Although this gives a clear indication of the specificity towards common proteins, specificity should be retested using the medium in which the aptamer is to be used. For hemoglobin, aptamers were selected after just one round of selection using non-SELEX despite the lack of a complex peak. This suggests that aptamers can still be selected in a blind type selection. Also from the reported bulk affinity K_D, there was a considerable difference in values when compared to the actual K_D reported for HB1. This may reinforce the view that the determination of bulk affinity K_D is not accurate and is merely a way to monitor the progress of

selection. Perhaps comparing the peak heights of the bound and unbound aptamer would be a better indication of the progress of reaction and be an indicator of whether a quenching effect is occurring. This could be especially useful when no complex peak is observed or if there is little sample available.

When comparing the method of non-SELEX described in this chapter and that of the CE-SELEX in chapter 2 it is difficult to make a direct comparison. The use of real time PCR was not available in this project so we had to use normal PCR with agarose gels instead. The non-SELEX was quicker to carry out than the CE-SELEX due to the lower number of rounds of selection but the fractions collected from the non-SELEX were more difficult to amplify due to the use of normal PCR and also because the template concentration gets progressively smaller in each round of non-SELEX. This problem could be overcome by using next generation sequencing which is more sensitive and convenient. However this technology was not accessible in the lab.

The aptamers generated from both CE-SELEX and non-SELEX showed quite similar binding affinities. This suggests that the two methods are comparable to one another. What needs to be address is our understanding of how aptamers interact with their targets and more characterization studies of these interactions need to be completed.

As previously stated there were a number of issues which needed to be addressed to improve on the non-SELEX procedure. Some of these problems have been improved upon in this study such as increasing the number of sequences and maximizing the stability and sensitivity of the complex peak. The number of sequences that are screened has been limited due to the extremely small diameter of the capillary. Our results showed that by using appropriate wide bore

capillaries the number of sequences that can be screened, could be maximized without causing significant Joule heating or deterioration of peak shape. Moreover, buffer optimization is also a lengthy procedure. Our results showed that by using selection buffer and run buffer of different ionic strengths, we could maintain the stability of the complex peak while inducing a stacking effect and improve upon the stability and size of the complex peak.

It is also worth noting that when choosing a method for K_D determination it may be worth considering that the properties of aptamers may change depending on the environment in which the aptamer is selected in and its application. It may be worthwhile to consider using a kinetic based assay which mimics the desired application to give more accurate kinetic parameters, although further investigation into the comparison of these techniques needs to be done to confirm this. The mechanism of binding will also be elucidated using x-ray crystallography

The aptamers selected in this chapter will be used in bioanalytical applications. Catalase was used to develop an aptamer based biosensor which is described in the next chapter. The hemoglobin aptamer selected will be used as an affinity probe in capillary electrophoresis.

5 Hybridised-SELEX of cholesterol esterase

5.1 Aim

In chapters 2 and 3 we developed aptamers using both the CE-SELEX and non-SELEX methods. These methods have allowed for the selection of aptamers in less than 4 rounds. However these methods suffer from one major drawback. They both can only screen a limited number of sequences from the DNA library.

Recently Jing *et al* developed a microfluidic based selection method using micro free flow electrophoresis (μFFE) [83]. This method allowed for 1.8 $x10^{14}$ sequences to be screened continuously in 30 minutes and was used to select aptamers for human IgE in the low nanomolar range using only 1 round of selection. However microfluidics suffers from poor reproducibility, has lower sensitivity when compared to CE and there are issues with biomolecule compatibility [128]. Also, micro free flow electrophoresis is not commercially available to the average biochemist.

In this chapter, the proof of principle of hybridised-selection to improve on the number of sequences selected for capillary based selection will be discussed. Hybridised-SELEX allows for the selection to be done using a classical method such as nitro cellulose filter (NC), followed by a capillary based method such as non-SELEX or CE-SELEX. The initial round of NC filtering will allow for a larger proportion of the library to be screened and selection can be carried out using fewer rounds of selection. As with the previous CE based methods, the hybridised-SELEX will also allow the selection to be carried out in free solution removing the need for immobilization of the target. The hybridised SELEX method involves incubating the target with

the DNA library and then passing the solution through the filter without blocking it using BSA or performing a negative selection step. The complex and the non-specific binders are retained on the filter, while the non-binding sequences pass through. The binding sequences are removed by denaturing with urea and the resultant solution is then purified using isopropanol precipitation.

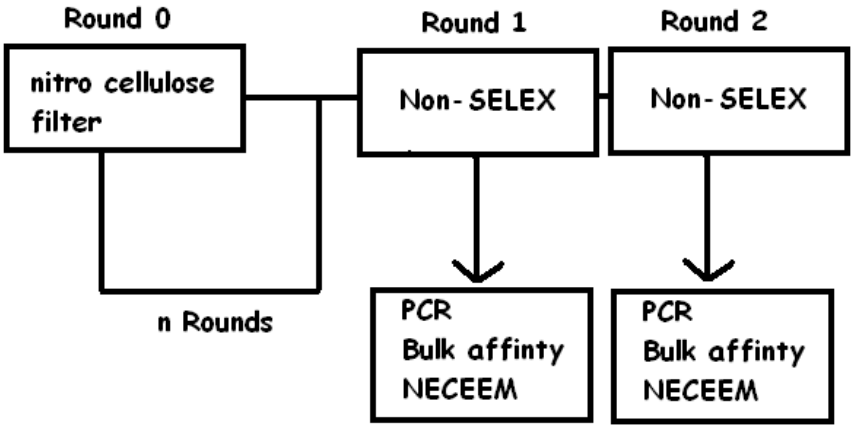

Figure 5.1 A general scheme for hybridized SELEX procedure; Round 0 involves passing an incubated mixture of target and DNA library on a NC membrane filter based partitioning. The recovered DNA can then be directly injected onto the capillary. If no complex peak is observed then the recovered DNA can be amplified and another round of NC filtering can be performed.

The bulk affinity K_D can be determined using NECEEM. This process is repeated until a complex peak is observed and then 1-2 rounds of non-SELEX can be carried out. The general scheme for hybridised SELEX is shown in **figure 5.1**. The model target used for this study was cholesterol esterase, a large acidic protein. The enzyme is responsible for the conversion of sterol esters to sterols. The structure of bovine cholesterol esterase is illustrated in **figure 5.2.** To the best of our knowledge, DNA aptamers for cholesterol esterase have not been previously reported.

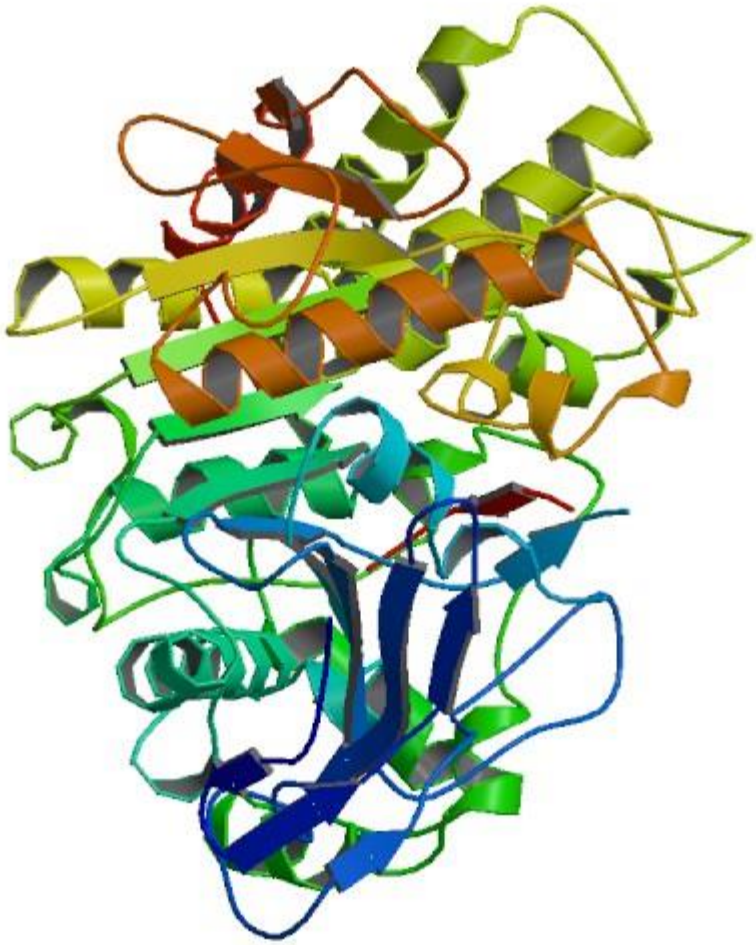

Figure 5.2 The structure of Cholesterol esterase from bovine *Bos Taurus*[129].

An aptamer developed for this protein would find use in biosensoring applications as well as immunology as an alternative to antibodies.

5.2 Results and discussion

5.2.1 The Hybridised -SELEX procedure

The time window was determined by injecting the protein and the DNA library separately. The protein gave several peaks starting at 1.2 min suggesting that the cholesterol esterase contained more than one isoform. The strong signal at 280nm also suggested that the protein contained a large proportion of aromatic containing amino acids. As with previous selections, the DNA library migrated last with a broad peak due to the heterogeneous nature of the sample. The time window was determined to be between 1.2 and 4.8 minutes and is shown in **figure 5.3**.

The analysis time was shortened for this selection by reducing the total and effective capillary lengths to 40 and 30cm respectively. This was to speed up the time for the selection. As a result, the separation current was too high when the existing buffer conditions were employed. Therefore we dissolved the protein target and the DNA library in water and the run buffer was 3x TGK. The electrophoretogram for the protein shows multiple peaks for the cholesterol esterase suggesting that the protein is made up of more than one isoform.

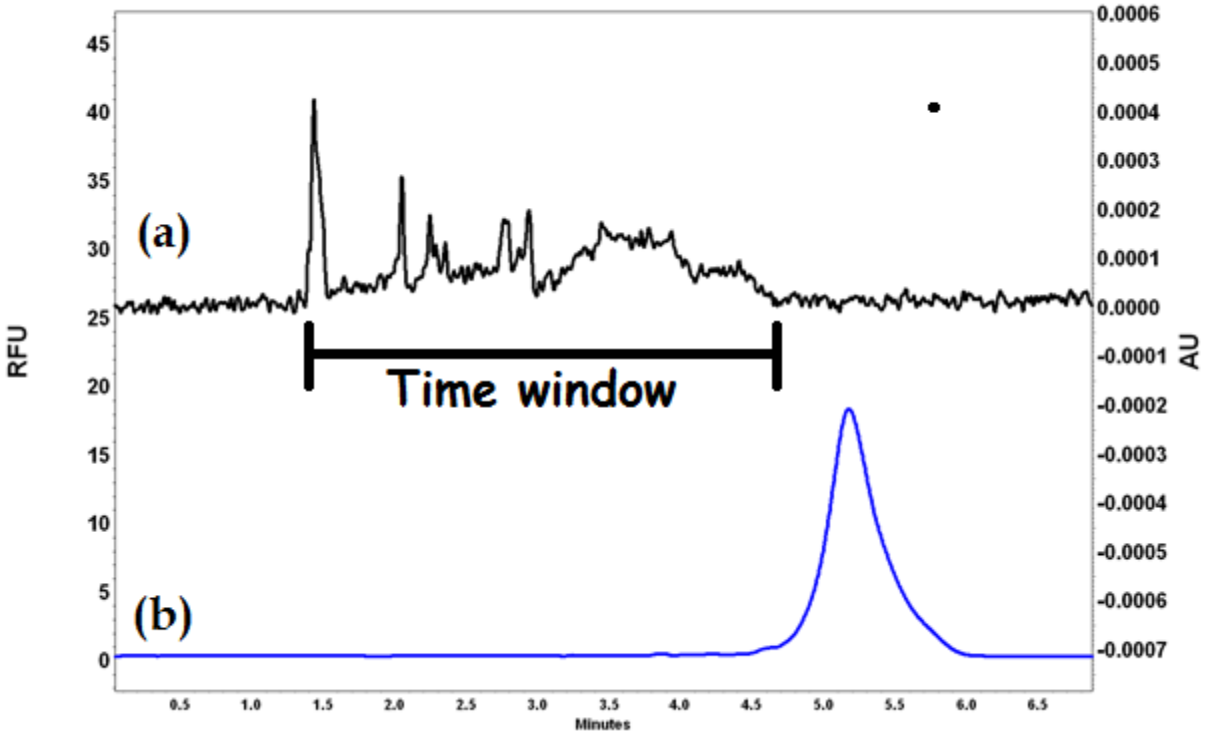

Figure 5.3 Time window determination (a) 1 µM Cholesterol esterase, 500 Vcm^{-1}, 9.90nl hydrodynamic injection with PDA 280nm detection; (b) Equilibrium mixture of 100nM DNA and 1.0 µM Cholesterol esterase; 500 Vcm^{-1} separation, LIF detection ,RB: 3xTGK, SB: nuclease-free water, 50 µm ID capillary.

Initial experiments on hybridized-SELEX involved combining magnetic beads based selection with non-SELEX. The use of magnetic beads involved biotinylation of the target followed by incubation with a streptavidin affinity capture step. The magnetic beads yielded very poor results in terms of recovery of DNA and it was decided that a hybridized SELEX involving nitro cellulose filters (NC) would give better results. The original selection of aptamers by NC membrane filters involves immobilizing the protein onto the membrane filter and blocking the remaining sites with BSA to prevent non-specific binding of DNA sequences to the filter. In our procedure, we chose not to immobilize the protein onto the membrane and instead incubated the DNA library with the target protein in solution and then added the DNA and target directly onto

the membrane. In theory the unbound DNA should pass directly through the filter leaving the complex stuck on the filter. As there is no blocking step, there was also a significant amount of nonspecific binders that were retained on the membrane. These non-specific DNA binders can be removed in the subsequent non-SELEX partitioning steps assuming that there is no interaction between the target and these sequences. The DNA on the membrane was eluted using 7 M urea which is known to denature DNA and disrupt the DNA protein target complex. The DNA can then be purified using chloroform: phenol extraction and isopropanol precipitation. The ssDNA was reconstituted in 10 µl of water and DNA library recovery was measured on the nanodrop spectrometer. From the recovery it was found that the DNA library can be incubated with the target and directly injected onto the capillary without a PCR amplification step.

The number of estimated sequences recovered was 10^{13} sequences and the number of sequences injected was 10^{10} sequences. All non-binding sequences have already been removed in the NC step. Also there is no need for immobilization of the target on the nitrocellulose filter and subsequent blocking with BSA. The complex is pre-formed in solution and the binding sequences were retained on the filter along with the non-specific binding sequences. These non-specific binding sequences were removed in the subsequent capillary electrophoresis rounds.

Table 5.1 A summary of the selection conditions and conditions for NECEEM bulk affinity determination of CE aptamers.

		Rounds of Selection		
		NC	1	2
NECEEM Conditions	**Protein concentration (µM)**	1.20	0.25	0.10
	DNA library concentration (µM)	0.110	0.190	0.197
Selection Conditions	**Protein concentration (µM)**	1.0	1.0	0.1
	DNA library concentration (µM)	50	0.172	Not Determined
	Bulk affinity K_D (nM)	1320	445.9	98.12

2 rounds of CE based partitioning were performed without intermittent amplification by PCR. Fractions were collected manually by determining the elution point using **equation 1.1** to calculate the elution factor. Fractions were collected into vials containing 5 µl of 0.1 µM protein. Fractions were collected 3 times for each round of selection. The outlet vial was then reinjected and 3 further fractions were collected. 2 rounds of CE based partitioning were performed. The fractions from each round of selection were amplified using PCR.

The bulk affinity K_D was determined on the recovered fraction collected from the nitrocellulose membrane and on the enriched fractions collected from each round of capillary electrophoresis. The bulk K_D was estimated using NECEEM. The estimated bulk binding affinities are shown in **table 5.1.** A decrease from 1320 nM to 98 nM in the final round of CE selection showed that the selection was progressing. **Figure 5.4** illustrates the bulk affinity electrophoretogram of the library after the NC round.

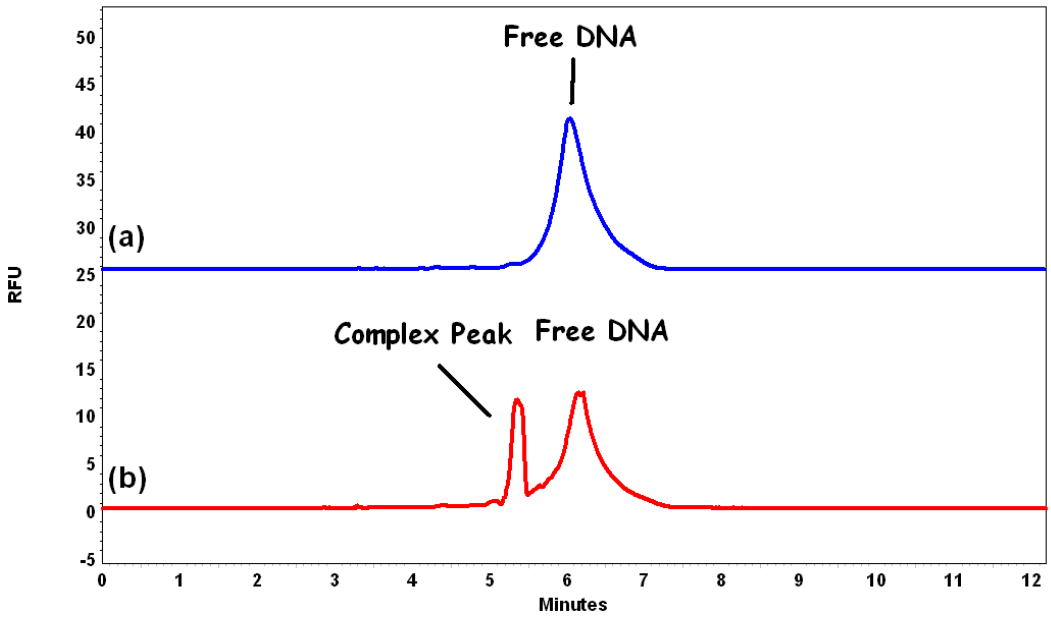

Figure 5.4 Bulk affinity determination post NC (round 0); (a) 100 nM DNA library; (b) Equilibrium mixture of 100nM DNA and 1.2 µM Cholesterol esterase; 500 Vcm-1 separation, LIF detection, RB: 3xTGK, SB: nuclease free water 50 µm ID capillary.

When compared to the initial library electrophoretogram, in **figure 5.3** we can observe the formation of the complex peak which confirms that the NC round allows for a considerable increase in the number of sequences that are selected and is comparable to classical methods. The electrophoretograms of rounds 1 and 2 also show the complex peak at even lower target concentrations (See appendix 4, **figure c.1** and **c.2**).

5.2.2 Validation of cholesterol esterase clone sequences

The enriched library from round 2 was cloned and sequenced and out of the 20 colonies selected, 6 sequences were successfully found. The secondary structure of each sequence (CES 1-6) was accessed for binding using oligoanalyzer 3.1 . As mentioned before, the folding is simulated using a NaCl concentration of 100mM and $MgCl_2$ concentration of 5mM. The secondary

structures of both the truncated and full structure and are shown in (Appendix 4, **figure c.3-c.8**). For CES 3 and CES 4, both the truncated and full structures show a well-defined conformation and the secondary structure of the truncated structure does not change upon removal of the constant region.

Table 5.2 A summary of the binding affinities of the full aptamer sequence using NECEEM.

Name	Random Region	NECEEM K_D
CES 1	CACTTCCTGCTTGTGCCAAGGGTGACGAGTTATTTTAAAA	3.6 ± 0.36 µM
CES 2	CTCGAGCCTAGGCTAGCTCTAGACCACACGTGTGGGGGCCC	211.17 ± 6.8 nM
CES 3	CTGTTTAAGACTGTAAATCATAAATTGCAATCTTTCGTGG	162.17 ± 28 nM
CES 4	TGTGTGAAATTGTTATCCGCTCACAATTCCACACAACATAC	116.6 ± 4.7 nM
CES 5	CCCCCTCTCCCGCGGGGGGGTATGTAAATATAAACAGGGGG	204.16 ± 8.6 nM
CES 6	CTAAGAATACTTTGGGCTACCGTATTTGGAGGTTCCATAA	541.17 ± 82 nM

The full structures clone sequences (CES 1-6) and truncated clone sequences (CES 3T and CES 4T) were validated using NECCEM. The binding affinities for aptamers CES 1-6 are shown in **table 5.2**. Aptamer CES 4 gave the best binding affinity with a K_D of 116.6 ± 4.7 nM. The binding affinities were lower than for the bulk affinity which confirms that the bulk affinity wasn't an accurate measure of actual binding affinities.

From the electrophoretogram shown in **figure 5.5**, it can be seen that after incubation, there are a number of complexes observed which shows that the aptamer forms complexes of different stoichiometry.

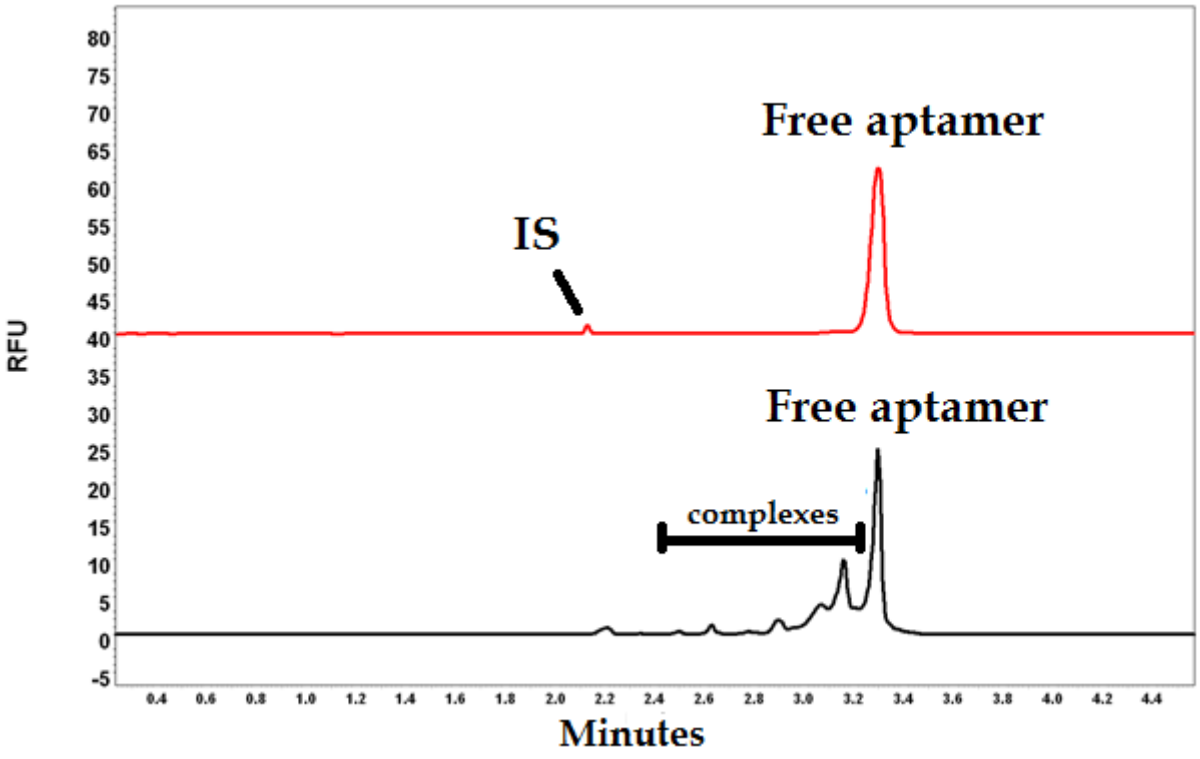

Figure 5.5 NEECEM analysis of CES4; 100nM aptamer and 200nM cholesterol esterase were incubated for 30 minutes and injected onto the capillary by hydrodynamic injection (9.90 nl), 500Vcm^{-1} separation with LIF detection. The areas of the free DNA, dissociated DNA and complex peak were used to determine K_D and 3 experiments were performed for each sequence.

This is due to the fact that cholesterol esterase is quite a big target for the selection allowing for multiple aptamers to bind. Also, as discussed previously, the protein has more than one isoform present. The electrophoretograms for aptamers CES 2, CES3 and CES 5 also gave multiple complex peaks and are shown in Appendix of chapter **figure c.9 - c.11**. From the binding analysis, the truncated structures of CES 4 and CES 3 demonstrated a good secondary structure with the random region conserving the same shape. A negative Gibbs free energy also suggested that the truncated structure could display the same binding as the full structure. Therefore we

validated the truncated structure of CES 4 and 3 using NECEEM. The binding affinities of CES 3T and CES 4T are shown in **table 5.3**.

Table 5.3 Summary of the binding affinities of the truncated aptamer sequence using NECEEM and Fluorescence polarization.

Name	Random Region	NECEEM K_D	Fluorescence polarization K_D
CES 3T	CTGTTTAAGACTGTAAATCATAAATTGCAATCTTTCGTGG	1.64 ± 0.386 µM	Not determined
CES 4T	TGTGTGAAATTGTTATCCGCTCACAATTCCACACAACATAC	203 ± 14 nM	248 ± 0.08 nM

The electrophoretogram of CES 4T is shown in **figure 5.6** and gave rise to a binding affinity of 203 ± 14 nM and 248 ± 0.08 nM using NECEEM and the fluorescence polarization methods respectively. When comparing the NECEEM electrophoretogram in **figure 5.5** to that of **figure 5.6**, there is an observed decrease in the number of complex peaks. There is also a shift in the migration times of the free truncated aptamer and complex peak which is due to the decrease in molecular weight of the aptamer and decrease in the hydrodynamic radius which reduces the electrophoretic mobility.

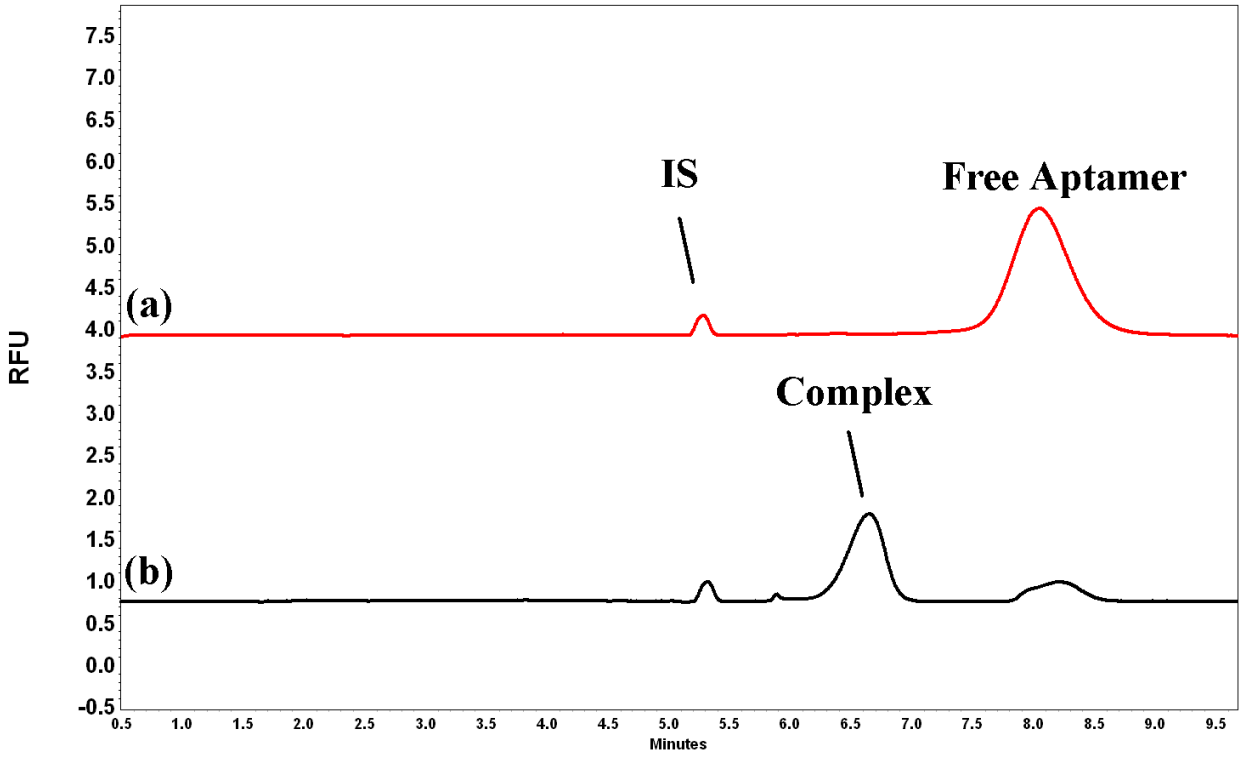

Figure 5.6 NEECEM analysis of CES 4T; 100nM aptamer and 1μM cholesterol esterase were incubated for 30 minutes and injected onto the capillary by hydrodynamic injection (9.90 nl), 500Vcm^{-1} separation with LIF detection. The areas of the free DNA, dissociated DNA and complex peak were used to determine K_D and 3 experiments were performed for each sequence. Fluorescein was used as the internal standard (IS)

The binding affinity of CES 4T was further confirmed by fluorescence polarization. The binding affinity decreased to 248 ± 0.08 nM. The Fluorescence polarization gave a slightly higher binding affinity when compared to NECEEM, but the two results are close to one another. The Fluorescence polarization plot is shown in **figure 5.7**.

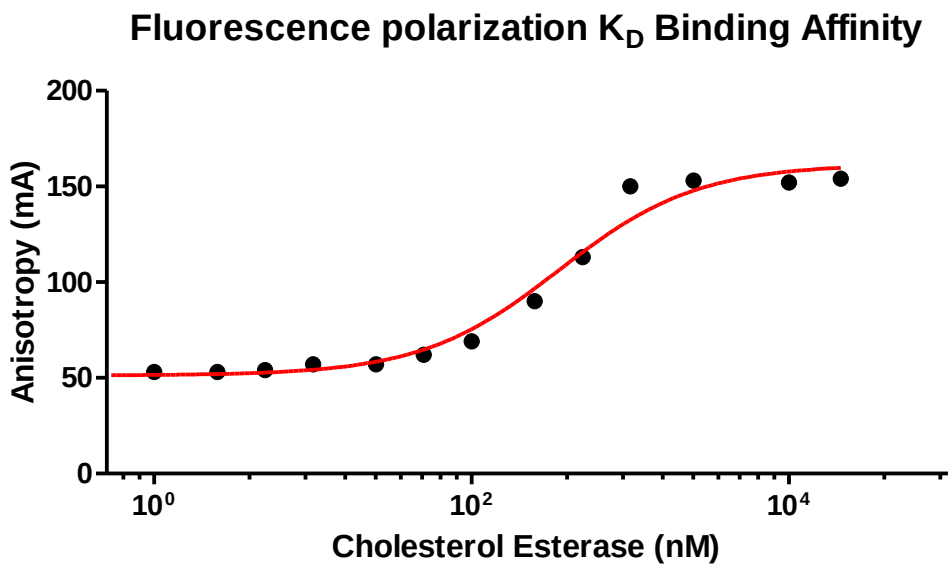

Figure 5.7 Fluorescence Polarization plot of Anistropy (mA) against the log cholesterol esterase concentration. Concentrations of cholesterol esterase were incubated with 10nM. CES 4T. K_D was determined by non-linear regression.

When comparing the binding affinities of both CES 4 and CES 4T, there is a decrease from 116 nM to 203 nM which suggests that the constant regions are involved in the binding and may give rise to the higher number of binding stoichiometries whereas the truncated structure only showed one peak although a broad peak is observed which may mask some of the other peaks.

The specificity was measured using NECEEM against several common acidic proteins (α glycol acid protein, amylose glycosylase, trypsin inhibitor and bovine catalase). The electrophoretogram of CES 4 aptamer incubated with different proteins is presented in **figure 5.8.**

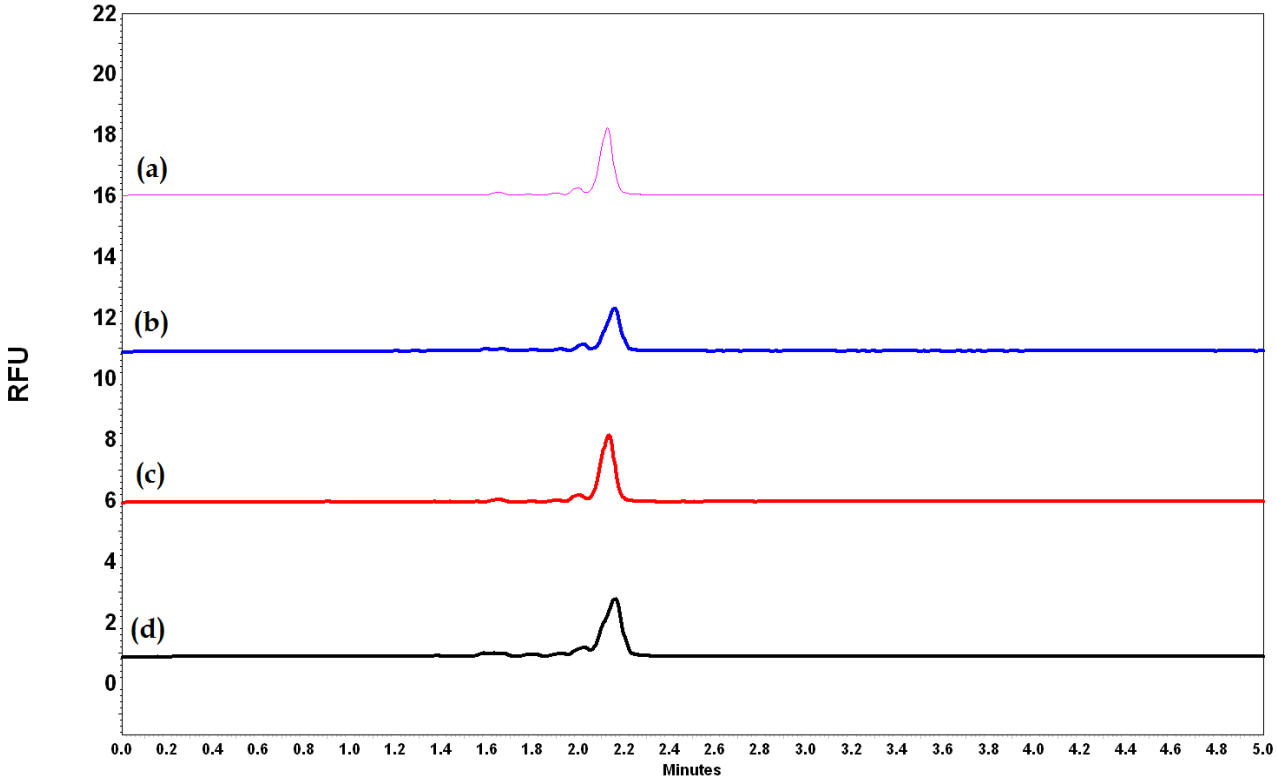

Figure 5.8 NECEEM based specificity for (a) 1 µM α glycol acid protein, (b) 1 µM amylose; (c) trypsin inhibitor and (d) bovine catalase proteins were incubated with 0.1 µM of CES 4 aptamer and injected onto the capillary by hydrodynamic injection (9.90 nl), 500Vcm^{-1} separation with LIF detection. The areas of the free DNA, dissociated DNA and complex peak were used to determine K_D and 3 experiments were performed for each sequence.

The K_D was determined by comparing the areas of the complex peak and free aptamer peak**.** CES4 aptamer shows a much greater specificity towards cholesterol esterase when compared to α glycol acid protein (8.86 µM), amylose glycosylase (9.23 µM), trypsin inhibitor (5.44 µM) and bovine catalase (8.90 µM). From the electrophoretogram**,** the area of the unbound DNA is much greater than the area of the complex peaks and these complex peaks are not observed when < 1µM of target is incubated with the aptamer. The specificity of CES T4 was also tested and gave comparable specificity to cholesterol esterase.

5.3 Summary

Aptamers for cholesterol esterase were successfully selected using a hybridised method of selection. The bulk affinity suggested that the CES 4 showed the highest binding affinity with a K_D of 116 nM although this is still not in the sub-nanomolar range. The other aptamers showed a wide range of binding affinities. The truncated structure CES 4T showed a slight decrease in the binding affinity down to 204 nM suggesting that the constant region was involved in the conformation formed by the aptamer. Fluorescence polarization gave a similar K_D of 248 nM. CES 4 showed good specificity towards cholesterol esterase and this selection suggests that there are benefits to combining the nitro cellulose membrane filter step with the non-SELEX. Although aptamers in the low nanomolar range were not found, aptamers with higher binding affinities were found suggesting that the number of sequences screened had increased. It may also be noted that because cholesterol esterase is not known to interact with ssDNA in nature and hence the selection may only give rise to lower binding and the wide range of binding affinities reported for different targets suggest that this might be the case. A selection on a target that has already been selected such as thrombin would confirm this method. Also it was shown that an increase in the number of sequences screened from our electrophoretogram data suggests a significant enrichment of the library after the nitrocellulose filter step. This technique could also be hybridised with other classical technique such as affinity columns and could also be used to select aptamers which bind to targets both in solution and immobilized onto a stationary phase allowing the aptamer to be used in different binding environments. It will also be worth using X-ray crystallography to elucidate the mechanism of binding between the target and aptamer.

6 The development of a aptamer based SPR sensor for the detection of catalase in milk samples

6.1 Aim

Mastitis is a disease which causes inflammation of the udder tissue in cattle and is the most common disease affecting the dairy industry today. This disease can increase the somatic cell count in milk (an indicator of milk quality) and is caused by a number of pathogens including *S. aureus*, *E. coli*, and *Streptococcus spp*. Catalase was identified as a possible bio indicator of mastitis disease in cattle and could be used to monitor the quality of the milk[130]. Catalase enters the milk by somatic cells and catalase levels correlated with bulk milk somatic cell counts [131]. A number of methods have been developed to determine the total somatic cell count which can include any bacterial cells. In 2009 Koskinen *et al* used a PCR based assay to identify mastitis pathogens[132]. A chip based method was recently developed to detect mastitis pathogens using a ligation detection reaction[133]. An online conductivity system for the detection of mastitis has been developed which identified a number of sub clinical quarters. Futo *et al* recently developed an amperometric based biosensor for the detection of catalase in milk samples by measuring indirectly, the degradation of hydrogen peroxide [134].

In this chapter we demonstrated the use of the aptamer selected against bovine catalase and used it to develop a highly sensitive and specific SPR based aptamer biosensor for the detection of catalase protein in milk samples. CAT 1 aptamer was synthesized with a biotin tag on the 3' end and was successfully immobilised onto a chip by affinity capture with immobilised streptavidin. Streptavidin was immobilised onto the gold surface of the chip. This biosensor was used to

measure the catalase directly in milk samples and could allow for the rapid determination of mastitis disease in milk.

6.1.1 Preparation of chips sensor – SensiQ

A mixed SAM was initially prepared by suspending the chip above a solution of the thiol solution allowing for only the SPR surface to be in contact with the solution. This technique seemed to be effective but resulted in the degradation of the adhesive used to glue the gold slide to the chip resulting in a unusable chip. We therefore choose to do the immobilization while the chip was docked into the machine. The SensiQ chip was normalized after docking to ensure that the response unit signal was adequate. The signal was checked by looking at the SPR dip signals for channel 1 and 2 which is shown in appendix 3, **figure d.1.** The sensiQ chip was coated with the mixed thiol by injecting the samples onto the surface of the docked chip which gave a comparable immobilization. As the gold slide is attached to the slide, characterization of the SAM is impossible on the sensiQ based chips. The initial affinity capture experiments were performed using avidin protein. It was quickly found that the non-specific binding of catalase to the avidin was significant. It was therefore decided that streptavidin would be a better choice of ligand which would minimise the extent of non-specific binding. Neutravidin which is a deglycosylated version of avidin, has a near neutral *pI* value and suffers the least from non-specific binding was another option but this protein is quite expensive to buy [135].

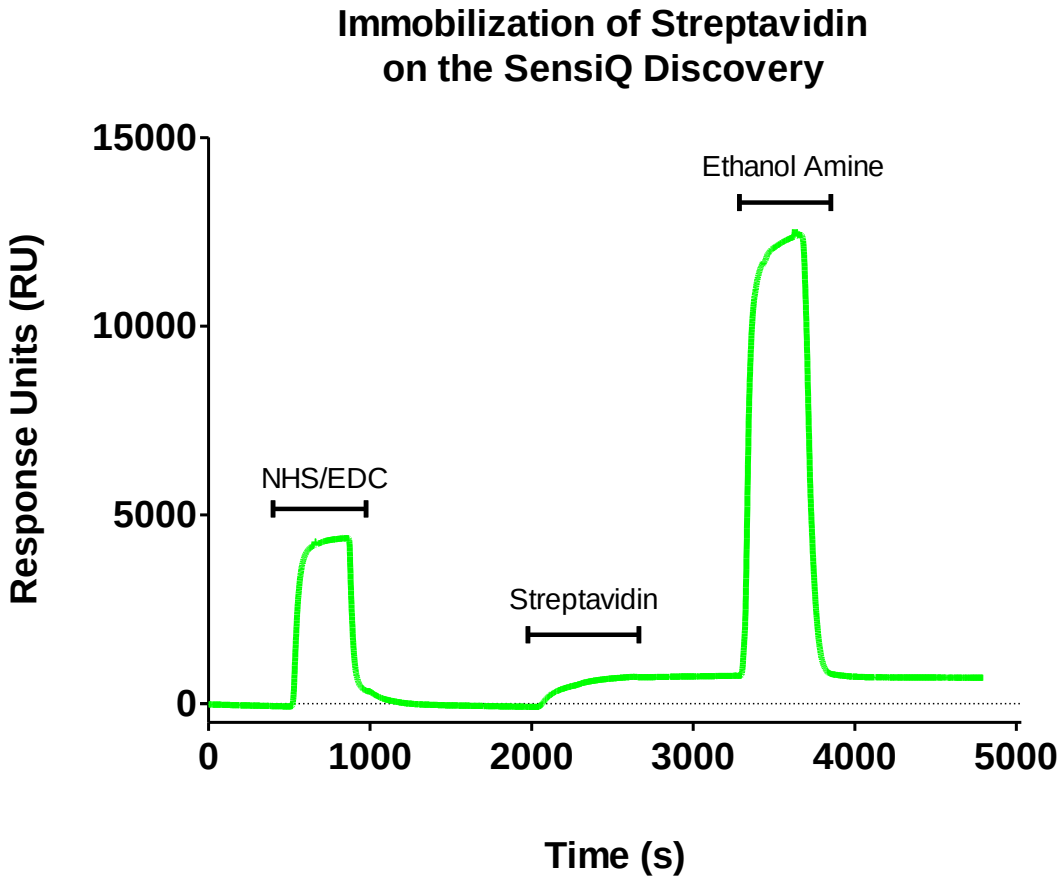

Figure 6.1 Immobilization of streptavidin on the SensiQ discovery. The flow buffer was sodium acetate buffer at pH 5 µl/min, 50µl of EDC/NHS solution, 50 µl of streptavidin(50µg/ml), biotin 50 µl of tagged aptamer (10 µM) and ethanol amine (1M) were injected.

The immobilization of streptavidin and the biotin tagged aptamer was monitored by measuring the relative response. The online response plot of the immobilization of streptavidin and the affinity capture of the biotin tagged aptamer on the sensiQ discovery is shown in **figure 6.1** and **figure 6.2**. The flow rate was set to 5µl/min in order to maximise the contact time of each reagent with the surface of the SAM. A run buffer of sodium acetate pH 5.0 was used for the immobilization of streptavidin in order to pre-concentrate the protein onto the sensor surface.

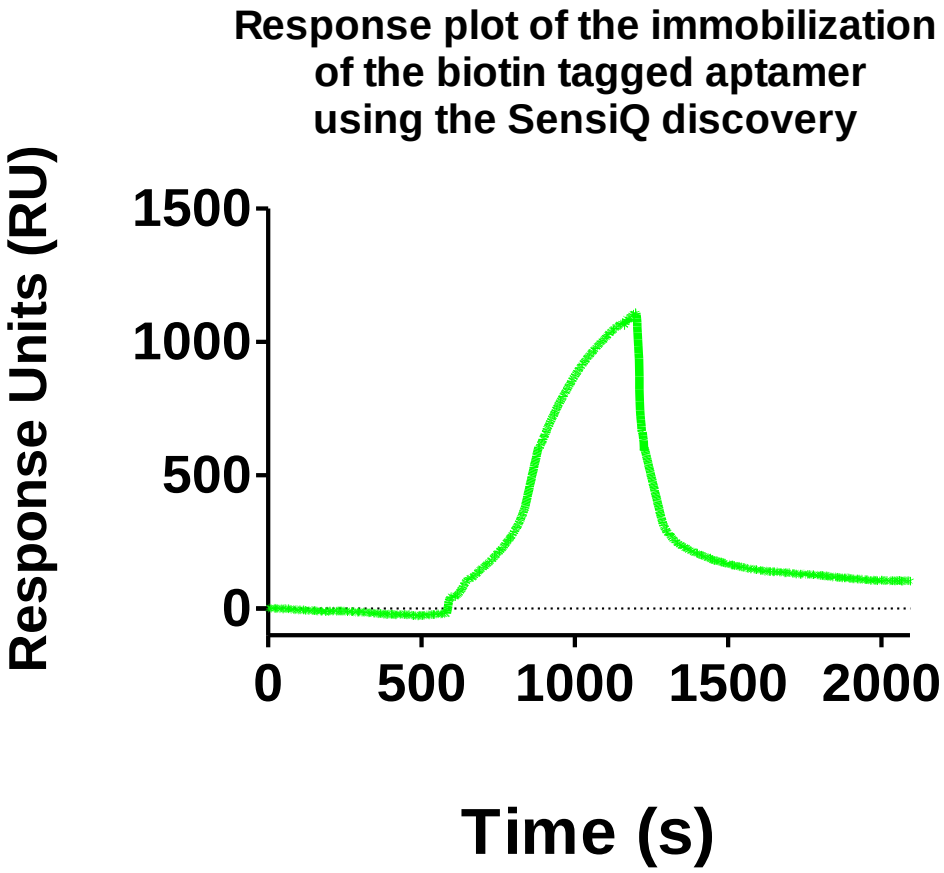

Figure 6.2 Affinity capture of 10 µM of biotin tagged CAT 1 aptamer (50 µl) at a ligand density of 105 RU on the SensiQ discovery. Flow buffer HKE buffer 5 µl /min.

The first injection was the NHS/EDC injection. The NHS and EDC allow for the activation of the carboxylic acid group on the alkane thiol by forming an activated ester. A successful reaction results in a difference in response before and after the injection of the reagent. The relative response was about 100 RU. As EDC and NHS are small molecules, the change in signal is small. An amine coupling was performed by injecting 50 µg/ml of streptavidin.

The streptavidin can undergo covalent coupling with the activated ester group on the SAM.

The Biotin tagged aptamer was injected at a concentration of 10 µM. The final step involved using a blocking agent to react with the remaining unreacted activated ester groups on the SAM.

Ethanol amine contains a primary amine that can undergo covalent coupling with the remaining unreacted activated ester groups on the surface. Ethanol amine is also basic can remove any unreacted ligands which may be attracted to the surface of the SAM via electrostatic interactions. The average response to immobilization was > 2000 RU. For the affinity capture of the biotin tagged aptamer, the run buffer was changed to HKE buffer due degradation of DNA when using acidic buffer via hydrolysis. The KCl salt concentration would also encourage binding between the immobilized streptavidin and biotin on the aptamer.

The overall response to the immobilization was 550 RU. The extent of immobilization between the two machines is comparable in terms of RU. This suggests that both methods used to form the SAM are acceptable in the preparation of the SPR sensor surface. It is worth noting that during the injection of NHS/EDC in the sensiQ discovery machine, the signal often would disappear due to bubbles forming. This phenomenon was not observed with any other reagent. We prevented this from happening in the other experiments by degassing the reagent.

6.1.2 Preparation of chips sensors – BIAcore

For the BIAcore, there is no need to normalize the signal and the mixed thiol SAM could be prepared outside the machine by immersing the gold film in the solution containing the 11-MUA and 2-ME. The sample container was purged with nitrogen and sealed to encourage the formation of a tightly packed monolayer. The chip was washed and dried and immediately docked into the machine.

Figure 6.3 shows the online response plot for the immobilization of streptavidin on the BIAcore chip. The surface was again activated using NHS/EDC which gave a response of about (100-200 RU).

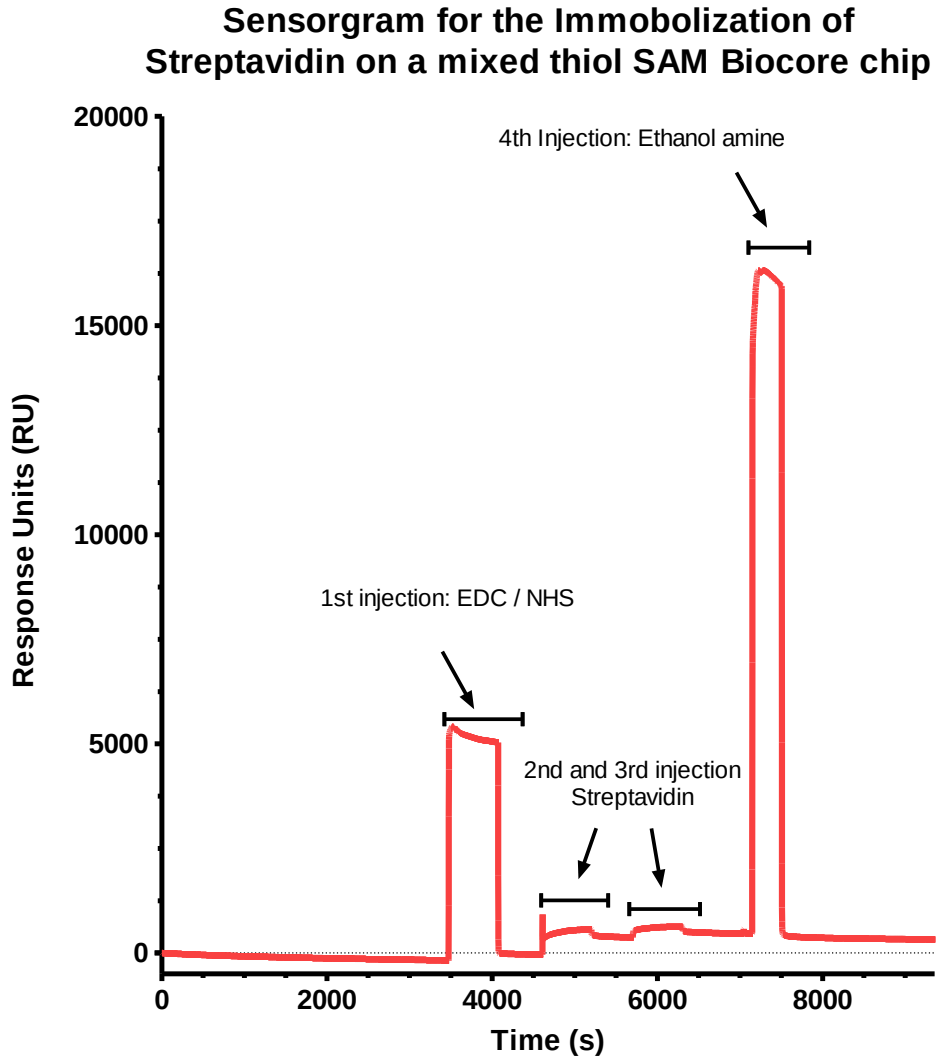

Figure 6.3 Immobilization of streptavidin on the Biacore T3000 SP, the flow buffer was 25mM sodium acetate buffer (pH 5.0) at 5 µl/min, 50µl of EDC/NHS solution, 50 µl of avidin (50 g/ml), biotin 50 µl of tagged aptamer (10 M) and ethanol amine (1M) were injected.

As with the sensiQ discovery, the buffer pH of the flow buffer and immobilization buffer was below the *pI* value of streptavidin allowing for a larger electrostatic interaction between the

carboxylic group and the streptavidin. The streptavidin was immobilized with a density of about 500 RU. The extent of immobilization between the two machines is comparable in terms of RU. This suggests that both methods used to form the SAM are acceptable in the preparation of the SPR sensor surface. The ethanol amine was again injected to react with the unreacted activated ester groups and to remove any unreacted protein that may have bound via electrostatic interactions. When compared to avidin, streptavidin gives a smaller response which was due to avidin having a high *pI* value.

The tagged aptamer was captured by injecting 50 µl at concentrations of (1 - 10 µM) with a flow rate of 5 µl/min and is shown in **figure 6.4**.

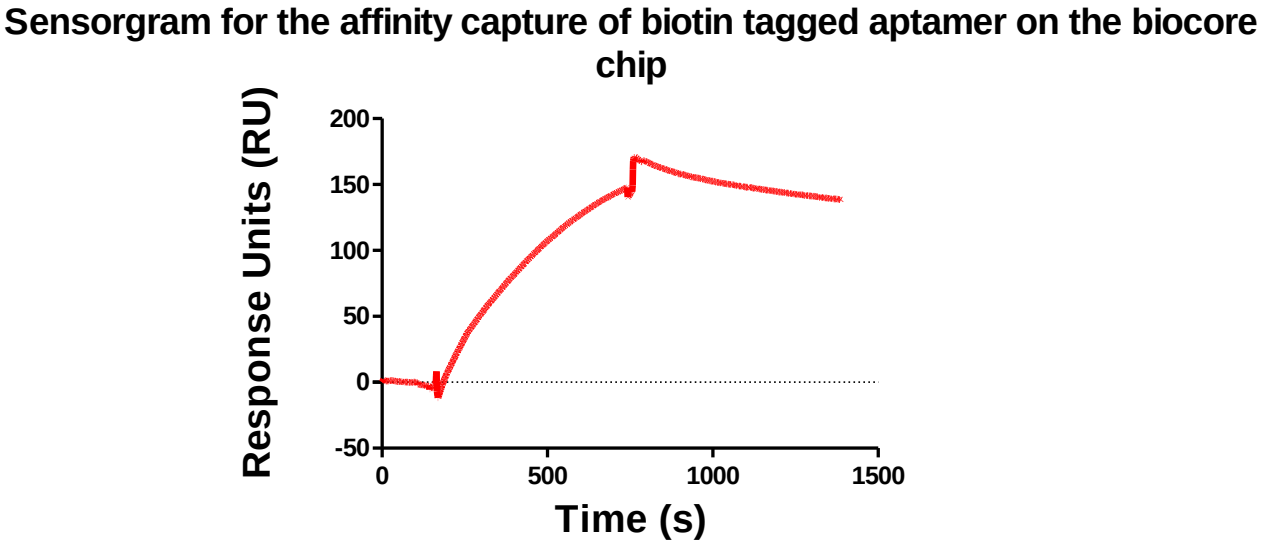

Figure 6.4 Response plot showing the affinity capture of 10 µM of biotin tagged CAT aptamer at a ligand density of 150 RU. Flow buffer HKE buffer 5 µl /min.

In general there was no improvement in the response at concentrations >10 µM. The binding buffer was changed to HKE buffer (pH 7.4) as the sodium acetate buffer would facilitate

degradation of the aptamer through hydrolysis. A flow rate of 5 µl/min was used again to allow for maximum contact time with the surface. The total immobilization density was about 650RU. This was found to be adequate for the analysis due to the fact that the analyte is much bigger than the ligand allowing for relatively large response changes with little need to immobilize much of the ligand.

The extent of immobilization between the two machines is comparable in terms of RU. This suggests that both methods used to form the SAM are acceptable in the preparation of the SPR sensor surface. Comparing the two machines, we can say that the extent of immobilization is comparable to one another allowing suggesting that both an injection based SAM formation and the solution based method can be used to immobilize ligands. Unfortunately both techniques can only be used exclusively with each particular machine.

6.1.3 Optimization of the aptamer based biosensor

The performance of both sensors was assessed on both the sensiQ and the BIAcore T3000 and the method was optimized by altering the injection volume, flow rate, buffer conditions and regeneration conditions. The injection volumes were optimized by injecting (0 - 100 µl) at a low flow rate of 5 µl/min. From the response plots it was found that larger volumes resulted in longer injection times, which is not practical in terms of developing calibration plots. It was also noted that at lower injection volumes, the response is quite small and from the response curves, it was observed that the analyte didn't have enough time to reach the steady state which is demonstrated by a levelling off of the response during the association stage after the start of the injection. We decided that an injection volume of 50 µl was a good compromise to give a good

exponential curve and allowing the injection to be carried out within 5 minutes. The response plot showed that catalase binds to the aptamer without dissociation as indicated by the fact that the relative response does not return to the base line after injection which could be the result of slow dissociation. Non-specific binding of the analyte was accounted for by using a streptavidin only surface as the negative control and adding 0.5 % BSA to the run buffer and the samples. The response plots further confirm that the selected aptamer has slow binding kinetics as suggested in the previous chapter from NECEEM analysis. This made it necessary to employ a regeneration buffer to remove the bound analyte after each injection. The regeneration buffer was developed by considering the nature of the surface and the analyte. Since an aptamer based system was used, acidic conditions would result in degradation of the aptamer. Therefore basic conditions were chosen for our regeneration buffer. Glycine-NaOH in 1.2 % ethanol has been reported as an effective regeneration buffer for oligonucleotide based aptasensors [136]. 50 µl of catalase was injected at 1 µM. This was followed by injection of regeneration buffers containing NaOH and glycine at different concentrations.

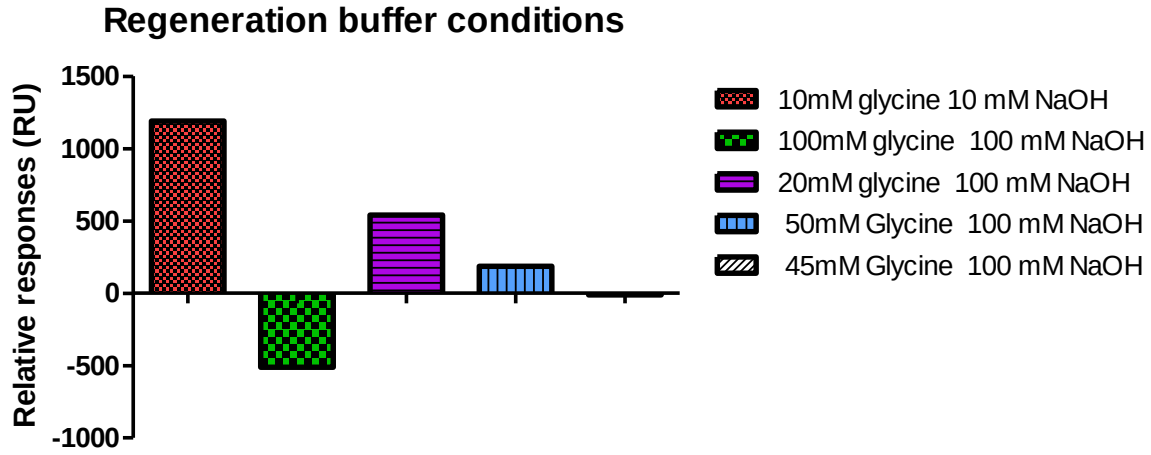

Figure 6.5 A graph showing the relative responses after injection of various Regeneration buffers using the BIAcore T3000. Firstly 50 µl of 1 µM catalase was injected followed by 50 µl of each regeneration buffer respectively. Relative responses were calculated by comparing the base line before the first injection and the base line after the second injection.

The difference in response between the initial baseline signal and the baseline after the injection of the regeneration buffer was taken to assess the performance of the regeneration buffer. If the basic conditions are too harsh then the surface can be degraded resulting in a decrease of the final baseline. If the basic conditions are too weak then the analyte will not be effectively removed, and would lead to an increased baseline signal. **Figure 4.5** shows the effect of regeneration buffer on the baseline signal before and after injection.

The regeneration buffer conditions varied a lot and the weaker regeneration buffer was found to give a higher baseline signal suggesting that some of the analyte stayed on the ligand (10 mM glycine, 100 mM NaOH and 20 mM glycine, 100 mM NaOH). The stronger conditions had the opposite effect of removing the ligand from the surface. The optimum was found to be 45 mM glycine 100 mM NaOH which showed very little difference in response after injection.

The flow rate was also optimized by injecting 1 µM catalase at various flow rates. From **figure 6.6**, it can be observed that as the flow rate is increased, the shape of the response curve changes. At a flow rate of 5 µl/min the curve is a smooth exponential curve that reaches steady state. As the flow rate is increased, the exponential curve becomes sharper and from15 µl/min the curve does not reach steady state suggesting a large mass transport effect. This can be detrimental to analysis as the reproducibility of each cycle can deteriorate. However at low flow rates, the time for injection was 20 minutes per injection which would result in a total of 40 minutes for each cycle including regeneration buffer. It was decided that a flow rate of 10µl / min gave reproducible results while allowing each cycle to be completed in 20 minutes. The flow rate selected allowed the assay to be completed within a day while allowing for adequate time for a stable baseline to be obtained after each injection and giving reproducible results.

Graphs showing the effect of flow rate on the response of catalase signal

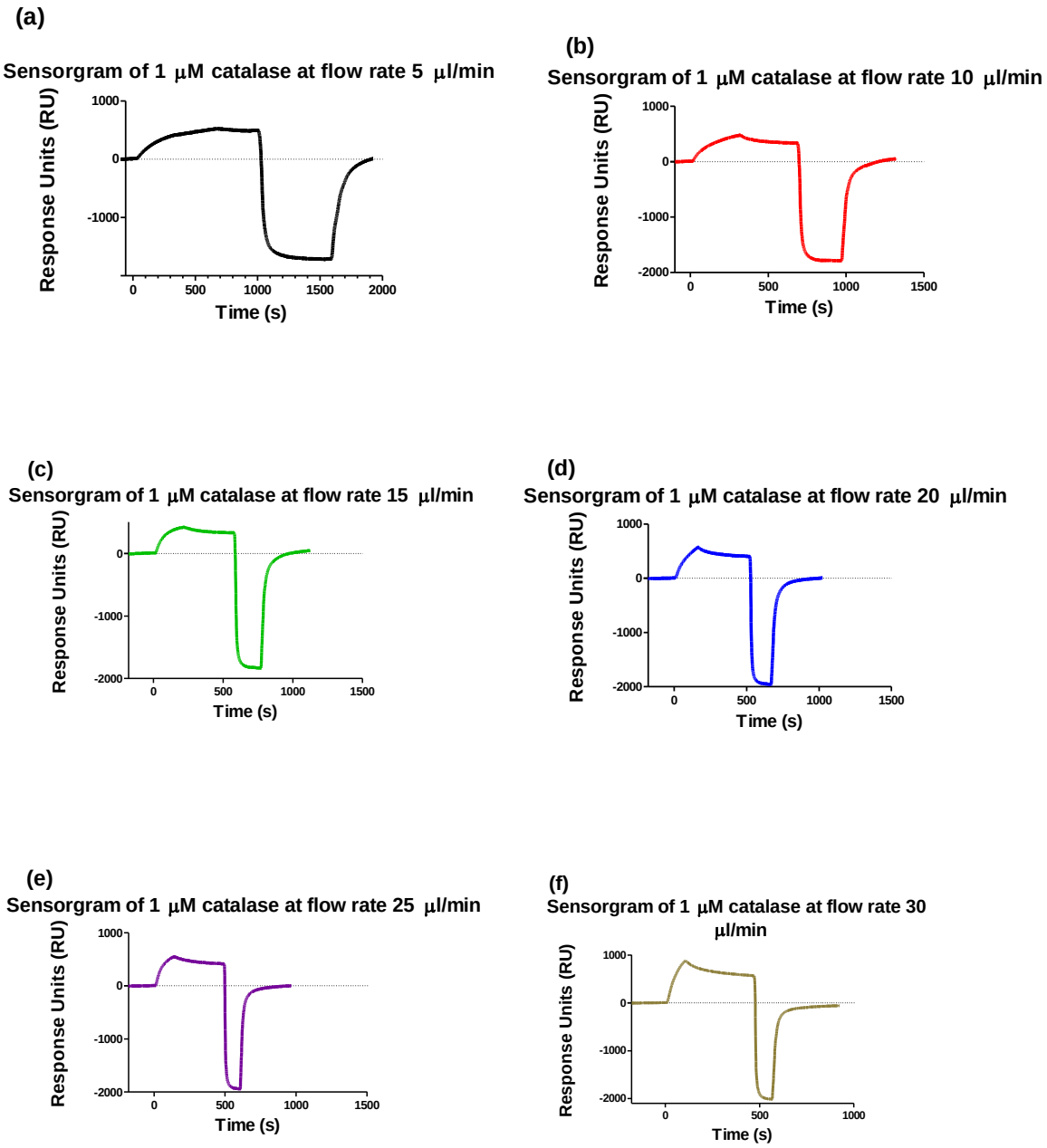

Figure 6.6 Graphs showing the response of injection of 50µl of 4 µM catalase at different flowrates; (a) 5 µl/min,(b) 10 µl/min, (c) 15 µl/min, (d) 20µl/min, (e) 25 µl/min and (f) 30 µl/min.

This allowed for the analysis to be performed in triplicate within a reasonable time frame. The next step in the development of the sensor was to retest the specificity of the aptamer towards the analyte. As the assay was to be performed in milk, we tested the aptamer against 3 of the most abundant milk proteins found in milk. The protein content in milk can be put into 2 main groups, namely caseins and whey proteins. For this experiment casein, beta lactoglobulin (whey protein) and albumin (whey protein) were selected to determine the specificity of the aptamer.

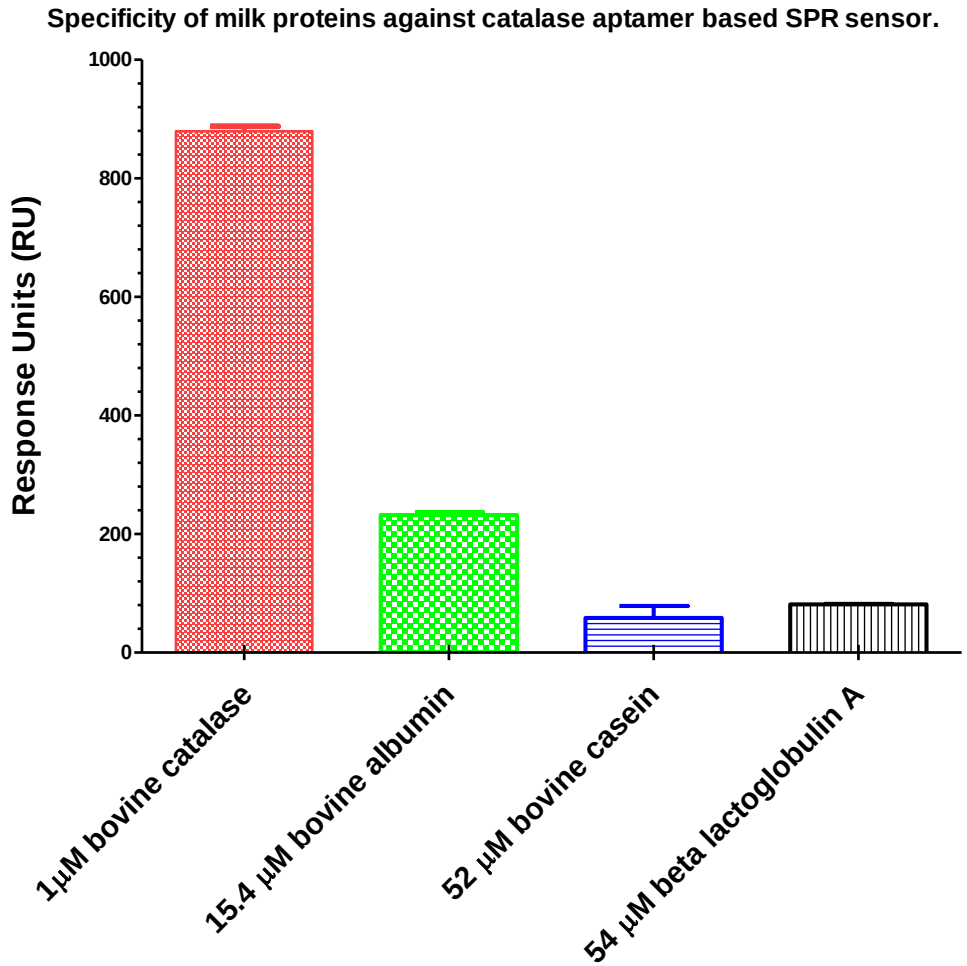

Figure 6.7 Graph showing specificity of the sensor chip surface towards different proteins found in milk. 50 µl of bovine catalase (1µM), bovine albumin (15.4 µM), bovine casein (52 µM) and beta lactoglobulin (54 µM) was injected, run buffer of HKE, 0.5 % BSA at a flow rate of 10 µl/min Regenerated using 45 mM glycine, 100mM NaOH in 1.2 % EtOH.

50 µl of each protein was injected at and the relative response was measured just before the end of the injection was measured to take into account both the response from refractive index changes and binding. From **figure 6.7**, catalase gave an average response of 820 RU when compared to the other proteins which confirmed that the aptamer ligand was specific towards catalase. It is also noted that from the response plot in **figure 6.8**, the relative response after injection for the 3 negative control proteins went back down near to the base line. This suggests that the negative control proteins response is caused by refractive index changes rather than a binding event or that the proteins in question dissociate much faster from the ligand.

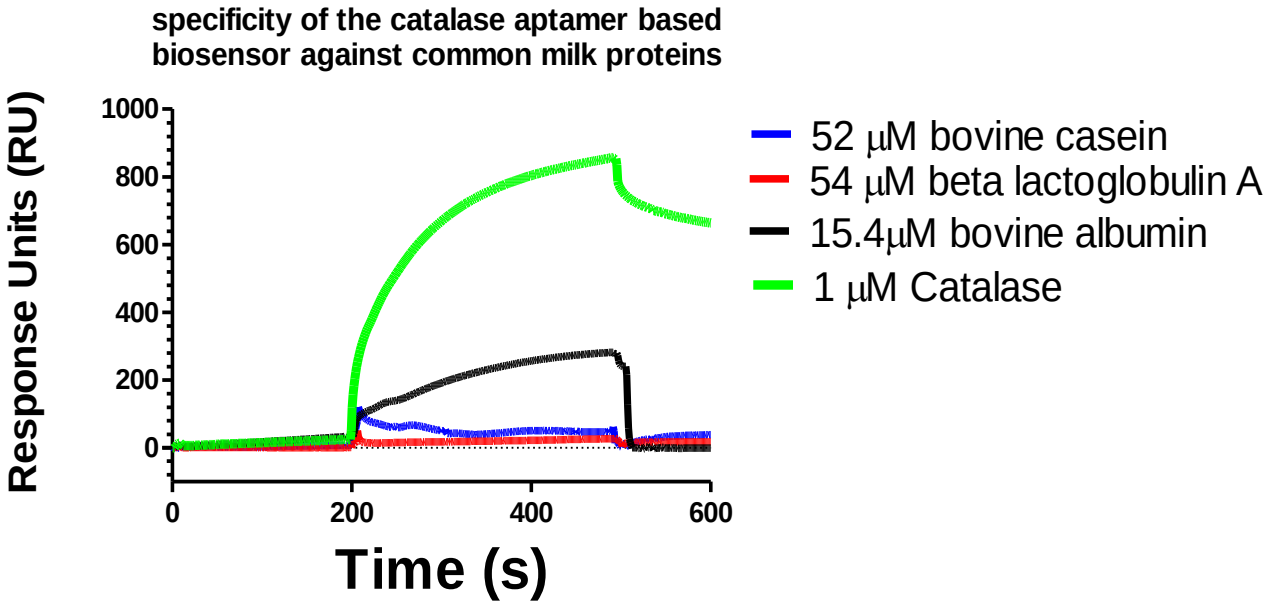

Figure 6.8 Response plot demonstrating the specificity of the sensor surface towards different common milk proteins; flow rate 10 µl/min, 50 µl of bovine catalase (1µM), bovine albumin (15.4 µM), bovine casein (52 µM) and beta lactoglobulin (54 µM) was injected, run buffer of HKE, 0.5 % BSA at a flow rate of 10 µl/min Regenerated using 45 mM glycine, 100mM NaOH in 1.2 % EtOH.

The catalase assay was initially performed on the SensiQ discovery. From our experiments, it was found that the performance of the sensor was quite poor and a dip signal deteriorated over time. The use of BSA in the run buffer also affected the performance of the machine by causing blockages to occur in tubing which also lead to an irreproducible method. It was decided that the method should be converted over to the BIAcore T3000 in order to get more robust results for the assay.

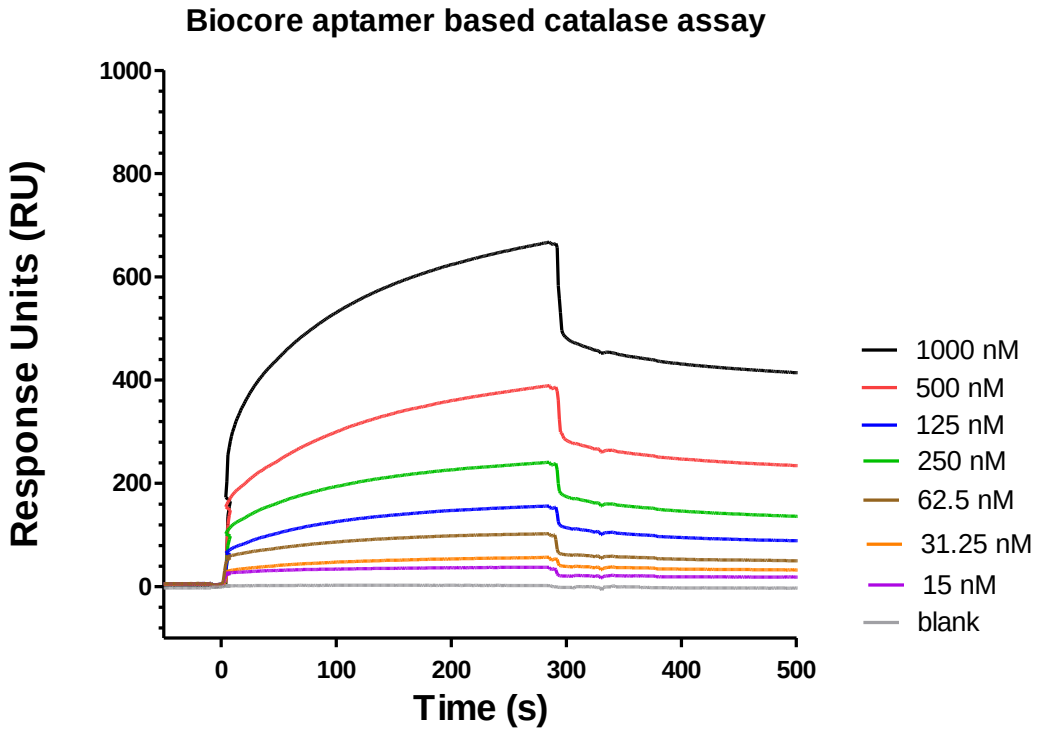

Figure 6.9 Response plot for the aptamer based catalase SPR biosensor in HKE buffer with 0.5 % BSA. Injections of 50 µl of catalase (15-1000 nM); flow rate: 10 µl/min HKE buffer; Regenerated using 0.1M NaOH in 1.2% EtOH.

Injections of 50 µl of catalase (15 - 1000nM) were made followed by injection of 50 µl the regeneration buffer. The response plot and linear regression calibration plot are shown in **figure 6.9** and **6.10**. The limit of detection (LOD) was determined to be 20.5 nM ± 3.12 and the

dynamic linear range was determined to be between 20.5 -1000 nM. The linear regression for the aptamer catalase interaction was y = 0.4750x + 1.048 (R^2 = 0.94, n=6).

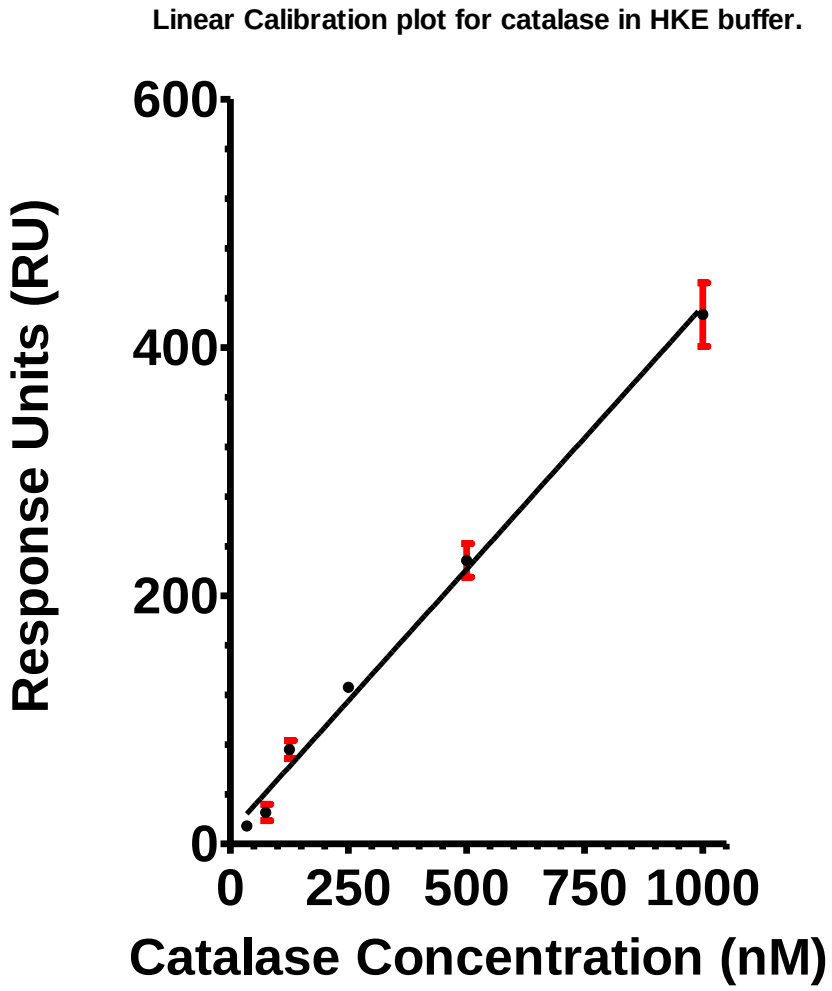

Figure 6.10 Calibration plot for the aptamer based catalase SPR biosensor in HKE buffer. Injections of 50 µl of catalase (15-1000 nM); flow rate: 10 µl/min HKE buffer. Regenerated using 0.1M NaOH in 1.2% EtOH. (LOD = 20.5 nM ± 3.12).

The standard deviation of injections was found to be higher at higher concentrations which may be due to the fact that the sensor was saturated at higher concentrations of analyte.

At lower concentrations the standard deviation was lower and within <10% RSD. The reproducibility of the biosensor was comparable to the other reported methods.

6.1.4 Real sample analysis

For the sensiQ system, the chip had to be immobilized by injecting the mixed thiol onto the chip while docked in the machine and stopping the syringe pump half way through the injection. This prevented characterization of the SAM. It was also found that the tubes in the sensiQ would often get blocked when BSA was used in the run buffer.

The sensor performance was then assessed in real milk samples. For this study standardized milk was used. Samples of milk were prepared by spiking the samples with catalase, centrifuging to remove the fat layer and filtering using 0.45µm filter. The centrifugation and filtering steps are necessary to remove particulates from the sample as this can ruin the machine. The spiked samples were injected at different concentrations (0-1000nM). The response plots are shown in **figure 6.11**.

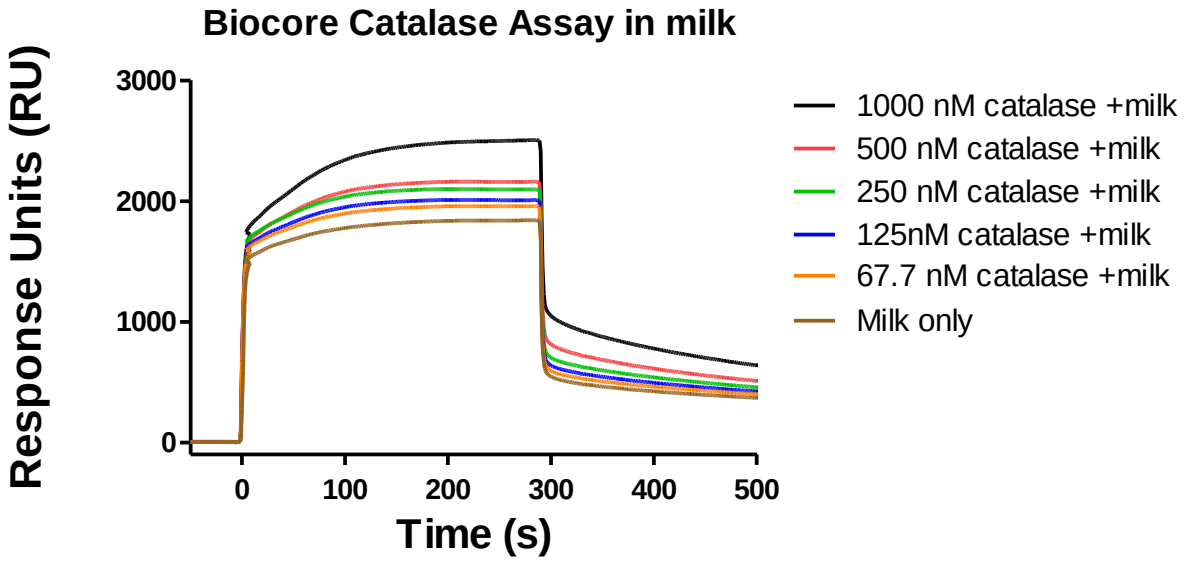

Figure 6.11 Response plot for the aptamer based catalase SPR biosensor in spiked milk samples with 0.5%BSA. Injections of 50 µl of catalase (0-1000 nM); flow rate: 10 µl/min HKE buffer; Regenerated using 0.1M NaOH in 1.2% EtOH.

All the samples including the blank milk sample showed a response due to the significant refractive index change of the milk sample compared to the run buffer. However the response of the spiked samples showed a correlation and the response gradually decreased with decreasing concentration. The milk only sample was used as the negative control in the assay and the corrected response plot and the linear calibration plot are shown in **figure 6.12** and **6.13.**

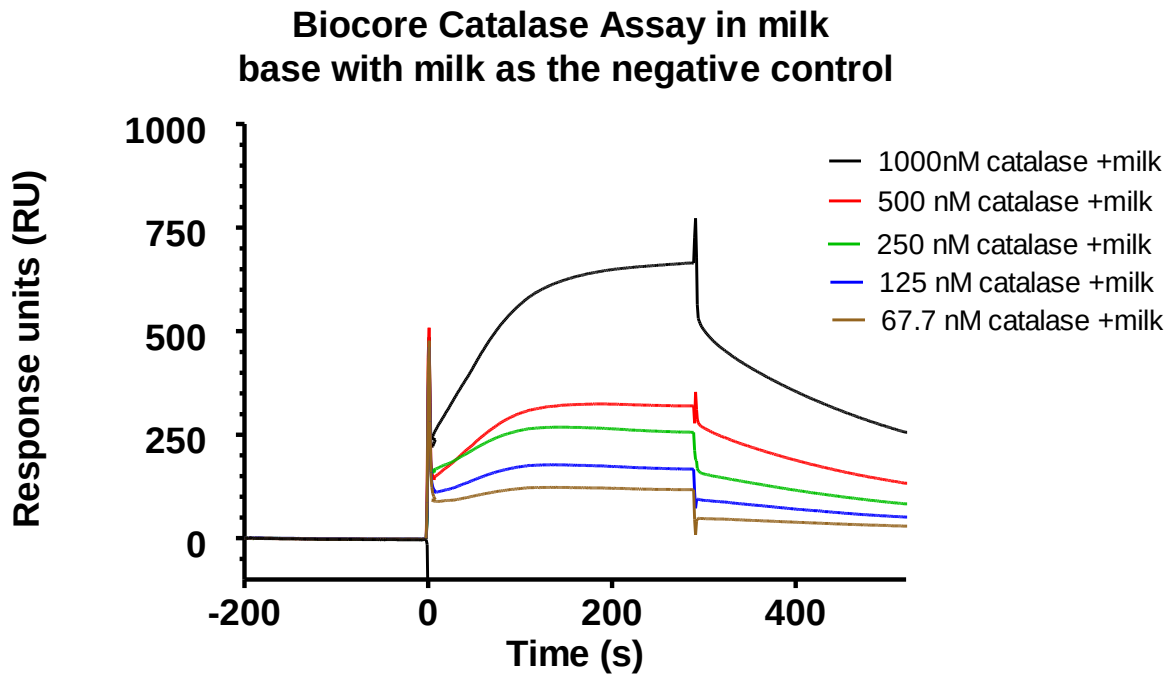

Figure 6.12 Corrected response plot for the aptamer based catalase SPR biosensor in spiked milk samples with 0.5%BSA. Injections of 50 µl of catalase (0-1000 nM); flow rate: 10 µl/min HKE buffer; Regenerated using 0.1M NaOH in 1.2% EtOH. The relative response was determined by subtracting the response from the milk only sample from each spiked response.

The shape of the corrected response plot for the spiked milk samples was significantly different from that with the standard calibration plots. Spikes in the signal are observed at the start and end of the injection due to the slight differences in the times of injection.

The spiked milk samples also show a linear response from 62.5 nM to 1000 nM. The linear regression equation for the catalase aptamer catalase interaction in milk was

$y = 0.5567x + 91.92$ ($R^2 = 0.998$, n =5).

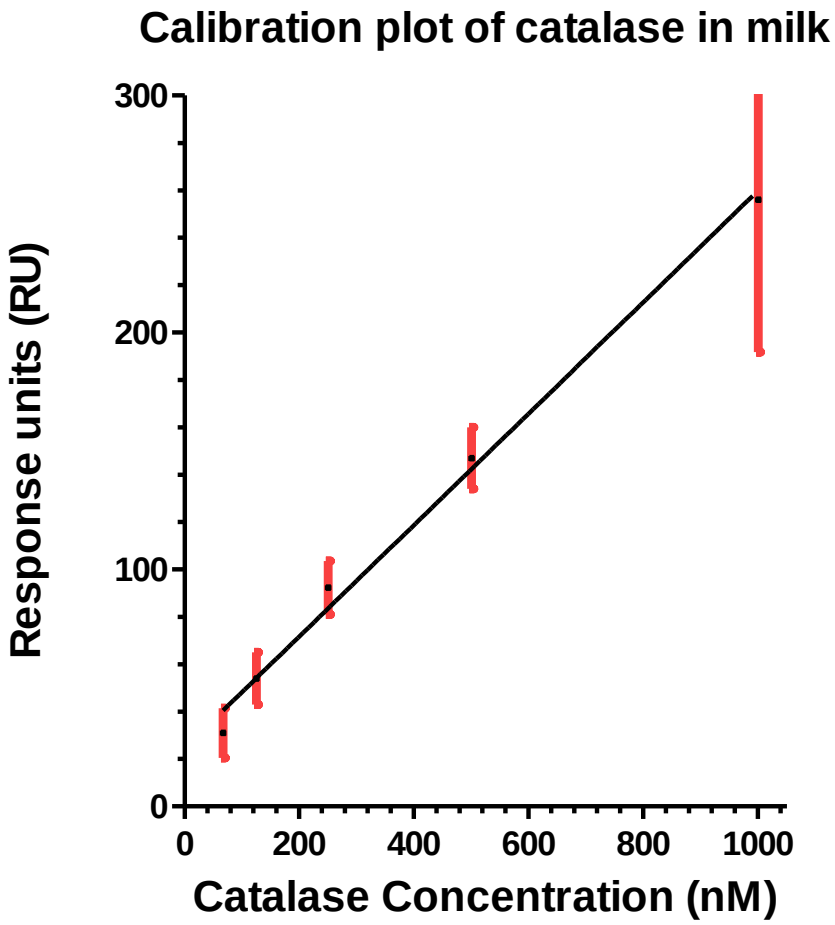

Figure 6.13 Calibration plot for the catalase spiked in milk, injections of 50 µl of catalase (20-1000 nM); flow rate: 10 µl/min HKE buffer. Regenerated using 0.1M NaOH in 1.2% EtOH and performed on the Biacore T3000.

The catalase recoveries were calculated for each spiked sample in milk from the calibration graph and are shown in **table 6.1.** Going from higher concentrations, the recoveries of catalase significantly improved as lower concentrations of spiked milk were injected with the 67.7 nM

catalase giving a recovery of 104 %. The slight differences can be explained by the sample matrix response.

Table 6.1 A summary of the percentage catalase recoveries from spiked milk samples (67 nM - 1000 nM).

Spiked concentration (nM)	**1000**	**500**	**250**	**125**	**67.7**
Calculated recovery (nM)	514.26	308.42	193.04	112.20	65.05
% recovery	51.42	61.68	77.21	89.76	104.1
% RSD	14.5	5.07	6.99	11.6	19.4

These results show that aptamers can be used in SPR based biosensors and is shown to have good sensitivity and specificity, although there are still issues to be solved in terms of interfering matrix effects. These results are comparable to previous studies on aptamer based SPR sensors such as by Lee *et al* who developed an aptamer based biosensor for the detection of RBP in human serum, reporting a similar K_D (0.2 µM) for the aptamer and LOD (75 nM) although the binding affinity K_D for the aptamer developed in this study was determined using non equilibrium capillary electrophoresis of equilibrium mixtures (NECEEM) and fluorecence intensity and gave a K_D of 0.237 µM and 0.430 µM respectively. The results obtained from this study show that aptamers are viable alterntive to antibodies and due to the large size of the analyte in comparison to the aptamer and also this means that nanomolar detection limits can be accomplished with relatively low levels of immobilization. They also demonstrate the ability of SPR to detect analytes in complex mixtures such as milk samples.

6.2 Summary

An SPR based aptamer biosensor was successfully developed to detect bovine catalase. A mixed thiol of 11-MUA and 2-ME (1:4 ratio) was used to coat the bare gold surface in order to prevent steric hindrance of the ligand during the amine coupling. Two different affinity capture strategies were used to immobilize the ligand onto the surface, namely avidin and streptavidin. Streptavidin was chosen due to the reduced non-specific binding exhibited and BSA was added to the run buffer to further reduce non-specific binding. The LOD was determined to be 20.5 nM for the catalase in buffer and spiked milk samples respectively. This sensor will allow for the direct measurement of catalase in milk samples with minimal sample preparation and with a high degree of specificity and sensitivity and shows that aptamers can be used as the recognition element in SPR based biosensors as an alternative to antibodies. It also demonstrates that an aptamer that was developed against larger targets, using an immobilization free selection process, can be immobilized onto a surface without any loss in binding affinity and specificity. This method could be used in routine screening of milk for mastitis disease. This aptamer could be applied as the recognition element in a lot of different biosensing platforms such as QCM, FRET based molecular beacons and quantum dots. The catalase aptamer could also be used in other sensing applications such as investigating oxidative stress in animals upon acute exposure to pollutants.

7 Conclusion and future work

7.1 Conclusion

In the course of this thesis, CE-SELEX, non-SELEX and hybridised-SELEX have been used to select aptamers for a number of proteins. One of these aptamers was used as the transduction element in an SPR based biosensor for the detection of catalase, a bio indicator of mastitis disease in milk samples.

In chapter 2, it was shown that CE-SELEX can be used to select aptamers for human leptin protein, a small 19 kDa protein. After 4 rounds of selection the bulk affinity showed no further improvement in K_D and 10 sequences were found, 4 of which showed good secondary structure folding. For validation of the clones, two methods, fluorescence intensity and NECEEM were chosen. From the results, a significant difference was observed between the two techniques for the absolute value of the binding affinity. It was concluded that this difference could be explained by a number of reasons such as the nature of free solution selection, the relative k_{off} rates of the aptamers, or systematic errors, although systematic errors should have been minimised. Nevertheless, the selection of aptamers using non-immobilized, small targets may be limited in use in free solution based applications, and it was suspected that this is only a problem for smaller targets.

In chapter 3, a closely related post CE-SELEX modification called non-SELEX was used to select aptamers. Aptamers were successfully selected against catalase, a 150 kDa protein and hemoglobin, a 67 kDa protein. Aptamers against catalase were selected in less than 3 rounds of selection and gave 4 sequences which showed good secondary structure, and these aptamers were

again, validated using NECEEM and fluorescence intensity, giving rise to CAT 1 with a K_D in the lower micromolar to high nanomolar range. The similarity of K_D's measured with both binding affinity assays suggest that the relative size of the target is important in the selection of aptamers using free solution methods.

Hemoglobin aptamers were selected after just 1 round of selection of non-SELEX. No complex peak was observed. Therefore a blind selection was effectively carried out and there was no improvement in bulk K_D after the subsequent round. ACE was used to measure the binding affinity instead of NECEEM due to the lack of a complex peak. HB 1 gave rise to a K_D in the lower micro molar to high nanomolar region. No sequences were found with low nanomolar range in the K_D's reported, which may be due to the number of sequences being too small or to the fact that binding affinities are defined by the nature of the target. The literature shows many examples of proteins with high binding affinities which are known to interact with nucleic acids in nature and tend to show higher binding affinities towards aptamers. When comparing the methods of non-SELEX described in this chapter and that of the CE-SELEX in chapter 2, it is difficult to make a direct comparison. The use of real time PCR was not available in the non-SELEX project, so normal PCR with agarose gels was used instead. The aptamers generated from both methods showed similar binding affinities. However, the number of sequences found in the CE-SELEX was higher due to the high efficiency of using real time PCR.

In the next chapter, a new method for screening aptamers was developed that would allow for a much higher number of sequences to be screened. Hybridising a classical method such as the nitrocellulose membrane with a capillary based technique such as non-SELEX would bring together the advantages of both techniques. The two techniques allowed for a higher proportion of sequences to be screened by using a nitrocellulose filter for the first round of selection while

increasing the efficiency of separation with capillary based techniques in subsequent rounds. It also removes the need for intermittent amplification using PCR, and in the case of acidic protein targets removes the necessity of a negative selection step. 6 aptamer sequences were found and validated using NECEEM. Aptamers with high nanomolar binding affinities were found and CES 4 had the highest binding affinity of 116 nM. The method allowed for the validation of the full structures and two truncated aptamers CES T4 and CES T3 were also tested using NECEEM and fluorescence polarization which resulted in a slightly lower binding affinity. This could allow for CE methods to be more widely adopted by the scientific community in aptamer selections and CE could be used as a complimentary technique in the partitioning step to speed up the selection process while still allowing for more of the library to be screened.

In the last part of the thesis, a SPR based aptamer biosensor was developed using CAT 1 aptamer. Originally, an avidin based system was used to capture the biotin tagged aptamer but to minimise the amount of non-specific binding, a streptavidin based affinity capture was used for the aptamer ligand. Initially the SPR experiments were performed on a sensiQ discovery but were later adapted to the BIAcore T3000 SPR machine. The LOD of the sensor was measured to be 20 nM in buffer. Upon spiking the milk samples with catalase, the recoveries of the catalase in spiked milk samples showed similar values between the measured values and recovered values. This research allows for the direct measurement of catalase in milk and could be used in the screening of mastitis disease in milk with minimal sample preparation. It was also shown for the first time that aptamers were compatible with milk samples proving that they are comparable to the antibodies.

7.2 Future work

The aptamers selected from chapter 3 against haemoglobin could be used as an affinity probe to analyse the total and glycosylated haemoglobin in blood serum samples. As the aptamer for the glycosylated haemoglobin (unpublished) has already been selected, the use of two aptamers in affinity capillary electrophoresis using LIF detection would make it possible to diagnose diabetes in patients[137-140]. The aptamers would be incubated with samples of hemoglobin and glycosylated hemoglobin to form the complexes. The complexes can then be separated from the unbound DNA and the total haemoglobin and glycosylated hemoglobin can be determined by comparing the peak heights and plotting a linear calibration graph. These aptamers could also be developed into molecular beacons to allow for an immobilization free FRET based biosensor which is complimentary to the selection technique.

The leptin aptamer developed in chapter 2 would be optimized further to improve the binding and specificity. Closed loop aptameric directed evolution (CLADE) is an array based method which allows for the selection and mutation of aptamers in silico. This would allow for a consensus sequence to be found and could help develop sequences with higher binding affinities. The aptamers could be used in molecular beacon design.

One of the greatest challenges in SELEX is in the development of aptamers for small molecules. Often classical methods are not suitable for the selection due to the immobilization of the target preventing adequate binding to the aptamer. A number of immobilization-free post-SELEX modifications have been developed which remove the need to immobilize the target.

Non-SELEX and CE-SELEX have been demonstrated against larger targets but to date these techniques have not been used on small molecules. As mentioned previously, Park et al developed a method called GO-SELEX[70]. This technique has the potential to be used to select aptamers for small molecules. Successive rounds of partitioning of cortisol bound aptamers from the unbound DNA using graphene oxide, followed by PCR and regeneration of ssDNA will be performed. A round of negative selection will also be performed by incubating the aptamers with other closely related small molecules. Aptamers from this study will be used to develop a resistive pulse sensing assay for the detection of cortisol in blood and urine samples[141]. Firstly the aptamer would be immobilized onto rod shaped nanoparticles. These nanoparticles have advantages over normal spherical nanoparticles in agglutination assays. These nanoparticles will be able to capture the analyte and form aggregates. The aggregations can be counted using tunable pores. This would find applications in the detection of cortisol in blood plasma and urine samples.

8 References

1. A.D. Keefe, S. Pai, and A. Ellington, Aptamers as therapeutics. Nature Reviews Drug Discovery 9 (**2010**) 537-550.

2. A.D. Keefe, S. Pai, and A. Ellington, Aptamers as therapeutics. Nature Reviews Drug Discovery 9 (**2010**) 660.

3. H. Ulrich, C.A. Trujillo, A.A. Nery, J.M. Alves, P. Majumder, R.R. Resende, and A.H. Martins, DNA and RNA aptamers: From tools for basic research towards therapeutic applications. Combinatorial Chemistry and High Throughput Screening 9 (**2006**) 619-632.

4. M. Mascini, I. Palchetti, and S. Tombelli, Nucleic acid and peptide aptamers: Fundamentals and bioanalytical aspects. Angewandte Chemie - International Edition 51 (**2012**) 1316-1332.

5. A.B. Iliuk, L. Hu, and W.A. Tao, Aptamer in bioanalytical applications. Analytical Chemistry 83 (**2011**) 4440-4452.

6. M. Mascini, Aptamers in Bioanalysis, Wiley, **2009**.

7. Q. Zhao, X.F. Li, and X.C. Le, Aptamer-modified monolithic capillary chromatography for protein separation and detection. Analytical Chemistry 80 (**2008**) 3915-3920.

8. T.S. Romig, C. Bell, and D.W. Drolet, Aptamer affinity chromatography: Combinatorial chemistry applied to protein purification. Journal of Chromatography B: Biomedical Sciences and Applications 731 (**1999**) 275-284.

9. Q. Zhao, X.F. Li, Y. Shao, and X.C. Le, Aptamer-based affinity chromatographic assays for thrombin. Analytical Chemistry 80 (**2008**) 7586-7593.

10. Y. Xu, J.A. Phillips, J. Yan, Q. Li, Z.H. Fan, and W. Tan, Aptamer-based microfluidic device for enrichment, sorting, and detection of multiple cancer cells. Analytical Chemistry 81 (**2009**) 7436-7442.

11. I. German, D.D. Buchanan, and R.T. Kennedy, Aptamers as ligands in affinity probe capillary electrophoresis. Analytical Chemistry 70 (**1998**) 4540-4545.

12. V. Pavski, and X.C. Le, Detection of human immunodeficiency virus type 1 reverse transcriptase using aptamers as probes in affinity capillary electrophoresis. Analytical Chemistry 73 (**2001**) 6070-6076.

13. M. Berezovski, R. Nutiu, Y. Li, and S.N. Krylov, Affinity analysis of a protein-aptamer complex using nonequilibrium capillary electrophoresis of equilibrium mixtures. Analytical Chemistry 75 (**2003**) 1382-1386.

14. C.C. Huang, Z. Cao, H.T. Chang, and W. Tan, Protein-protein interaction studies based on molecular aptamers by affinity capillary electrophoresis. Analytical Chemistry 76 (**2005**) 6973-6981.

15. Electrochemical Aptamer-Based Biosensors: Recent Advances and Perspectives. International Journal of Electrochemistry 2011 (**2011**).

16. X. Liu, R. Freeman, E. Golub, and I. Willner, Chemiluminescence and Chemiluminescence Resonance Energy Transfer (CRET) Aptamer Sensors Using Catalytic Hemin/G-Quadruplexes. ACS Nano 5 (**2011**) 7648-7655.

17. Y. Wang, L. Bao, Z. Liu, and D.-W. Pang, Aptamer Biosensor Based on Fluorescence Resonance Energy Transfer from Upconverting Phosphors to Carbon Nanoparticles for Thrombin Detection in Human Plasma. Analytical Chemistry 83 (**2011**) 8130-8137.

18. R. Nutiu, J.M.Y. Yu, and Y. Li, Signaling aptamers for monitoring enzymatic activity and for inhibitor screening. Chembiochem 5 (**2004**) 1139-1144.

19. W. Li, X. Yang, K. Wang, W. Tan, Y. He, Q. Guo, H. Tang, and J. Liu, Real-time imaging of protein internalization using aptamer conjugates. Analytical Chemistry 80 (**2008**) 5002-5008.

20. H. Chang, L. Tang, Y. Wang, J. Jiang, and J. Li, Graphene fluorescence resonance energy transfer aptasensor for the thrombin detection. Analytical Chemistry 82 (**2010**) 2341-2346.

21. N. Hamaguchi, A. Ellington, and M. Stanton, Aptamer Beacons for the Direct Detection of Proteins. Analytical Biochemistry 294 (**2001**) 126-131.

22. J. Li, Z.C. Cao, Z. Tang, K. Wang, and W. Tan, Molecular beacons for protein-DNA interaction studies. Methods in molecular biology (Clifton, N.J.) 429 (**2008**) 209-224.

23. Z. Cao, and W. Tan, Molecular aptamers for real-time protein-protein interaction study. Chemistry - A European Journal 11 (**2005**) 4502-4508.

24. J.J. Li, X. Fang, and W. Tan, Molecular aptamer beacons for real-time protein recognition. Biochemical and Biophysical Research Communications 292 (**2002**) 31-40.

25. L.S. Green, D. Jellinek, R. Jenison, A. Östman, C.H. Heldin, and N. Janjic, Inhibitory DNA ligands to platelet-derived growth factor B-chain. Biochemistry 35 (**1996**) 14413-14424.

26. C.-W. Chi, Y.-H. Lao, Y.-S. Li, and L.-C. Chen, A quantum dot-aptamer beacon using a DNA intercalating dye as the FRET reporter: Application to label-free thrombin detection. Biosensors and Bioelectronics 26 (**2011**) 3346-3352.

27. J.G. Bruno, T. Phillips, M.P. Carrillo, and R. Crowell, Plastic-adherent DNA aptamer-magnetic bead and quantum dot sandwich assay for Campylobacter detection. Journal of Fluorescence 19 (**2009**) 427-435.

28. E. Gizeli, and C.R. Lowe, Biomolecular Sensors, Taylor & Francis, **2002**.

29. C. Yao, T. Zhu, Y. Qi, Y. Zhao, H. Xia, and W. Fu, Development of a quartz crystal microbalance biosensor with aptamers as bio-recognition element. Sensors 10 (**2010**) 5859-5871.

30. S.R. Hong, and S. Hong, Application of QCM DNA biosensor to detect a marine derived pathogenic virus VHSV, **2009**, pp. 197-200.

31. S. Tombelli, M. Minunni, E. Luzi, and M. Mascini, Aptamer-based biosensors for the detection of HIV-1 Tat protein. Bioelectrochemistry 67 (**2005**) 135-141.

32. Q. Chen, W. Tang, D. Wang, X. Wu, N. Li, and F. Liu, Amplified QCM-D biosensor for protein based on aptamer-functionalized gold nanoparticles. Biosensors and Bioelectronics 26 (**2010**) 575-579.

33. S. Peeters, T. Stakenborg, G. Reekmans, W. Laureyn, L. Lagae, A. Van Aerschot, and M. Van Ranst, Impact of spacers on the hybridization efficiency of mixed self-assembled DNA/alkanethiol films. Biosensors and Bioelectronics 24 (**2008**) 72-77.

34. C. Ananthanawat, T. Vilaivan, W. Mekboonsonglarp, and V.P. Hoven, Thiolated pyrrolidinyl peptide nucleic acids for the detection of DNA hybridization using surface plasmon resonance. Biosensors and Bioelectronics 24 (**2009**) 3544-3549.

35. N. Patel, M.C. Davies, M. Hartshorne, R.J. Heaton, C.J. Roberts, S.J.B. Tendler, and P.M. Williams, Immobilization of protein molecules onto homogeneous and mixed carboxylate-terminated self-assembled monolayers. Langmuir 13 (**1997**) 6485-6490.

36. Z. Altintas, Y. Uludag, Y. Gurbuz, and I. Tothill, Development of surface chemistry for surface plasmon resonance based sensors for the detection of proteins and DNA molecules. Analytica Chimica Acta 712 (**2012**) 138-144.

37. S. Löfås, and B. Johnsson, A novel hydrogel matrix on gold surfaces in surface plasmon resonance sensors for fast and efficient covalent immobilization of ligands. Journal of the Chemical Society, Chemical Communications (**1990**) 1526-1528.

38. S.H. Jung, J.W. Jung, I.B. Suh, S.Y. Jong, W.J. Kim, Y.C. Eui, Y.M. Kim, and K.S. Ha, Analysis of C-reactive protein on amide-linked N-hydroxysuccinimide-dextran arrays with a

spectral surface plasmon resonance biosensor for serodiagnosis. Analytical Chemistry 79 (**2007**) 5703-5710.

39. E. Wijaya, C. Lenaerts, S. Maricot, J. Hastanin, S. Habraken, J.-P. Vilcot, R. Boukherroub, and S. Szunerits, Surface plasmon resonance-based biosensors: From the development of different SPR structures to novel surface functionalization strategies. Current Opinion in Solid State and Materials Science 15 (**2011**) 208-224.

40. R. Zheng, B.W. Park, D.S. Kim, and B.D. Cameron, Development of a highly specific amine-terminated aptamer functionalized surface plasmon resonance biosensor for blood protein detection. Biomedical Optics Express 2 (**2011**) 2731-2740.

41. Y. Liu, Y. Dong, J. Jauw, M.J. Linman, and Q. Cheng, Highly sensitive detection of protein toxins by surface plasmon resonance with biotinylation-based inline atom transfer radical polymerization amplification. Analytical Chemistry 82 (**2010**) 3679-3685.

42. H. Bai, R. Wang, B. Hargis, H. Lu, and Y. Li, A SPR aptasensor for detection of avian influenza virus H5N1. Sensors (Switzerland) 12 (**2012**) 12506-12518.

43. S.J. Lee, B.-S. Youn, J.W. Park, J.H. Niazi, Y.S. Kim, and M.B. Gu, ssDNA Aptamer-Based Surface Plasmon Resonance Biosensor for the Detection of Retinol Binding Protein 4 for the Early Diagnosis of Type 2 Diabetes. Analytical Chemistry 80 (**2008**) 2867-2873.

44. Y.H. Kim, J.P. Kim, S.J. Han, and S.J. Sim, Aptamer biosensor for lable-free detection of human immunoglobulin E based on surface plasmon resonance. Sensors and Actuators, B: Chemical 139 (**2009**) 471-475.

45. C.-C. Chang, S. Lin, C.-H. Lee, T.-L. Chuang, P.-R. Hsueh, H.-C. Lai, and C.-W. Lin, Amplified surface plasmon resonance immunosensor for interferon-Gamma based on a streptavidin-incorporated aptamer. Biosensors and Bioelectronics 37 (**2012**) 68-74.

46. C. Tuerk, and L. Gold, SYSTEMATIC EVOLUTION OF LIGANDS BY EXPONENTIAL ENRICHMENT - RNA LIGANDS TO BACTERIOPHAGE-T4 DNA-POLYMERASE. Science 249 (**1990**) 505-510.

47. A.D. Ellington, and J.W. Szostak, INVITRO SELECTION OF RNA MOLECULES THAT BIND SPECIFIC LIGANDS. Nature 346 (**1990**) 818-822.

48. C.L.A. Hamula, H. Zhang, F. Li, Z. Wang, X. Chris Le, and X.-F. Li, Selection and analytical applications of aptamers binding microbial pathogens. TrAC Trends in Analytical Chemistry 30 (**2011**) 1587-1597.

49. B. Waybrant, T.R. Pearce, P. Wang, S. Sreevatsan, and E. Kokkoli, Development and characterization of an aptamer binding ligand of fractalkine using domain targeted SELEX. Chemical Communications 48 (**2012**) 10043-10045.

50. Y. Takagaki, and J.L. Manley, RNA recognition by the human polyadenylation factor CstF. Molecular and Cellular Biology 17 (**1997**) 3907-3914.

51. S.Y. Low, J.E. Hill, and J. Peccia, A DNA aptamer recognizes the Asp f 1 allergen of Aspergillus fumigatus. Biochemical and Biophysical Research Communications 386 (**2009**) 544-548.

52. H. Feng, J. Beck, M. Nassal, and K.-h. Hu, A SELEX-Screened Aptamer of Human Hepatitis B Virus RNA Encapsidation Signal Suppresses Viral Replication. PLoS ONE 6 (**2011**) e27862.

53. M. Kim, H.-J. Um, S. Bang, S.-H. Lee, S.-J. Oh, J.-H. Han, K.-W. Kim, J. Min, and Y.-H. Kim, Arsenic Removal from Vietnamese Groundwater Using the Arsenic-Binding DNA Aptamer. Environmental Science & Technology 43 (**2009**) 9335-9340.

54. S. Weiss, D. Proske, M. Neumann, M.H. Groschup, H.A. Kretzschmar, M. Famulok, and E.L. Winnacker, RNA aptamers specifically interact with the prion protein PrP. Journal of Virology 71 (**1997**) 8790-8797.

55. M. Dobbelstein, and T. Shenk, In vitro selection of RNA ligands for the ribosomal L22 protein associated with Epstein-Barr virus-expressed RNA by using randomized and cDNA-derived RNA libraries. Journal of Virology 69 (**1995**) 8027-8034.

56. S.J. Kim, M.Y. Kim, J.H. Lee, J.C. You, and S. Jeong, Biochem. Biophys. Res. Commun. 291 (**2002**) 925-931.

57. R. Stoltenburg, C. Reinemann, and B. Strehlitz, FluMag-SELEX as an advantageous method for DNA aptamer selection. Analytical and Bioanalytical Chemistry 383 (**2005**) 83-91.

58. J.C. Cox, and A.D. Ellington, Automated selection of anti-protein aptamers. Bioorganic and Medicinal Chemistry 9 (**2001**) 2525-2531.

59. S.C.B. Gopinath, K. Kawasaki, and P.K.R. Kumar, Nucleic Acids Symp ser 49 (**2005**) 85.

60. S.C.B. Gopinath, Y. Sakamaki, K. Kawasaki, and P.K.R. Kumar, An efficient RNA aptamer against human influenza B virus hemagglutinin. Journal of Biochemistry 139 (**2006**) 837-846.

61. S.C.B. Gopinath, T.S. Misono, K. Kawasaki, T. Mizuno, M. Imai, T. Odagiri, and P.K.R. Kumar, An RNA aptamer that distinguishes between closely related human influenza viruses and inhibits haemagglutinin-mediated membrane fusion. Journal of General Virology 87 (**2006**) 479-487.

62. B. Hall, S. Arshad, K. Seo, C. Bowman, M. Corley, S.D. Jhaveri, and A.D. Ellington, In Vitro Selection of RNA Aptamers to a Protein Target by Filter Immobilization, Current Protocols in Molecular Biology, John Wiley & Sons, Inc., **2001**.

63. D. Ogasawara, H. Hasegawa, K. Kaneko, K. Sode, and K. Ikebukuro, Screening of DNA aptamer against mouse prion protein by competitive selection. Prion 1 (**2007**) 248-254.

64. T.W. Wiegand, P.B. Williams, S.C. Dreskin, M.H. Jouvin, J.P. Kinet, and D. Tasset, High-affinity oligonucleotide ligands to human IgE inhibit binding to Fcε receptor I. Journal of Immunology 157 (**1996**) 221-230.

65. R. Conrad, L.M. Keranen, A.D. Ellington, and A.C. Newton, Isozyme-specific inhibition of protein kinase C by RNA aptamers. Journal of Biological Chemistry 269 (**1994**) 32051-32054.

66. A. Geiger, P. Burgstaller, H. von der Eltz, A. Roeder, and M. Famulok, RNA aptamers that bind L-arginine with sub-micromolar dissociation constants and high enantioselectivity. Nucleic acids research 24 (**1996**) 1029-1036.

67. K.B. Jensen, B.L. Atkinson, M.C. Willis, T.H. Koch, and L. Gold, Using in vitro selection to direct the covalent attachment of human immunodeficiency virus type 1 Rev protein to high-affinity RNA ligands. Proceedings of the National Academy of Sciences of the United States of America 92 (**1995**) 12220-12224.

68. K.N. Morris, K.B. Jensen, C.M. Julin, M. Weil, and L. Gold, High affinity ligands from in vitro selection: Complex targets. Proceedings of the National Academy of Sciences of the United States of America 95 (**1998**) 2902-2907.

69. D. Shangguan, Y. Li, Z. Tang, Z.C. Cao, H.W. Chen, P. Mallikaratchy, K. Sefah, C.J. Yang, and W. Tan, Aptamers evolved from live cells as effective molecular probes for cancer study. Proceedings of the National Academy of Sciences of the United States of America 103 (**2006**) 11838-11843.

70. J.W. Park, R. Tatavarty, D.W. Kim, H.T. Jung, and M.B. Gu, Immobilization-free screening of aptamers assisted by graphene oxide. Chemical Communications 48 (**2012**) 2071-2073.

71. S.D. Mendonsa, and M.T. Bowser, In vitro selection of high-affinity DNA ligands for human IgE using capillary electrophoresis. Analytical Chemistry 76 (**2004**) 5387-5392.

72. M.T. Bowser, S.D. Mendonsa, and R. Mosing, CE-selex: In vitro selection of DNA APTAMERS using capillary electrophoresis. Abstracts of Papers of the American Chemical Society 229 (**2005**) 308-ANYL.

73. R.K. Mosing, S.D. Mendonsa, and M.T. Bowser, Capillary electrophoresis-SELEX selection of aptamers with affinity for HIV-1 reverse transcriptase. Analytical Chemistry 77 (**2005**) 6107-6112.

74. S.D. Mendonsa, and M.T. Bowser, In vitro selection of aptamers with affinity for neuropeptide Y using capillary electrophoresis. Journal of the American Chemical Society 127 (**2005**) 9382-9383.

75. P. Mallikaratchy, R.V. Stahelin, Z.H. Cao, W.H. Cho, and W.H. Tan, Selection of DNA ligands for protein kinase C-delta. Chemical Communications (**2006**) 3229-3231.

76. J. Tang, J. Xie, N. Shao, and Y. Yan, The DNA aptamers that specifically recognize ricin toxin are selected by twoin vitro selection methods. Electrophoresis 27 (**2006**) 1303-1311.

77. P. Ruff, R.B. Pai, and F. Storici, Real-Time PCR-Coupled CE-SELEX for DNA Aptamer Selection. ISRN Molecular Biology 2012 (**2012**) 9.

78. M. Berezovski, M. Musheev, A. Drabovich, and S.N. Krylov, Non-SELEX selection of aptamers. Journal of the American Chemical Society 128 (**2006**) 1410-1411.

79. M.V. Berezovski, M.U. Musheev, A.P. Drabovich, J.V. Jitkova, and S.N. Krylov, Non-SELEX: selection of aptamers without intermediate amplification of candidate oligonucleotides. Nature Protocols 1 (**2006**) 1359-1369.

80. M. Berezovski, A. Drabovich, S.M. Krylova, M. Musheev, V. Okhonin, A. Petrov, and S.N. Krylov, Nonequilibrium capillary electrophoresis of equilibrium mixtures: A universal tool for development of aptamers. Journal of the American Chemical Society 127 (**2005**) 3165-3171.

81. A. Drabovich, M. Berezovski, and S.N. Krylov, Selection of smart aptamers by equilibrium capillary electrophoresis of equilibrium mixtures (ECEEM). Journal of the American Chemical Society 127 (**2005**) 11224-11225.

82. J. Tok, J. Lai, T. Leung, and S.F.Y. Li, Selection of aptamers for signal transduction proteins by capillary electrophoresis. Electrophoresis 31 (**2010**) 2055-2062.

83. M. Jing, and M.T. Bowser, Isolation of DNA aptamers using micro free flow electrophoresis. Lab on a Chip 11 (**2011**) 3703-3709.

84. A.P. Drabovich, M.V. Berezovski, M.U. Musheev, and S.N. Krylov, Selection of smart small-molecule ligands: The proof of principle. Analytical Chemistry 81 (**2009**) 490-494.

85. M. Jing, and M.T. Bowser, Methods for measuring aptamer-protein equilibria: A review. Analytica Chimica Acta 686 (**2011**) 9-18.

86. Y. Li, C.R. Geyer, and D. Sen, Recognition of anionic porphyrins by DNA aptamers. Biochemistry 35 (**1996**) 6911-6922.

87. M. Del Toro, R. Gargallo, R. Eritja, and J. Jaumot, Anal. Biochem. 379 (**2008**) 8-15.

88. J.S. Choi, S.G. Kim, M. Lahousse, H.Y. Park, H.C. Park, B. Jeong, J. Kim, S.K. Kim, and M.Y. Yoon, Screening and Characterization of High-Affinity ssDNA Aptamers against Anthrax Protective Antigen. Journal of Biomolecular Screening 16 (**2011**) 266-271.

89. F. Chen, Y. Hu, D. Li, H. Chen, and X.L. Zhang, CS-SELEX generates high-affinity ssDNA aptamers as molecular probes for hepatitis C virus envelope glycoprotein E2. PLoS ONE 4 (**2009**).

90. C. Di Primo, E. Dausse, and J.-J. Toulmé, Surface Plasmon Resonance Investigation of RNA Aptamer–RNA Ligand Interactions. in: J. Goodchild, (Ed.), Therapeutic Oligonucleotides, Humana Press, **2011**, pp. 279-300.

91. S. Tsuji, T. Tanaka, N. Hirabayashi, S. Kato, J. Akitomi, H. Egashira, I. Waga, and T. Ohtsu, RNA aptamer binding to polyhistidine-tag. Biochemical and Biophysical Research Communications 386 (**2009**) 227-231.

92. M. Müller, J.E. Weigand, O. Weichenrieder, and B. Suess, Thermodynamic characterization of an engineered tetracycline-binding riboswitch. Nucleic acids research 34 (**2006**) 2607-2617.

93. Q. Deng, I. German, D. Buchanan, and R.T. Kennedy, Retention and separation of adenosine and analogues by affinity chromatography with an aptamer stationary phase. Analytical Chemistry 73 (**2001**) 5415-5421.

94. J.A. Cruz-Aguado, and G. Penner, Determination of ochratoxin A with a DNA aptamer. Journal of Agricultural and Food Chemistry 56 (**2008**) 10456-10461.

95. S. Jaouen, L. De Koning, C. Gaillard, E. Muselíková-Polanská, M. Štros, and F. Strauss, Determinants of specific binding of HMGB1 protein to hemicatenated DNA loops. Journal of Molecular Biology 353 (**2005**) 822-837.

96. O. Kensch, B.A. Connolly, H.J. Steinhoff, A. McGregor, R.S. Goody, and T. Restle, Hiv-1 reverse transcriptase-pseudoknot RNA aptamer interaction has a binding affinity in the low picomolar range coupled with high specificity. Journal of Biological Chemistry 275 (**2000**) 18271-18278.

97. L.M. Hellman, and M.G. Fried, Electrophoretic mobility shift assay (EMSA) for detecting protein-nucleic acid interactions. Nature Protocols 2 (**2007**) 1849-1861.

98. D. Sekkai, E. Dausse, C. Di Primo, F. Darfeuille, C. Boiziau, and J.J. Toulmé, In vitro selection of DNA aptamers against the HIV-1 TAR RNA hairpin. Antisense and Nucleic Acid Drug Development 12 (**2002**) 265-274.

99. P. Zhang, N. Zhao, Z. Zeng, Y. Feng, C.H. Tung, C.C. Chang, and Y. Zu, Using an RNA aptamer probe for flow cytometry detection of CD30-expressing lymphoma cells. Laboratory Investigation 89 (**2009**) 1423-1432.

100. M. Berezovski, and S.N. Krylov, Nonequilibrium capillary electrophoresis of equilibrium mixtures - A single experiment reveals equilibrium and kinetic parameters of protein-DNA interactions. Journal of the American Chemical Society 124 (**2002**) 13674-13675.

101. D.D. Buchanan, E.E. Jameson, J. Perlette, A. Malik, and R.T. Kennedy, Effect of buffer, electric field, and separation time on detection of aptamer-ligand complexes for affinity probe capillary electrophoresis. Electrophoresis 24 (**2003**) 1375-1382.

102. J. Cruz-Toledo, M. McKeague, X. Zhang, A. Giamberardino, E. McConnell, T. Francis, M.C. DeRosa, and M. Dumontier, Aptamer base: A collaborative knowledge base to describe aptamers and SELEX experiments. Database 2012 (**2012**).

103. J.F. Lee, J.R. Hesselberth, L.A. Meyers, and A.D. Ellington, Aptamer database. Nucleic acids research 32 (**2004**) D95-D100.

104. L.T. Cherney, M. Kanoatov, and S.N. Krylov, Method for determination of peak areas in nonequilibrium capillary electrophoresis of equilibrium mixtures. Analytical Chemistry 83 (**2011**) 8617-8622.

105. A.M. Brennan, and C.S. Mantzoros, Drug Insight: the role of leptin in human physiology and pathophysiology - emerging clinical applications. Nature Clinical Practice Endocrinology & Metabolism 2 (**2006**) 318-327.

106. J.M. Friedman, and J.L. Halaas, Leptin and the regulation of body weight in mammals. Nature 395 (**1998**) 763-770.

107. F. Zhang, M.B. Basinski, J.M. Beals, S.L. Briggs, L.M. Churgay, D.K. Clawson, R.D. DiMarchi, T.C. Furman, J.E. Hale, H.M. Hsiung, B.E. Schoner, D.P. Smith, X.Y. Zhang, J.-P. Wery, and R.W. Schevitz, Crystal structure of the obese protein Ieptin-E100. Nature 387 (**1997**) 206-209.

108. P. Yang, Y. Ma, A.W.M. Lee, and R.T. Kennedy, Measurement of dissociation rate of biomolecular complexes using CE. Electrophoresis 30 (**2009**) 457-464.

109. L.C. Bock, L.C. Griffin, J.A. Latham, E.H. Vermaas, and J.J. Toole, Selection of single-stranded DNA molecules that bind and inhibit human thrombin. Nature 355 (**1992**) 564-566.

110. P. Chelikani, I. Fita, and P.C. Loewen, Diversity of structures and properties among catalases. Cellular and Molecular Life Sciences 61 (**2004**) 192-208.

111. M.R.N. Murthy, T.J. Reid Iii, A. Sicignano, N. Tanaka, and M.G. Rossmann, Structure of beef liver catalase. Journal of Molecular Biology 152 (**1981**) 465-499.

112. J.B. Sumner, and A.L. Dounce, CRYSTALLINE CATALASE. Science 85 (**1937**) 366-367.

113. B. Maitre, L. Jornot, and A.F. Junod, Effects of inhibition of catalase and superoxide dismutase activity on antioxidant enzyme mRNA levels. American Journal of Physiology - Lung Cellular and Molecular Physiology 265 (**1993**) L636-L643.

114. L. Góth, Catalase Deficiency and Type 2 Diabetes. Diabetes Care 31 (**2008**) e93.

115. K.T. Kim, S.J. Klaine, J. Cho, S.-H. Kim, and S.D. Kim, Oxidative stress responses of Daphnia magna exposed to TiO(2) nanoparticles according to size fraction. Science of the Total Environment 408 (**2010**) 2268-2272.

116. C.C.W. Hsia, Respiratory Function of Hemoglobin. New England Journal of Medicine 338 (**1998**) 239-248.

117. A. Riccio, L. Vitagliano, G. Di Prisco, A. Zagari, and L. Mazzarella, The crystal structure of a tetrameric hemoglobin in a partial hemichrome state. Proceedings of the National Academy of Sciences of the United States of America 99 (**2002**) 9801-9806.

118. A. Vergara, M. Franzese, A. Merlino, G. Bonomi, C. Verde, D. Giordano, G. Di Prisco, H.C. Lee, J. Peisach, and L. Mazzarella, Correlation between hemichrome stability and the root effect in tetrameric hemoglobins. Biophysical Journal 97 (**2009**) 866-874.

119. M.F. Perutz, M.G. Rossmann, A.F. Cullis, H. Muirhead, G. Will, and A.C.T. North, Structure of Haemoglobin: A Three-Dimensional Fourier Synthesis at 5.5-[angst]. Resolution, Obtained by X-Ray Analysis. Nature 185 (**1960**) 416-422.

120. M. Paoli, R. Liddington, J. Tame, A. Wilkinson, and G. Dodson, Crystal Structure of T State Haemoglobin with Oxygen Bound At All Four Haems. Journal of Molecular Biology 256 (**1996**) 775-792.

121. S.D. Jayasena, Aptamers: An emerging class of molecules that rival antibodies in diagnostics. Clinical Chemistry 45 (**1999**) 1628-1650.

122. S. Shin, I.H. Kim, W. Kang, J.K. Yang, and S.S. Hah, An alternative to Western blot analysis using RNA aptamer-functionalized quantum dots. Bioorganic & Medicinal Chemistry Letters 20 (**2010**) 3322-3325.

123. I. Mannelli, M. Minunni, S. Tombelli, R. Wang, M. Michela Spiriti, and M. Mascini, Direct immobilisation of DNA probes for the development of affinity biosensors. Bioelectrochemistry 66 (**2005**) 129-138.

124. L.H. Cazares, D.A. Troyer, B.H. Wang, R.R. Drake, and O.J. Semmes, MALDI tissue imaging: from biomarker discovery to clinical applications. Analytical and Bioanalytical Chemistry 401 (**2011**) 17-27.

125. S. Stewart, A. Syrett, A. Pothukuchy, S. Bhadra, A. Ellington, and E. Anslyn, Identifying Protein Variants with Cross-Reactive Aptamer Arrays. Chembiochem 12 (**2011**) 2021-2024.

126. B. Feng, Y.P. Luo, F. Ge, L. Wang, L.Q. Huang, and Y.Z. Dai, Site-oriented immobilization of fusion antigen directed by an affinity ligand, and its validation in an immunoassay. Surface and Interface Analysis 43 (**2011**) 1304-1310.

127. M. Kanoatov, and S.N. Krylov, DNA Adsorption to the Reservoir Walls Causing Irreproducibility in Studies of Protein-DNA Interactions by Methods of Kinetic Capillary Electrophoresis. Analytical Chemistry 83 (**2011**) 8041-8045.

128. T. Das, and S. Chakraborty, Biomicrofluidics: Recent trends and future challenges. Sadhana 34 (**2009**) 573-590.

129. J.C.H. Chen, L.J.W. Miercke, J. Krucinski, J.R. Starr, G. Saenz, X. Wang, C.A. Spilburg, L.G. Lange, J.L. Ellsworth, and R.M. Stroud, Structure of bovine pancreatic cholesterol esterase at 1.6 Å: Novel structural features involved in lipase activation. Biochemistry 37 (**1998**) 5107-5117.

130. L.M.T.E. Lansbergen, M. Nielen, T.J.G.M. Lam, A. Pengov, Y.H. Schukken, and K. Maatje, Evaluation of a Prototype On-Line Electrical Conductivity System for Detection of Subclinical Mastitis. Journal of Dairy Science 77 (**1994**) 1132-1140.

131. H. Hamed, A. El Feki, and A. Gargouri, Total and differential bulk cow milk somatic cell counts and their relation with antioxidant factors. Comptes Rendus Biologies 331 (**2008**) 144-151.

132. M.T. Koskinen, J. Holopainen, S. Pyörälä, P. Bredbacka, A. Pitkälä, H.W. Barkema, R. Bexiga, J. Roberson, L. Sølverød, R. Piccinini, D. Kelton, H. Lehmusto, S. Niskala, and L. Salmikivi, Analytical specificity and sensitivity of a real-time polymerase chain reaction assay for identification of bovine mastitis pathogens. Journal of Dairy Science 92 (**2009**) 952-959.

133. P. Cremonesi, G. Pisoni, M. Severgnini, C. Consolandi, P. Moroni, M. Raschetti, and B. Castiglioni, Pathogen detection in milk samples by ligation detection reaction-mediated universal array method. Journal of Dairy Science 92 (**2009**) 3027-3039.

134. P. Fűtő, G. Markus, A. Kiss, and N. Adányi, Development of a Catalase-Based Amperometric Biosensor for the Determination of Increased Catalase Content in Milk Samples. Electroanalysis 24 (**2012**) 107-113.

135. Y. Hiller, J.M. Gershoni, E.A. Bayer, and M. Wilchek, Biotin binding to avidin. Oligosaccharide side chain not required for ligand association. Biochem. J. 248 (**1987**) 167-171.

136. K. Andersson, M. Hämäläinen, and M. Malmqvist, Identification and optimization of regeneration conditions for affinity- based biosensor assays. A multivariate cocktail approach. Analytical Chemistry 71 (**1999**) 2475-2481.

137. A. Yan, and A.D. Ellington, Aptamers as potential diagnostic reagents for diabetes. Diabetes Technology and Therapeutics 4 (**2002**) 339-346.

138. P.J. Beisswenger, B.S. Szwergold, and K.T. Yeo, Glycated proteins in diabetes. Clinics in Laboratory Medicine 21 (**2001**) 53-78.

139. W.J. Schnedl, A. Liebminger, R.E. Roller, and R.W. Lipp, HbA(1c) determination and predicting the clinical status of diabetic patients [6]. Diabetes Care 23 (**2000**) 1597.

140. W.J. Schnedl, A. Liebminger, R.E. Roller, R.W. Lipp, and G.J. Krejs, Hemoglobin variants and determination of glycated hemoglobin (HbA1c). Diabetes/Metabolism Research and Reviews 17 (**2001**) 94-98.

141. M. Platt, G.R. Willmott, and G.U. Lee, Resistive pulse sensing of analyte-induced multicomponent rod aggregation using tunable pores. Small 8 (**2012**) 2436-2444.

a. Appendix of chapter 3

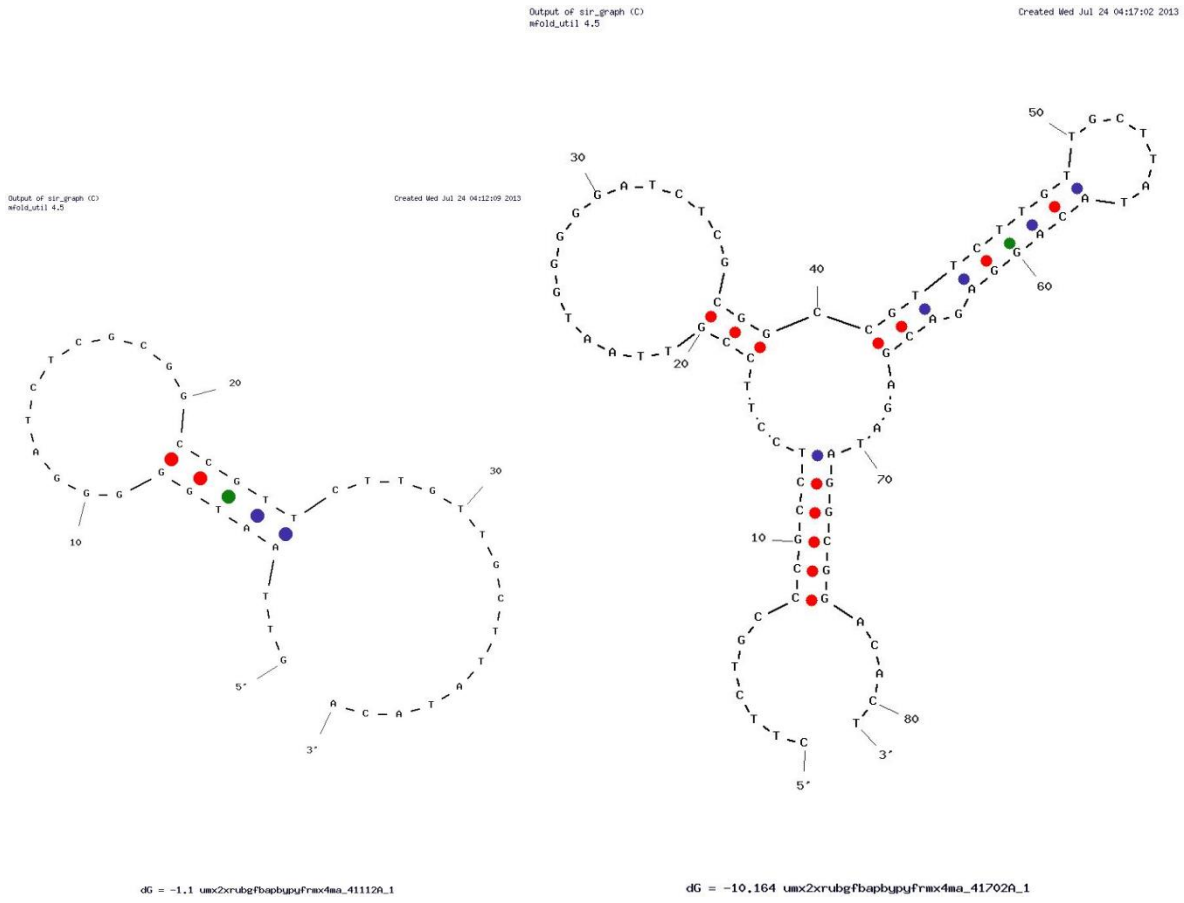

Figure a.1 Full secondary structure of Lep 3 Aptamer. Analyzed by OligoAnalyzer 3.1 software using 100mM NaCl and 10mM $MgCl_2$ concentration

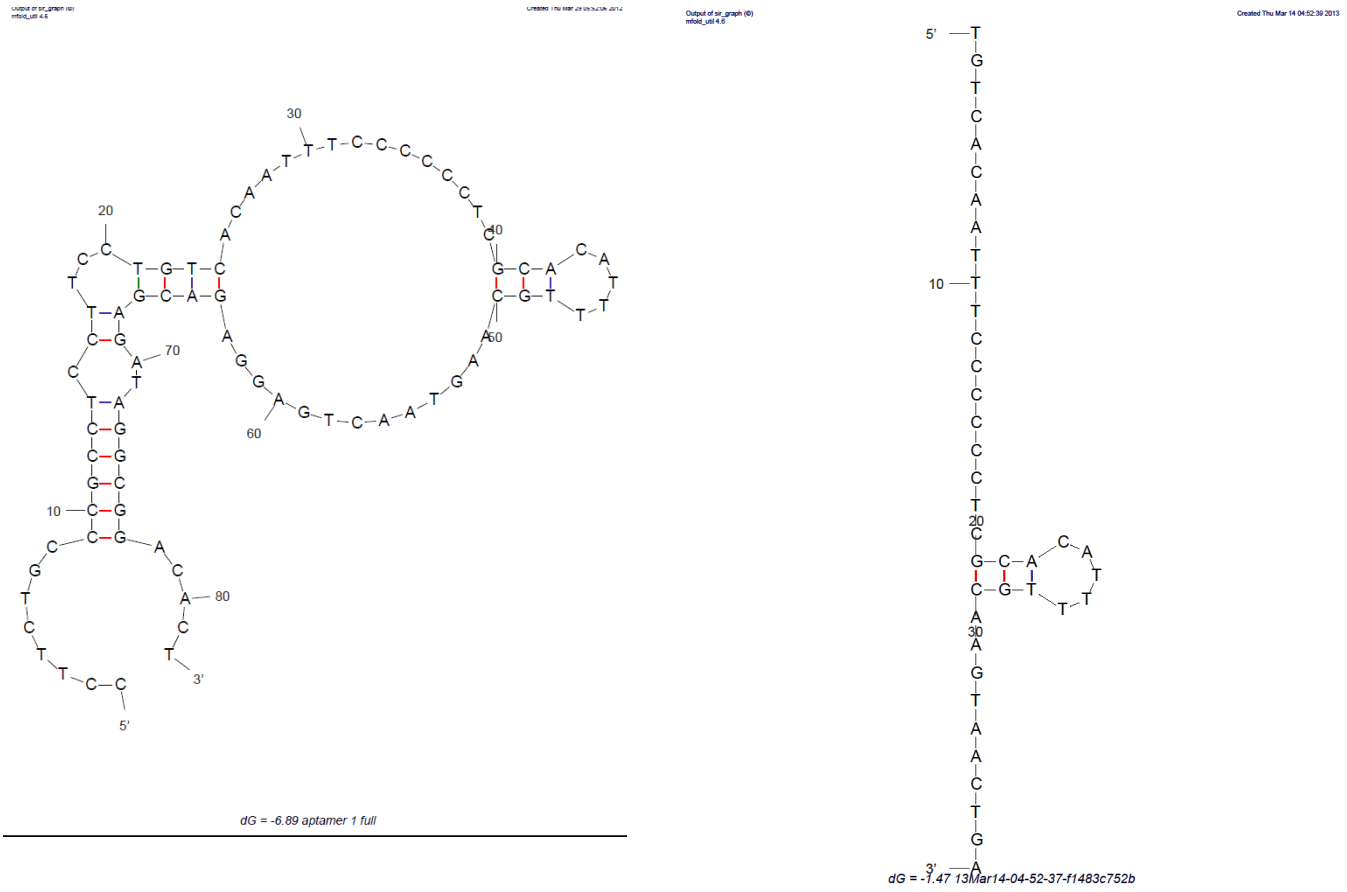

Figure a.2 Secondary structure of Lep 1 and Lep 1T aptamer, analyzed on mfold software using 100mM NaCl and 10mM $MgCl_2$ for the ionic conditions

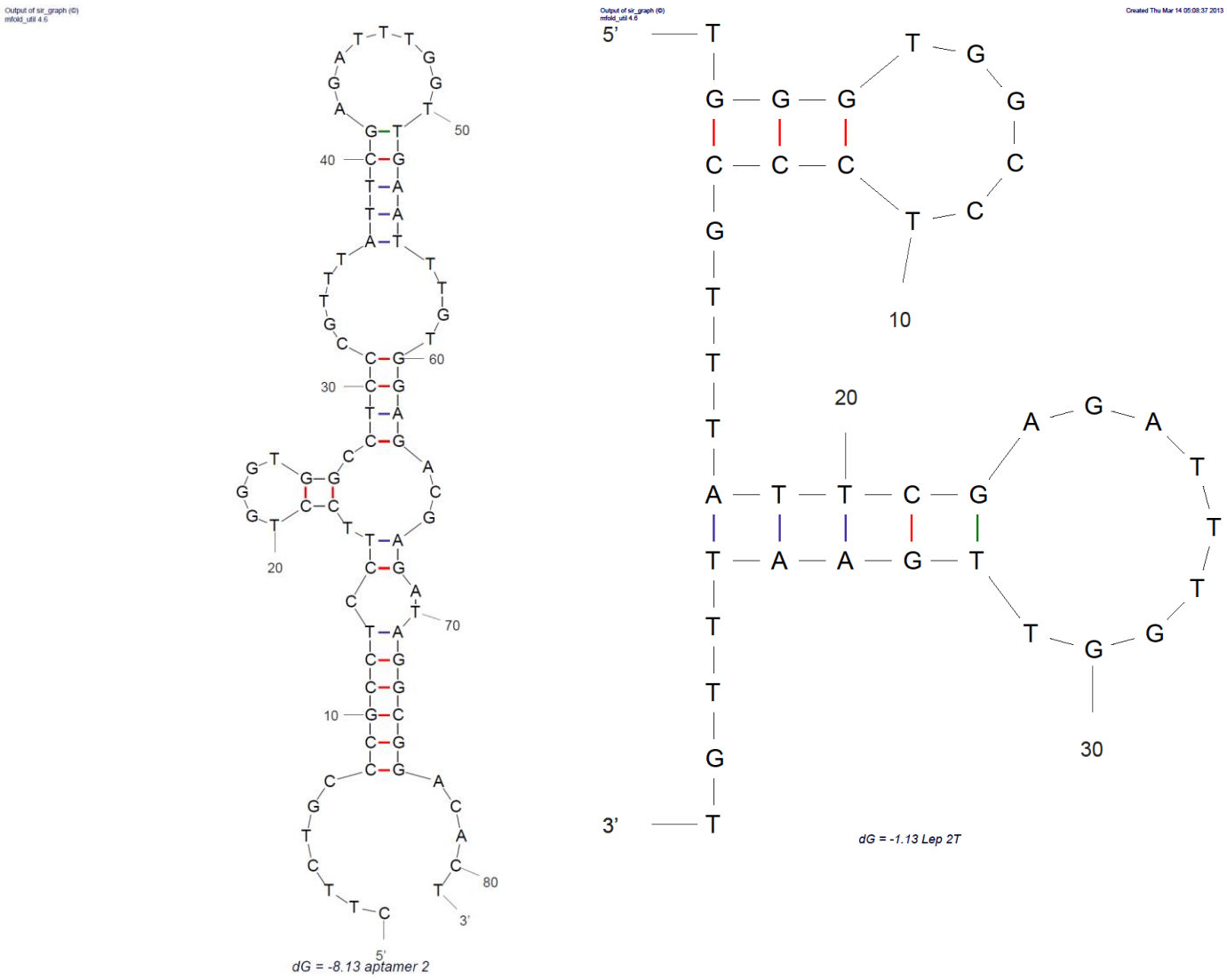

Figure a.3 Secondary structure of Lep 2 and Lep 2T aptamer, analyzed on mfold software using 100mM NaCl and 10mM $MgCl_2$ for the ionic conditions

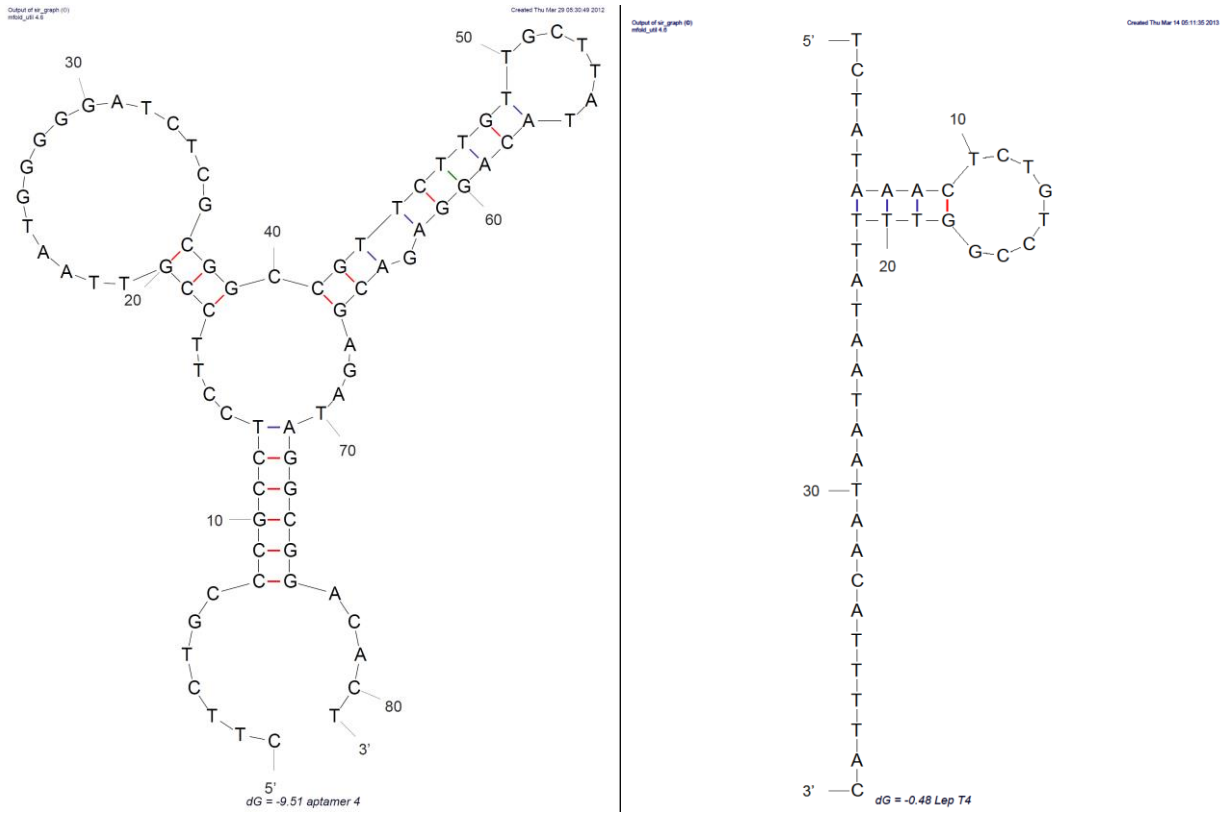

Figure a.4 Secondary structures of Lep 4 and Lep 4T aptamer, analyzed on mfold software using 100mM NaCl and 10mM $MgCl_2$ for the ionic conditions

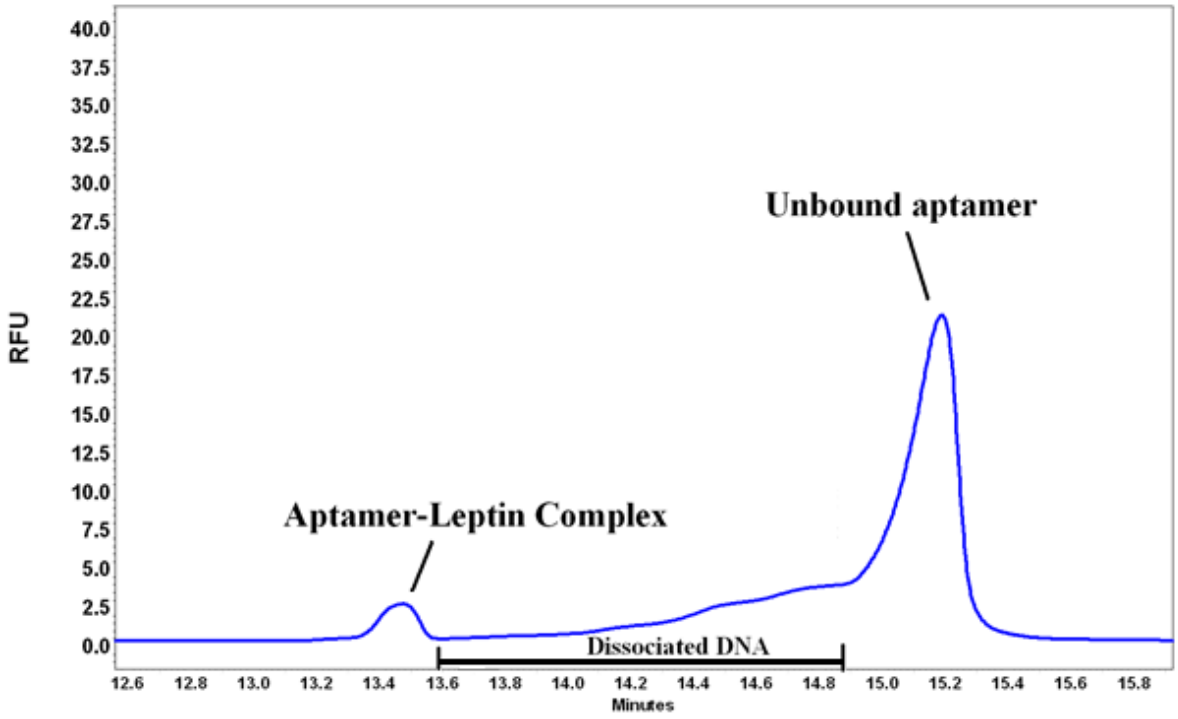

Figure a.5 NECEEM analysis electrophoretogram of Lep 1; 100nM aptamer and 500nM leptin were incubated for 30 minutes and injected onto the capillary by hydrodynamic injection (411nl), 333Vcm^{-1} separation with LIF detection. The areas of the free DNA, dissociated DNA and complex peak were used to determine K_D and 3 experiments were performed for each sequence.

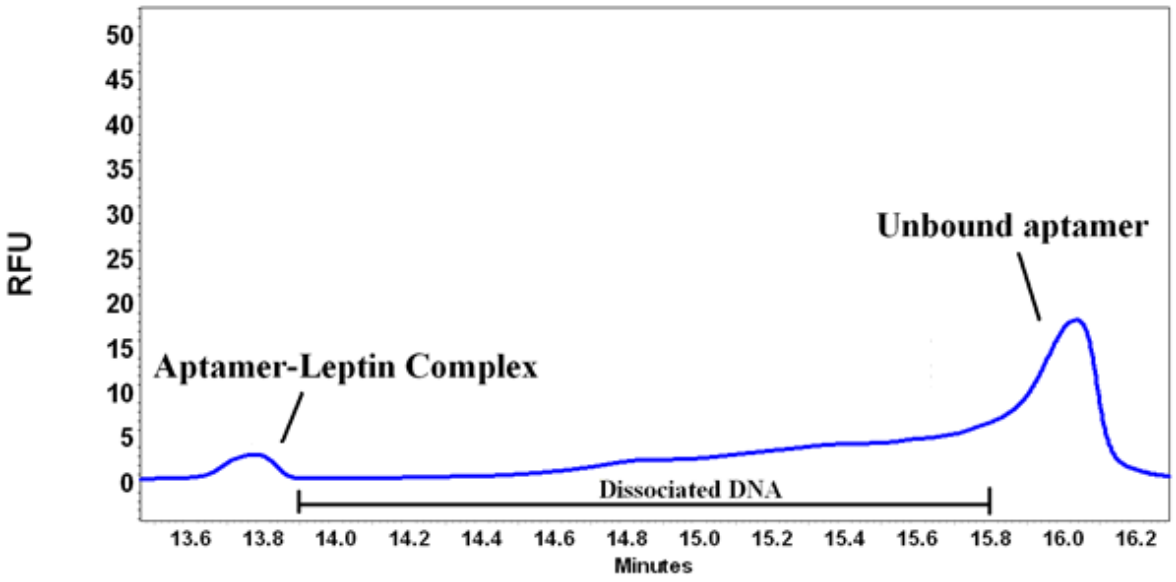

Figure a.6 NEECEM analysis electrophoretogram of Lep 2; 100nM aptamer and 500nM leptin were incubated for 30 minutes and injected onto the capillary by hydrodynamic injection (411nl), 333Vcm^{-1} separation with LIF detection. The areas of the free DNA, dissociated DNA and complex peak were used to determine K_D and 3 experiments were performed for each sequence.

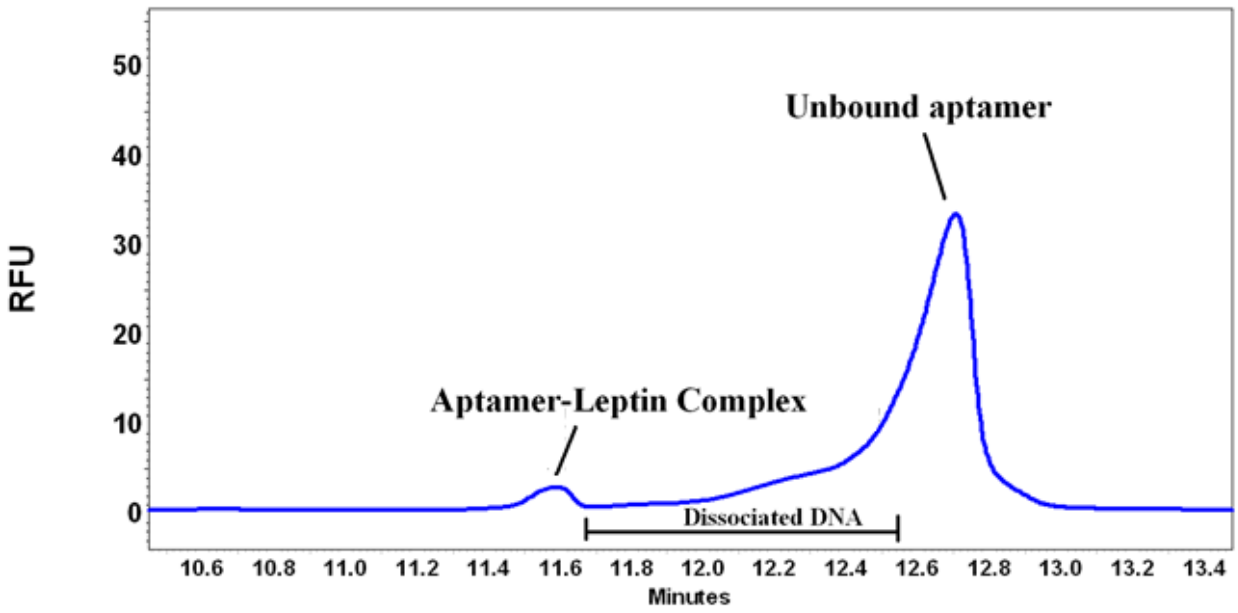

Figure a.7 NEECEM analysis electrophoretogram of Lep 4; 100nM aptamer and 500nM leptin were incubated for 30 minutes and injected onto the capillary by hydrodynamic injection (411nl), 333Vcm^{-1} separation with LIF detection. The areas of the free DNA, dissociated DNA and complex peak were used to determine K_D and 3 experiments were performed for each sequence.

b. Appendix of chapter 4

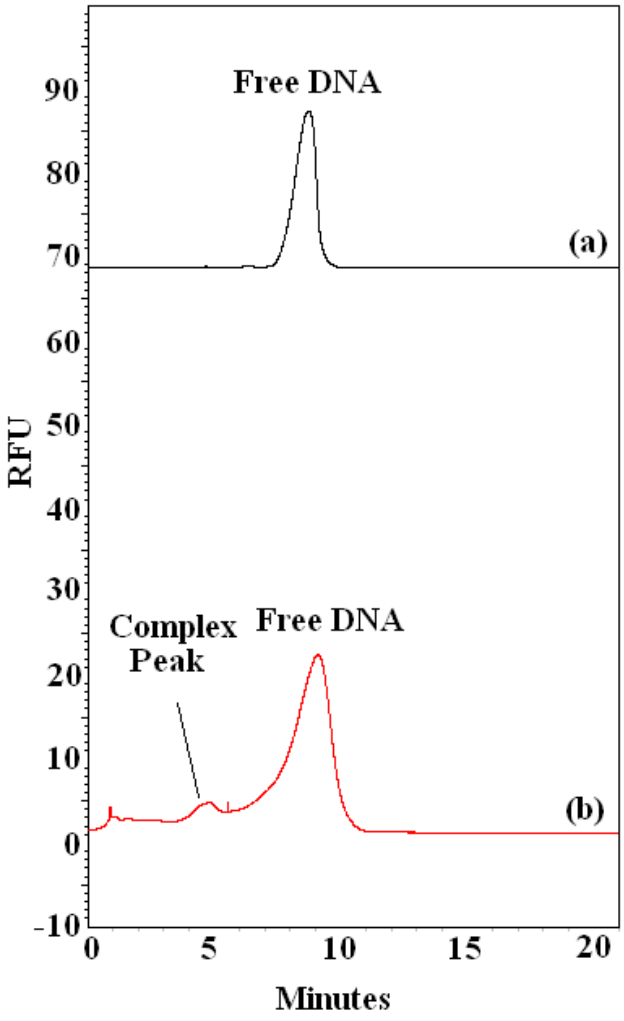

Figure b.1 Bulk affinity analysis electrophoretogram of the 1st enriched library using NECEEM, Run buffer: 3xTGK and selection buffer 1xTGK, 20kV 13 second injection 1psi, 100μm ID capillary (a) Enriched DNA library with LIF detection; (b) Enriched DNA library with 1μM Catalase protein with LIF detection

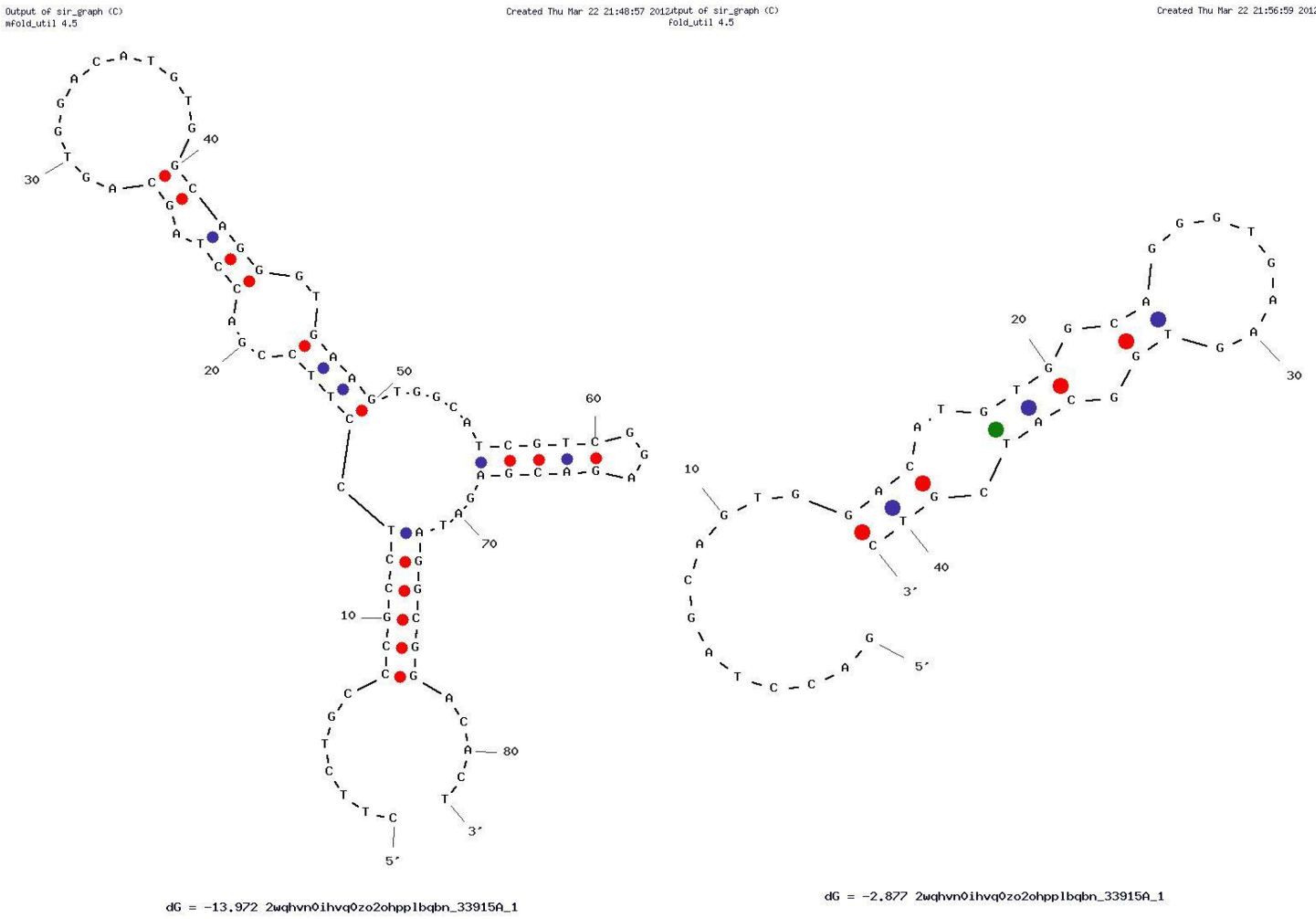

Figure b.2 Full secondary structure of aptamer CAT 1 and CAT 1T, checked on the OligoAnalyzer 3.1 program using the ionic conditions of 100mM [Na^{+}] and 5mM [Mg^{2+}] ion concentration.

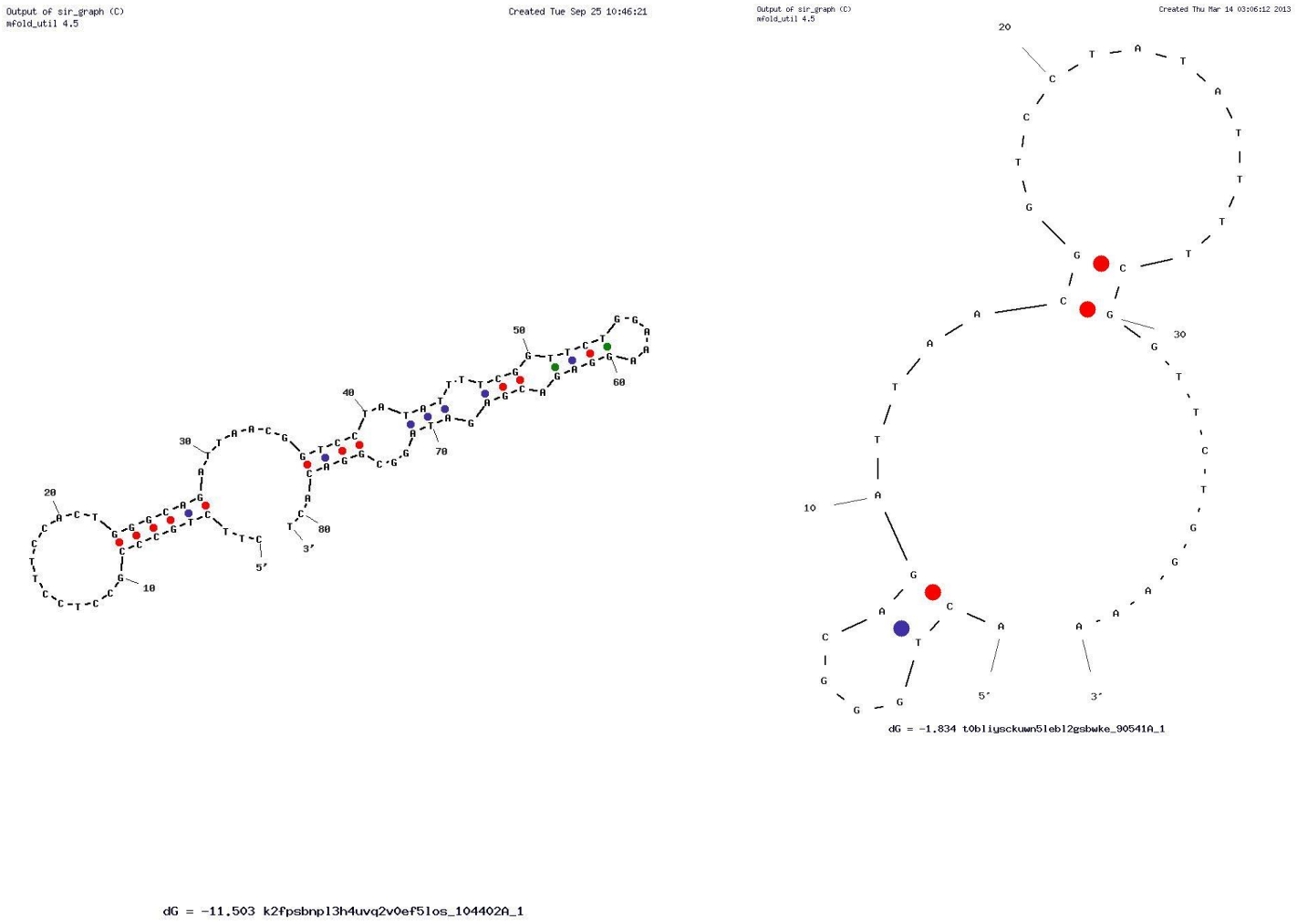

Figure b.3 The secondary structures of aptamer CAT 2 and CAT 2T, checked on the OligoAnalyzer 3.1 program using the ionic conditions of 100mM [Na^+] and 5mM [Mg^{2+}] ion concentration

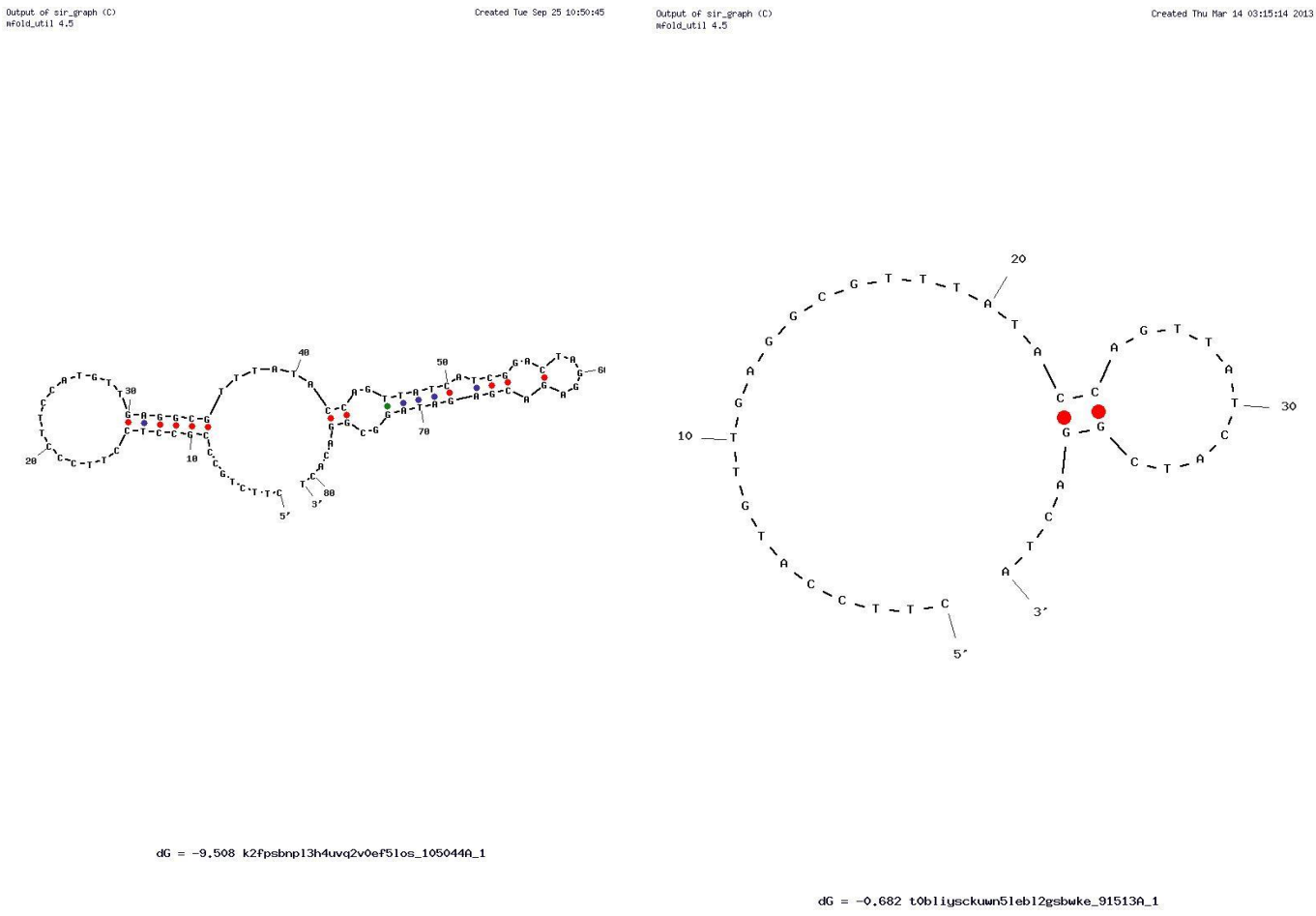

Figure b.4 The secondary structures of aptamer CAT 3 and CAT 3T, checked on the OligoAnalyzer 3.1 program using the ionic conditions of 100mM [Na^{+}] and 5mM [Mg^{2+}] ion concentration

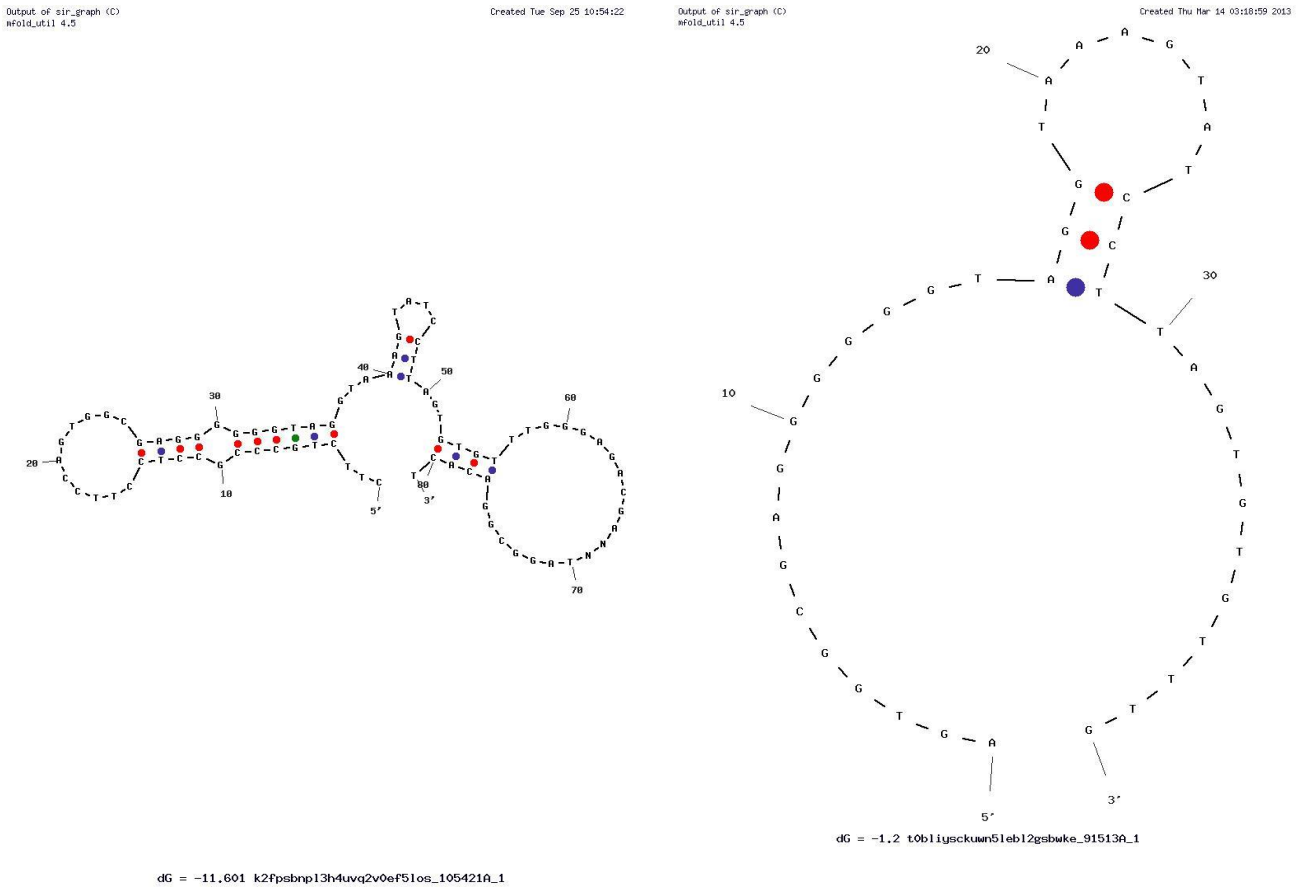

Figure b.5 The secondary structures of aptamer CAT 4 and CAT 4T, checked on the OligoAnalyzer 3.1 program using the ionic conditions of 100mM [Na^{+}] and 5mM [Mg^{2+}] ion concentration

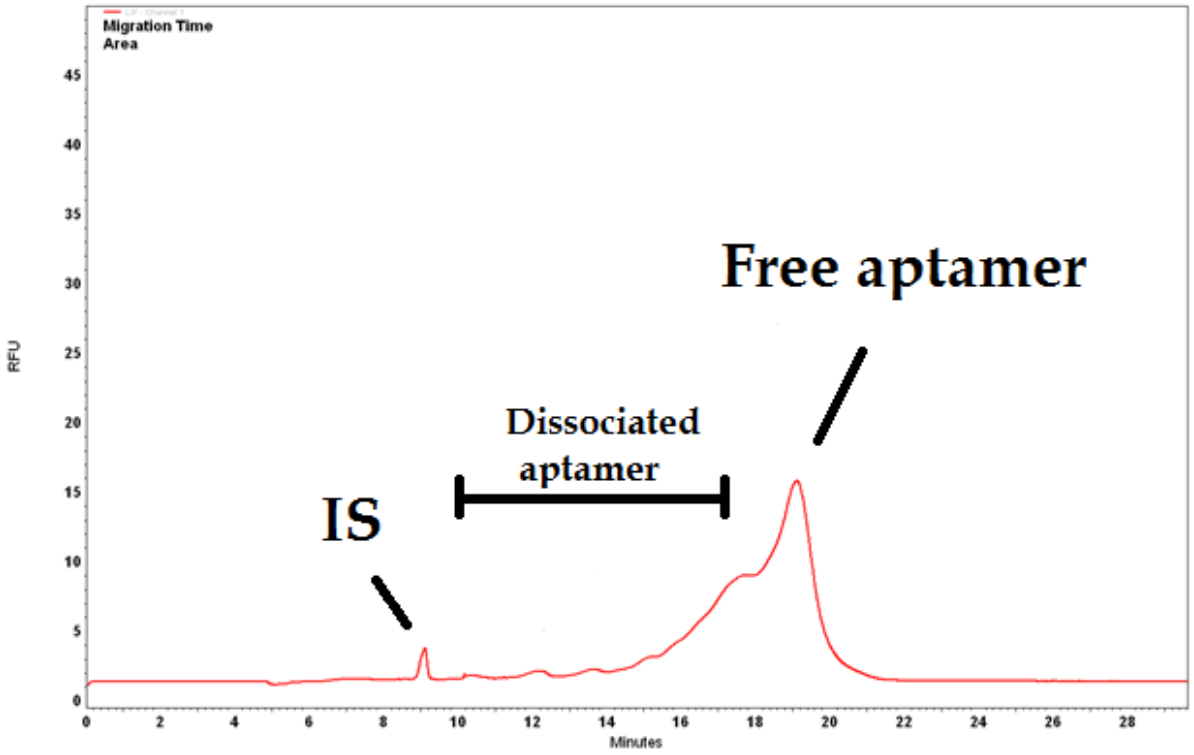

Figure b.6 NECEEM analysis electrophoretogram of CAT 2 aptamer; Run buffer: 3xTGK and selection buffer 1xTGK, 20kV 13 second injection 1psi, 100μm ID capillary; (a) 100nM DNA library with LIF detection; (b) incubated mixture of 4μM catalase, 100nM catalase aptamer 1 and 10nM FAM internal standard with LIF detection.

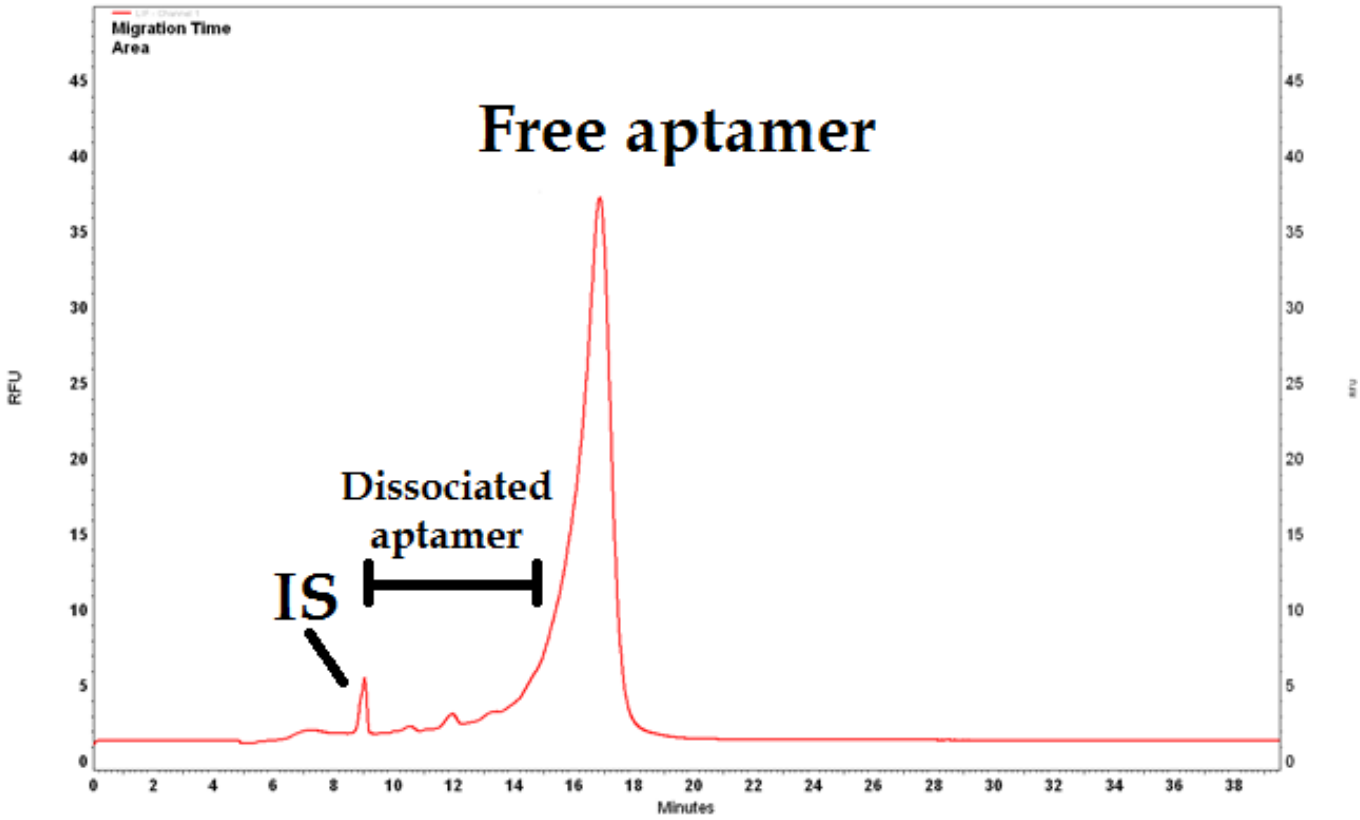

Figure b.7 NECEEM analysis electrophoretogram of CAT 3 aptamer; Run buffer: 3xTGK and selection buffer 1xTGK, 20kV 13 second injection 1psi, 100μm ID capillary; (a) 100nM DNA library with LIF detection; (b) incubated mixture of 4μM catalase, 100nM catalase aptamer 1 and 10nM FAM internal standard with LIF detection.

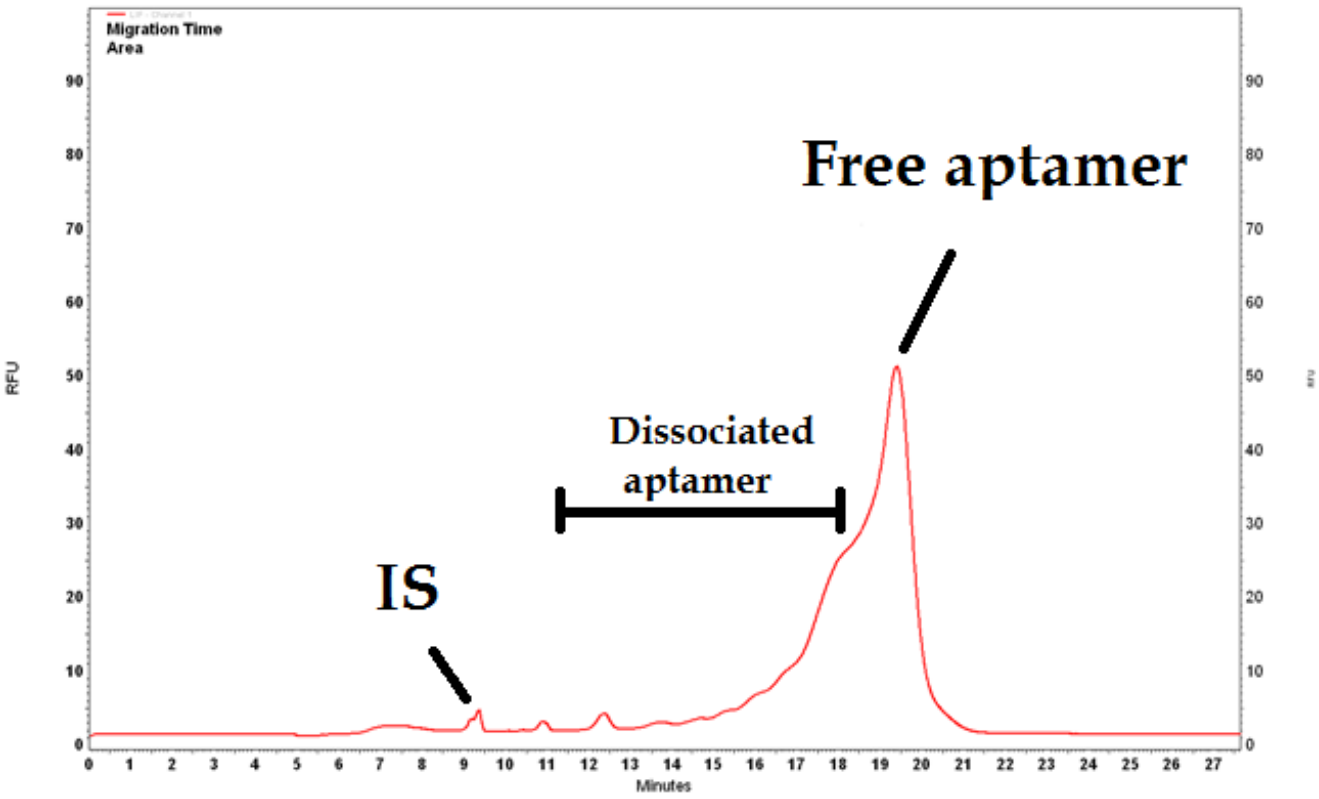

Figure b.8 NECEEM analysis electrophoretogram of CAT4 aptamer; Run buffer: 3xTGK and selection buffer 1xTGK, 20kV 13 second injection 1psi, 100μm ID capillary; (a) 100nM DNA library with LIF detection; (b) incubated mixture of 4μM catalase, 100nM catalase aptamer 1 and 10nM FAM internal standard with LIF detection.

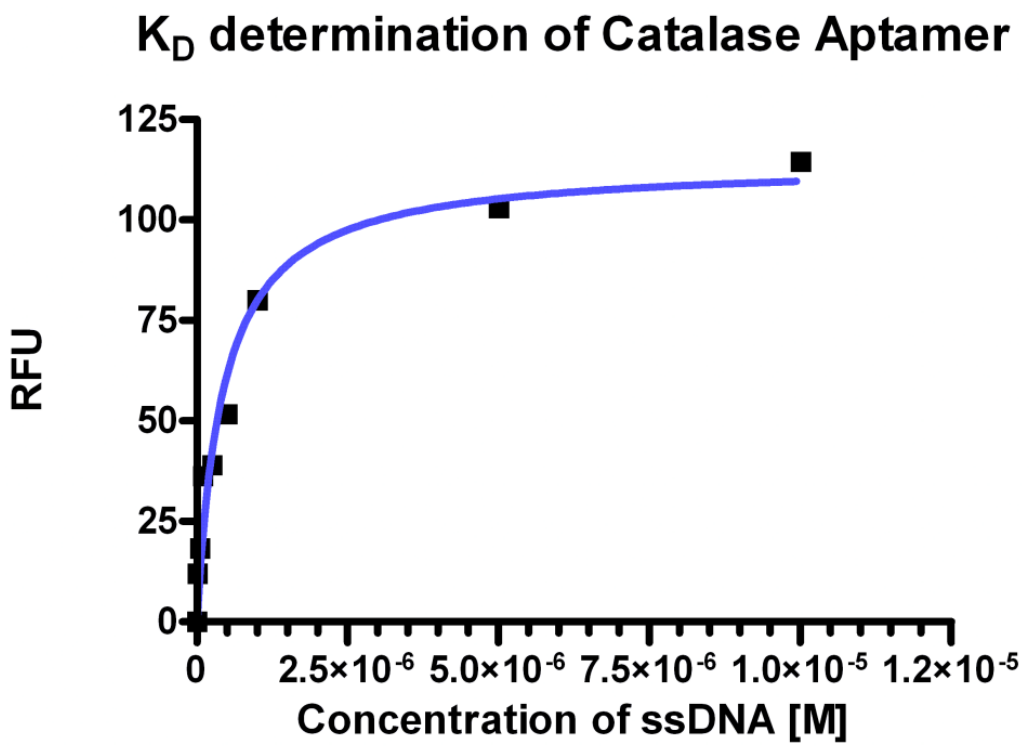

Figure b.9 Saturation curve for the affinity analysis of CAT 1 aptamer incubated with immobilized aptamer concentrations using fluorescence intensities. K_D was determined through through non-linear regression plotting fluorescence intensity against ssDNA concentration

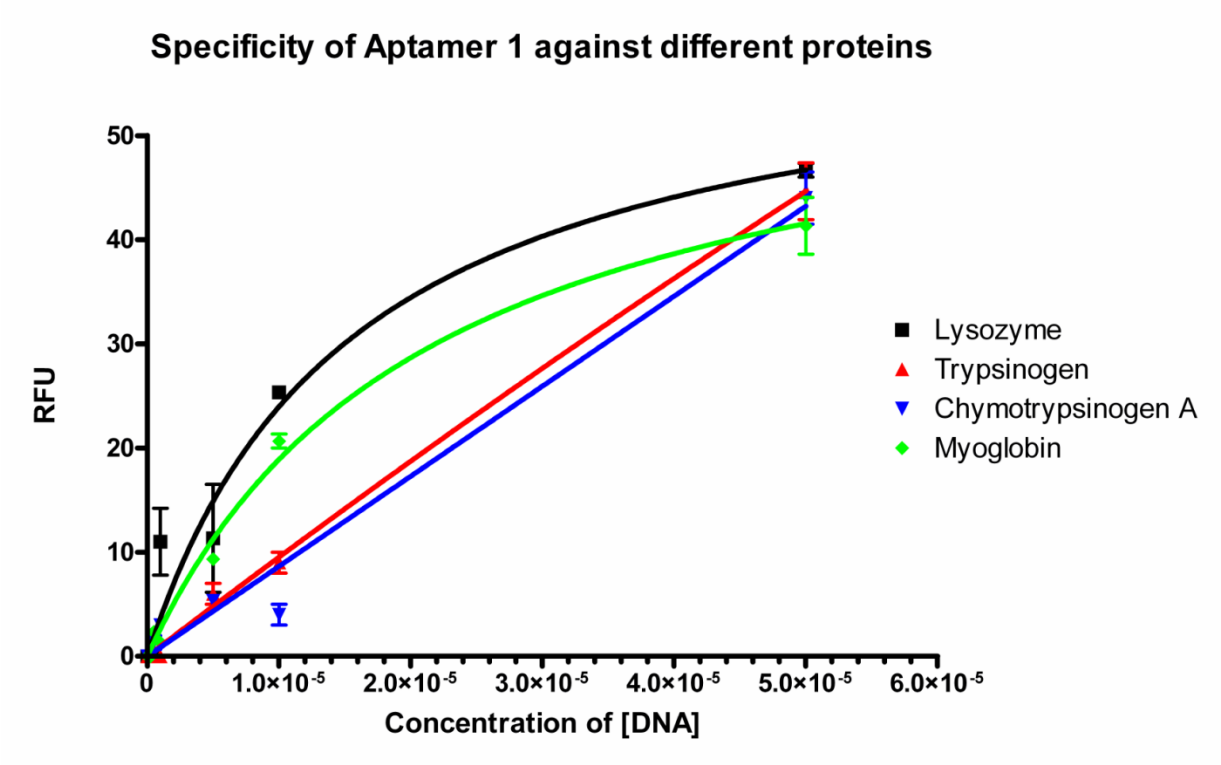

Figure b.10 Saturation curve to show the specificity of CAT 1 aptamer against different proteins. The catalase protein shows a 100 fold increase in binding compared to the other proteins.

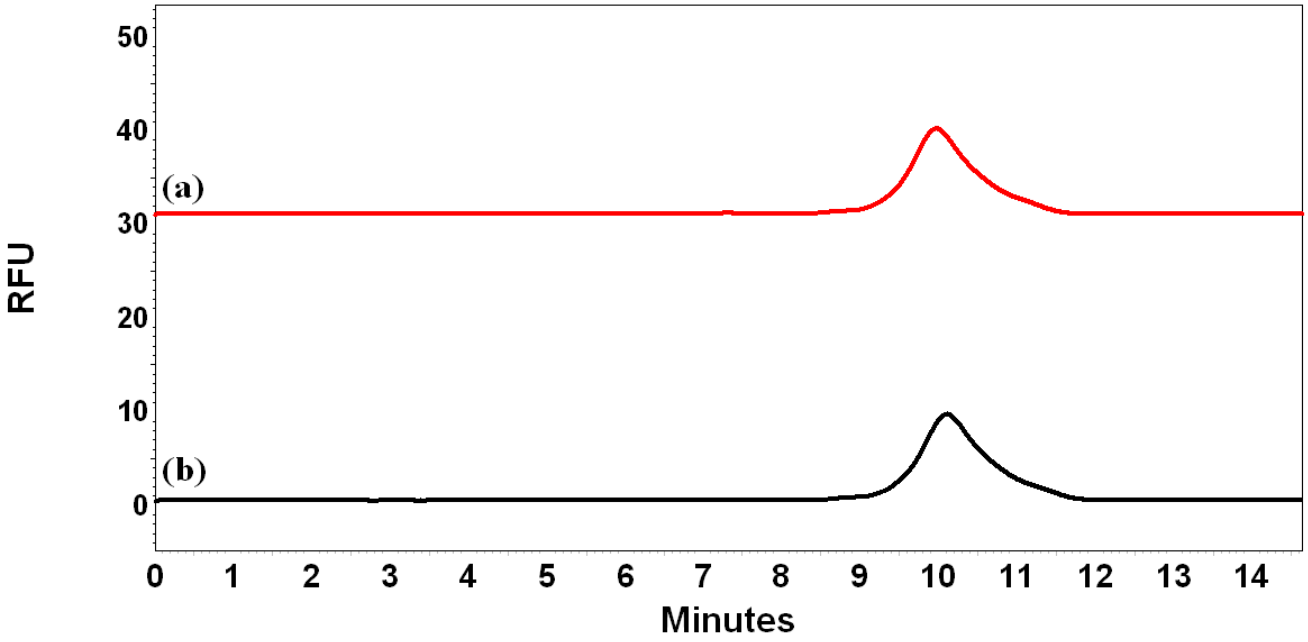

Figure b.11 **Electophoreogram of the initial haemoglobin library using capillary electrophoresis; Run buffer: 3xTGK and selection buffer 1xTGK, 333Vcm^{-1} 13 second injection 1psi, 100μm ID capillary; (a); 100nM random library with LIF detection (b) 13.9 μM hemoglobin protein and 100nM enriched DNA library with LIF detection**

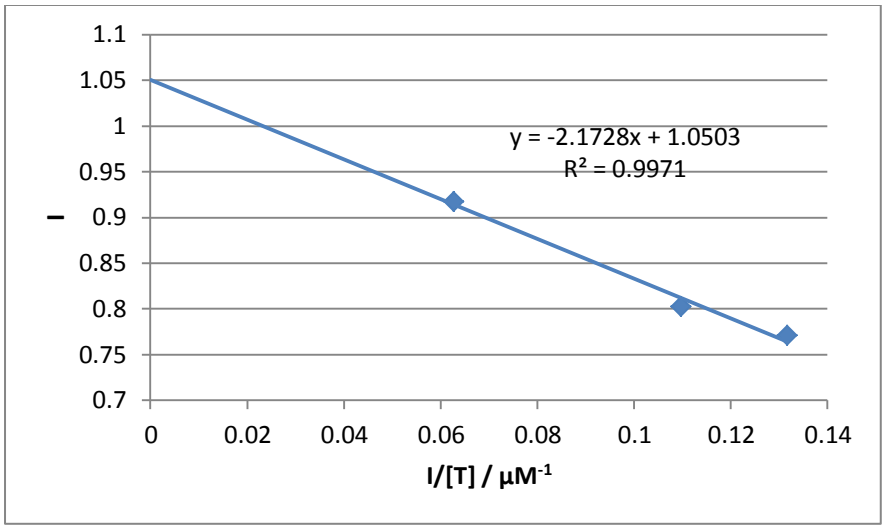

Figure b.12 **Eadie-Hofstee Plot for bulk affinity determination of the enriched library from round 1 of selection**

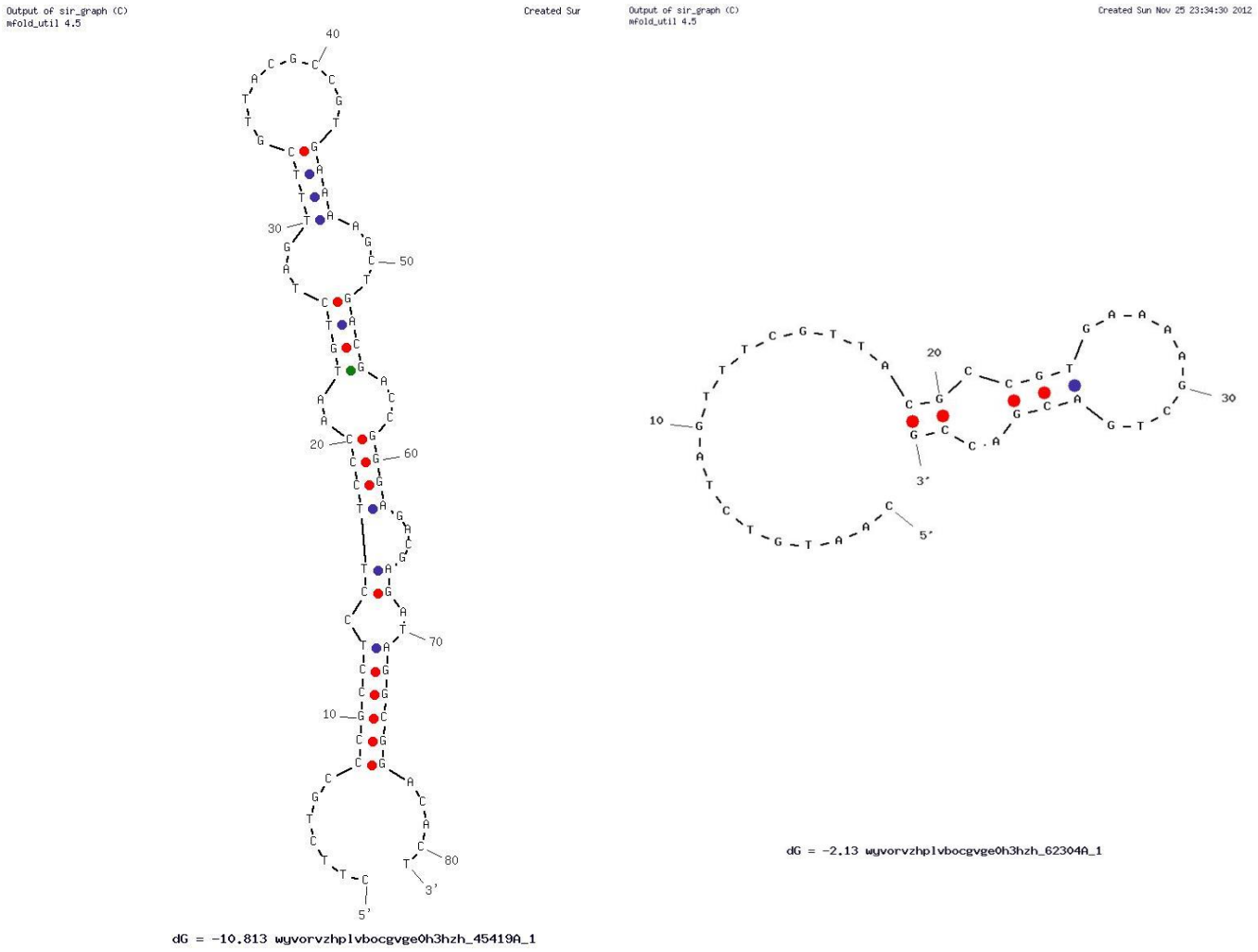

Figure b.13 The secondary structures of aptamer HB 1 and HB 1T. The secondary structure is checked on the OligoAnalyser 3.1 program using ionic conditions of 100mM [Na^+] and 5mM [Mg^{2+}] ion concentration.

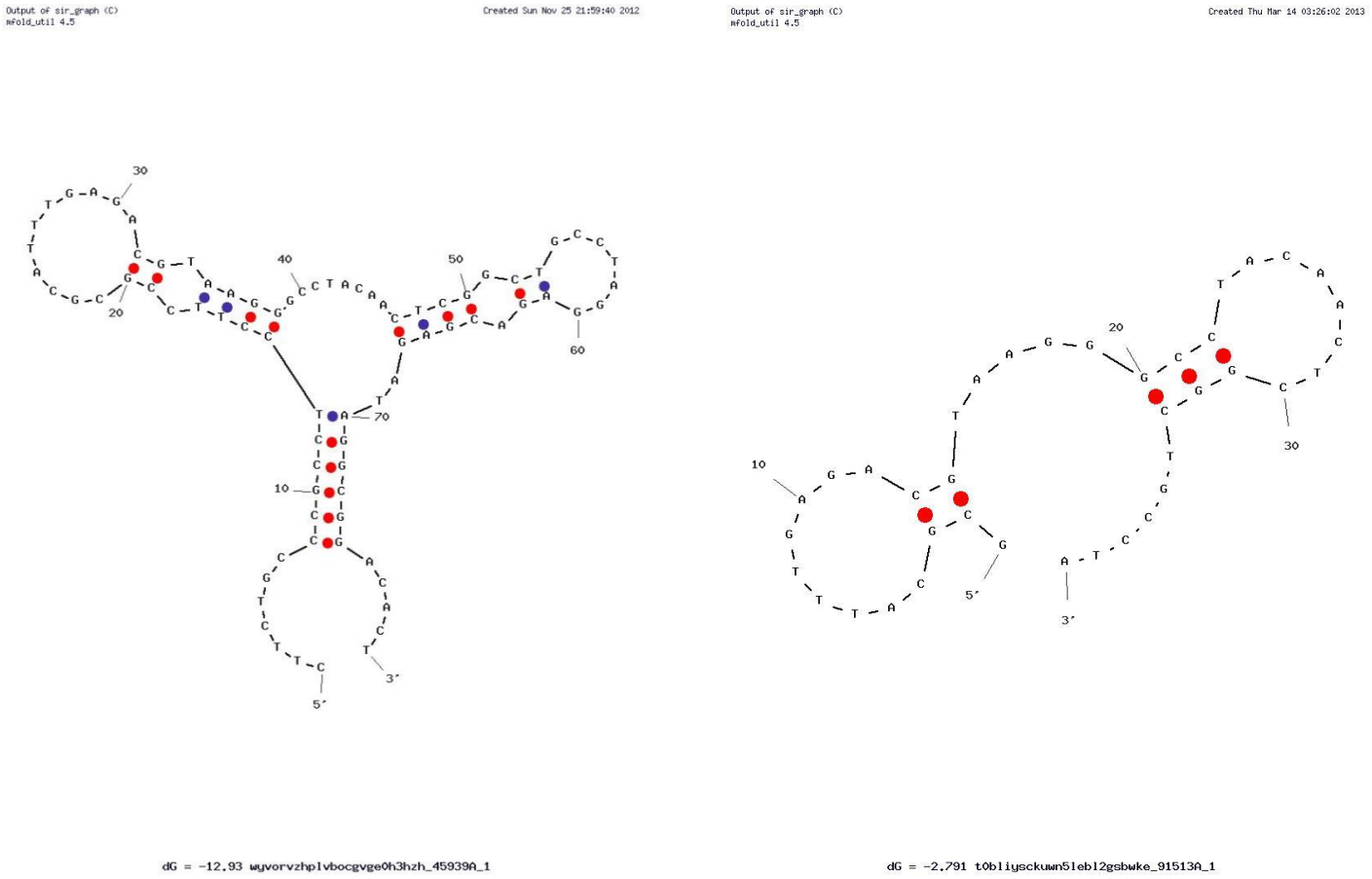

Figure b.14 The secondary structures of aptamer HB 2 and HB 2T checked on the OligoAnalyzer 3.1 program using ionic conditions of 100mM [Na^{+}] and 5mM [Mg^{2+}] ion concentration.

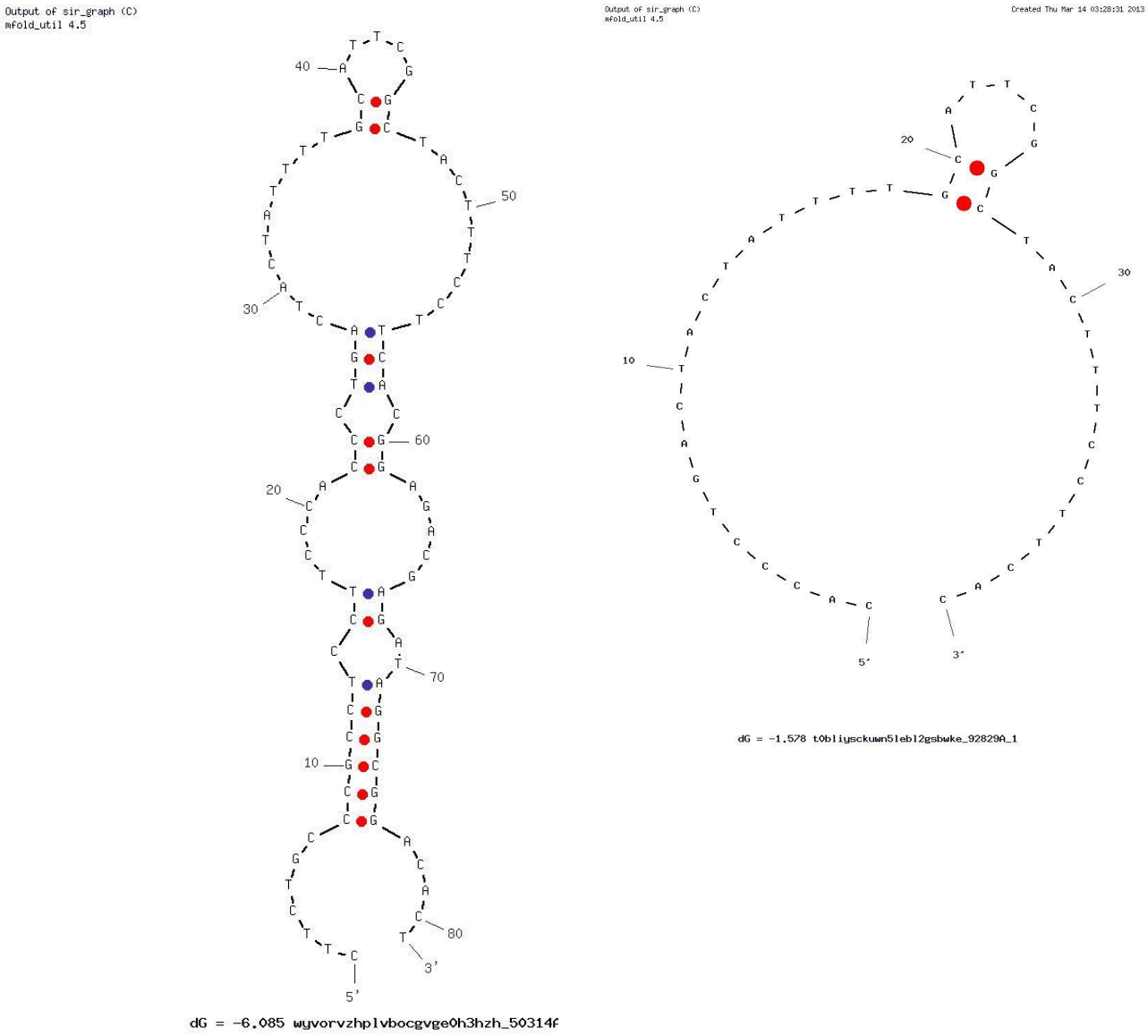

Figure b.15 Full secondary structures of aptamer HB 3 and HB 3T, checked on the OligoAnalyzer 3.1 program using the ionic conditions of 100mM [Na^+] and 5mM [Mg^{2+}] ion concentration.

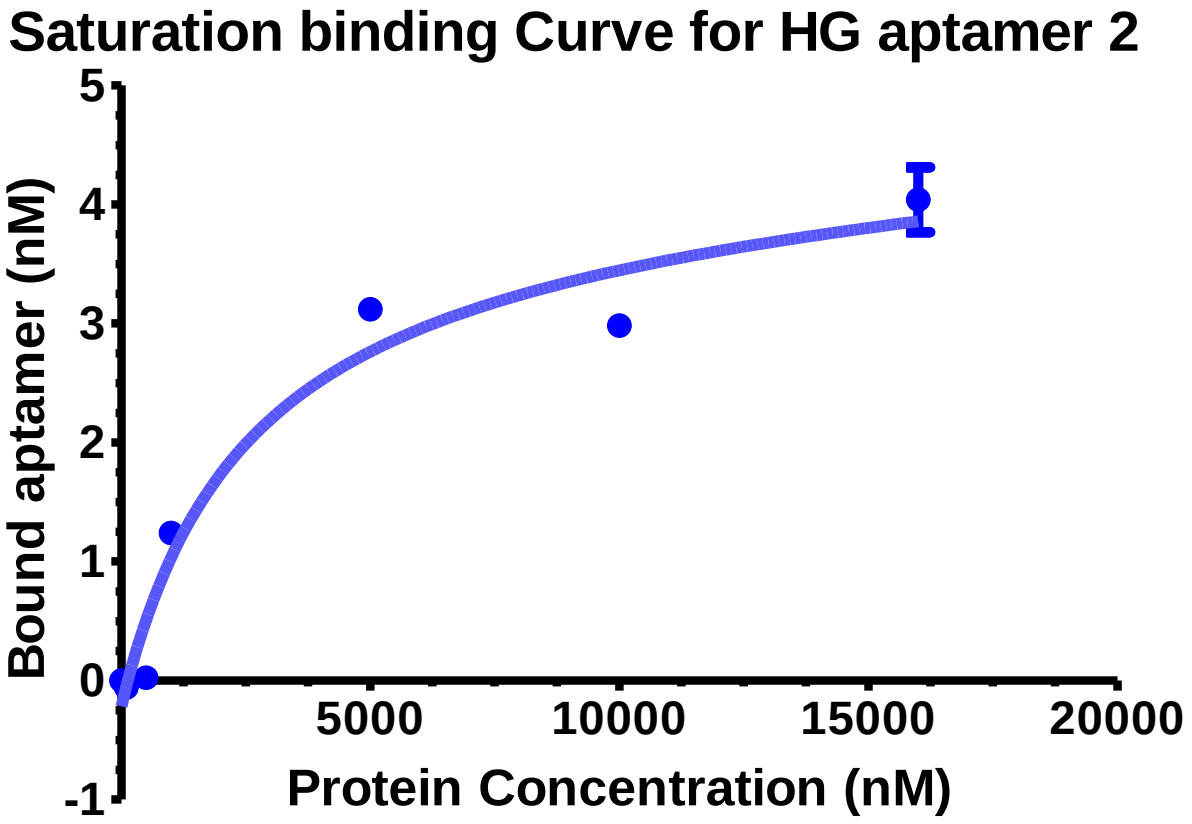

Figure b.16 Non-Linear regression analysis of HB2 aptamer; The ratio of bound DNA was plotted against protein concentration. K_D was determined using equation 1.1 on GraphPad Prism 5

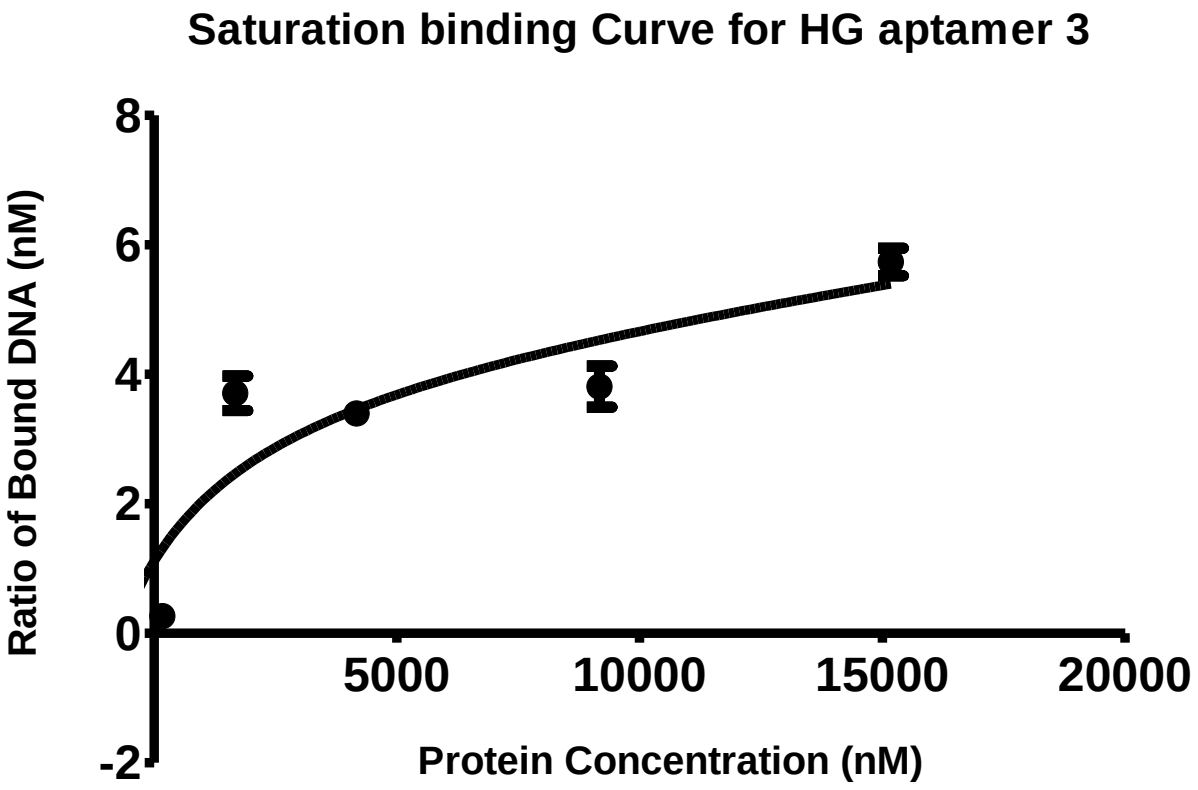

Figure b.17 Non-Linear regression analysis of HB3 aptamer; The ratio of bound DNA was plotted against protein concentration. K_D was determined using equation 1.1 on GraphPad Prism 5

c. Appendix of chapter 5

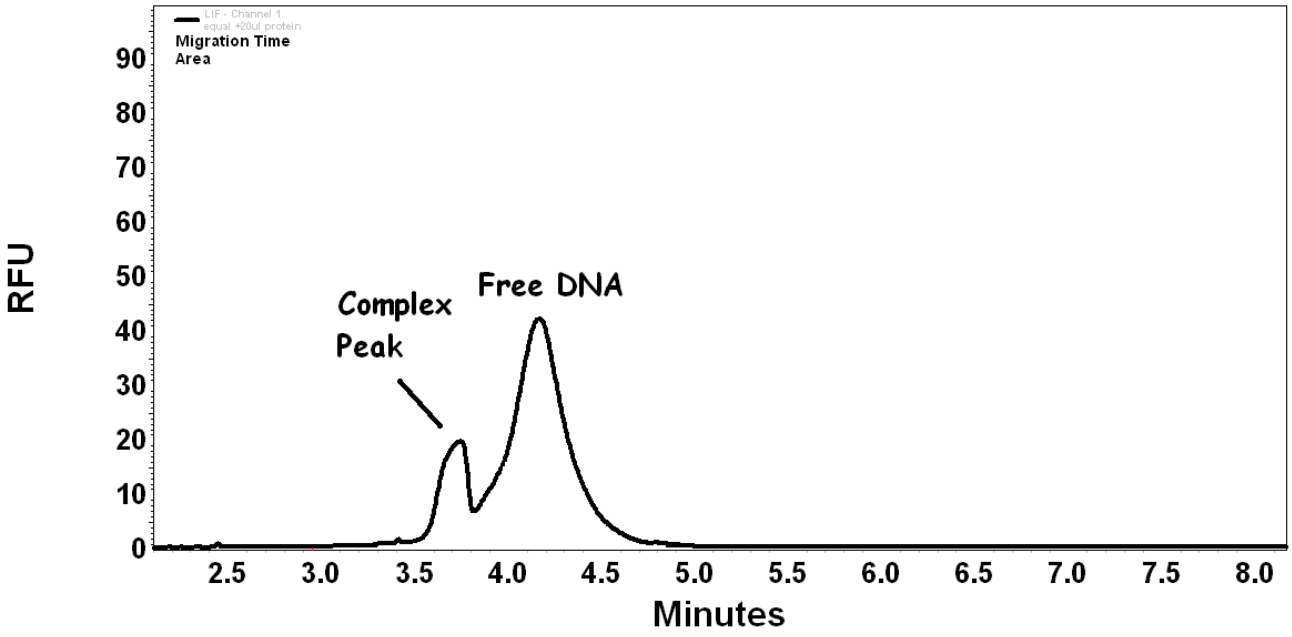

Figure c.1 Bulk affinity determination of the equilibrium mixture of round 1 hybridised SELEX 190nM DNA and 250 nM Cholesterol esterase; 500Vcm^{-1} separation, LIF detection , RB: 3xTGK, SB: water, 50µm ID capillary.

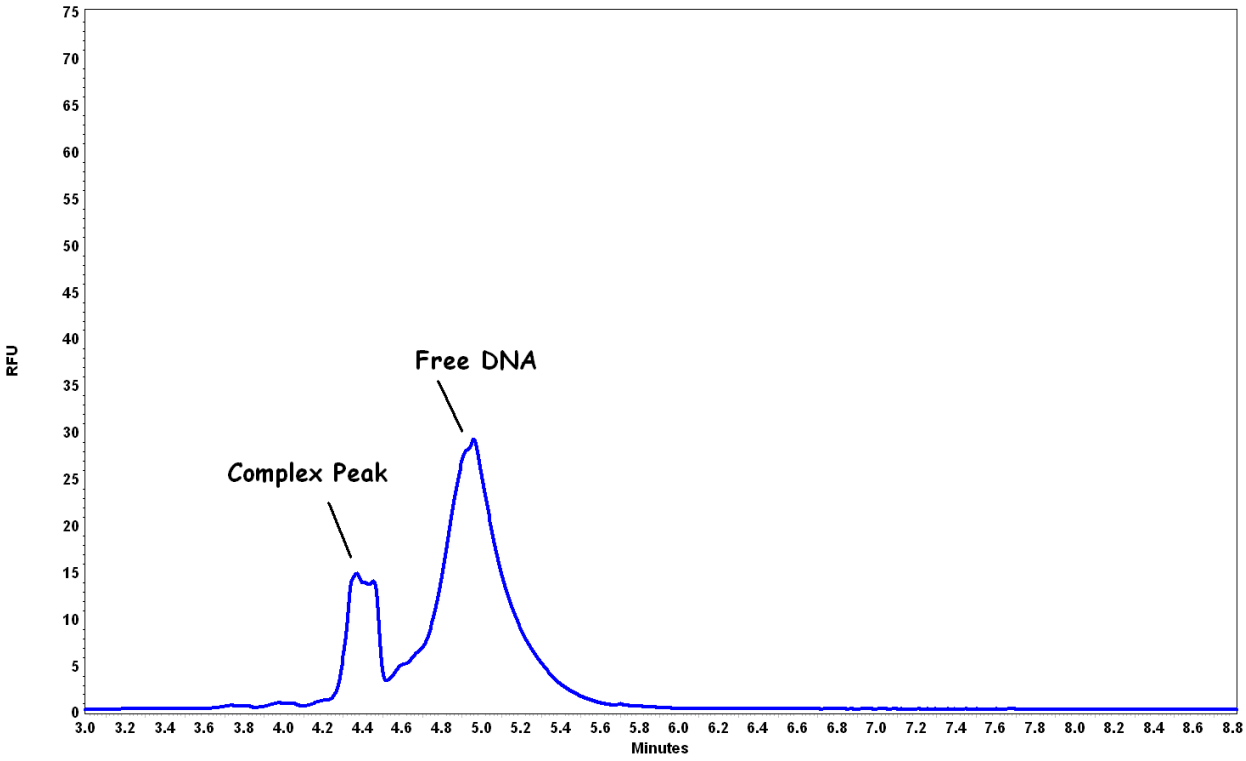

Figure c.2 (a) 100nM DNA library; (b) Equilibrium mixture of 100nM DNA and 100nM Chlorestrol esterase; 500Vcm^{-1} separation, LIF detection ,RB: 3xTGK, SB: water, 50µm ID capillary.

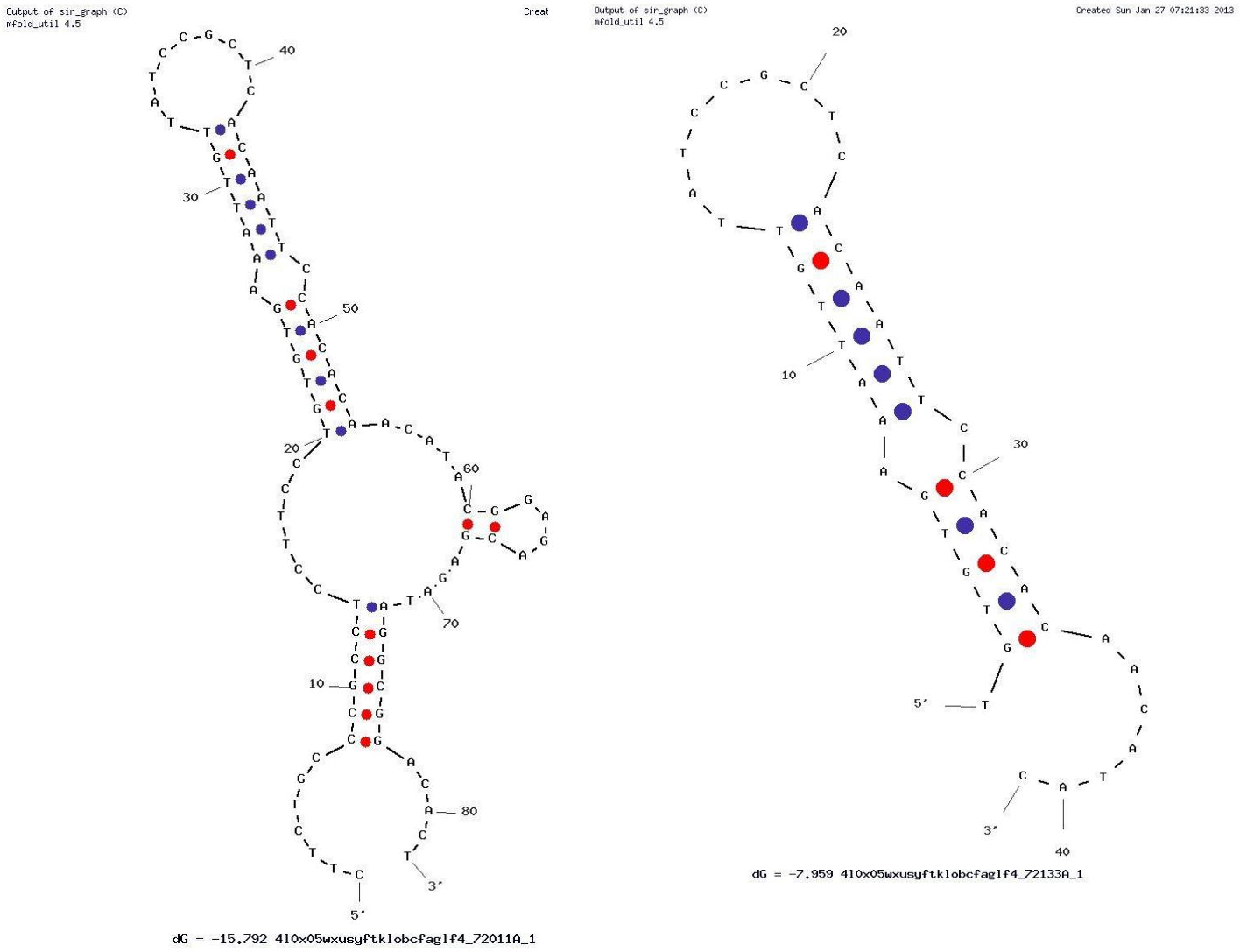

Figure c.3 The secondary structure of aptamer CES 4 and CES 4T checked on the OligoAnalyser 3.1 program using the ionic conditions of 100mM [Na^+] and 5mM [Mg^{2+}] ion concentrations

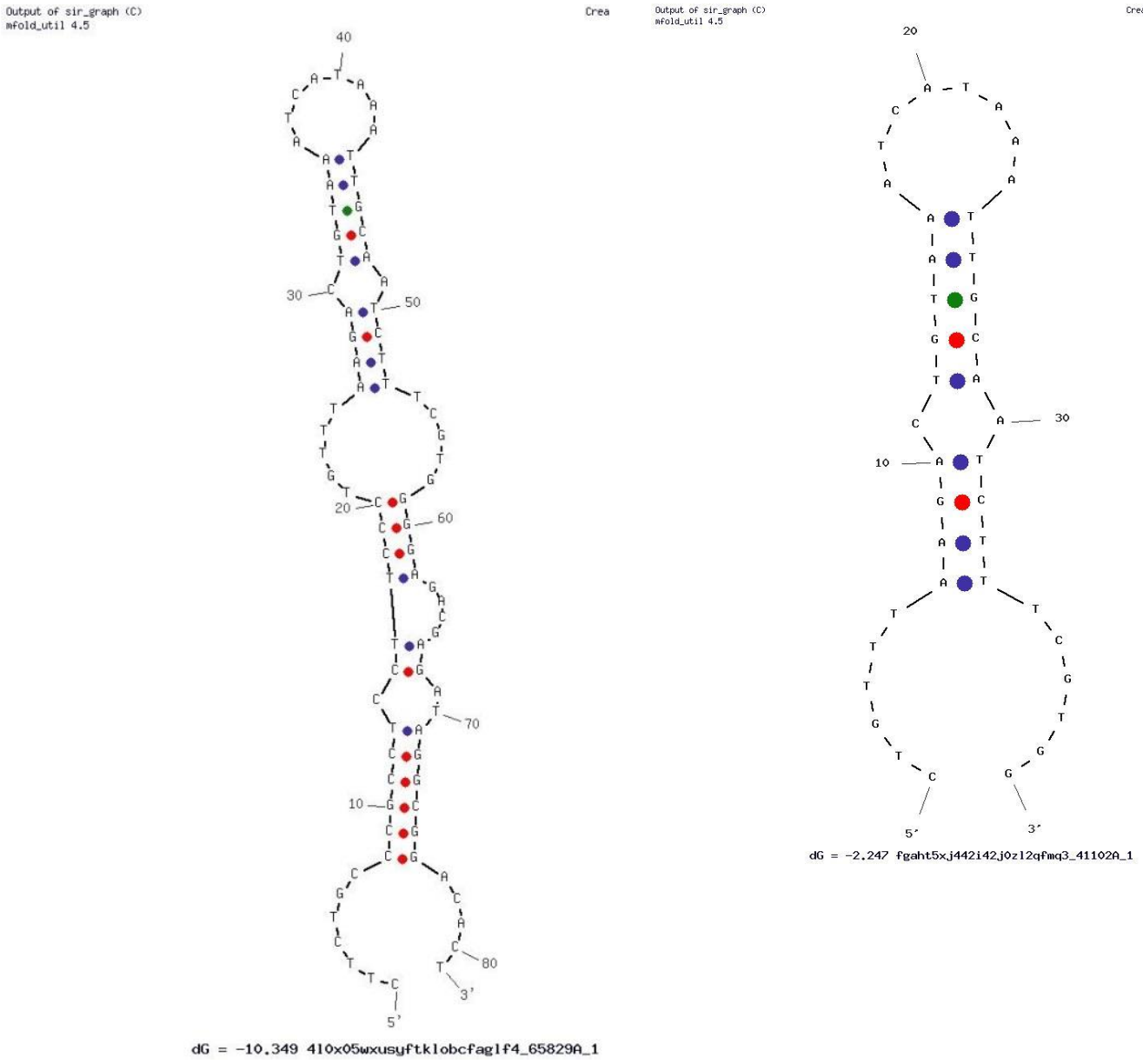

Figure c.4 The secondary structure of aptamer CES 3 and CES 3T checked on the OligoAnalyser 3.1 program using the ionic conditions of 100mM [Na^{+}] and 5mM [Mg^{2+}] ion concentrations.

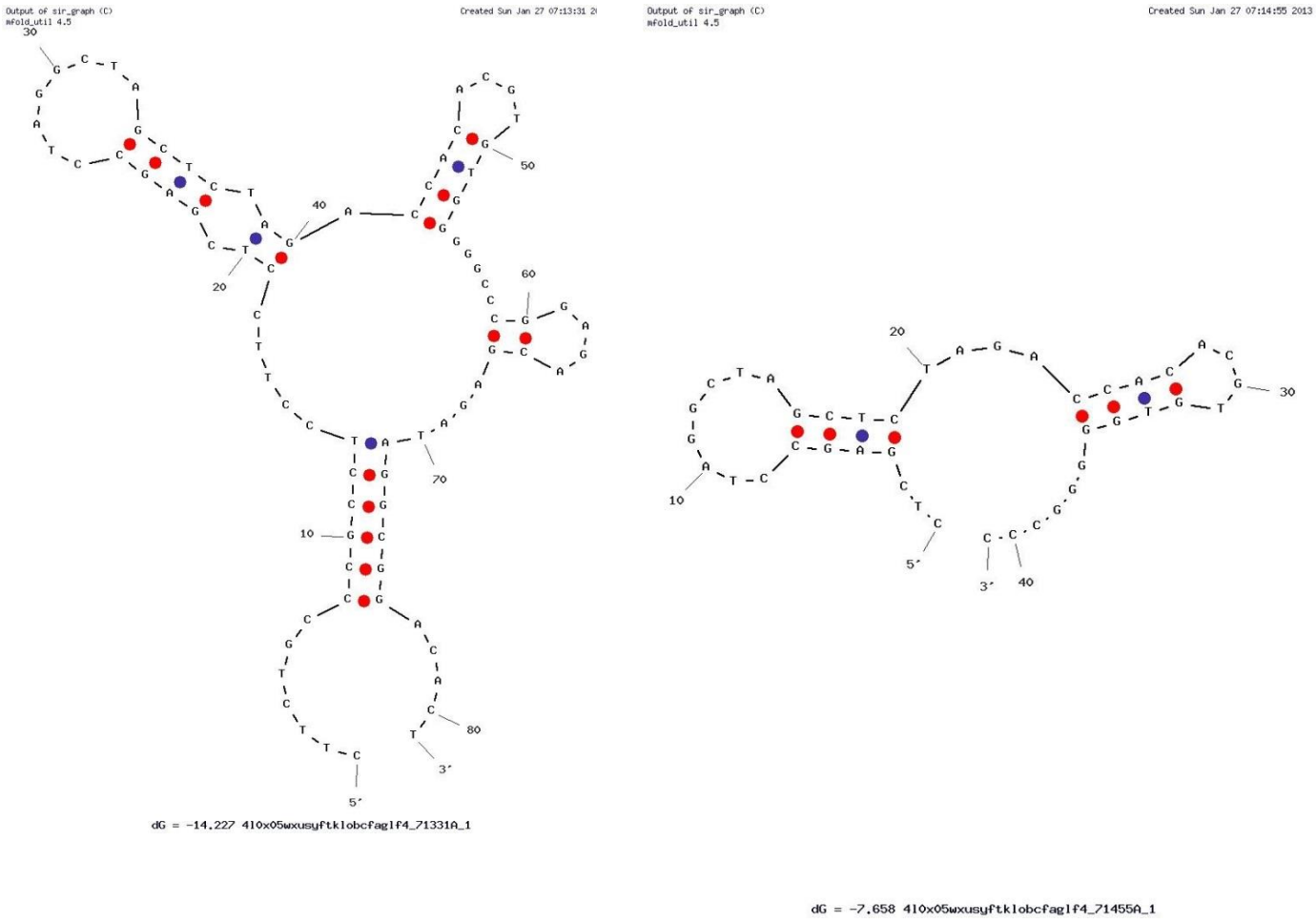

Figure c.5 The secondary structure of aptamer CES 2 and CES 2T checked on the OligoAnalyser 3.1 program using the ionic conditions of 100mM [Na^{+}] and 5mM [Mg^{2+}] ion concentrations.

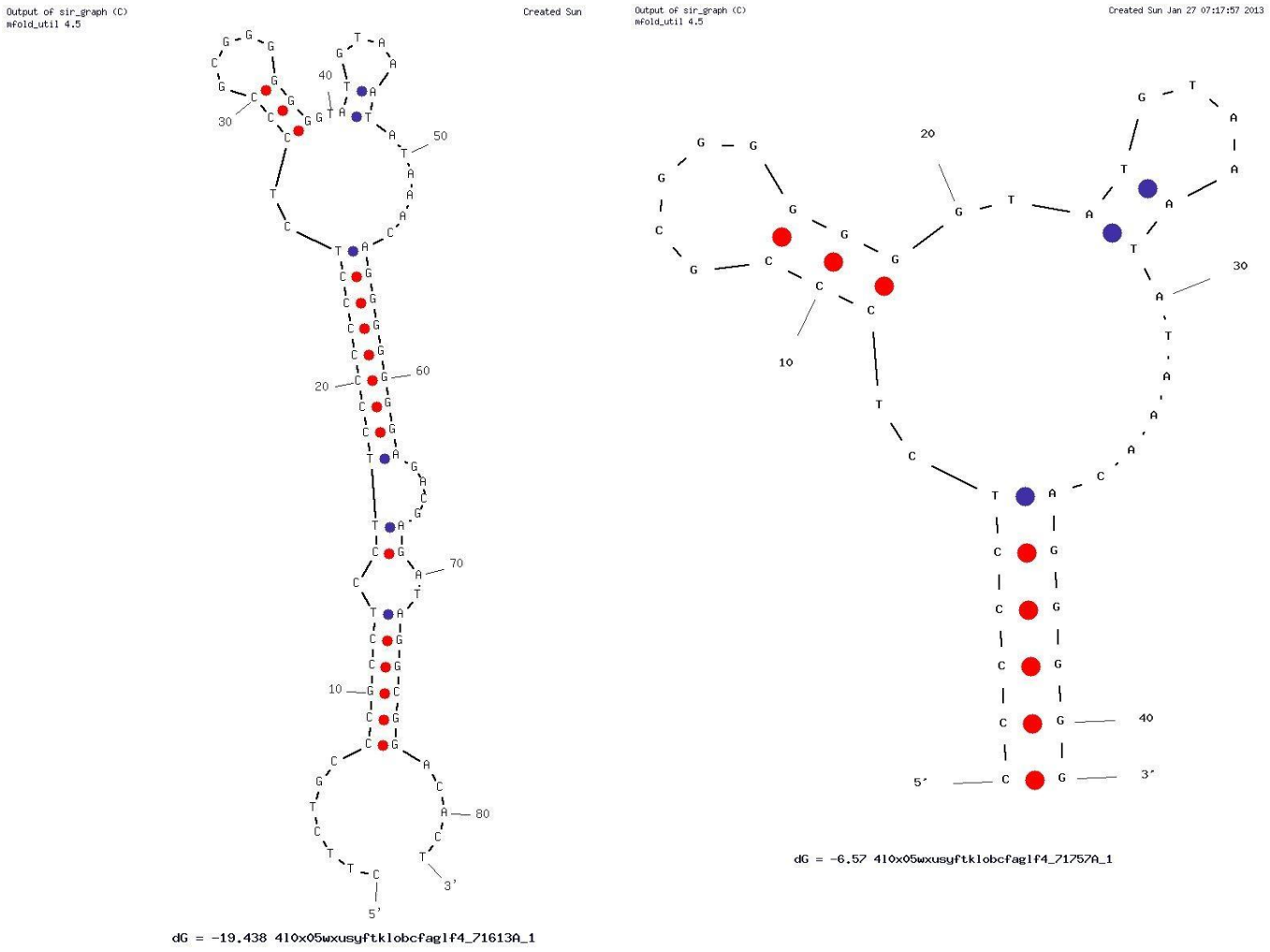

Figure c.6 The secondary structures of aptamer CES 5 and CES 5T, checked on the OligoAnalyser 3.1 program using the ionic conditions of 100mM [Na^+] and 5mM [Mg^{2+}] ion concentrations.

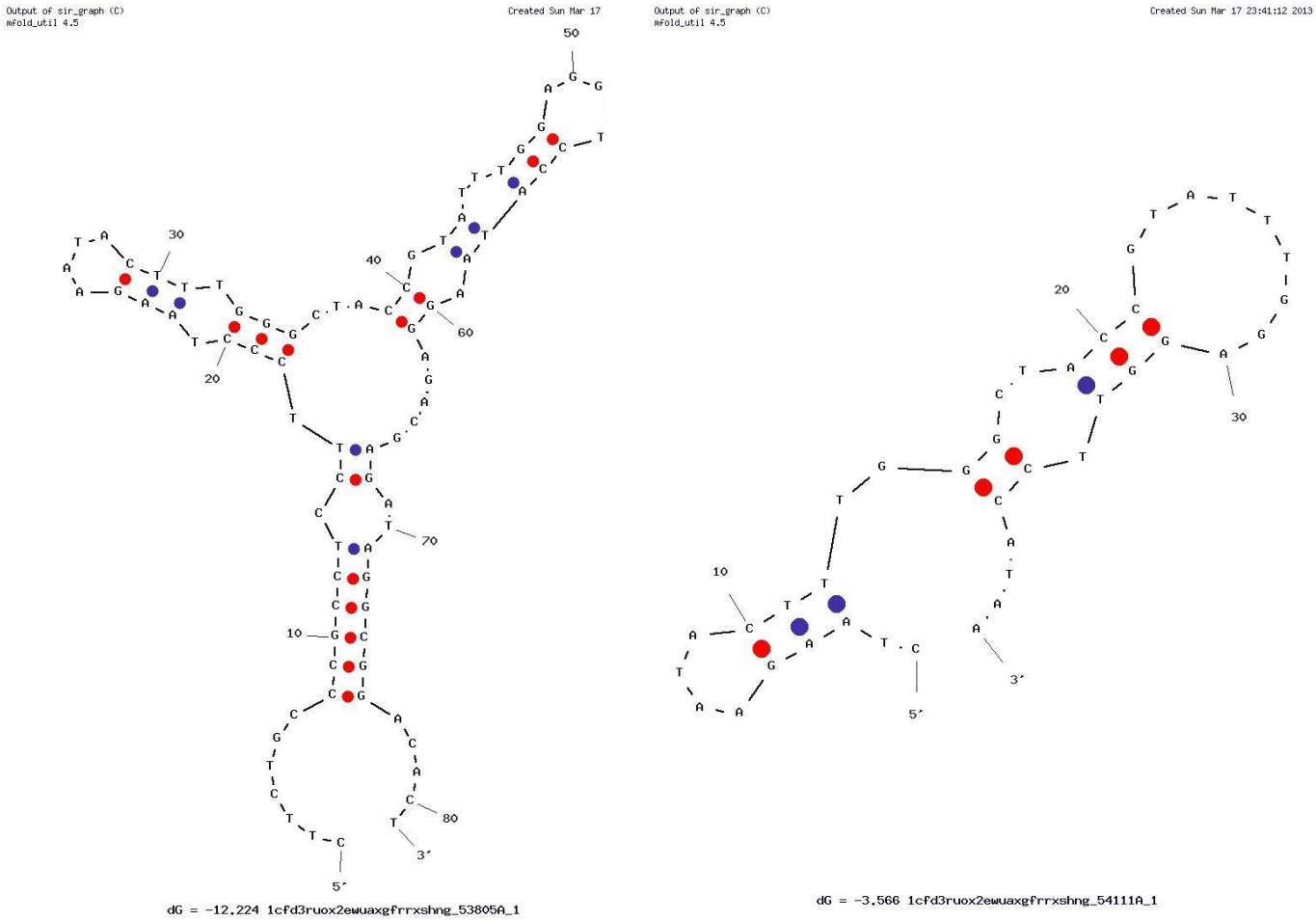

Figure c.7 The secondary structures of aptamer CES 6 and CES 6T, checked on the OligoAnalyser 3.1 program using the ionic conditions of 100mM [Na^+] and 5mM [Mg^{2+}] ion concentrations.

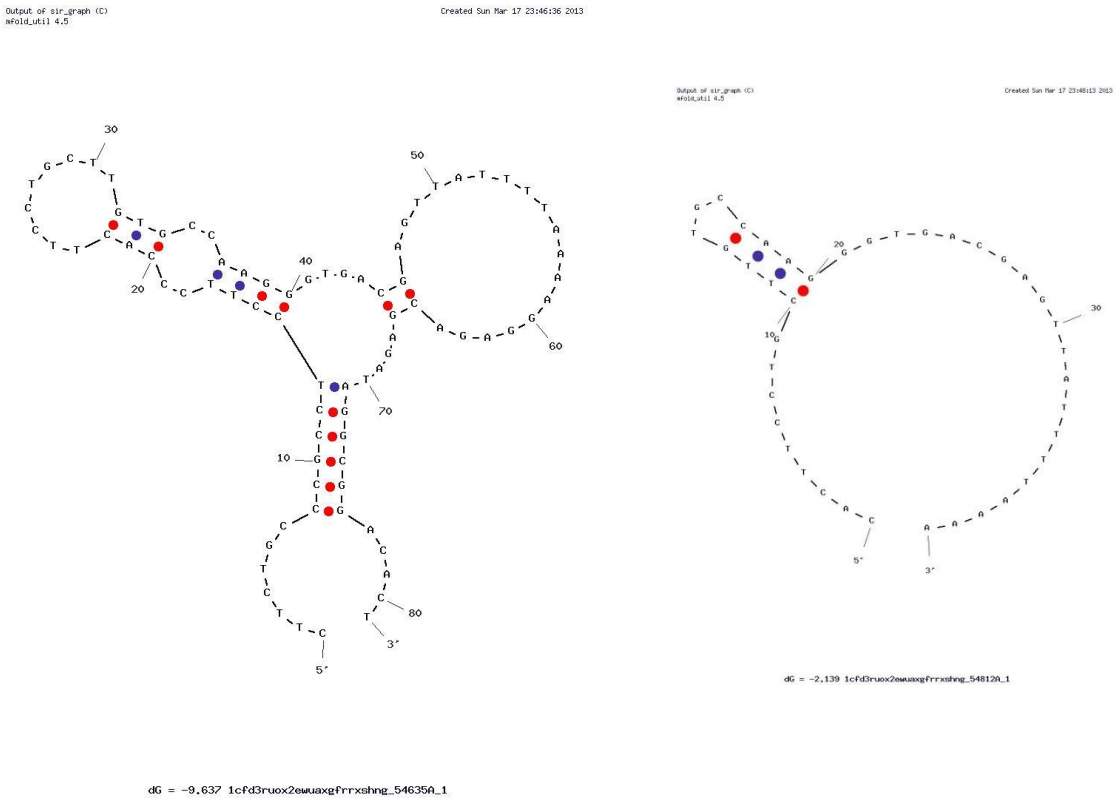

Figure c.8 The secondary structures of aptamer CES 6 and CES 6T, checked on the OligoAnalyser 3.1 program using the ionic conditions of 100mM [Na^{+}] and 5mM [Mg^{2+}] ion concentrations.

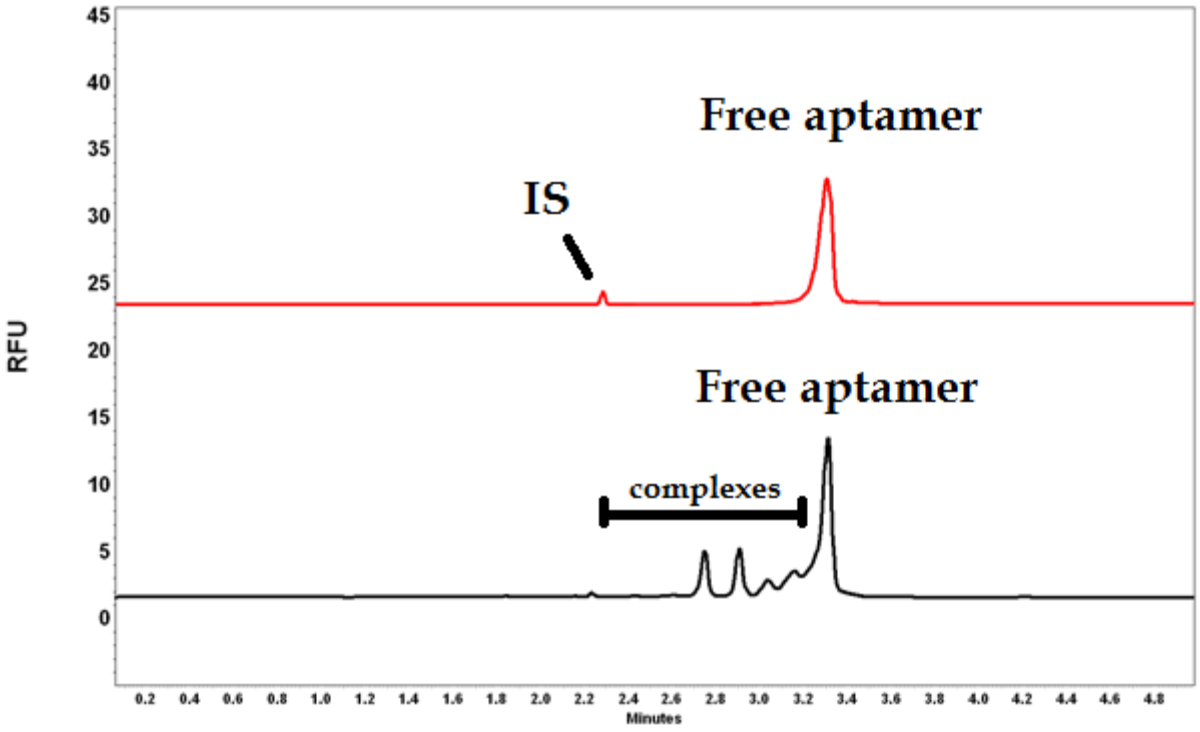

Figure c.9 NEECEM analysis of CES 3 aptamer; 100nM aptamer and 500nM leptin were incubated for 30 minutes and injected onto the capillary by hydrodynamic injection (9.90 nl), 666Vcm^{-1} separation with LIF detection. The areas of the free DNA, dissociated DNA and complex peak were used to determine K_D and experiments were performed in triplicate.

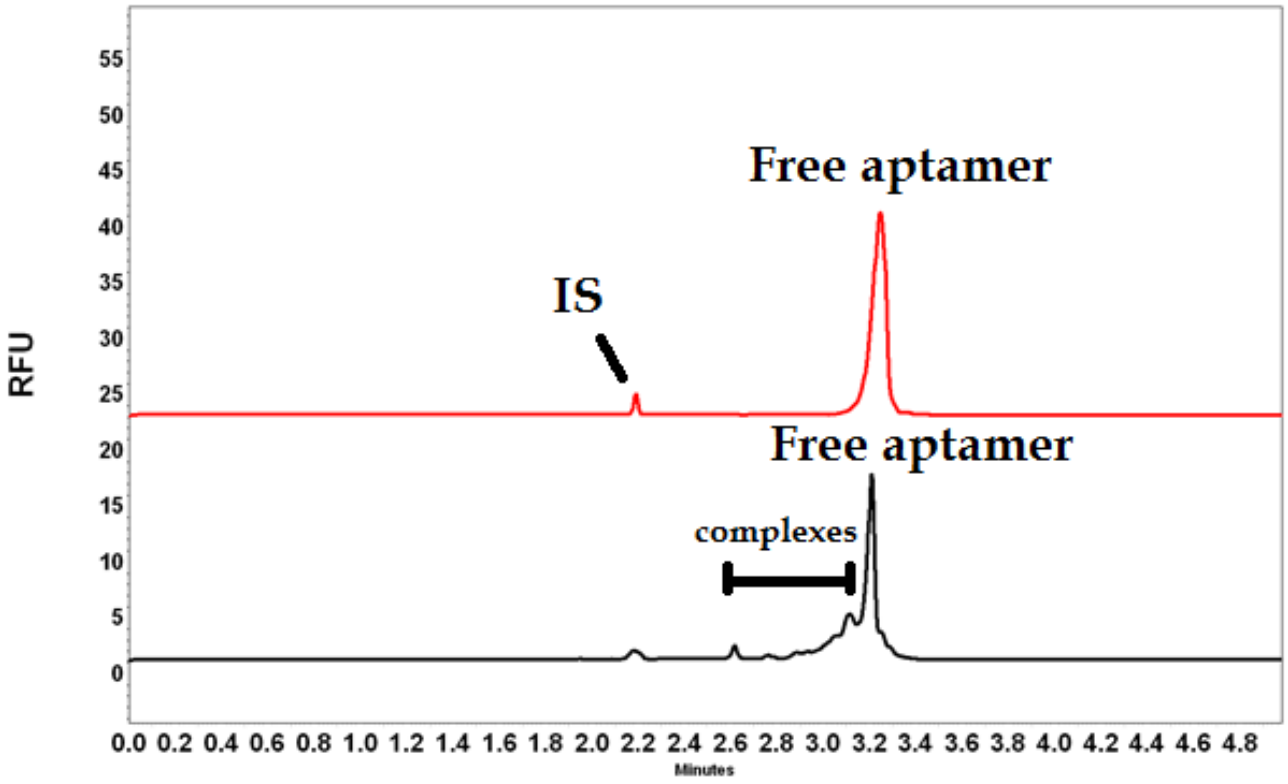

Figure c.10 NEECEM analysis of CES 5; 100nM aptamer and 500nM leptin were incubated for 30 minutes and injected onto the capillary by hydrodynamic injection (9.90 nl), 666Vcm^{-1} separation with LIF detection. The areas of the free DNA, dissociated DNA and complex peak were used to determine K_D and experiments were performed in triplicate.

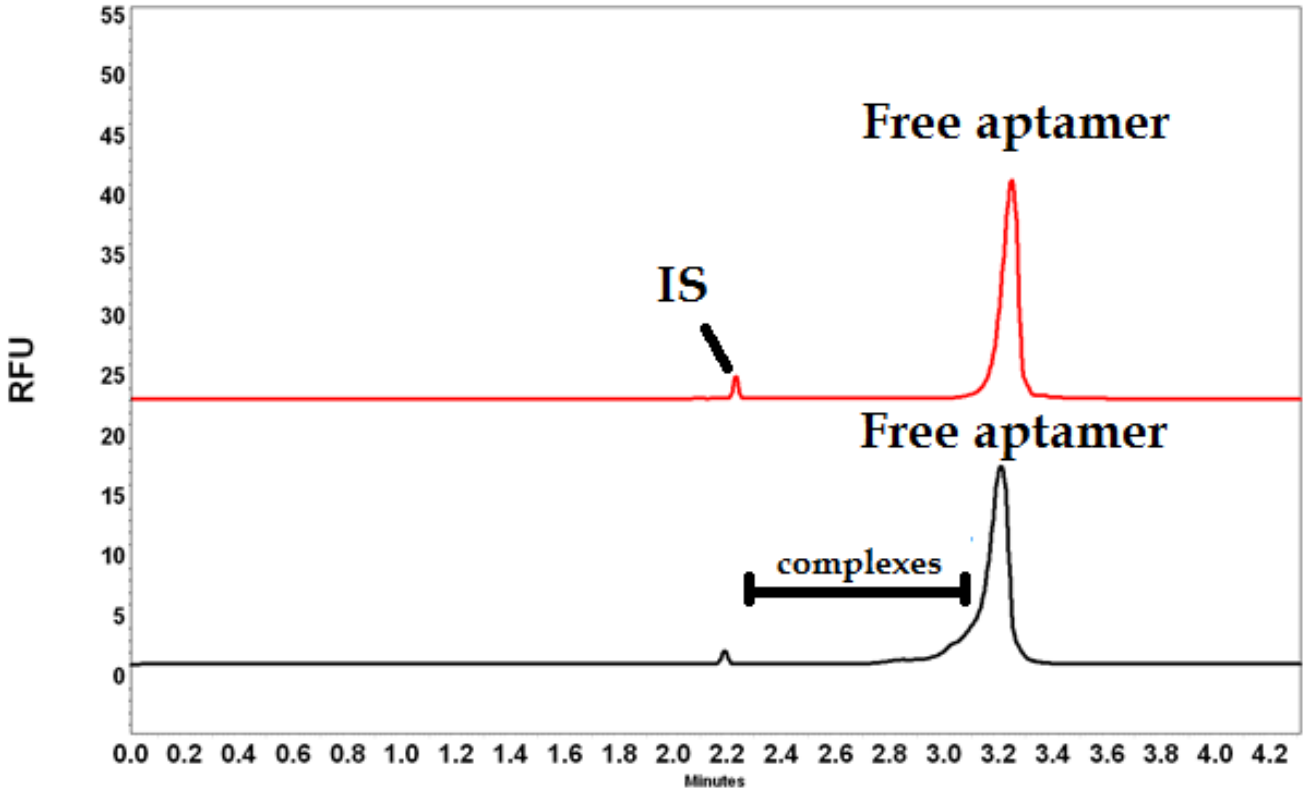

Figure c.11 NEECEM analysis of CES 2; 100nM aptamer and 500nM leptin were incubated for 30 minutes and injected onto the capillary by hydrodynamic injection (9.90 nl), 666Vcm^{-1} separation with LIF detection. The areas of the free DNA, dissociated DNA and complex peak were used to determine K_D and experiments were performed in triplicate.

d. Appendix of chapter 6

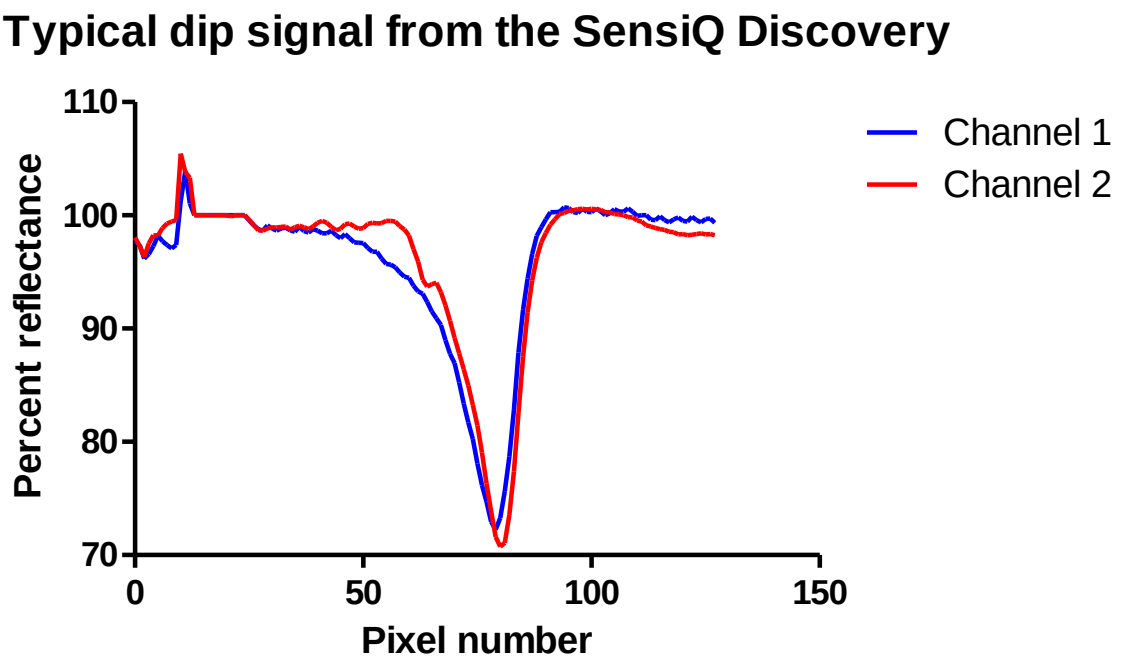

Figure d.1 Dip signal for the SensiQ discovery

9 List of Publications

1. Ashley J, Ji K, Li SFY: Selection of bovine catalase aptamers using non-SELEX. *Electrophoresis* 2012; 33:2783-2789.
2. J. Ashley, and S.F.Y. Li, Three-dimensional selection of leptin aptamers using capillary electrophoresis and implications for clone validation. *Analytical Biochemistry* 434 (2013) 146-152.
3. J. Ashley, and Li SFY An aptamer based surface plasmon resonance biosensor for the detection of bovine catalase in milk. *Biosensors and Bioelectronics* 48 (2013) 126–131
4. J. Ashley, W. S. Lim, K. Ji and Li SFY Non-SELEX of human haemoglobin aptamers (to be submitted).
5. J.Ashley and Li SFY Hybridised-SELEX: a capillary electrophoresis based method for maximising the number of aptamers screened (to be submitted).